Calabi-Yau Manifolds and Feynman Integral Computations

The Family of Banana Feynman Graphs

Dissertation
zur
Erlangung des Doktorgrades (Dr. rer. nat.)
der
Mathematisch-Naturwissenschaftlichen Fakultät
der
Rheinischen Friedrich-Wilhelms-Universität Bonn

von
Christoph Nega
aus
Waldbröl

Bonn, September 2021

Angefertigt mit Genehmigung der Mathematisch-Naturwissenschaftlichen Fakultät der Rheinischen Friedrich-Wilhelms-Universität Bonn

1. Gutachter:	Prof. Dr. Albrecht Klemm
2. Gutachter:	Prof. Dr. Claude Duhr
Tag der Promotion:	21.12.2021
Erscheinungsjahr:	2022

To my parents and friends.

Acknowledgements

At this point I would like to thank all the people who helped and encouraged me during my PhD.

First of all, I have to show my gratitude to Albrecht Klemm for his supervision during my PhD. It was always a pleasure for me to work with him on interesting questions in physics. All the meetings and discussions where very important in developing the ideas to solve the problems in my PhD. In particular, I am so happy and grateful that he pointed me into the connection between Feynman integral computations and string theory. This is a very interesting field which captured me. But nearly the same thank goes to Claude Duhr my second supervisor. My first contact with him was on a fruitful conference in Zurich which was trendsetting for my PhD. But also the other discussions, in particular, during my last project with him were very important for me. A similar thank goes to the other members of my PhD committee, Klaus Desch and Valentin Blomer.

I thank also my collaborators Kilian Bönisch, Claude Duhr, Fabian Fischbach, Albrecht Klemm and Reza Safari for very fruitful and interesting projects and discussions. Without them I could not have finished my PhD projects.

Moreover, I would like to thank Spencer Bloch, Martijn Hidding, Matt Kerr and Rene Klausen for helpful discussions. In particular, I thank Matt Kerr for pointing us to the complete intersection geometry and other useful references.

Furthermore, my gratitude is for all members and former members of the string theory group of Albrecht Klemm. My thank goes to Mahsa Barzegar, Kilian Bönisch, Cesar Fierro Cota, Fabian Fischbach, Andreas Gerhardus, Thaisa Guio, Hans Jockers, Abhinav Joshi, Marvin Kohlmann, Urmi Ninad, Rongvoram Nivesvivat, Reza Safari, Yannik Schüler, Thorsten Schimannek, Xin Wang for the constant open doors for questions not only about physics. But I thank also the other members of the Bethe Center for Theoretical Physics. Specially to Stefan Förste, Dominik Köhler and Hans Peter Nilles for the conversations during lunch and the coffee breaks afterwards. But also former members as Joshua Kames-King, Christoph Liyanage and Max Wiesner get my gratitude for their open offices and funny conversations. Without the help of Christa Börsch, Petra Weiß, Andreas Wisskirchen and Patrica Zündorf the institute would not be such an amazing place such that I am engaged for a big thank you. Additionally, I want to thank the Physics Institut and the Bonn-Cologne Graduate School of Physics and Astronomy for financial support.

Additionally, I thank my old student colleges Philip Hauer and Thilo vom Hövel that we managed it to pass first our physics studies and hopefully also our PhD in physics.

Of course, I am also deeply happy that I got a lot of support from my other friends, partly also from physics Arne, Benedict, Dominik, Florin, and Martin, in particular, for many amazing big rides. Also I thank my sports team at TTG St. Augustin for many nice and great table tennis hours. Moreover, I thank my friends Alex, Heinz and Lukas for nice vacations and one or more glasses of beer.

Finally, my biggest gratitude goes to my family. My parents Birgit and Bernd who supported my not only my PhD and studies at the university but also during my whole life. Often also with a necessary financial support, thanks for this. Also my sister Catharina encouraged me during all periods of my life. At the end I also thank my girlfriend Katharina who supported me always during my PhD and in all other situations. She was my rock and guided me through my long time as a PhD student which is now more or less accomplished.

Summary

In this thesis we use geometrical and string theoretic inspired methods to compute Feynman integrals. We analyze the family of l-loop banana Feynman graphs which is a very prominent and important infinite family of Feynman graphs. Using our methods we compute the banana integrals to high loop order and also for generic masses which was not possible before. We relate the abstract l-loop Feynman integral in $D = 2$ dimensions to geometric period integrals of a $(l-1)$-dimensional Calabi-Yau manifold M_{l-1} such that the maximal cut contours correspond to the integral homology $H_{l-1}(M_{l-1}, \mathbb{Z})$.

The first part of the thesis introduces basic concepts of the theory of Feynman graph computations. Different integral representations of Feynman diagrams and important structures deduced therefrom are elucidated. In particular, integration by parts relations, relations between different Feynman integrals and the concept of maximal cuts are introduced and illustrated through examples. Secondly, fundamentals of differential equations and solution techniques thereof are explained. Moreover, it is argued that Feynman integrals satisfy homogeneous differential equations which can actually be used to determine them. Properties of these special differential equations are discussed. Additionally, we explain how they can be solved with the Frobenius method. In a third review part the mathematics of Calabi-Yau manifolds is mentioned, including their general structure as well as their properties. More importantly, the consequences of these structures in the context of Feynman integral computations are stressed. For example, bilinear relations between Feynman integrals result from Griffiths transversality between Calabi-Yau period integrals. Similarly, important structures such as variations of (mixed) Hodge structures, the point of maximal unipotent monodromy, the GKZ system and the Frobenius method for computing periods are discussed. We further review basics of mirror symmetry and explain main concepts as the $\widehat{\Gamma}$-class.

In the second part we use all of the previously introduced structures and techniques to solve the l-loop banana integral. First, we solve the equal-mass case. Using the bilinear relations between the maximal cuts of the banana graphs we can write down a very simple and elegant solution of the whole banana integral valid to arbitrary loop order. This generalizes the $l \leq 3$ cases. Then we give two different Calabi-Yau geometries associated to the l-loop banana diagram, namely a hypersurface and a complete intersection motive. Using the GKZ system and the Frobenius method we are able to find the periods for both geometries. We extend the GKZ system such that it also includes the contributions of the full Feynman integral not just the maximal cuts. Then we can linearly combine all periods to obtain the full integral. The subsequent chapter uses the techniques of the $\widehat{\Gamma}$-class to find the correct

linear combination of periods for the full Feynman integral purely through geometrical data at the point of maximal unipotent monodromy. This enables us to solve for the first time the generic-mass banana integral for $l \geq 3$ in $D = 2$ dimensions. Finally, the banana graphs are solved in dimensional regularization, i.e. $D = 2 - 2\epsilon$ dimensions. We first find a hypergeometric series expansion of the banana integral which serves as a generalization of the $\widehat{\Gamma}$-class to dimensional regularization. Furthermore, we present a technique to find differential equations describing the hypergeometric expansion purely from combinatorics such that one can analytically continue the integral in the whole parameter space.

List of Publications

This thesis is based on the following publications:

Feynman Integrals in Dimensional Regularization and Extensions of Calabi-Yau Motives, *K. Bönisch, C. Duhr, F. Fischbach, A. Klemm, C.N.*, In: (August 2021) arXiv: 2108.05310 [hep-th]

Analytic Structure of all Loop Banana Amplitudes, *K. Bönisch, F. Fischbach, A. Klemm, C.N., R. Safari*, In: *JHEP* 05 (2021), p. 066. DOI: 10.1007/JHEP05(2021)066, arXiv: 2008.10574 [hep-th]

The l-loop Banana Amplitude from GKZ Systems and relative Calabi-Yau Periods, *A. Klemm, C.N., R. Safari*, In: *JHEP* 04 (2020), p. 088. DOI: 10.1007/JHEP04(2020)088, arXiv: 1912.06201 [hep-th]

Contents

1 Introduction **1**

2 Basics of Feynman Graph Computations **5**
2.1 Feynman diagrams in quantum field theory . . . 5
2.2 Feynman graphs . . . 6
2.3 Momentum space representation . . . 7
2.3.1 Concept of dimensional regularization . . . 8
2.3.2 Integration by parts identities . . . 9
2.3.3 Master integrals for the banana graphs . . . 12
2.4 Symanzik representation and graph polynomials . . . 14
2.4.1 Some graph theory . . . 16
2.5 Schwinger representation . . . 18
2.5.1 Dimensional shift relations . . . 19
2.6 Baikov representation . . . 20
2.7 Maximal cuts of Feynman integrals . . . 23
2.8 Discontinuities, Cut Feynman integrals and the Optical theorem . . . 26

3 Differential Equational Approach to Feynman Integrals **29**
3.1 Differential equations for Feynman integrals . . . 29
3.2 Gauss-Manin type differential equations . . . 30
3.3 Picard-Fuchs type differential equations . . . 33
3.3.1 One-parameter Picard-Fuchs-type differential equations . . . 34
3.3.2 Multi-parameter Picard-Fuchs operators . . . 36

4 Mathematics of Calabi-Yau Spaces in the Context of Feynman Integrals **39**
4.1 Calabi-Yau varieties and their complex structure moduli spaces $\mathcal{M}_{cs}$ . . . 39
4.1.1 Complex families of Calabi-Yau n-folds. . . . 40
4.2 Geometric structures in the complex moduli space and period integrals . . . 41
4.2.1 On the bulk of $\mathcal{M}_{cs}$ . . . 42
4.2.2 Quadratic relations from Griffiths transversality . . . 46
4.2.3 Monodromy and limiting mixed Hodge structure on the boundary of $\mathcal{M}_{cs}$ . . . 48

5 The Equal-Mass Banana Graphs **61**
5.1 Frobenius method for equal-mass banana graphs . . . 61
5.2 Bilinear relations for equal-mass banana graphs . . . 63
5.3 Explicit set of master integrals for banana graphs . . . 66

6 Hypersurface Motive of the Banana Graphs **69**
6.1 Hypersurface geometry associated to the l-loop banana graph . . . 69
6.1.1 Calabi-Yau hypersurfaces in toric ambient spaces . . . 70
6.1.2 Period integrals of the hypersurface model M_{l-1} . . . 75
6.1.3 GKZ method for the banana integrals . . . 78
6.1.4 Mori cone generators and subslice problem . . . 80
6.2 The complete banana diagram and inhomogeneous differential equations . . . 80
6.3 Example: The generic mass three-loop banana integral . . . 81

7 Complete Intersection Motive of the Banana Graphs **85**
7.1 A complete intersection Calabi-Yau for the l-loop banana graph . . . 85
7.1.1 Frobenius method for complete intersection geometry . . . 88
7.2 Comparison of the hypersurface motive and the complete intersection motive 90
7.3 The four-loop generic-mass banana integral . . . 92

8 Mirror Symmetry and the $\widehat{\Gamma}$-Class **95**
8.1 Mirror symmetry . . . 95
8.2 The $\widehat{\Gamma}$-class . . . 97

9 Banana Feynman Integrals in Dimensional Regularization **103**
9.1 A hypergeometric series representation of the banana integral . . . 103
9.2 Differential equations for banana Feynman integrals . . . 106
9.2.1 Comments on the number of solutions . . . 111
9.3 Some comments on the equal-mass case . . . 112
9.4 Special solutions and cut integrals . . . 113

10 Conclusion **117**

A Differential operators for the three-loop banana integral **119**

B Differential operators for the four-loop banana integral **121**

Bibliography **123**

CHAPTER 1

Introduction

Many modern theories in physics are expressed in the language of quantum field theory. For example, the fundamental forces like electromagnetism, the weak and the strong force are described as a quantum field theory known as the Standard Model of particle physics. One of the successes of quantum field theories is that they give precise theoretical predictions for the scattering amplitudes of fundamental particles which can be tested in experiments. The Standard Model of particle physics is a quantum field theory which has passed over several decades many experimental checks. On the experimental side one uses for example bigger and stronger particle colliders as the Large Hadron Collider to obtain more precision on the experimental data but also to test the theory at different energy levels. But also the theoretical side has to improve their predictions to compare theory and experiment more accurately. A common technique is to use perturbative quantum field theory which allows for explicit calculations though only giving an approximate prediction.

The cornerstone of perturbative quantum field theory is the computation of multi-loop Feynman diagrams. To acquire the desired precision, high loop orders have to be reached. This is only possible if one has a precise understanding of the mathematical structures underlying Feynman integrals and additionally if efficient methods to evaluate them are known and well under control. Since the last century many different techniques have been developed to tackle the computation of these integrals. In recent years it has become clear that there is a strong connection between the techniques from Feynman integrals and certain branches of pure mathematics such as geometry, algebra and number theory. For instance, it was shown that Feynman integrals are actually period integrals in the sense of Kontsevich and Zagier [1] such that the physical parameters, i.e. the momenta and masses, can be seen as the moduli of these periods. This observation opens a link between geometric periods of algebraic varieties and abstract integrals related to Feynman graphs. As an example, periods of algebraic varieties satisfy linear differential equations describing the variations of the mixed Hodge structures of these varieties. Depending on the formulation of these equations they are called Gauss-Manin connection or Picard-Fuchs differential ideal and they are well known in mathematics for several decades or even centuries. But also Feynman integrals

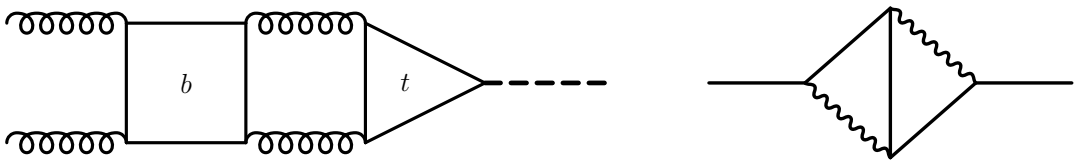

Figure 1.1: A three loop contribution to Higgs production via gluon fusion with a bottom and a top quark running in the loops (left panel). The scalar kite Feynman graph with two massless and three propapagators of equal mass (right panel).

satisfy first-order differential equations as observed in [2–6]. From a geometric point of view this is quite obvious because they are periods but from a purely physics perspective this was a new and interesting observation [7, 8]. In this thesis I want to elaborate on this connection and show many situations where geometry can give precise and often new predictions for Feynman integrals. But also the other way is possible meaning that mathematics can learn something from physics since the mathematics needed for multi-loop Feynman integral computations is on the frontier of pure mathematics and by far fully developed.

The running example in my thesis will be the so-called family of banana graphs shown in figure 2.2. On the first glance these diagrams do not look realistic and important at high loop orders since the valence of their vertices is too high. But actually these graphs appear almost everywhere as sub-topologies of any higher-loop process and are therefore necessary in most computations of phenomenologically relevant processes. Using integration by parts identities and in advance tensor reductions to obtain scalar Feynman integrals from tensor ones one can show that banana graphs enter relevant Feynman integral computations. For example, the two-loop banana graph appears as a building block for computing the so-called kite diagram in figure 1.1 which is a two-loop correction to the electron self-energy [9]. The next higher banana graph is a sub-topology of a three-loop correction for Higgs production via gluon fusion, see also figure 1.1. Notice that here different masses of the banana integral are necessary as well as for the three-loop correction to the ρ-parameter [10]. Even the four-loop banana graph is relevant for calculating the anomalous magnetic moment of the electron [11]. So we see that the role of this family of Feynman graphs is significant and should not be underestimated. With the techniques I develop in this thesis it is possible to compute for the first time these diagrams in the equal– as well as in the generic-mass case to nearly arbitrary loop order. Besides the phenomenological implications of this there are also new achievements in mathematics as a product of analyzing these Feynman integrals, e.g. a novel $\widehat{\Gamma}$-class, new insights into higher dimensional Calabi-Yau manifolds, iterated integrals of Calabi-Yau periods and many more.

One common strategy in the computation of Feynman integrals is to restrict the function space of a given Feynman graph. Here one searches for the most generic set of functions such that one can build the Feynman integral from them. The structure of Feynman integrals is strongly determined from fundamental physical principles. For example, the branch cut structure of Feynman graphs reflects the thresholds of the involved particles. This severely restricts the possible functions appearing. It has been found that many Feynman

integrals can be expressed through so-called multiple polylogarithms having the required branching behavior. This is a class of functions introduced by Poincaré, Kummer and Lappo-Danilevsky [12, 13] which has recently reappeared in both mathematics [14–16] and physics [17–19]. But it turns out that the function space of polylogarithms is not large enough to capture all Feynman integrals. Even the two-loop banana graph can not be computed from this set of functions. In a fantastic paper [20] Bloch and Vanhove showed that the generic-mass two-loop banana graph can be solved in terms of a so-called elliptic dilogarithm, a generalization of the usual polylogarithms [21–23]. In the equal-mass case one can use iterated integrals of Eisenstein series [24, 25]. With these kinds of functions many multi-loop and massive Feynman graphs have been computed [10, 24–40]. But still the theory of these functions has to be developed from a physics as well as from a mathematical, in particular, numerical side [37, 41, 42].

In recent years examples of three-loop graphs were found which can not even been computed with these additional functions. These are the three-loop generic-mass banana graph [43–45] and the so-called train track graphs [46]. The period integrals appearing in the corresponding Feynman integrals could be related to period integrals of K3 surfaces. These geometric integrals are the natural extensions of the ones at lower loops. At two loops these periods form the class of elliptic integrals which are known to the physics community since the Kepler problem. At higher loops they correspond to Calabi-Yau period integrals which are well studied objects in string theory. In this spirit one has to understand the structure of higher dimensional Calabi-Yau periods to understand the Feynman integrals properly. For the banana family I wanted to clarify this connection within my PhD projects [44, 45, 47] and collect the most important observations in my PhD thesis here. For this we used methods from string theory, or more generally, geometry, such as the theory of periods of algebraic varieties and mirror symmetry to compute the banana integrals.

In this approach as a first step one has to identify the geometry associated to the l-loop banana diagram, which is a $(l-1)$-dimensional Calabi-Yau manifold M_{l-1}. In $D = 2$ dimensions one can relate the maximal cuts of the banana graphs exactly to the periods of these Calabi-Yau spaces. In fact, we will give two topologically different manifolds which still describe the appropriate periods for the banana graphs. In more detail, the maximal cuts are the periods of M_{l-1} over cycles in integral homology $H_{l-1}(M_{l-1}, \mathbb{Z})$. These can be computed at the point of maximal unipotent monodromy (short MUM-point) using the Picard-Fuchs differential ideal and the Frobenius method to obtain first a non-integer basis of periods. Using the $\widehat{\Gamma}$-class this non-geometric basis can be related to the geometric, integral basis of maximal cuts. This technique was developed in mirror symmetry [48, 49]. We show that this method can be extended also for the full banana integral which is an open chain integral on the Calabi-Yau M_{l-1}. This will lead us to a novel $\widehat{\Gamma}$-class for the Fano ambient space F_l of M_{l-1} which has now been proven in [50]. Finally, this determines completely the full l-loop generic-mass and equal-mass banana Feynman integral in the large momentum regime in $D = 2$ dimensions.

In another step we extend these results to dimensional regularization in $D = 2 - 2\epsilon$ dimensions. This extension is inspired by the previous geometrical methods and shows

that they are not only applicable and useful in $D = 2$ dimensions but also with generic ϵ-dependence. Using a Mellin-Barnes integral representation of the l-loop banana integral one can derive a generalized hypergeometric series representation charing similar features than the Calabi-Yau periods. For instance, we can construct a differential ideal describing these hypergeometric series such that they can be evaluated in the whole parameter space. Furthermore, we show that this series expansion extends the asymptotic of the banana integral to dimensional regularization which was previously described by the $\widehat{\Gamma}$-class for vanishing ϵ. In the limit $\epsilon \to 0$ we exactly reproduce the Calabi-Yau results.

Hopefully, we have already made clear that the connection between Feynman integral computations and Calabi-Yau manifolds, or more general algebraic objects such as motives, has to be extended and deepened. With this thesis I hope that I can introduce interesting mathematics and therefrom insights and techniques for the Feynman integral community. This shall motivate to proceed the interplay between the Feynman integral community, string theorists and pure mathematicians.

My PhD thesis is roughly assembled in two parts including several chapters. The first part contains the chapters 2 - 4 and also section 8.2 and gives a review of the necessary material to understand this thesis. Chapters 5 - 9 show how the banana integrals can be calculated.

In more detail, chapter 2 is an introduction to the theory of Feynman integrals. Important concepts such as Feynman graphs, integration by parts, different integral representations and maximal cuts are introduced and exemplified with the banana diagrams. Afterwards in chapter 3 general differential equational techniques are introduced which will be necessary for the computations in the second part of the thesis. In particular, the Frobenius method at the MUM-point is explained. The mathematics of Calabi-Yau manifolds is introduced in chapter 4 and also important implications for Feynman integrals such as bilinear relations coming from Griffiths transversality are discussed. Then all these methods are used in chapter 5 to compute the equal-mass banana graphs. Chapters 6 and 7 give two different Calabi-Yau geometries which both can be used to solve the generic-mass banana graphs. The explicit Calabi-Yau periods and operators are written down (see also appendices A and B). Mirror symmetry and together with the $\widehat{\Gamma}$-class are explained in chapter 8. The last chapter 9 deals with the banana integrals in dimensional regularization.

CHAPTER 2

Basics of Feynman Graph Computations

In this chapter we introduce some important concepts relevant in the field of Feynman graph computations. We define a Feynman graph and give different but equivalent integral representations of it. The start of our discussion is the traditional and probably best known one, namely the momentum space representation. But also other representations, in particular parametric ones, are discussed. We do not cover all possible representations known in the area of Feynman graph computations but focus on special ones which can be used to deduce important features of Feynman integrals, for instance the existence of integration by parts identities, dimensional shift relations, relations to geometric objects, etc.. Furthermore, the concept of cuts and specially of maximal cuts will be explained. All these concepts are demonstrated with the so-called family of banana diagrams.

2.1 Feynman diagrams in quantum field theory

Quantum field theory is a model for the description of fundamental particles and their behavior. For example, it describes the collision or scattering behavior of fundamental particles in terms of cross sections or scattering amplitudes. These quantities can often not be computed analytically in closed form. To circumvent this issue a common method is to use perturbation theory. In this approach one expands the desired expression in a certain small coupling constant. This should at least give an approximate, maybe not a convergent, series expansion. This expansion can be graphically visualized by so-called *Feynman graphs* which can be translated by knowing the *Feynman rules* to precise mathematical integral expressions. By this approach there are in principle three steps necessary: First, one has to identify all Feynman graphs relevant for the actual amplitude to be computed. Then, secondly, one has to translate each diagram into an integral which afterwards has to be evaluated. And lastly, one has to combine the results from all Feynman integrals correctly to obtain the desired scattering amplitude. All three steps are difficulty in themselves and many techniques [51] and references in there have been established in the last years or even decades. In my thesis we want to focus on the second step the computation of *Feynman*

integrals. Therefore, we want to first explain how one can construct the Feynman integral from the graph and secondly which techniques can be used to evaluate it.

Scine we want to focus in this thesis on the concepts and the mathematical structures behind Feynman integrals we only concentrate on scalar integrals. Of course, realistic theories as QED or QCD also have non-scalar integrals but there are powerful techniques [52–54] known for example as tensor reduction or Dirac algebra manipulations which reduce a non-scalar integral to a scalar one. By this process one typically exhibits additional factors in the numerator and/or higher powers in the propagators as given by the original non-scalar integral. This is one reason why we generalize later the textbook definition of a Feynman integral.

We emphasize the textbooks [55–58] as standard references for an introduction to quantum field theory and in particular to Feynman graphs and integrals.

2.2 Feynman graphs

So let us start with the definition of a *Feynman graph* G. We define a Feynman graph G to be a connected and oriented graph given by the following data:

- We have a set of *vertices* $V_G = \{v_i\}_{i=1,\dots,v}$ of length $v = |V_G|$.
- Another set $E_G = \{e_i\}_{i=1,\dots,n}$ of length $n = |E_G|$ contains all *internal edges* of the graph G, where each edge is incident to exactly two vertices in V_G. We do not restrict the maximum number of edges which are incident to the same vertex. For every edge e_i we associate a *momentum*[1] $q_i \in \mathbb{R}^D$, where the *dimension* D can be arbitrary first, and a *mass* m_i such that m_i^2 is a positive real number. Additionally, we denote for every edge e_i an integer ν_i.
- The N *external edges* e_i^{ext} are contained in the set $E_G^{\text{ext}} = \{e_i^{\text{ext}}\}_{i=1,\dots,N}$. These are only incident to a single vertex. An external edge e_i^{ext} comes also along with a momentum $p_i \in \mathbb{R}^D$.
- Moreover, we assume *momentum conservation* at each vertex, i.e. $\sum_{e_j \text{ incident to } v_i} q_j + \sum_{e_j^{\text{ext}} \text{ incident to } v_i} p_j = 0$ for all $v_i \in V_G$.
- We assume that all external momenta $p_i \in E_G^{\text{ext}}$ are flowing inwards. Then over all momentum conservation implies that $\sum_{i=1}^{N} p_i = 0$.

Note that if $\nu_i = 0$ for some edge e_i of the graph G then the graph G is equivalent to the graph $\tilde{G}$ which is obtained from G after contraction of the edge e_i.

Due to momentum conservation at all vertices not all internal momenta q_i are independent. The number of independent internal momenta is defined as the *loop number* l sometimes

[1] This can also mean that we take momenta in Minkowski space $\mathbb{R}^{(1,D-1)}$ with signature $(+,-,\dots,-)$.

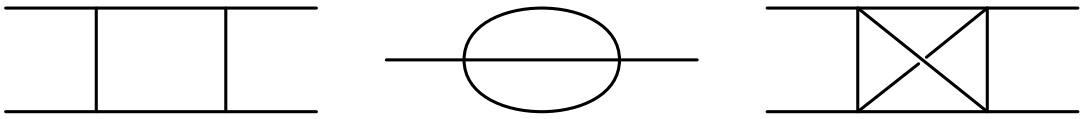

Figure 2.1: Three examples of Feynman graphs having different characteristics as the loop number, number of external particles, vertices, propagators and planarity.

also-called the first Betti number of the graph G which is related to the number of edges and vertices by

$$l = n - v + 1\,. \tag{2.1}$$

Another characteristic of a Feynman graph is if it can be drawn on a plane without crossings of some edges. In this case one talks about *planar* Feynman graphs, otherwise they are called *non-planar* graphs.

To illustrate these definitions we have drawn some Feynman graphs in figure 2.1. Here the first graph is called a one-loop box diagram. This is, of course, a planar graph as well as the two-loop sunset graph shown as the second graph in figure 2.1. The last Feynman graph is a non-planar three-loop box diagram.

2.3 Momentum space representation

Each Feynman graph encodes a precise mathematical prescription of an integral. So given a Feynman graph G we can associate to it a *Feynman integral* by standard Feynman rules in momentum space

$$I^G_{\underline{\nu}}(\underline{s}; D) := \int \left(\prod_{j=1}^{l} \frac{\mathrm{d}^D k_j}{i\pi^{D/2}} \right) \left(\prod_{i=1}^{n} \frac{1}{D_i^{\nu_i}} \right) , \tag{2.2}$$

where the propagators are defined by $D_i = q_i^2 - m_i^2 + i0^+$ with the $i0^+$-prescription[2] meaning that we have assigned a small negative imaginary part to the masses m_i^2. Here label the k_j for $j = 1, \ldots, l$ the independent loop momenta and D denotes again the space-time dimension and is at this point arbitrary. The variable $\underline{s}$ collects all kinematic information which we specify later. We have generalized here the standard textbook definition of a Feynman integral by allowing for arbitrary integer powers $\nu_i \in \mathbb{Z}$ of the propagators.

Notice that the internal momenta q_i are due to momentum conservation linear combinations of the external momenta p_j and the loop momenta k_m. We can write this as

$$\underline{q} = \boldsymbol{\kappa}\underline{k} + \boldsymbol{\rho}\underline{p}\,, \tag{2.3}$$

[2] Later we see that the $i0^+$-prescription tells us how we have to analytically continue the Feynman integral appropriate.

with $\underline{k} = (k_1, \ldots, k_l)$ and $\underline{p} = (p_1, \ldots, p_N)$. The entries of the matrices $\boldsymbol{\kappa}$ and $\boldsymbol{\rho}$ take only values in $\{-1, 0, 1\}$ depending whether the corresponding momentum contributes to the internal momentum q_i.

We consider the Feynman integral (2.2) as a function of the space-time dimension D, of the masses m_i^2 and the external momenta p_j. Due to Lorentz invariance the integral actually depends only on the dot products between the independent external momenta[3], i.e., one can build $\frac{(N-1)N}{2}$ independent dot products of the form $p_{j_1} \cdot p_{j_2}$. We call these parameters, the masses and dot products, the scales of the Feynman integral, which we collect into the vector $\underline{s} = (m_1^2, \ldots, m_n^2, p_1 \cdot p_1, p_1 \cdot p_2, \ldots, p_{N-1} \cdot p_{N-1})$. The space spanned by the scales $\underline{s}$ is called the kinematic space[4] of the Feynman integral and sometimes one even considers the complexified kinematic space by allowing complex values for the scales $\underline{s}$.

Every Feynman integral has a well defined *scaling dimension* given by

$$\dim(I_{\underline{\nu}}^G) = \frac{lD}{2} - \sum_{i=1}^{n} \nu_i \,, \tag{2.4}$$

which states how a Feynman integral changes if the scales $\underline{s}$ are rescaled, i.e. $p_j \to \lambda\, p_j$ and $m_i^2 \to \lambda^2\, m_i^2$. For the examples in figure 2.1 we have as scaling dimensions $D/2 - 4$, $D - 3$ and $3D/2 - 6$ if we assume that all propagator powers ν_i are equal to one.

Due to the scaling behavior (2.4) we can actually reduce the number of parameters a Feynman integral has by one simply by an appropriate rescaling of the parameters. Therefore, the Feynman integral has in total only $N_z = n + \frac{(N-1)N}{2} - 1$ parameters or moduli which we represent by the vector $\underline{z} = (s_1/s_{N_z+1}, \ldots, s_{N_z}/s_{N_z+1})$ where as a possible choice we have rescaled by the last scale s_{N_z+1}. In the following we assume that after such a rescaling the Feynman integral (2.2) is only a function of these variables $\underline{z}$ and the dimension D.

2.3.1 Concept of dimensional regularization

It turns out that most of the Feynman integrals (2.2) are actually divergent, in particular if they are evaluated in $D = 4$ dimensions. To deal with this problem and to give the Feynman integral in $D = 4$ a meaningful result one has to *regularize* the integral. There are many different techniques known, for example the introduction of a cut off parameter or the Pauli-Villars regularization [56]. They have their own advantages and disadvantages as the first ist not gauge invariant and the second not gauge covariant but on the other hand quite simple in their definition and convenient in chiral problems, respectively. Here we want to concentrate on another method namely *dimensional regularization* which has the big advantage that it does not destroy the symmetries of the theory and can be applied generally

[3] Due to overall energy-momentum conservation we have only $N - 1$ independent external momenta from which we can compute independent dot products.

[4] Sometimes we also call it the parameter space or moduli space in a geometric context.

to the Feynman integrals we are considering in this thesis.

The idea of dimensional regularization is that one considers the dimension D to be an arbitrary number, even a complex one. For generic complex values of D the Feynman integral (2.2) is convergent and the result can be analytically continued to $D = 4$ dimensions. Poles developed during the analytic continuation describe the divergencies. In this picture the Feynman integral is considered to be a meromorphic function in the dimension D with poles at most at integer values of D [59, 60]. Commonly, one writes the dimension as $D = D_0 - 2\epsilon$ with D_0 a fixed non-negative integer and computes the Laurent expansion of the Feynman integral in terms of the parameter ϵ

$$I^G_{\underline{\nu}}(\underline{z}; D) \longrightarrow I^G_{\underline{\nu}}(\underline{z}; D_0 - 2\epsilon) = \sum_{k \geq k_0} I^G_{\underline{\nu},k}(\underline{z})\, \epsilon^k \,. \tag{2.5}$$

If $k_0 < 0$ the Feynman integral has a highest pole of order k_0 and is therefore divergent in D_0 dimensions. The choice of D_0 is in principle arbitrary but typically one takes four or two dimensions, since in the latter Feynman integrals more often converge. Later we will see why it is also important or useful to choose an even D_0.

2.3.2 Integration by parts identities

One of the corner stones in Feynman integral computations is the existence und usage of so-called *integration by parts identities* (or short IBP identities). Before we introduce these relations and, in particular, show their significance we have to introduce some vocabulary.

Given a Feynman graph G we define its *topology* $\mathfrak{T}$ as the set of Feynman graphs which share the same propagators D_i for $i = 1, \ldots, n$ but differ in their values of the exponents ν_i. We are mostly interested in topologies of Feynman graphs which have an additional property which describes that they are in some sense large enough or complete. For this notion we first introduce the ring $\mathcal{R}_s$ of scalar products between loop momenta and also external momenta involved in the Feynman graph G. Let again $\underline{k} = (k_1, \ldots, k_l)$ be the loop momenta and $\underline{p} = (p_1, \ldots, p_N)$ be the external momenta were only $N - 1$ of them are linearly independent due to overall energy-momentum conservation. We can put them into the vector $\underline{\mathfrak{q}} = (k_1, \ldots, k_l, p_1, \ldots, p_{N-1})$ of all independent momenta. Then we can form the dot products

$$s_{i,j} = s_{j,i} = \mathfrak{q}_i \cdot \mathfrak{q}_j \quad \text{for } i \leq l \text{ and } i \leq j \leq l + N - 1 \,, \tag{2.6}$$

which are in total $N_{\mathfrak{s}} = \frac{l(l+1)}{2} + l(N-1)$ different ones. Theses dot products do at least involve one loop momentum and we collect them into the vector $\underline{\mathfrak{s}} = (s_{i,j})_{i \leq l, i \leq j \leq l+N-1}$. The ring $\mathcal{R}_s$ is now defined as the polynomial ring generated by these dot products

$$\mathcal{R}_s = \mathbb{C}[s_{i,j},\, i \leq l \text{ and } i \leq j \leq l + N - 1] \,. \tag{2.7}$$

There are certainly more dot products for $l < i \leq l + N - 1$ which are purely consisting of external momenta but these are part of the scales $\underline{s}$ or their rescaled versions $\underline{z}$, see section 2.3, and are not considered here. On the other hand we have the topology $\mathfrak{T}$ which gives us a set of propagators D_i for $i = 1, \ldots, n$ which are linear functions of the dot products

$$D_i = \mathfrak{A}_i \, \underline{\mathfrak{s}} + \mathfrak{b}_i \,, \tag{2.8}$$

where $\mathfrak{b}_i$ are functions of the scales $\underline{s}$. The entries of the matrices $\mathfrak{A}_i$ take only values in $\{0, \pm 1, \pm 2\}$. The propagators generate a subring in the ring $\mathcal{R}_s$

$$\mathcal{I}_{\mathfrak{T}} = \langle D_i \rangle_{i=1,\ldots,n} \subseteq \mathcal{R}_s \,, \tag{2.9}$$

where the scales $\underline{s}$ are considered as parameters in these rings. We now say that the topology $\mathfrak{T}$ is *complete* if $\mathcal{R}_s = \mathcal{I}_{\mathfrak{T}}$, i.e., we can express all dot products in terms of propagators. Remark that obviously $n = N_{\mathfrak{s}}$ for a complete topology. If the topology $\mathfrak{T}$ is not complete we can extend it by the inclusion of additional propagators D_{n+j} such that the whole set $\{D_1, \ldots, D_n, D_{n+1}, \ldots, D_{N_{\mathfrak{s}}}\}$ is linearly independent and therefore generates a complete topology $\tilde{\mathfrak{T}}$. Different completions of the ideal $\mathfrak{T}$ do in general produce different complete topologies $\tilde{\mathfrak{T}}$ but they have a common intersection which is the only relevant part for the graphs build from the topology $\mathfrak{T}$. Therefore, one can complete the topology $\mathfrak{T}$ in different ways but at the end this does not effect the set of IBP relations of $\mathfrak{T}$ as long as the final set of propagators is linearly independet. Also a different labeling of the propagators and the internal loop momenta does not effect this. So we see that we can always extend a topology $\mathfrak{T}$ associated to a graph G to a complete topology $\tilde{\mathfrak{T}}$ such that $\mathfrak{T} \subseteq \tilde{\mathfrak{T}}$.

Every element in the topology $\mathfrak{T}$ defines a point in a lattice $\mathbb{Z}^n$ by its integer exponents ν_i, $i = 1, \ldots, n$. In the topology $\mathfrak{T}$ we want to group elements together which share the same propagators but with possibly different exponents. These groups are called sectors. It turns out that elements in the same sector share similar features as we will see later. To define a sector we consider the Heaviside step function

$$\Theta(x) = \begin{cases} 1, \text{ if } x > 0 \,, \\ 0, \text{ if } x \leq 0 \,, \end{cases} \tag{2.10}$$

which we can let act on the lattice $\mathbb{Z}^n$ and then by extension also on the topology $\mathfrak{T}$ by the map $\vartheta : \mathbb{Z}^n \to \{0, 1\}^n$ defined as

$$\vartheta(\underline{\nu}) = (\Theta(\nu_i))_{1 \leq i \leq n} \tag{2.11}$$

for a vector $\underline{\nu} = (\nu_1, \ldots, \nu_n)$ build from the exponents of the propagators. Then we say that $I_{\underline{\nu}}$ and $I_{\underline{\nu}'}$ belong to the same sector if $\vartheta(\underline{\nu}) = \vartheta(\underline{\nu}')$. A sector can be labeled by a cornerpoint of a

sector which is a vector $\underline{\nu}^c = (\nu_1^c, \ldots, \nu_n^c)$ with $\nu_i^c \in \{0, 1\}$ for all $i = 1, \ldots, n$. Moreover, there is a natural partial order on sectors given by $\vartheta(\underline{\nu}) \leq \vartheta(\underline{\nu}')$ if and only if $\Theta(\nu_i') - \Theta(\nu_i) \geq 0$ for all $1 \leq i \leq n$.

Now there exist relations between the elements of the lattice $\mathbb{Z}^n$ or in other words between different Feynman integrals in the topology $\mathfrak{T}$. These relations are known as IBP identities and can be derived form the fact that in dimensional regularization total derivates of a Feynman integral vanish

$$0 = \int \frac{\mathrm{d}^D k}{i\pi^{D/2}} \frac{\partial}{\partial k^\mu} \left(q^\mu \prod_{i=1}^{n} \frac{1}{D_i^{\nu_i}} \right) , \tag{2.12}$$

where q^μ is a linear combination of the external momenta $\underline{p}$ and the loop momentum k^μ. For simplicity we have here only written down the IBP relation for one-loop but, of course, for the higher loop case the same is true for every loop integration and any total derivative. Equation (2.12) can be proven using the Lorentz invariance of the Feynman integral, see [61–63]. One strength of the IBP relations is that they can be written down easily. Moreover, they give exact relations between Feynman integrals in dimensional regularization.

To see that the IBP identities give relations between different elements in a topology we make the following small calculation. Let us consider the one-loop equal-mass banana integral[5] also-called bubble integral

$$I^{\text{Bub}}_{\nu_1,\nu_2} = \int \frac{\mathrm{d}k}{i\pi^{D/2}} \frac{1}{D_1^{\nu_1}} \frac{1}{D_2^{\nu_2}} = \int \frac{\mathrm{d}k}{i\pi^{D/2}} \frac{1}{(k^2 - m^2)^{\nu_1}} \frac{1}{((p-k)^2 - m^2)^{\nu_2}} . \tag{2.13}$$

The corresponding topology $\mathfrak{T}^{\text{Bub}}$ is complete, since we have two propagators and two dot products k^2 and $k \cdot p$. To see that the IBP identities give relations between different elements in $\mathfrak{T}^{\text{Bub}}$ we consider the sector $(0, \nu_2)$ as an example. We use eq. (2.12) with $q^\mu = p^\mu$ and find

$$p^\mu \frac{\partial}{\partial k^\mu} \frac{1}{D_2^{\nu_2}} = 2\nu_2 \frac{p^2 - k \cdot p}{D_2^{\nu_2+1}} = 2\nu_2 \frac{\frac{1}{2}p^2 + \frac{1}{2}((p-k)^2 - m^2) - \frac{1}{2}(k^2 - m^2)}{D_2^{\nu_2+1}} = \nu_2 \frac{p^2 + D_2 - D_1}{D_2^{\nu_2+1}} , \tag{2.14}$$

such that we obtain after integrating (2.14) the following relation between different members of the topology $\mathfrak{T}^{\text{Bub}}$

$$I^{\text{Bub}}_{0,\nu_2} = I^{\text{Bub}}_{-1,\nu_2+1} - p^2 I^{\text{Bub}}_{0,\nu_2+1} . \tag{2.15}$$

The crucial step in this computation is the second identity in eq. (2.14) where we could replace the two dot products p^2 and $k \cdot p$ through the propagators D_1 and D_2 which is in

[5] The corresponding Feynman graph looks like the middle diagram in figure 2.1 where the middle propagator is absent.

general only possible in a complete topology. Furthermore, we see that also propagators in the numerator can show up. Although we have not done this small computation for the generic element (ν_1, ν_2) in $\mathfrak{T}^{\text{Bub}}$ we can still see that in (2.15) different elements in $\mathfrak{T}^{\text{Bub}}$ are related. Another IBP relation for the bubble integral can be found if one uses $q^\mu = k^\mu$ in eq. (2.12). Then both IBP relations generate all relations on the topology $\mathfrak{T}^{\text{Bub}}$.

So we see from the last calculation the importance to have a topology $\mathfrak{T}$ which is complete to guarantee that the IBP identities give back only elements again living in $\mathfrak{T}$. In general, we see that the IBP identities yield *recursive relations* on the lattice $\mathbb{Z}^n$.

It turns out that using all IBP identities, i.e., by solving the recursive relations, one can reduce the infinite number of elements in the topology $\mathfrak{T}$ to a *finite set of elements* [64–66]. These elements form a basis of Feynman integrals corresponding to the topology $\mathfrak{T}$ and are named *master integrals*. A priori, there does not exist a preferred choice of a set of master integrals. Notice that through the master integrals a generic element in the topology $\mathfrak{T}$ can be written as a linear combination of the former where the coefficients are still polynomials or rational functions in the scales $\underline{s}$ or their rescaled ones $\underline{z}$ and the dimension D.

The strategy is in principle the following: Given a Feynman graph G one first has to check whether its topology $\mathfrak{T}$ is complete or not. If not one has to extend with appropriate additional propagators. Then one analysis the IBP identities and can solve the resulting recursive relations. From this one can pick out a set of master integrals such that a generic element in the topology $\mathfrak{T}$ is related to the master integrals and can be computed from them. The master integrals themselves can directly not be computed only from the IBP relations. For example, one can compute them from differential equations where we give in the next chapters different techniques how these can be obtained and solved. If the master integrals together with the appropriate recursive relations are known and under control every element in the topology $\mathfrak{T}$ can be evaluated. This would be the ideal approach to compute a given Feynman integral or even better its whole topology. But unfortunately, there is not a general method known which does all these steps at least in a reasonable amount of time.

2.3.3 Master integrals for the banana graphs

In this thesis we will mostly consider the so-called *banana Feynman graphs*. This is a family of l-loop Feynman graphs shown in figure 2.2. In the middle of figure 2.1 we have already

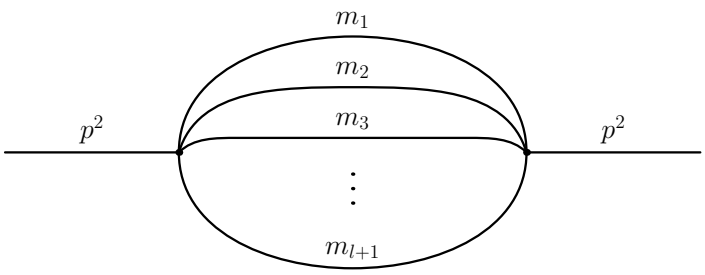

Figure 2.2: The l-loop banana graph with external momentum p and internal masses m_i.

seen the two-loop banana graph which is also known as the sunset graph. The one-loop banana graph is the bubble graph we considered in the previous subsection. We consider the banana integrals in dimensional regularization in $D = 2 - 2\epsilon$ dimensions. They have at l-loop $l+1$ propagators which are given by

$$\begin{aligned} D_j &= k_j^2 - m_j^2\,, \qquad 1 \leq j \leq l\,, \\ D_{l+1} &= (k_1 + \ldots + k_l - p)^2 - m_{l+1}^2\,. \end{aligned} \tag{2.16}$$

As we have explained in the last sections these Feynman integrals depend on the scales $\underline{s} = (p^2, m_1^2, \ldots, m_{l+1}^2)$ or after a suitable rescaling (see eq. (2.4)) on the ratios of scales $\underline{z} = (m_1^2/p^2, \ldots, m_{l+1}^2/p^2)$. In total there are $2^{l+1} - 1$ master integrals which are distributed among $l+2$ sectors. These sectors are divided in $l+1$ sectors of the form $\vartheta(\underline{\nu}) = (1, \ldots, 1, 0, 1, \ldots, 1)$ which give rise to a l-loop tadpole integral. For $1 \leq i \leq l+1$ we define:

$$J_{l,i}(\underline{z};\epsilon) = \frac{(-1)^{l+1}}{\Gamma(1+l\epsilon)} (p^2)^{l\epsilon} \epsilon^l \; I^{\text{Ban}}_{1,\ldots,1,0,1,\ldots,1}(\underline{x}; 2-2\epsilon) = -\frac{\Gamma(1+\epsilon)^l}{\Gamma(1+l\epsilon)} \prod_{\substack{j=1 \\ j\neq i}}^{l+1} z_j^{-\epsilon}\,. \tag{2.17}$$

The sector $(1, \ldots, 1)$ adds $2^{l+1} - l - 2$ master integrals, one for each $\underline{k} \in \{0,1\}^{l+1}$ with $1 \leq |\underline{k}| \leq l-1$ and $|\underline{k}| = \sum_{j=1}^{l+1} k_j$:

$$\begin{aligned} J_{l,\underline{0}}(\underline{z};\epsilon) &= \frac{(-1)^{l+1}}{\Gamma(1+l\epsilon)} (p^2)^{1+l\epsilon} \; I^{\text{Ban}}_{1,\ldots,1}(\underline{x}; 2-2\epsilon) \\ J_{l,\underline{k}}(\underline{z};\epsilon) &= (1+2\epsilon)\cdots(1+|\underline{k}|\epsilon)\; \partial_{\underline{z}}^{\underline{k}} J_{l,\underline{0}}(\underline{z};\epsilon)\,, \end{aligned} \tag{2.18}$$

with $\partial_{\underline{z}}^{\underline{k}} =: \prod_{i=1}^{l+1} \partial_{z_i}^{k_i}$. We have explicitly checked for the first few loop orders that these integrals form a basis of master integrals. Moreover, it matches with the results of ref. [67]. Note that the number M of master integrals may change discontinuously in the limit where some scales vanish or become equal. In the equal-mass case, i.e., $m_i^2 =: m^2$ for $1 \leq i \leq l+1$, the symmetry implies that there are only $l+1$ master integrals, which can be chosen as:

$$\begin{aligned} J_{l,0}(z;\epsilon) &= \frac{(-1)^{l+1}}{\Gamma(1+l\epsilon)} (m^2)^{l\epsilon} \epsilon^l \; I^{\text{Ban}}_{1,\ldots,1,0}(p^2, m^2; 2-2\epsilon) = -\frac{\Gamma(1+\epsilon)^l}{\Gamma(1+l\epsilon)}\,, \\ J_{l,1}(z;\epsilon) &= \frac{(-1)^{l+1}}{\Gamma(1+l\epsilon)} (m^2)^{1+l\epsilon} \; I^{\text{Ban}}_{1,\ldots,1}(p^2, m^2; 2-2\epsilon)\,, \\ J_{l,k}(z;\epsilon) &= (1+2\epsilon)\cdots(1+k\epsilon)\; \partial_z^{k-1} J_{l,1}(z;\epsilon)\,, \qquad \text{for } 2 \leq k \leq l\,, \end{aligned} \tag{2.19}$$

where we defined $z := \frac{m^2}{p^2}$.

We note that the number of master integrals changes also discontinuously when ϵ takes special values. In particular, in the generic-mass case, for $\epsilon = 0$ we have only $2^{l+1} - \binom{l+2}{\lfloor \frac{l+2}{2} \rfloor}$

independent master integrals instead of $2^{l+1}-(l+1)-1$ in the sector $(1,\dots,1)$. We note that this corresponds to the even primitive vertical cohomology $H^{k,k}_{\text{vert}}(W^{\text{CI}}_{l-1})$ for $k=0,\dots,l-1$ of W^{CI}_{l-1} given in eq. (7.5), or the horizontal middle cohomology $H^{l-1}_{\text{hor}}(M^{\text{CI}}_{l-1})$ of its mirror M^{CI}_{l-1} (see section 4 for an introduction to Calabi-Yau periods and their corresponding mathematics). Similar to eq. (2.18), in the latter picture the derivatives with respect to the z_i for $i=1,\dots,l+1$ generate the cohomology groups in $H^{l-1-k,k}_{\text{hor}}(M^{\text{CI}}_{l-1})$, $k=0,\dots,l-1$, see also eq. (4.15). However, keeping in mind the linear dependencies of these derivatives in the cohomology of M^{CI}_{l-1}, one finds that there are less independent elements and one finds as many elements as given in eq. (7.15).

2.4 Symanzik representation and graph polynomials

Let us now introduce another representation of a Feynman graph, namely the so-called *Symanzik* oder *graph polynomial representation*. A good review and introduction to this concept are [55, 68]. The starting point is the introduction of Feynman parameters x_i for every propagator which can be done in the most generic situation with the following relation

$$\prod_{i=1}^{n}\frac{1}{D_i^{\nu_i}}=\frac{\Gamma(\nu)}{\prod_{i=1}^{n}\Gamma(\nu_i)}\int_0^\infty \mathrm{d}^n x\left(\prod_{i=1}^{n}x_i^{\nu_i-1}\right)\delta\left(1-\sum_{i=1}^{n}x_i\right)\frac{1}{\left(\sum_{i=1}^{n}x_iD_i\right)^{\nu_i}}\,. \tag{2.20}$$

Now we can first perform the integration over the l D-dimensional loop momenta k_i. This is a tedious task and the details of this computation can be found for example in [55, 60]. The idea behind this computation is that one uses the translational invariance of the loop integrations to shift the loop momenta k_i such that they complete the square in the denominator of (2.20). Then the resulting integrals can be performed. The final expression can be written down in a compact form if we introduce some notation. The Feynman parameters and the loop momenta are related by

$$-\sum_{i=1}^{n}x_iD_i=-\underline{k}^T\mathbf{M}\underline{k}+2\underline{Q}\underline{k}+J\,, \tag{2.21}$$

where the $l\times l$ matrix $\mathbf{M}$ has as entries polynomials in the Feynman parameters x_i and the vector $\underline{Q}$ is a polynomial in x_i and the external momenta p_i. From these terms we can build the so-called *graph* or *first and second Symanzik polynomials*

$$\mathcal{U}=\det(\mathbf{M})\qquad\text{and}\qquad\mathcal{F}=\det(\mathbf{M})(J+\underline{Q}^T\mathbf{M}^{-1}\underline{Q})\,. \tag{2.22}$$

With $\mathcal{U}$ and $\mathcal{F}$ we can finally write the Symanzik integral representation of the Feynman

graph

$$I^G_{\underline{\nu}}(\underline{s};D) = (-1)^n \frac{\Gamma(\nu - lD/2)}{\prod_{i=1}^n \Gamma(\nu_i)} \int_0^\infty \mathrm{d}^n x \left(\prod_{i=1}^n x_i^{\nu_i - 1}\right) \delta\left(1 - \sum_{i=1}^n x_i\right) \frac{\mathcal{U}^{\nu-(l+1)D/2}}{\mathcal{F}^{\nu - lD/2}} \tag{2.23}$$

with $\nu = \sum_{i=1}^{l+1} \nu_i$.

Before we continue let us make some important remarks about the graph polynomials in eq. (2.22). Some of the facts about the graph polynomials will become more clear from a different definition we make in the next subsection as from the definition in eq. (2.22). First of all, the graph polynomials $\mathcal{U}$ and $\mathcal{F}$ are both homogeneous polynomials in the Feynman parameters x_i. More precisely, $\mathcal{U}$ is of homogeneous degree l and depends only linearly on each x_i whereas $\mathcal{F}$ is of degree $l+1$ and only linear in x_i if all internal masses are set to zero. Secondly, it is remarkable that the $\mathcal{U}$ polynomial has neither a dependence on the internal masses nor the external momenta. Each monomial entering in $\mathcal{U}$ has actually $+1$ as coefficient. All the kinematic dependence is packaged in the $\mathcal{F}$ polynomial. In other words, if for a given Feynman integral the dependence of the $\mathcal{F}$ polynomial drops out in eq. (2.23) then the Feynman integral has no non-trivial dependence on the kinematics. Moreover, it is interesting that the dimension D where the Feynman integral is evaluated does only enter via the exponents of the graph polynomials and the gamma factors but not in the definition of $\mathcal{U}$ and $\mathcal{F}$.

The $\mathcal{F}$ polynomial has in general positive and negative coefficients in front of each monomial which are in general actually polynomials in the kinematics. A region in the kinematic space where all dot products of external particles are negative or zero and the internal masses are chosen positive or zero is called euclidean region. From eq. (2.23) it is pretty obvious that the Feynman integral $I^G_{\underline{\nu}}$ is real along such a region in the kinematic space. Outside of this region the $+i0^+$ prescription is important to guarantee the convergence of the Feynman integral. Notice that the euclidean region is generically not the same as the physical region where dot products of external momenta are typically positive. Furthermore, for non-planar diagrams with non-vanishing dot products and masses sometimes there does even not exist a euclidean region and the integral is then generically complex.

Before we give an example let us make another comment about the Symanzik integral representation. Observe that the integral (2.23) is invariant under rescaling of the coordinates, i.e. $(x_1, \ldots, x_n) \mapsto (\lambda x_1, \ldots, \lambda x_n)$. Therefore, we can also write it down as an integral in projective space

$$I^G_{\underline{\nu}}(\underline{x};D) = (-1)^n \frac{\Gamma(\nu - lD/2)}{\prod_{i=1}^n \Gamma(\nu_i)} \int_{\sigma_{n-1}} \left(\prod_{i=1}^n x_i^{\nu_i - 1}\right) \frac{\mathcal{U}^{\nu-(l+1)D/2}}{\mathcal{F}^{\nu - lD/2}} \, \mu_{n-1}\,, \tag{2.24}$$

with the holomorphic $(n-1)$-dimensional measure μ_{n-1} of projective space $\mathbb{P}^{n-1}$ defined

by

$$\mu_{n-1} = \sum_{k=1}^{n} (-1)^{k+1} x_k \, \mathrm{d}x_1 \wedge \ldots \wedge \widehat{\mathrm{d}x_k} \wedge \ldots \wedge \mathrm{d}x_n \tag{2.25}$$

and the $(n-1)$-real-dimensional integration domain σ_{n-1} given by

$$\sigma_{n-1} = \{[x_1 : \ldots : x_n] \in \mathbb{P}^{n-1} | x_i \in \mathbb{R}_{\geq 0} \text{ for all } 1 \leq i \leq n\} \,. \tag{2.26}$$

As usual, the hat indicates the omission of a differential. This representation (2.24) was the starting point for us in the works [44, 45, 47] to relate Feynman integrals to geometric or so-called period integrals as we will also show in this thesis later.

Before we make some examples we turn to the next subsection where we show another method to compute the graph polynomials $\mathcal{U}$ and $\mathcal{F}$.

2.4.1 Some graph theory

In the previous section we have seen that the graph polynomials $\mathcal{U}$ and $\mathcal{F}$ can be computed from (2.22) together with the relation in (2.21). Here we want to present another possibility namely to use techniques from graph theory to compute them. We follow quite closely the excellent work of [68] on this topic.

So let G be as in the previous sections a graph with n edges, v vertices and N external lines. They are related to the loop number l through eq. (2.1). We define a *spanning tree* T of the graph G to be a sub-graph of G such that:

- T contains all vertices of G,
- the loop number of T is zero,
- T is connected.

This means that we can construct T out of G if we delete l edges. A graph G has in general many different spanning trees.

By neglecting the last property in the definition of a spanning tree we get the definition of a *spanning forest*, i.e., a spanning forest F of G is a sub-graph of the later such that

- F contains all vertices of G,
- the loop number of F is zero.

We see that F can have many components. If it has k connected components then it is called a spanning k-forest. Obviously, a spanning tree is a spanning one-forest. F is constructed from G if we delete $l + k - 1$ edges.

Some further notations are necessary. By $\mathcal{T}$ we denote the set of spanning trees of a given graph G and by $\mathcal{T}_k$ the set of spanning k-forests of G. So obviously, we have $\mathcal{T} = \mathcal{T}_1$. An

element in $\mathcal{T}_k$ is given by a collection of connected components $(T_1, \dots, T_k)$. Moreover, we can associate to a component T_i the set of external momenta attached to it, which we denote by P_{T_i}.

With all these definitions we can now give the graph theoretic definition of the Symanzik polynomials

$$\begin{aligned} \mathcal{U} &= \sum_{T \in \mathcal{T}} \prod_{e_i \notin T} x_i \,, \\ \mathcal{F} &= \mathcal{F}_0 + \mathcal{U} \sum_{i=1}^{n} m_i^2 x_i \,, \\ \mathcal{F}_0 &= \sum_{(T_1,T_2)\in\mathcal{T}_2} (-s(T_1,T_2)) \left(\prod_{e_i \notin (T_1,T_2)} x_i \right) \end{aligned} \tag{2.27}$$

with the short hand notation for squares of external momenta

$$s(T_1, T_2) = -\left(\sum_{p_i \in P_{T_1}} p_i \right) \cdot \left(\sum_{p_j \in P_{T_2}} p_j \right) . \tag{2.28}$$

We see that the sums in the definitions of $\mathcal{U}$ and $\mathcal{F}$ run over spanning trees and two-forests, respectively. Therefore, we can easily see that the $\mathcal{U}$ polynomial is of homogeneous degree l since we have to delete l edges to obtain a spanning forest. Similarly, the degree of $\mathcal{F}$ is $l+1$ since we have to delete $l+1$ edges. Since we can delete an edge only ones it is also clear that $\mathcal{U}$ and $\mathcal{F}_0$ are linear in each Feynman parameter x_i. Moreover, we easily see that $\mathcal{U}$ has only positive monomials and $\mathcal{F}$ can have monomials with positiv and negative sign. This agrees or even justifies the remarks made after eq. (2.23).

So now let us make an example to explain and visualize our definitions. We consider again the l-loop banana family already introduced in subsection 2.3.3. These graphs are shown in figure 2.2 and 2.3. We want to use the above introduced graph theory to compute the two

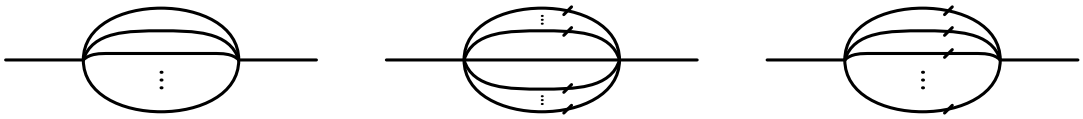

Figure 2.3: The left Feynman diagram is the l-loop banana graph. In the middle a generic spanning tree for the l-loop banana graph is shown. On the right there is the unique spanning two-forest for the banana graph drawn. The crossed edges are the deleted edges.

graph polynomials for the l-loop banana graph. To compute the $\mathcal{U}$ polynomial we have to find all possible spanning forests, i.e., we have to delete l edges such that after deletion all vertices of the original banana graph are connected without a loop. This is combinatorially quite simple because we have to delete all edges up to one. There are $l+1$ possibilities to do that. A generic spanning forest is shown in the middle of figure 2.3 and the $\mathcal{U}_l^{\text{Ban}}$ polynomial

is the sum of the product of the deleted edge variables, i.e.

$$\mathcal{U}_l^{\text{Ban}} = \sum_{i=1}^{l+1} x_1 \cdots x_{i-1}\, \hat{x}_i\, x_{i+1} \cdots x_{l+1} = \left(\sum_{i=1}^{l+1} \frac{1}{x_i}\right) \prod_{i=1}^{l+1} x_i\,, \tag{2.29}$$

where the $\hat{}$ means omission of the corresponding variable. For the $\mathcal{F}_l^{\text{Ban}}$ polynomial we have to find all spanning two-forests which is again not too hard because there is only one possibility namely to cut all edges. This is shown on the right graph in figure 2.3. Moreover, we call the external momenta of the banana graphs p and $-p$, respectively. So we find

$$\mathcal{F}_l^{\text{Ban}} = -p^2 \prod_{i=1}^{l+1} x_i + \mathcal{U}_l^{\text{Ban}} \sum_{i=1}^{l+1} m_i^2 x_i = \left(-p^2 + \left(\sum_{i=1}^{l+1} \frac{1}{x_i}\right)\left(\sum_{i=1}^{l+1} m_i^2 x_i\right)\right) \prod_{i=1}^{l+1} x_i\,. \tag{2.30}$$

As a small check we see that the degrees of the monomials and their signs in (2.29) and (2.30) match with the expectations. So finally, we can write down the Symanzik representation (2.24) of the l-loop banana integral

$$I_{\underline{\nu}}^{\text{Ban}}(p^2, \underline{m}^2; D) = (-1)^{l+1} \frac{\Gamma(\nu - lD/2)}{\prod_{i=1}^{l+1} \Gamma(\nu_i)} \int_{\sigma_l} \left(\prod_{i=1}^{l+1} x_i^{1+\nu_i}\right) \frac{\mathcal{U}^{\nu-(l+1)\frac{D}{2}}}{\mathcal{F}^{\nu - l\frac{D}{2}}}\, \mu_l\,, \tag{2.31}$$

where we dropped the sub– and superscripts of the graph polynomials for clarity. Later in the thesis we will see that this representation of the banana graph is the starting point to relate it to a geometry.

2.5 Schwinger representation

Another parametric integral representation of a Feynman graph G is given by the so-called *Schwinger representation* which again uses the graph polynomials $\mathcal{U}$ and $\mathcal{F}$ from (2.22) or (2.27). One can derive this representation by first noticing the so-called Schwinger trick

$$D_i^{\nu_i} = \frac{1}{(q_i^2 - m_i^2 + i0^+)^{\nu_i}} = \frac{1}{\Gamma(\nu_i)} \int_0^\infty \mathrm{d}x_i\, x_i^{\nu_i - 1} \mathrm{e}^{-x_i(q_i^2 - m_i^2 + i0^+)}\,, \tag{2.32}$$

which expresses a propagator D_i as an integral over the Schwinger parameter x_i. Plugging this relation into the general momentum space representation (2.2) and performing, similarly as for the Symanzik representation, first the Gaussian integrals over the loop momenta k_i one obtains the Schwinger representation

$$I_{\underline{\nu}}^{G}(\underline{s}; D) = (-1)^{\nu} \mathrm{e}^{-i\frac{\pi}{2}(\nu - l\frac{D}{2})} \int_0^\infty \mathrm{d}^n x \prod_{i=1}^{n} \frac{x_i^{\nu_i - 1}}{\Gamma(\nu_i)}\, \mathcal{U}^{-D/2} e^{i\mathcal{F}/\mathcal{U}} \tag{2.33}$$

with the same graph polynomials $\mathcal{U}, \mathcal{F}$ as in the Symanzik representation.

For the banana integral (2.31) one can check, for example with numerical integration, that both integral representation agree.

2.5.1 Dimensional shift relations

From the Schwinger representation we can deduce a very interesting and important property of Feynman integrals, namely that one can relate the result of a Feynman integral in D dimensions to $D \pm 2$ dimensions, in particular in dimensional regularization. This is known under the name *dimensional shift relations* [69]. To see this we first notice the following relation

$$\mathcal{U}(\partial_{m_i^2})\, e^{i\sum_{i=1}^{n} m_i^2 x_i} = i^l\, \mathcal{U}(x_i)\, e^{i\sum_{i=1}^{n} m_i^2 x_i}\,, \tag{2.34}$$

where by $U(\partial_{m_i^2})$ we mean that we take the $\mathcal{U}$ polynomial and replace the Schwinger parameter x_i by derivatives with respect to m_i^2. With this relation it is easy to see that the following is true

$$\mathcal{U}(\partial_{m_i^2})\, I^G_{\underline{\nu}}(\underline{s}; D) = (-1)^l I^G_{\underline{\nu}}(\underline{s}; D-2)\,. \tag{2.35}$$

We can interpret relation (2.35) as follows: Assume that we know the master integral $I^G_{\underline{\nu}}(\underline{s}; D)$ and the rest of the master integrals in D dimensions but we want to compute $I^G_{\underline{\nu}}$ in $D-2$ dimensions. First, we can perform the derivatives $\mathcal{U}(\partial_{m_i^2})$ which in general will not give back master integrals. But in a second step we can use the master integrals of the graph G in D dimensions to express the result after differentiation purely in terms of master integrals which were assumed to be known in D dimensions. Thus, we obtained a relation between the master integrals in D dimensions and the desired integral $I^G_{\underline{\nu}}$ in $D-2$ dimensions.

To be honest, this relation is first of all only valid in the generic mass case. But in the case of equal or even vanishing masses one can first perform the derivate operation and later one sets the masses equal or to zero. The reduction to the master integrals is in this limit often simpler compared to the generic mass case.

Furthermore, notice that a similar relation as in eq. (2.35) exists and relates by the same reasoning the result in $D-2$ dimensions, which is now assumed to be known, to the D-dimensional one. So generically, one can relate the master integrals in D dimensions to the ones in $D-2$ dimensions. This means that one can in some sense start the computation of a given Feynman graph in a preferred dimension if it is an even integer away from the desired dimension. Often this allows one to start in a dimension where the Feynman integral is actually convergent and the divergency in the preferred dimension results only through the dimensional shift relation (2.35). As a caveat one has to do this in dimensional regularization

since it can happen that the number of master integrals in exactly $D = 2$ and $D = 4$ can be different so one can not relate them completely. We will see later that this is the case for the l-loop banana integral where in $D = 2$ dimensions one has muss less master integrals compared to $D = 4$, see the remark at the end of subsection 2.3.3. But in dimensional regularization the number of master integrals is the same and one can use the dimensional shift relations for all master integrals.

We have so far seen two different types of linear relations between Feynman integrals. First, we have seen IBP relations and now as a second type of linear relations the dimensional shift relations. Actually, it is conjectured that these are the only linear relations between Feynman integrals. For fixed dimension D the IBP relations alone even generate all linear relations between Feynman integrals. To the author there is now proof of this conjecture known but as it is with other important statements in the Feynman graph business it is strongly believed that this is true and no counterexamples are known. Hence, other relations coming for instance from Lorentz invariance are only linear combinations of the IBP and dimensional shift relations.

2.6 Baikov representation

As a last representation we want to introduce the so-called *Baikov representation*. In the Symanzik representation we had a quite simple form of the integration contour namely a $(n-1)$-dimensional simplex σ_{n-1}. In contrast, the integrand was quite complicated involving a fraction of the graph polynomials $\mathcal{U}$ and $\mathcal{F}$ raised to some power depending on the dimension D. In the Baikov representation we somehow change the perspective and give the integrand a relatively simple form whereas the integration contour is quite involved. This is done by changing the integration over the loop momenta to an integration over the independent dot products of loop momenta which we collected in the vector $\underline{\mathfrak{s}}$. As a very good reference and foundation of our discussion about the Baikov representation we refer to [63, 70], the lecture notes [71] and to the older works [72, 73].

So let us be more concrete. Again we have a graph G with propagators D_i for $i = 1, \dots, n$ which gives rise to the complete topology $\mathfrak{T}$. The independent dot products of loop momenta are collected in $\underline{\mathfrak{s}}$ as explained around eq. (2.6). Here it is once again important that we really have a complete topology, i.e., we have the same number of propagators as independent dot products $n = N_{\mathfrak{s}}$. If not one has to extend the set of propagators as described after eq. (2.9). The dot products $\underline{\mathfrak{s}}$ shall now be used as the integration variables in the Baikov representation[6]. To be more precise, at the end we do not directly want the $s_{i,j}$ as integration variables but instead the propagators D_i. Remember that the D_i are linear functions of the dot products as can be seen from eq. (2.8). Therefore, we we have to solve equation (2.8) for the $s_{i,j}$. This will only work if we have a complete topology $\mathfrak{T}$, as we have assumed, i.e. $n = N_{\mathfrak{s}}$. In this case we can invert equation (2.8) and use the propagators D_i for $i = 1, \dots, n$

[6] Do not interchange them with the scales $\underline{s}$ which are also build from dot products but purely from external momenta. They are the parameters of the final integrals not their integration variables.

as integration variables which we then call again x_i similarly as the integration variables in the other Feynman integral representations.

The actual change of variables from $k_1, \ldots, k_l$ to the $\underline{s}$ parameters is as for the other representations quite complicated and a lot of book keeping is needed. For details of this computation we refer to [63]. The idea of the computation is that one splits the i^{th} loop integration over k_i into a parallel and transverse part corresponding to the subspace spanned by the momenta $k_{i+1}, \ldots, k_l, p_1, \ldots, p_{N-1}$. Then parts of this integral can explicitly be performed. Finally, if the involved changes of variables are correctly performed one arrives at

$$I^G_{\underline{\nu}}(\underline{s}; D) = C \int \frac{\mathrm{d}x_1 \ldots \mathrm{d}x_n}{x_1^{\nu_1} \ldots x_n^{\nu_n}} P(x_1, \ldots, x_n)^{\frac{D-l-N}{2}} , \tag{2.36}$$

where the normalization C is given by

$$C = \frac{\pi^{-l(l-1)/4 - l\frac{N-1}{2}}}{\prod_{k=1}^{l} \Gamma\left(\frac{d-l-N+k+1}{2}\right)} G(p_1, \ldots, p_{N-1})^{(N-D)/2} J \tag{2.37}$$

with J being the Jacobian going from the $s_{i,j}$ variables to the propagators D_i and the Baikov polynomial P is defined by

$$P(x_1, \ldots, x_n) = G(k_1, \ldots, k_l, p_1, \ldots, p_{N-1})|_{s_{i,j}=s_{j,i}=s_{i,j}(x_k)} , \tag{2.38}$$

meaning that we have expressed the dot products through the propagators x_k by inverting eq. (2.8). In these definitions we used the Gram determinant G which is given for m momenta $q_1, \ldots, q_m$ by

$$G(q_1, \ldots, q_m) = \det(q_i \cdot q_j) . \tag{2.39}$$

So far we have not specified the integration region in the Baikov representation (2.36) of a Feynman graph. This is in general very complicated and different ways of defining the integration range are known in the literature, see [63, 72, 73]. One way is that the boundary of the integration region in (2.36) is given by the vanishing locus of the Baikov polynomial. This locus is for most cases not analytically computable and obey a too complicated structure which is why the Baikov representation is not used for actual computations of the whole Feynman integral. But this is not really a big problem since many other properties of the Feynman integral, as we see in the following, can be derived from the Baikov representation without knowledge of the exact integration region.

Before we state these properties we make a short remark. The changes of variables involved in the derivation of the Baikov representation for multi-loop and multi-external particle graphs are getting fast very difficult. Fortunately, there is a good `mathematica`

code available with the paper [70] in which one has only to give a complete set of propagators to receive the Baikov representation. In the example of the two-loop banana graph below we used this program to obtain the Baikov representation without going through the tedious changes of variables.

In the Baikov representation it is as in the standard momentum space representation or in the Schwinger representation possible to derive the integration by parts relations and the dimensional shift relations, respectively. For the first, one observes that the generators of the IBP relations can be found from requiring that they annihilate the Baikov polynomial. For the later, one notices that the Baikov representation in $D+2$ can be related to the D-dimensional one since $P^{\frac{(D+2)-l-N}{2}} = P^{\frac{D-l-N}{2}} P$ and the second P factor then changes the exponents ν_i of the x_i integration variables. These can then be related to the master integrals in D dimensions such that the $(D+2)$-dimensional integral is expressed purely through D-dimensional master integrals. Since we have discussed theses properties of Feynman integrals already in the previous sections we do not focus here again on them but refer to [70, 71] for more details. However, there is an additional feature we have not discussed so far. This is the so-called maximal cut of a Feynman graph which can be defined and computed quite generically in the Baikov representation. Since this is a very important and often not clearly defined concept in the Feynman graph literature we dedicate to it the subsequent section.

So let us make an example. We consider again the banana graphs and focus on the equal-mass two-loop sunset graph for simplicity (figure 2.1 middle graph). We can use the `mathematica` code from [70] to generate the Baikov representation. Since the sunset topology is not complete we have to extend it with two additional propagators. We made the following choice of propagators

$$\begin{aligned} &D_1 = k_1^2 - m^2 \qquad &&D_2 = k_2^2 - m^2 \qquad &&D_3 = (p - k_1 - k_2)^2 - m^2 \\ &D_4 = (p - k_1)^2 \qquad &&D_5 = (p - k_2)^2 \end{aligned} \tag{2.40}$$

such that we find for the Baikov polynomial

$$\begin{aligned} P_2^{\text{Ban}}(x_1, \ldots, x_5) = {} & (m-p)p^2(m+p)(3m^2+p^2) - p^2x_1^2 + 2m^2p^2x_2 - 2p^4x_2 - p^2x_2^2 \\ & + 2m^2p^2x_3 + 2p^4x_3 + 2p^2x_2x_3 - p^2x_3^2 + 4m^2p^2x_4 + 4p^4x_4 + 4p^2x_2x_4 - 4p^2x_3x_4 - 4m^2x_4^2 \\ & - 4p^2x_4^2 - 4x_2x_4^2 + 4(m^2+p^2+x_2-x_3-2x_4)(p^2-x_4)x_5 - 4(m^2+p^2-2x_4)x_5^2 \\ & + 2x_1\left((m-p)p^2(m+p) + p^2x_2 + p^2x_3 + 2\left(p^2 - x_5\right)(x_4+x_5)\right) . \end{aligned} \tag{2.41}$$

The Baikov polynomial P^{Ban} is of multi-degree three and in principle we could find closed analytic expressions for its root and therefore also for the exact integration range. But this would involve very complicated root expressions which are hard to handle and other Feynman integral representations would be superior. As said this is a common problem with the Baikov representation but we will see in the next section that we can still deduce an

important quantity, the maximal cut, from the Baikov representation of the banana integral.

2.7 Maximal cuts of Feynman integrals

The concept of *maximal cut integrals* goes back till the analytic S-matrix theory. Cut integrals were originally defined by replacing a certain subset of the propagators $q_i^2 - m_i^2$ for $i = 1, \ldots, n_c \leq n$ of a given Feynman integral by delta distributions $\delta(q_i^2 - m_i^2)$ or in more physical words these propagators were set on-shell. Maximal then means that we do this replacement for every propagator appearing in a given Feynman graph. This should first of all simplify the computation of the integral but still give parts of the information about the full Feynman integral, for example, of the kind of singularities and functions involved. In particular, maximal cut integrals satisfy the homogeneous differential equation of the full Feynman integral. The argument for this is the following: First of all, the delta distributions should be considered as computing residues around the propagators $q_i^2 - m_i^2 = 0$ which is slightly more general than the strict delta function prescription. So if we let the homogeneous differential equation of the full Feynman integral let act on the differential form of the maximal cut we first get also inhomogeneous contributions. These inhomogeneous terms correspond to subtolopogies which have less propagators. If we know perform all residues for the maximal cut each subtopology has at least a single residue which gets zero simply because the corresponding propagator does not show up in the subtopology. Therefore, all subtopologies vanish and the maximal cut satisfies the homogeneous differential equation of the full integral. We refer to the references [74–77] for more details and also to a modern view.

As already mentioned the strict definition via delta distributions is too restrictive or not adequate for the desired purposes. As the basic property of a maximal cut one really wants that it satisfies the homogeneous differential equation associated to the full integral. For example, for the box diagram the delta functions do not have a support in the reals and therefore the maximal cut would simply be vanishing. So to generalize the notion of a maximal cut one attempt is that a maximal cut is defined in the momentum representation as a cycle which encircles all the singularities of the propagators $D_i = q_i^2 - m_i^2 = 0$ for $i = 1, \ldots, n$. There can in general be different such cycles but they have to be chosen such that total derivatives rising up during the integration by parts process still vanish on the maximal cut cycles. These total derivatives would correspond to subtopologies of the Feynman graph. These subtopologies life in a subsector of the Feynman graph since they have less propagators than the original one. Therefore, they would only enter the differential equation of the full Feynman graph as inhomogeneities which should vanish per definition for the maximal cuts. Thus, one has to guarantee that the cycles chosen for the maximal cut are such that if one integrates the subtopologies over them they vanish. For some examples [74] it was possible to construct these cycles with the correct properties explicitly and compute their corresponding maximal cuts. Unfortunately, for an arbitrary Feynman integral there is yet no general rigorous definition of a maximal cut known in the

literature, at least not known to the author.

In this thesis we give two different definitions or concepts of a maximal cut integral which we believe are equivalent but we have no proof for it so far. The first definition starts also with the equations $D_i = 0$ for $i = 1, \dots, n$. These equations which we assume are generic are considered to be relations in the lD-dimensional space of loop momenta cutting out a $lD - n$ variety V. One can now look at the different $lD - n$ dimensional cycles Γ_i of this variety V. These are classified by the homology group $H_{lD-n}(V)$. A maximal cut is then an integral as in eq. (2.2) but with integration domain Γ_i

$$M_{\underline{\nu}}^{G,\Gamma_k}(\underline{s}; D) := \int_{\Gamma_k} \left(\prod_{j=1}^{l} \frac{d^D k_j}{i\pi^{D/2}} \right) \left(\prod_{i=1}^{n} \frac{1}{D_e^{\nu_e}} \right) \quad \text{for } k = 1, \dots, \dim(H_{lD-n}(V)) \,. \tag{2.42}$$

The other definition starts with the Baikov polynomial P of a given graph G. Here the definition of the variety V, which we think is equivalent and therefore we take the same letters here, is given by the constraints $P = 0$ and the first n propagators set to zero, i.e. $x_i = 0$ for $i = 1, \dots, n$. For a graph G having $N_{\mathfrak{s}}$ propagators, i.e., it gives directly rise to a complete topology $\mathfrak{T}$, we would set all propagators x_i to zero and the Baikov polynomial P would be trivial. Then the resulting variety V would be trivial and the maximal cut is an algebraic function. For other graphs G we obtain a $(N_{\mathfrak{s}} - n - 1)$-dimensional variety for which we can again consider $(N_{\mathfrak{s}} - n - 1)$-dimensional cycles Γ_i[7]. Then the complicated domain of integration in the Baikov representation[8] is replaced by the cycle Γ_i

$$M_{\underline{\nu}}^{G,\Gamma_k}(\underline{x}; D) := \int_{\Gamma_k} \mathrm{d}x_{n+1} \dots \mathrm{d}x_{N_{\mathfrak{s}}} \, P(0, \dots, 0, x_{n+1}, \dots, x_{N_{\mathfrak{s}}})^{\frac{d-l-N}{2}} \,. \tag{2.43}$$

From both definitions it is absolutely not clear that they give rise to the same notion of a maximal cut integral. Also it is not clear that within a definition of a maximal cut a change in the choice of loop momenta does not effect the definition of the variety V and therefore also of the cycles Γ_i. But to make our definitions at least plausible and meaningful we give later the example of the banana graphs where we can explicitly compute the maximal cut integrals. For $l > 3$ these maximal cuts where were not been computed and understood so far.

Before that we want to point out some confusion or unclearness in the literature. In some references the usage of delta functions to indicate the maximal cut is still common but often with knowing that a generalized residue integral is meant. Moreover, sometimes people are talking about the maximal cut integral while many Feynman integrals have more than a

[7] Notice that although we have used the same notation for the cycles in both of our definitions of a maximal cut they are not necessary the same. We still use here the same notation to show that at the end they should give rise to the same definition of maximal cut integrals.

[8] The maximal cut integrals have an ambiguity in their normalization. A priori there does not exist a preferred normalization. We have chosen a normalization to simplify and shorten the formulas.

single maximal cut. This, let us say special, maximal cut is defined as a $(n-1)$-dimensional torus integral in the Symanzik representation (2.24)

$$\tilde{M}^G_{\underline{\nu}}(\underline{x};D) = (-1)^n \frac{\Gamma(\nu - lD/2)}{\prod_{i=1}^n \Gamma(\nu_i)} \int_{T^{n-1}} \left(\prod_{i=1}^n x_i^{\nu_i - 1} \right) \frac{\mathcal{U}^{\nu-(l+1)D/2}}{\mathcal{F}^{\nu - lD/2}} \, \mu_{n-1} \,. \tag{2.44}$$

To be more precise, this is in general only a single maximal cut and others can exist. The only advantage of this particular maximal cut is that the cycle T^{n-1} can be written down for every Feynman integral. This integral, as we will see later for banana graphs, can be evaluated with known techniques if the external momenta and internal masses are in the right parameter range. It is not clear in general that this integral can easily be computed but if, it can give us some information, in particular about the geometry of the maximal cut integrals.

Now we can come back to the example of the sunset from the end of section 2.6. In (2.41) we have already found the Baikov polynomial. For the maximal cuts of the sunset graph we have to compute the residues around the first three propagators. This is quite simple and one only has to set $x_1 = x_2 = x_3 = 0$ and obtains

$$\begin{aligned} P_3^{\text{max, Ban}}(X,Y) :=& P_2^{\text{Ban}}(0,0,0,X,Y) = 3m^4p^2 - \left(p^2 - 2X\right)\left(p^2 - 2Y\right)\left(p^2 - 2(X+Y)\right) \\ & - 2m^2\left(p^4 - 2p^2(X+Y) + 2\left(X^2 + XY + Y^2\right)\right) , \end{aligned} \tag{2.45}$$

where we have conveniently used X, Y as final integration variables. The polynomial $P_3^{\text{max, Ban}}(X,Y) = 0$ defines an elliptic curve in $\mathbb{P}^2$. This is the maximal cut geometry V_2^{Ban} which in the case of an elliptic curve has two independent cycles since $H_1(V) = 2$. Therefore, we have two different maximal cut integrals which, for example, can be chosen as

$$\begin{aligned} M^{\text{Ban}, \Gamma_a}_{1,1,1} &= \int_{\Gamma_a} \mathrm{d}X\mathrm{d}Y \, \frac{1}{P_3^{\text{max, Ban}}(X,Y)} \\ M^{\text{Ban}, \Gamma_a}_{1,1,1} &= \int_{\Gamma_b} \mathrm{d}X\mathrm{d}Y \, \frac{1}{P_3^{\text{max, Ban}}(X,Y)} \end{aligned} \tag{2.46}$$

with Γ_a, Γ_b a basis of $H_1(V_2^{\text{Ban}})$, i.e. the A– and B-cycle of an elliptic curve.

Before we move on let us make some further comments about the elliptic curve defined by $P_3^{\text{max, Ban}}(X,Y) = 0$ in the sunset case. From the Symanzik representation (2.29) - (2.31) we can also associate an elliptic curve to the sunset graph. Here we simply take the second graph polynomial $\mathcal{F}_2^{\text{Ban}}$ as defining equation. In affine coordinates, i.e. $x_3 = 1$, we get again a cubic polynomial but different to the one in eq. (2.45). But as it turns out both lead to the same elliptic curve up to isogeny. This means that one can compute the τ-parameter which is given as the ratio of both maximal cut integrals and finds that the one coming from

the Symanzik representation is the squared of the Baikov one. We recommend also [24, 78] for more details about this observation and the later chapters of this thesis of how one can compute the maximal cuts of the banana graphs and the corresponding τ-parameter or Kähler paramters t^i.

2.8 Discontinuities, Cut Feynman integrals and the Optical theorem

In the previous section we have introduced the concept of a maximal cut integral. Obviously, one can also study less cut Feynman diagrams. The basic idea behind the cutting of Feynman integrals is that a cut diagram is much easier to compute than the full Feynman integral but still gives important information about the whole graph. The incorporation of a delta function or better a residue computation reduces the necessary integration processes. So cutting more and more up to the maximal cut should in principle simplify the computation. Similar as for the maximal cut the rules for computing cut Feynman integrals are not developed as good as for calculating the full Feynman integral. In particular, subtleties concerning the precise definition of the integration range, i.e. the choice of cycle as for the maximal cut, which depends also on the given integral representation have to be rigorously defined which is as far as the author knows not done in the literature for generic loop order.

Another reason for computing cut diagrams is that by the optical theorem they can be related to the discontinuities of the full Feynman integral. From a physics point of view these discontinuities show up if particles can go on-shell. Let s be a variable of the Feynman integral I, e.g. a Mandelstam invariant, then we define the discontinuity

$$\mathrm{Disc}_s(I(s \pm i0)) = \lim_{\delta \to 0} \{I(s \pm i\delta) - I(s \mp i\delta)\} \ . \tag{2.47}$$

If there is no branch for a considered kinematic region or the integral I does not depend on the variable s then of course the discontinuity is zero. On the other hand we can also define a cut Feynman integral in the variable s. By this we consider the sum of all cut diagrams which are obtained by cutting the original Feynman graph into two pieces such that the momentum transfer q from one piece of the cut diagram to the other is given by the Mandelstam variable $s = q^2$. In our example of the banana family (see figure 2.3) we see that there is only a single cut diagram for the cut in the momentum variable p^2 which is additionally a maximal cut. For this example we will see later in this thesis that a particular maximal cut of the banana integral is the discontinuity of the whole integral as expected. In general all cut diagrams corresponding to the variable s contribute to the discontinuity. How they have to be add up precisely and how each individual cut integral has to be evaluated is in general not rigorously described in the literature. A good introduction to theses concepts is given in [79, 80] where in [80] all examples could be expressed through multiple polylogarithms. How the definition and computation of cut integrals which contain elliptic or even more complicated functions has to be extended is so far not known completely at least not for

the author. For the banana integrals we will later generalize the definitions known in the literature such that we can also describe or interpret non-maximal cut integrals. This will clarify at least for the banana integrals the role of the discontinuity, the maximal cuts and the non-maximal cuts.

Finally, let us make another short remark about the usefulness of cut diagrams. There are attempts [80] which try to reconstruct the full Feynman integral from the knowledge of all cut integrals using dispersion relations. For so-called single unitarity cuts dispersion relations are known and the cut result can be uplifted to the whole integral. In the general situation of multi unitarity cuts the knowledge or even the existence of the dispersion relations is not given so far.

CHAPTER 3

Differential Equational Approach to Feynman Integrals

In most of the cases it is not possible to compute multi-loop Feynman integrals directly by using known integral identities. So instead of trying to evaluate the Feynman integral directly one possible and often applied method is to use differential equations. Every Feynman integral satisfies differential equations and together with an appropriate boundary condition one can reconstruct a given Feynman integral from the basis of solutions to these differential equations. In this chapter we will first explain how one can derive these differential equations and how they can be solved. There are in principle two different ways of writing down the differential equations of a Feynman graph, a first-order linear system or a single higher-order equation. For both ways we show solution strategies. These methods are explained for the single- and multi-parameter case.

This chapter follows in parts my third publication [47] and in there the second section.

3.1 Differential equations for Feynman integrals

So let G be a Feynman graph we want to compute and $\mathfrak{T}$ the corresponding topology. Assume that we have already solved the IBP relations such that we have identified a certain set of master integrals which we collect into the vector $\underline{I}(\underline{s}; D) = (I_1(\underline{s}; D), \ldots, I_M(\underline{s}; D))^T$, where M denotes the number of master integrals. Moreover, we know from the IBP relations how we can express a generic element in the topology $\mathfrak{T}$ of G in terms of the master integrals $\underline{I}(\underline{s}; D)$.

The strategy now is similar as for the derivation of the IBP relations itself. By taking a derivative with respect to an external momentum p_i one obtains back elements in the topology $\mathfrak{T}$ but with shifted exponents compared to the original one. In a second step one can use the IBP relations to relate these integrals back to the master integrals. By this one has obtained a *differential relation* between the master integrals. The same can be repeated for all external momenta p_i and also for the internal masses m_i^2 to find a whole set of differential

equations which now describes the whole master integrals.

As we have seen in the last chapter a Feynman integral does only depend via Lorentz invariant scalar products on the external momenta p_i. Moreover, one has to take care that the external momenta fulfill momentum conservation which gives additional constraints. One has even a rescaling degree of freedom such that the true parameters of the Feynman integral are not the scales $\underline{s}$ directly but only the dimensionless ratios $z_i = s_i/s_1$ for $i = 2, 3, \ldots, N_s = \#s$, where as a choice we have rescaled by s_1. So at the end the differential equations should be expressed through the parameters $\underline{z}$ as we will do later.

There are many computer programs, for example `FIRE`, `Reduce`, `LiteRed` and others, known in the literature which do exactly the steps described. They first solve the IBP relations and identify a set of master integrals and then they compute derivatives with respect to the parameters and relate them to the master integrals back. For low loop orders and not to many scales these programs work quite well and produce the desired differential equations. For high loop orders as for example the three-loop banana integral with generic masses these programs do not terminate in a feasible amount of time which is why we will explain later our methods of finding and solving differential equations for Feynman graphs, in particular for the banana family.

3.2 Gauss-Manin type differential equations

Having so far explained how in principle one can compute differential equations for Feynman integrals let us now, first, analyze these differential equations in general by presenting some properties of them and, second, explain how we can solve them.

With the vector $\underline{I}(\underline{s}; D)$ of master integrals we can write down the differential equations from the previous section as a system of first-order linear differential equations [2, 3, 6, 81, 82]

$$\mathrm{d}\underline{I}(\underline{s}; D) = \mathbf{A}(\underline{s}; D)\, \underline{I}(\underline{s}; D)\,, \tag{3.1}$$

where the total differential is given by $\mathrm{d} = \sum_{k=1}^{N_s} \mathrm{d}s_k \partial_{s_k}$ and $\mathbf{A}(\underline{s}; D)$ is a matrix of rational one-forms. The entries are rational functions of $\underline{s}$ because by the IBP relations only rational functions can appear. This set of first-order differential equations is also known as the *Gauss-Manin system* for the family of Feynman integrals under consideration. Indeed, from a geometrical point of view, we can interpret the M-dimensional vector space spanned by the family of Feynman integrals as a rank M vector bundle over the base defined by the scales $\underline{s}$. On this vector bundle there exists a *flat connection* called the *Gauss-Manin connection* and the matrix $\mathbf{A}(\underline{s}; D)$ is the corresponding connection one-form. The flatness property can be seen from the following argument. From the integrability condition $\mathrm{d}^2\underline{I} = 0$ we find

$$0 = \mathrm{d}^2\underline{I} = (\mathrm{d}\mathbf{A})\underline{I} - \mathbf{A} \wedge \mathrm{d}\underline{I} = (\mathrm{d}\mathbf{A})\underline{I} - \mathbf{A} \wedge \mathbf{A}\underline{I} \tag{3.2}$$

by using eq. (3.1) for the last equality. This means that the curvature $\mathrm{d}\mathbf{A} - \mathbf{A} \wedge \mathbf{A}$ has to vanish so the connection is flat.

The choice of a set of master integrals is, of course, not unique. One can perform a *gauge transformation* to obtain another set of master integrals. So let $\mathbf{M}(\underline{s}; D)$ be an invertible matrix. Then a new set of master integrals is given by

$$\begin{aligned} \underline{I}(\underline{s}; D) &= \mathbf{M}(\underline{s}; D)\underline{J}(\underline{z}; D) \quad \text{with} \\ \mathrm{d}\underline{J}(\underline{z}; D) &= \tilde{\mathbf{A}}(\underline{z}; D)\underline{J}(\underline{z}; D) \end{aligned} \tag{3.3}$$

and the new connection one-form $\tilde{\mathbf{A}}(\underline{z}; D)$ is related to the old one by

$$\tilde{\mathbf{A}}(\underline{z}; D) = \mathbf{M}(\underline{s}; D)^{-1} \left(\mathbf{A}(\underline{s}; D)\mathbf{M}(\underline{s}; D) - \mathrm{d}\mathbf{M}(\underline{s}; D)\right) . \tag{3.4}$$

Here we have also transformed to the dimensionless variables $\underline{z}$. One tries to use the matrix $\mathbf{M}(\underline{s}; D)$ sucht that the new differential equation is as simple as possible. It was argued in [83] that it is always possible to change basis to a so-called *ϵ-regular basis*, where the master integrals $J_i(\underline{z}; D_0 - 2\epsilon)$ are finite and non-zero as $\epsilon \to 0$ (see also ref. [84] for a closely related concept). It is easy to see that in this case also the matrix $\tilde{\mathbf{A}}(\underline{z}; D_0 - 2\epsilon)$ remains regular as $\epsilon \to 0$, and we define $\mathbf{A}_0(\underline{z}) := \lim_{\epsilon\to 0} \tilde{\mathbf{A}}(\underline{z}; D_0 - 2\epsilon)$. In the following we assume $\mathbf{A}_0(\underline{z})$ is finite, though we may allow bases that are not necessarily ϵ-regular, i.e., they can possibly start with $\mathcal{O}(\epsilon)$ and can therefore vanish as $\epsilon \to 0$.

There is one special form of the Gauss-Manin system which can be solved in general. This form is known as the *canonical form* introduced by Henn [6]. One can bring the Gauss-Manin system (3.1) into this form if one can find a matrix $\mathbf{M}(\underline{s}; D)$ that is rational in D and algebraic in $\underline{s}$ such that $\tilde{\mathbf{A}}(\underline{z}; D_0 - 2\epsilon) = \epsilon \mathbf{A}_1(\underline{z})$. The the Gauss-Manin system can be solved by a path-ordered exponential

$$\underline{J}(\underline{z}; D) = \mathbb{P} \exp\left(\epsilon \int_{\underline{z}_0}^{\underline{z}} \mathbf{A}_1(\underline{z}')\right) \underline{J}(\underline{z}_0; D) , \tag{3.5}$$

where the integral is over a path from the point $\underline{z}_0$ to the point $\underline{z}$. The big advantage of this representation is that one can compute the path-ordered exponential by expanding around $\epsilon = 0$. The expansion can be truncated easily after a few terms. The coefficient ϵ^k will involve iterated integrals over algebraic one-forms. The same conclusion holds if we can find $\mathbf{M}(\underline{s}; D)$ such that $\mathbf{A}_0(\underline{z}) = 0$, although the system may not be strictly speaking in canonical form.

If one cannot find such a transformation[1] $\mathbf{M}(\underline{s}; D)$ to bring the Gauss-Manin system to canonical form we can still find a transformation which sorts the master integrals by the

[1] However, canonical form may be reached by a transcendental rotation $\mathbf{M}(\underline{s}; D)$, see [29–31, 35, 85].

partial order on the sectors, i.e.

$$\underline{J}(\underline{z};D) = (\underline{J}_1(\underline{z};D)^T,\ldots,\underline{J}_r(\underline{z};D)^T)^T\,, \tag{3.6}$$

such that the master integrals in $\underline{J}_k(\underline{z};D)$ are in the same sector and thus have the same propagators. Such a rotation can always be found und then the connection one-form $\tilde{\mathbf{A}}(\underline{z};D)$ is block-triangluar. In each sector the master integrals $\underline{J}_k(\underline{z};D)$ satisfy an inhomogeneous differential equation of the form

$$\mathrm{d}\underline{J}_k(\underline{z};D) = \mathbf{B}_k(\underline{z};D)\,\underline{J}_k(\underline{z};D) + \underline{N}_k(\underline{z};D) \quad \text{for } 1 \leq k \leq r\,. \tag{3.7}$$

Here the inhomogeneity $\underline{N}_k(\underline{z};D)$ collects contributions form Feynman integrals from lower sectors, which we assume are known. The maximal cuts of $\underline{J}_k(\underline{z};D)$ satisfy the homogeneous equation of (3.7). They are obtained from residues around the propagators as explained in section 2.7. If the basis $\underline{J}(\underline{z};D)$ is ϵ-regular, then so are $\mathbf{B}_k(\underline{z};D)$ and $\underline{N}_k(\underline{z};D)$. We define $\mathbf{B}_{k,0}(\underline{z}) \coloneqq \lim_{\epsilon\to 0}\mathbf{B}_k(\underline{z},D_0-2\epsilon)$.

Now, assume that we have found the general solution of the homogeneous equation for $\epsilon = 0$. If $\underline{J}_k(\underline{z};D)$ has M_k elements, this general solution can be conveniently cast in the form of an $(M_k \times M_k)$-matrix $\mathbf{W}_k(\underline{z})$ which we call the *Wronskian*. The Wronskian is governed by the homogeneous equation

$$\mathrm{d}\mathbf{W}_k(\underline{z}) = \mathbf{B}_{0,k}(\underline{z})\,\mathbf{W}_k(\underline{z})\,. \tag{3.8}$$

Since the columns of $\mathbf{W}_k(\underline{z})$ form a basis for the solution space, this matrix must have full rank for generic values of $\underline{z}$. Define

$$\underline{L}_k(\underline{z};D) = \mathbf{W}_k(\underline{z})^{-1}\,\underline{J}_k(\underline{z};D) \tag{3.9}$$

such that we obtain the equation

$$\mathrm{d}\underline{L}_k(\underline{z};D) = \tilde{\mathbf{B}}_k(\underline{z};D)\,\underline{L}_k(\underline{z};D) + \tilde{\underline{N}}_k(\underline{z};D) \tag{3.10}$$

with

$$\begin{aligned}\tilde{\mathbf{B}}_k(\underline{z};D) &= \mathbf{W}_k(\underline{z})^{-1}\left(\mathbf{B}_k(\underline{z};D) - \mathbf{B}_{k,0}(\underline{z})\right)\mathbf{W}_k(\underline{z})\,,\\ \tilde{\underline{N}}_k(\underline{z};D) &= \mathbf{W}_k^{-1}\,\underline{N}_k(\underline{z};D)\,.\end{aligned} \tag{3.11}$$

Notice that by construction we have $\lim_{\epsilon\to 0}\tilde{\mathbf{B}}_k(\underline{Z};D_0)$. Hence, we can solve the Gauss-Manin system in eq. (3.10) order-by-order in ϵ. Since $\underline{L}_k$ and $\underline{N}_k$ must be regular for $\epsilon \to 0$, they

admit a Taylor expansion

$$\underline{L}_k(\underline{z}; D_0 - 2\epsilon) = \sum_{j=0}^{\infty} \epsilon^j \underline{L}_k^{(j)}(\underline{z}) \quad \text{and} \quad \underline{\tilde{N}}_k(\underline{z}; D_0 - 2\epsilon) = \sum_{j=0}^{\infty} \epsilon^j \underline{\tilde{N}}_k^{(j)}(\underline{z}) \,. \tag{3.12}$$

In particular, the leading order in ϵ leads to the equation

$$\mathrm{d}\underline{L}_k^{(0)}(\underline{z}) = \underline{\tilde{N}}_k^{(0)}(\underline{z}) \,, \tag{3.13}$$

which can easily be solved by quadrature

$$\underline{L}_k^{(0)}(\underline{z}) = \underline{L}_k^{(0)}(\underline{z}_0) + \int_{\underline{z}_0}^{\underline{z}} \underline{\tilde{N}}_k^{(0)}(\underline{z}') \,. \tag{3.14}$$

We can iteratively solve eq. (3.10) order by order in ϵ by inserting this solution into its ϵ-expansion. This strategy was successfully applied to several complicated Feynman integrals for which no canonical form can be reached via an algebraic transformation matrix $\mathbf{M}(\underline{s}; D)$, see also [83, 86–92].

3.3 Picard-Fuchs type differential equations

Instead of solving the system of first-order differential equations for the vector $\underline{I}(\underline{s}; D)$ of master integrals, it is also possible to consider an inhomogeneous higher-order differential equation satisfied by each master integral:

$$\mathcal{L}_{k,D}\, I_k(\underline{s}; D) = R_k(\underline{s}; D) \,, \tag{3.15}$$

where the inhomogeneity $R_k(\underline{s}; D)$ is related to master integrals from lower sectors, and the differential operator $\mathcal{L}_{k,D}$ has the form

$$\mathcal{L}_{k,D} = \sum_{j_1,\ldots,j_{N_s} \geq 0} Q_{k,j_1\ldots j_{N_s}}(\underline{s}; D)\, \partial_{s_1}^{j_1} \ldots \partial_{s_{N_s}}^{j_m} \,, \tag{3.16}$$

where $Q_{k,j_1\ldots j_{N_s}}(\underline{s}; D)$ are polynomials in $\underline{s}$ and D. The operator $\mathcal{L} := \mathcal{L}_{k,D_0}$ will annihilate the maximal cuts of $I_k(\underline{s}; D_0)$. Geometrically, these higher-order equations are also known as *Picard-Fuchs differential equations*. They describe the periods of algebraic varieties. This will be explained further in the subsequent chapter 4. The higher-order differential equations can for example be obtained by decoupling the first-order Gauss-Manin system. However, this may not be the only way to obtain them, and indeed, in the case of the banana integrals, we

will see that it is easier to derive the decoupled higher-order differential equations directly without passing through the coupled first-order system.

In the remainder of this section we review some general strategies to solve homogeneous linear higher-order differential equations (inhomogeneous equations can be brought into homogeneous form by acting with a suitable differential operator). Moreover, we want to introduce our notation and conventions. The material in this section is well known in the literature (see, e.g., refs. [93–95]), but it will play an important role to understand the properties of the banana integrals, as studied in refs. [44, 45]. We start by reviewing in some detail the case of a single variable z (which corresponds to the case of Feynman integrals depending on two scales), and briefly comment on the multi-variate generalization at the end.

3.3.1 One-parameter Picard-Fuchs-type differential equations

Consider a differential equation of the form

$$\mathcal{L}f(z) = 0 \qquad \text{with} \qquad \mathcal{L} = q_n(z)\partial_z^n + q_{n-1}(z)\partial_z^{n-1} + \ldots + q_0(z)\,, \qquad q_n(z) \neq 0\,, \tag{3.17}$$

where the $q_i(z)$ are polynomials, and we assume that the $q_i(z)$ do not have any common zero. The leading coefficient $q_n(z) =: \mathrm{Disc}(\mathcal{L})$ is called the *discriminant*. It will often be convenient to write the differential operator in the equivalent form

$$\mathcal{L} = \tilde{q}_n(z)\theta^n + \tilde{q}_{n-1}(z)\theta^{n-1} + \ldots + \tilde{q}_0(z) \qquad \text{with } \theta = \theta_z := z\,\partial_z\,. \tag{3.18}$$

One can relate both forms simply by the relations

$$\theta^n = \sum_{i=1}^{n} s_2(n,k) z^k \partial_z^k \qquad \text{or} \qquad z^n\partial_z^n = \prod_{i=0}^{n-1}(\theta - i)\,, \tag{3.19}$$

with the Stirling numbers of second kind $s_2(n,k) = \frac{1}{k!}\sum_{i=0}^{k}(-1)^i\binom{k}{i}(k-i)^n$. In particular, we have $q_n(z) = z^n\tilde{q}_n(x)$.

This equation has n independent solutions $f_i(z)$ for $1 \leq i \leq n$. The solution space $\mathrm{Sol}(\mathcal{L})$ is the $\mathbb{C}$-vector space generated by the $f_i(z)$. Let $p_i(z) := q_i(z)/q_n(z)$, $0 \leq i < n$. We want to understand the singularities of the solutions. We say that the differential equation (3.17) has an *ordinary point* at $z = z_0$ if the coefficient functions $p_i(z)$ are analytic in a neighbourhood of z_0 for all $0 \leq i < n$. A point z_0 is called *regular singular point* if the $(z - z_0)^{n-i}p_i(z)$ are analytic in a neighbourhood of z_0. An *irregular singular point* is neither an ordinary nor a regular singular point. Note that all singular points $z_0 \neq \infty$ are zeroes of the discriminant, $\mathrm{Disc}(\mathcal{L})|_{z=z_0} = q_n(z_0) = 0$. For the point at infinity $z_0 = \infty$ one introduces the variable $t = 1/z$ and makes the analysis around $t = 0$. A differential equation without irregular singular points is called a *Fuchsian* differential equation. Feynman integrals are expected to

have only regular singularities, and no irregular singularities can appear. We therefore do not distinguish between regular and irregular singularities from now on.

Let us now briefly review how one can obtain a basis for the solution space using the well-known *Frobenius method*. The goal will be to construct for every point $z_0 \in \mathbb{C}$ n linearly independent local solutions. Each local solution will be given in terms of power series convergent up to the nearest singularity. These local solutions can be analytically continued to multivalued global solutions over the whole parameter space. In the following we assume without loss of generality $z_0 = 0$ (if not, we perform a variable substitution $z \to z' = z - z_0$ or $z' = 1/z$). Our starting point is the indicial equation

$$\tilde{q}_n(0)\alpha^n + \tilde{q}_{n-1}(0)\alpha^{n-1} + \ldots + \tilde{q}_0(0)\alpha = 0\,, \tag{3.20}$$

The solutions of eq. (3.20) are called the *indicials* or *local exponents* at $z_0 = 0$.

We now discuss the structure of the solution space close to an ordinary or regular-singular point z_0. If $z_0 = 0$ is an ordinary point, then there are n different solutions $\alpha_1, \ldots, \alpha_n$ to eq. (3.20). The n-dimensional solution space is then spanned by:

$$z^{\alpha_i}\,\Sigma_{i,0}(z) = z^{\alpha_i}\sum_{k=0}^{\infty} a_{i,k}\,z^k\,, \qquad a_{i,0} \neq 0\,, \qquad 1 \leq i \leq n\,, \tag{3.21}$$

where the $\Sigma_{i,0}(z)$ are power series around $z_0 = 0$ with non-vanishing radius of convergence and normalized according to $\Sigma_{i,0}(0) = 1$. The coefficients $a_{i,k}$ can be computed from recurrence relations obtained by applying the operator $\mathcal{L}$ on the ansatz in eq. (3.21).

If $z_0 = 0$ is a regular-singular point, there are still n independent local solutions, but the solution space contains also solutions other than those in eq. (3.21). Again one analyzes the indicial equation (3.20), but now some solutions appear with multiplicities. Let us sort them as $(\alpha_1, \ldots, \alpha_1, \alpha_2, \ldots, \alpha_2, \ldots, \alpha_m, \ldots, \alpha_m)$. For all indicials $\alpha_1, \ldots, \alpha_r$ such that $\alpha_i - \alpha_j \notin \mathbb{Z}$ for pairwise distinct i, j, one gets r power series-type solutions as in eq. (3.21). The missing $n - r$ solutions contain powers of $\log(z)$ and are constructed by the following procedure. For an indicial $\alpha_i \in \{\alpha_1, \ldots, \alpha_r\}$ appearing with multiplicity s, one has $s - 1$ different logarithmic solutions containing up to s powers of $\log(z)$. They are given by

$$z^{\alpha_i}\sum_{j=0}^{k}\frac{1}{(k-j)!}\,\log^{k-j}(z)\,\Sigma_{i,j}(z) \quad \text{for } 0 \leq k \leq s-1\,, \tag{3.22}$$

where again $\Sigma_{i,j}(z)$ are power series convergent until the nearest singularity, normalized such that $\Sigma_{i,j}(z) = \delta_{j0} + \mathcal{O}(z)$ for $j \geq 1$. For indicials α_i and α_k such that $\alpha_i - \alpha_k \in \mathbb{Z}$, one has to check case by case whether one obtains a power series-type solution as in eq. (3.21) or a logarithmic solution as in eq. (3.22).

For some Fuchsian differential equations there is a special singular point where all indicials are equal. Close to such a point the solution space can be characterized by an increasing hierarchical structure of logarithmic solutions, i.e., there exists a power series-type solution ϖ_0, a

single logarithmic solution ϖ_1, and so on, up to $\log^{n-1}(z)$. Such a point is also-called a *point of maximal unipotent monodromy* (MUM-point), and the associated basis $\varpi_0(z), \ldots, \varpi_{n-1}(z)$ is called a *Frobenius basis*.

It may be convenient to collect the information about all singular points and their indicials in the so-called *Riemann $\mathcal{P}$-symbol*. Let $\{z_1, \ldots, z_s\}$ be the singular points of the n-th order operator $\mathcal{L}$, including possibly also the point at infinity. We denote the indicials for the singular point $z_i \in \{z_1, \ldots, z_s\}$ by $\{\alpha_1^{(i)}, \ldots, \alpha_n^{(i)}\}$ (some indicials may be equal). The Riemann $\mathcal{P}$-symbol is then:

$$\mathcal{P}\left\{\begin{array}{cccc} z_1 & z_2 & \ldots & z_s \\ \hline \alpha_1^{(1)} & \alpha_1^{(2)} & \ldots & \alpha_1^{(s)} \\ \vdots & \vdots & \ddots & \vdots \\ \alpha_n^{(1)} & \alpha_n^{(2)} & \ldots & \alpha_n^{(s)} \end{array}\right\} . \tag{3.23}$$

The sum of all indicials fulfills the so-called *Fuchsian relation*:

$$\sum_{i=1}^{s}\sum_{j=1}^{n} \alpha_j^{(i)} = \frac{n(n-1)(s-2)}{2} . \tag{3.24}$$

3.3.2 Multi-parameter Picard-Fuchs operators

Let us conclude by making some brief comments about how the Frobenius method generalizes to the multi-parameter case. In the multi-parameter case one has a set of differential operators $\mathcal{D} = \{\mathcal{L}_1, \ldots, \mathcal{L}_r\}$, and we are looking for functions $f(\underline{z})$ that are simultaneously annihilated by all elements in $\mathcal{D}$. The solution space $\mathrm{Sol}(\mathcal{D})$ is the $\mathbb{C}$-linear span of all common solutions, i.e.,

$$\mathrm{Sol}(\mathcal{D}) := \{f(\underline{z}) | \mathcal{L}_i f(\underline{z}) = 0 \text{ for all operators } \mathcal{L}_i \in \mathcal{D}\} . \tag{3.25}$$

The set $\mathcal{D}$ actually generates a *(left-)ideal of differential operators*. Indeed, if $\mathcal{L}_i \in \mathcal{D}$ and $f \in \mathrm{Sol}(\mathcal{D})$, we have $\tilde{\mathcal{L}}\mathcal{L}_i f(\underline{z}) = 0$, for every differential operator $\tilde{\mathcal{L}}$.

It is possible to generalize the Frobenius method to the multi-variate case. Close to an ordinary point (in the sense of section 3.3.1), one again finds a basis of local solutions in terms of generalized power series-type solutions

$$\left(\prod_{i=1}^{m} z_i^{\alpha_i}\right) \sum_{j_1,\ldots,j_m \geq 0} a_{j_1,\ldots,j_m} z_1^{j_1} \cdots z_m^{j_m} \tag{3.26}$$

with indicials $(\alpha_1, \ldots, \alpha_m)$. At singular points also multi-variate logarithmic solutions can show up, and we have

$$\left(\prod_{i=1}^{m} z_i^{\alpha_i}\right) \sum_{\substack{j_1,\ldots,j_m \geq 0 \\ k_1,\ldots,k_m \geq 0}} a_{j_1,\ldots,j_m,k_1,\ldots,k_m} \log^{j_1}(z_1) \cdots \log^{j_m}(z_m) z_1^{k_1} \cdots z_m^{k_m} , \tag{3.27}$$

where $j_1 + \ldots + j_m$ depends on the multiplicity and the differences of the local indicials. Similarly to the one-parameter case, the local basis can be analytically continued to a global solution. In the multi-parameter case, however, this is a much harder problem, and may require blow ups at certain singular points, see, e.g., refs. [96, 97]. As a side remark we note that if the singularity is too 'bad' due to a crossing of many singular loci, choosing a good set of coordinates $(z_1, \ldots, z_m)$ can be important. It may happen that with the wrong choice of coordinates the Frobenius method does not produce all expected solutions. For a more thorough discussion we refer again to refs. [96, 97].

There may be different ways to choose the set of differential operators, or more precisely, how to choose a representation of the differential ideal generated by $\mathcal{D}$. There can be different sets of operators, e.g., $\mathcal{D} = \{\mathcal{L}_1, \ldots, \mathcal{L}_s\}$ and $\mathcal{D}' = \{\mathcal{L}'_1, \ldots, \mathcal{L}'_{s'}\}$, which generate the same ideal, and thus they have the same solution space, i.e.,

$$\text{Sol}(\mathcal{D}) = \text{Sol}(\mathcal{D}') \,. \tag{3.28}$$

Note that the sets $\mathcal{D}$ and $\mathcal{D}'$ can have different lengths, $s \neq s'$, and also the degrees of the operators can be different. Sometimes even a single but complicated operator is enough to generate the complete ideal. A clever choice of how to represent the ideal can have an impact on how complicated it is to find all the solutions. In particular, the higher-order differential operators obtained by decoupling the Gauss-Manin-type system is only one possible way to choose a set $\mathcal{D}$ that generates the ideal of differential operators; other, equivalent, choices are possible, and may lead to simplifications. We will exploit this freedom in later sections to obtain the differential equations satisfied by banana graphs at high loop orders.

Let us conclude with a comment. In the case of differential operators in one variable, it is always possible to choose a single differential operator that generates the differential ideal completely. More precisely, in appendix A of [47] it was shown that the ring of linear differential operators in one variable with rational coefficients is a principle left-ideal domain, i.e., every differential operator in this ideal is of the form $\mathcal{L}\mathcal{L}_0$, for some distinguished differential operator $\mathcal{L}_0$.

CHAPTER 4

Mathematics of Calabi-Yau Spaces in the Context of Feynman Integrals

In this chapter we will introduce the most important concepts of Calabi-Yau manifolds and motives useful for computations of Feynman integrals. We will apply these methods on the banana family in the subsequent chapters.

This chapter follows strongly parts of the third chapter of my third publication [47]. For more details, in particular, about Calabi-Yau motives and their arithmetic– and number-theoretic properties we suggest the full third chapter in [47]. We dedicate an additional whole chapter to mirror symmetry and the $\widehat{\Gamma}$-conjecture which was one big achievement presented in my second publication [45] and summarized also in [47]. This is why we do not discuss these topics in this chapter.

4.1 Calabi-Yau varieties and their complex structure moduli spaces $\mathcal{M}_{\text{cs}}$

We consider n-dimensional *Calabi-Yau manifolds* M_n, often only called Calabi-Yau n-folds, which are complex n-dimensional *Kähler manifolds*. They are equipped with a *Kähler form* ω of Hodge-type $(1,1)$ that resides in the cohomology group $H^{1,1}(M_n,\mathbb{Z})$. The extra condition of being Calabi-Yau implies the existence of a *non-trivial holomorphic* $(n,0)$*-form* Ω spanning $H^{n,0}(M_n,\mathbb{C})$. In the case of a family of elliptic curves, which are one-dimensional Calabi-Yau manifolds, the former is the volume form on the elliptic curve and the latter generalizes the familiar holomorphic $(1,0)$-form $\mathrm{d}x/y$. The two forms Ω and ω are so characteristic for the Calabi-Yau manifold that one often refers to the triple (M_n,Ω,ω) as a Calabi-Yau manifold. They are related via the unique volume form $\omega^n/n! = (-1)^{n(n-1)/2}(i/2)^n\Omega\wedge\bar{\Omega}$. One can show that the existence of the form Ω (which is unique up to a phase) is equivalent to the fact that the holonomy group is $\mathrm{SU}(n)$, from which it follows that the first Chern class is trivial, $c_1(M_n)=0$. This in turn implies by the famous Theorem of Yau that a Ricci-flat

Kähler metric $g_{i\bar{j}}$ exists on every Calabi-Yau manifold [98],[1] i.e., $R_{i\bar{j}}(g_{i\bar{j}}) = 0$. We want the holonomy group to be the full $\mathrm{SU}(n)$ group, which implies that the cohomology groups $H^{k,0}(M_n, \mathbb{C})$ vanish unless $k = 0$ or $k = n$, in which case its dimension is one. This is due to the fact that $\mathrm{SU}(n)$ acts canonically on these forms and the only invariant representations available are the trivial and the totally antisymmetric one.

Another important property of Calabi-Yau manifolds M_n is that their *complex structure moduli space* $\mathcal{M}_{\mathrm{cs}}$ has particularly nice and simple structures. The first-order deformations of a complex manifold are given by (finitely) many linearly independent elements in the cohomology group $H^1(M_n, TM_n)$ [99]. For Calabi-Yau manifolds this space is isomorphic to the space of harmonic $(n-1,1)$-forms

$$H^1(M_n, TM_n) \cong H^{n-1,1}(M_n)\,, \tag{4.1}$$

where the isomorphism is simply provided by contracting the elements in $H^1(M_n, TM_n)$ with Ω. First-order complex structure deformations can in general be globally obstructed by higher-order obstructions, which generically depend on the position in the complex moduli space. One can think of these obstructions as higher terms in a potential W that obstructs the movement of a particle in a specific direction. Tian [100] and Todorov [101] have proven the important fact that for Calabi-Yau varieties M_n the complex $h^{n-1,1}$-dimensional moduli space $\mathcal{M}_{\mathrm{cs}}$ of complex structure deformations is globally unobstructed, i.e., in the picture with the potential, one has $W(\underline{z}) \equiv 0$ on $\mathcal{M}_{\mathrm{cs}}$.

4.1.1 Complex families of Calabi-Yau n-folds.

It is natural to consider *complex families of Calabi-Yau n-folds* $\mathcal{M}_n$ with projection $\pi : \mathcal{M}_n \to \mathcal{M}_{\mathrm{cs}}$ over the complex moduli space $\mathcal{M}_{\mathrm{cs}}$. This means that at each point $\underline{z}_0 \in \mathcal{M}_{\mathrm{cs}}$ we have a fiber being a Calabi-Yau n-fold, i.e., $\pi^{-1}(\underline{z}_0) = M_n^{\underline{z}_0}$ with a fixed complex structure. In this picture one understands easily that $\mathcal{M}_{\mathrm{cs}}$ can have special so-called *critical*[2] divisors. At these codimension one loci in $\mathcal{M}_{\mathrm{cs}}$, the manifold itself, i.e., the fiber of the family, becomes singular. For example, at a point in the one-dimensional complex moduli space of an elliptic curve a cycle S^1 might shrink to a point, and the elliptic curve develops a nodal singularity. More generally, a *nodal singularity* corresponds to a S^n shrinking. This is the most generic type of singularity for n-dimensional Calabi-Yau manifolds. The corresponding critical divisor in $\mathcal{M}_{\mathrm{cs}}$ is called a *conifold divisor*. However, n-dimensional Calabi-Yau manifolds can acquire a much greater variety of more interesting singularities, which are only classified up to $n = 2$ by the celebrated ADE-type classification of canonical surface singularities. Families

[1] Calabi constructed some of these metrics $g_{i\bar{j}}$ explicitly for non-compact Calabi-Yau manifolds. For elliptic curves ($n = 1$), Ricci-flatness implies flatness of the metric, $g_{1\bar{1}} = \mathrm{const}$. For higher-dimensional compact Calabi-Yau manifolds starting with the complex K3 surfaces ($n = 2$) the Ricci-flat metric is not known explicitly.

[2] Sometimes they are called singular divisors. However, since a divisor D can itself be singular in $\mathcal{M}_{\mathrm{cs}}$ (see below), we call them critical.

of higher-dimensional Calabi-Yau manifolds have in general a higher-dimensional moduli space, $\dim_{\mathbb{C}}(\mathcal{M}_{\text{cs}}) = h_{n-1,1}$. The divisors at which the fiber M_n is singular will intersect in higher codimensional sub-loci in $\mathcal{M}_{\text{cs}}$. This produces over the intersection locus an even more singular Calabi-Yau n-fold fibre. Generically, these critical divisors are given by the vanishing locus of algebraic equations, $\Delta_i(\underline{z}) = 0$, $i = 1, \ldots, r$. These loci can itself have singularities and non-generic intersections. There are mathematical techniques suggesting that within Calabi-Yau moduli spaces these singularities can be resolved by a finite sequence of blow ups to divisors with normal crossings [102].

One of the most important properties of a family of complex manifolds is the monodromy that its periods or its homology groups undergo if one encircles the critical divisors in a normal crossing model of the moduli space $\overline{\mathcal{M}}_{\text{cs}}$. The local monodromy reflects the nature of the singularity of the fibres and the degeneration of the periods. The global monodromy often restricts the class of functions that can be periods. For example, for elliptic families these are weight-one modular forms for a congruence subgroup of $\text{SL}(2, \mathbb{Z})$, determined by the global monodromy of the family. We will discuss these concepts further in section 4.2.3.

4.2 Geometric structures in the complex moduli space and period integrals

Next, we discuss some features of the structures appearing in the complex moduli space, in particular period integrals. We focus on the concepts that we expect to be most relevant for the application to Feynman integrals showing up in this thesis. For more general details we refer as mentioned to [47]. We start with section 4.2.1 where we focus on the interior of the moduli space, commonly called the *bulk*. We give the conceptual explanations, together with many references, that underly the most useful tools developed over a long period of time in mathematics, for example the concept of periods, the Gauss-Manin connection, the Picard-Fuchs differential ideal and the Griffiths transversality. As we will show in section 4.2.2, the latter leads straightforwardly to quadratic relations between maximal cuts of Feynman integrals. In section 4.2.3 we review concepts relevant to describe the possible degenerations of the geometry and the Feynman integrals at the critical divisors, i.e., at the boundary of the moduli space.

The mathematical properties of periods on compact smooth Kähler manifolds are captured by a so-called *variation of a pure Hodge structure*, characterized by its *decreasing Hodge filtration* in eq. (4.9). In a series of spectacular papers [103–105], Deligne generalized that notion to the variation of *mixed Hodge structures* to include open smooth, complete singular and general varieties. In addition to the decreasing Hodge filtration, one defines in these situations a second increasing filtration, the so-called *monodromy weight filtration*. For many applications to Feynman integrals the generalization to open manifolds is essential, as their integration domain is open. In our discussion, however, we concentrate on the case of complete singular spaces, as our main point is the study of the generalization of elliptic periods to Calabi-Yau periods, because they appear as the maximal cuts of (at least) the banana integrals. At the

same time, our discussion is a prerequisite for the final step to describe the analytic structure of the banana integrals in terms of the generalized $\widehat{\Gamma}$-class. A standard reference on mixed Hodge structures is the book of Peters and Steenbrink [106]; some applications to mirror symmetry are discussed in the book by Cox and Katz [107].

4.2.1 On the bulk of $\mathcal{M}_{\text{cs}}$

Away from the critical divisors, i.e., in the bulk, $\mathcal{M}_{\text{cs}}$ is a nicely behaved globally-defined Kähler manifold of dimension $h^{n-1,1}(M_n)$, where the real *Kähler potential* $K(z,\bar{z})$ is given by

$$e^{-K(\underline{z},\underline{\bar{z}})} = i^{n^2} \int_{M_n} \Omega(\underline{z}) \wedge \bar{\Omega}(\underline{\bar{z}}) = i^{n^2} \underline{\Pi}^{\dagger}(\underline{z})\, \mathbf{\Sigma}\, \underline{\Pi}(\underline{z})\,. \tag{4.2}$$

For the last equal sign in eq. (4.2) will be explained in the subsequent text, in particular, the definition of the vector of period functions $\underline{\Pi}(\underline{z}) := (\Pi_i(\underline{z}))_{1\leq i\leq b_n}$ (with $b_k := \dim H_k(M_n,\mathbb{Z})$ the Betti numbers) and the intersection pairing $\mathbf{\Sigma}$ will follow. Note that there is a 'gauge freedom' to rescale $\Omega(\underline{z}) \to e^{f(\underline{z})}\Omega(\underline{z})$ with $f(\underline{z})$ a holomorphic function, under which the Kähler potential $K(\underline{z},\underline{\bar{z}})$ undergoes a Kähler gauge transformation

$$K(\underline{z},\underline{\bar{z}}) \to K(\underline{z},\underline{\bar{z}}) - f(\underline{z}) - \bar{f}(\underline{\bar{z}})\,. \tag{4.3}$$

Most geometrical structures on Calabi-Yau manifolds, e.g., the Kähler metric, are invariant under the gauge transformation in eq. (4.3), but the Feynman integral is taken in a specific Kähler gauge.[3] In eq. (4.2) one understands the form $\Omega(\underline{z})$ to depend on the complex structure parameters $\underline{z}$ such that the $\Omega(\underline{z}_0)$ is of type $(n,0)$ exactly for the complex structure defined by $\underline{z} = \underline{z}_0$. For each point $\underline{z}_0$, the fibre $M_n^{\underline{z}_0}$ over it enjoys a Hodge decomposition, in particular, of its middle dimensional cohomology:[4]

$$H^n(M_n,\mathbb{C}) = \bigoplus_{p+q=n} H^{p,q}(M_n) \quad \text{with} \quad \overline{H^{p,q}(M_n)} = H^{q,p}(M_n)\,, \tag{4.4}$$

and a canonical polarization, i.e., for $\omega^{p,q} \in H^{p,q}(M_n)$ and $\omega^{r,s} \in H^{r,s}(M_n)$ with $p+q = r+s = n$, one has

$$\begin{aligned} \int_{M_n} \omega^{p,q} \wedge \omega^{r,s} &= 0 \qquad \text{unless} \quad p = s \ \text{ and } q = r\,, \\ i^{p-q} \int_{M_n} \omega^{p,q} \wedge \overline{\omega^{p,q}} &> 0 \qquad \text{for } \ \omega^{p,q} \neq 0\,. \end{aligned} \tag{4.5}$$

[3] This means concretely that the holomophic $(n,0)$-form could be modified by an $e^{f(z)}$ factor, but we make an explicit choice in eq. (6.17).

[4] We suppress the dependence on the point $\underline{z}_0$ to ease the notation.

The *periods* of M_n are pairings between the middle homology and the middle cohomology. They carry information about how the Hodge structure varies in the family. One fixes an integral topological basis Γ_i, $1 \leq i \leq b_n$ for the middle homology $H_n(M_n, \mathbb{Z})$. The choice of this basis is topological, and it does not depend on the complex structure. In particular, the intersection pairing in this fixed topological basis $\Sigma_{ij} = \Gamma_i \cap \Gamma_j$ is given by an integer $b_n \times b_n$-matrix.[5] If n is odd, then it is skew-symmetric and can be chosen to be the standard symplectic pairing $\mathbf{\Sigma} = \begin{pmatrix} 0 & \mathbb{1} \\ -\mathbb{1} & 0 \end{pmatrix}$. Instead, if n is even, $\mathbf{\Sigma}$ is symmetric, and general lattice arguments restrict its further, see [47].

Concretely, the periods are the pairing $\Pi : H_n(M_n, \mathbb{Z}) \times H^n(M_n, \mathbb{C}) \to \mathbb{C}$ given by the integrals

$$\Pi_{ij} = \int_{\Gamma_i} \hat{\Gamma}^j \,, \tag{4.6}$$

with $\hat{\Gamma}^j$ some basis of $H^n(M_n, \mathbb{C})$. One can fix a basis $\gamma_j \in H^n(M_n, \mathbb{C})$ with $\int_{\Gamma_i} \gamma^j = \delta_i^j$ and $\int_{M_n} \gamma^i \wedge \gamma^j = \Sigma^{ij} = \Sigma_{ij}$. Then one expands $\Omega(\underline{z}) \in H^n(M_n, \mathbb{C})$ in terms of the period functions $\Pi_i(\underline{z})$ in this fixed cohomology basis:

$$\Omega(\underline{z}) = \sum_i \left(\int_{\Gamma_i} \Omega(\underline{z}) \right) \gamma^i = \sum_i \Pi_i(\underline{z}) \gamma^i \,. \tag{4.7}$$

As an example, for an elliptic curve E with modulus z one may choose a symplectic basis $S_a^1, S_b^1 \in H_1(E, \mathbb{Z})$, with $S_a^1 \cap S_b^1 = -S_b^1 \cap S_a^1 = 1$ and $S_a^1 \cap S_a^1 = S_b^1 \cap S_b^1 = 0$ in integral homology, and a dual symplectic basis $\alpha, \beta \in H^1(E, \mathbb{Z})$ with $\int_E \alpha \wedge \beta = -\int_E \beta \wedge \alpha = 1$ and $\int_E \alpha \wedge \alpha = \int_E \beta \wedge \beta = 0$ in integral cohomology. Then $\Pi_a(z) = \int_{S_a^1} \mathrm{d}x/y$, $\Pi_b(z) = \int_{S_b^1} \mathrm{d}x/y$ are the well-known elliptic integrals, and one can evaluate eq. (4.2) in terms of these periods. The elliptic periods can in turn be evaluated in terms of complete elliptic integrals of the first kind. For the two-loop banana and train-track integrals (also known as the sunrise and the elliptic double-box integrals, respectively), the maximal cuts evaluate to the periods of an elliptic curve, cf., e.g., refs. [7, 108–110]. Introducing the parameter $\tau = \Pi_b(z)/\Pi_a(z)$ on the upper half-plane, and keeping in mind that $\Pi_a(z)$ (and $\Pi_b(z)$) are holomorphic, we can evaluate from eq. (4.2), with $G_{\tau\bar{\tau}} = \partial_\tau \bar{\partial}_{\bar{\tau}} K = 1/(2\mathrm{Im}(\tau))^2$, the famous parabolic metric on the upper half-plane (the Teichmüller space of E). Moreover, using τ as complex structure variable one can express the periods of the elliptic curve as modular forms of weight one in τ [111]. The Calabi-Yau periods generalize this relationship between periods and maximal cuts to higher-loop banana and train-track integrals, cf., e.g., refs. [44–46, 112, 113].

[5] Here $\cap$ denotes the standard intersection pairing on cycles.

The variation of the Hodge structure on the middle cohomology.

As pointed out, for a given complex structure specified by, let us say, $\underline{z}_0$ the form $\Omega(\underline{z}_0)$ is of Hodge type $(n,0)$. At $\underline{z}_0$ one can, due to (4.4), choose a basis $\tilde{\gamma}^i_{p,q}$ of specific Hodge type (p,q), $p+q=n$, and express them with constant coefficients in terms of the topologically basis γ^i at $\underline{z}_0$, cf. eq. (4.7). If we vary the complex structure, say $\underline{z}_0 \to \underline{z}_0 + \delta z$, then in particular the n-form $\Omega(\underline{z}_0 + \delta z)$ gets admixtures of forms of other types compared to the original complex structure at $\underline{z}_0$. The period functions $\Pi_i(\underline{z})$ describe this *variation of Hodge structure*, cf. eq. (4.7). One could have studied analogs of eq. (4.7) for all forms of Hodge type $\tilde{\gamma}^i_{p,q}$ but for Calabi-Yau manifolds the period functions $\Pi_i(\underline{z})$ over the unique holomorphic form $\Omega(\underline{z}_0)$ play a special role, and many seemingly more general questions follow from them.

Mathematically, one captures this variation of the Hodge decomposition of the middle cohomology $H^n(M_n,\mathbb{C})$ in eq. (4.4)[6] in terms of the so-called *Hodge filtration of weight* $m=n$ with[7]

$$F^p H^m = \bigoplus_{l\geq p} H^{l,m-l}\,, \tag{4.8}$$

such that

$$H^m = F^0 H^m \supset F^1 H^m \supset \cdots \supset F^m H^m \supset F^{m+1} H^m = 0\,. \tag{4.9}$$

One can recover the Hodge decomposition in eq. (4.4) from the Hodge filtration $F^\bullet$ via the relations:

$$F^p H^m \oplus \overline{F^{m-p+1} H^m} = H^m \qquad \text{and} \qquad H^{p,m-p} = F^p H^m \cap \overline{F^{m-p} H^m}\,. \tag{4.10}$$

The Hodge cohomology groups come from what is more generally known as the *associated graded complex* of the filtered complex

$$\mathrm{Gr}_F^p H^m = F^p H^m / F^{p+1} H^m \cong H^{p,m-p}\,. \tag{4.11}$$

Unlike the $H^{p,q}$, the $F^p H^m$ vary holomorphically with the complex structure and fit into locally free constant sheaves $\mathcal{F}^p$ over $\mathcal{M}_{cs}$, with the inclusions $\mathcal{F}^p \subset \mathcal{F}^{p-1}$. This defines a *decreasing varying Hodge filtration* of the Hodge bundle $\mathcal{H}$ for the family

$$\mathcal{H} = \mathcal{F}^0 \supset \mathcal{F}^1 \supset \cdots \supset \mathcal{F}^n \supset \mathcal{F}^{n+1} = 0\,, \tag{4.12}$$

[6] We will often suppress the dependence of the cohomology groups on the manifold M_n, i.e., we simply write H^m for $H^m(M_n)$.

[7] A good and more thorough treatment of the variation of the Hodge structure and the limiting mixed Hodge structure can be found in ref. [106] and in relation with mirror symmetry in ref. [107].

where we suppressed the dependence on H^m since we understand that we work in the middle cohomology $m = n$. By construction $\mathcal{F}^0 = R^n\pi_*\mathbb{C} \otimes \mathcal{O}_{\mathcal{M}_{cs}}$ contains a local system, namely the locally constant sheaf $R^n\pi_*\mathbb{C}$. This defines a flat connection called the *Gauss-Manin connection*

$$\nabla : \mathcal{F}^0 \mapsto \mathcal{F}^0 \otimes \Omega^1_{\mathcal{M}_{cs}} . \tag{4.13}$$

The flat sections of the Gauss-Manin connection coincide with the local system $R^n\pi_*\mathbb{C}$, i.e., for f a holomorphic function on $\mathcal{M}_{\text{cs}}$ and s a flat section of $R^n\pi_*\mathbb{C}$, one defines ∇ by $\nabla(s \otimes f) = s \otimes \mathrm{d}f$. As before, one chooses in $\mathcal{H}$ the locally constant subsheaf $\mathcal{H}_{\mathbb{C}} = R^n\pi_*\mathbb{C}$, and within that an integer subsheaf $\mathcal{H}_{\mathbb{Z}} = R^n\pi_*\mathbb{Z}$. The quadruple $(\mathcal{H}, \nabla, \mathcal{H}_{\mathbb{Z}}, \mathcal{F}^\bullet)$ is called a variation of pure Hodge structures. One of the most important features is the *Griffiths transversality* of ∇:

$$\nabla\mathcal{F}^p \subset \mathcal{F}^{p-1} \otimes \Omega^1_{\mathcal{M}_{\text{cs}}} . \tag{4.14}$$

A modern language proof of eq. (4.14) can be found in ref. [114]. In every coordinate system that corresponds to a local trivialization of $\mathcal{H}$, the connection ∇ is the normal derivative, and for $\Omega(\underline{z}) \in \mathcal{F}^n$ one gets in particular [115]

$$\partial^k_{\underline{z}}\Omega(\underline{z}) \in \mathcal{F}^{n-|k|} , \tag{4.15}$$

with $\partial^k_{\underline{z}} := \partial^{k_1}_{z_1} \ldots \partial^{k_r}_{z_r}$ and $|k| = \sum_{i=1}^{h^{n-1,1}} k_i$. Let us note in passing that one can define a non-holomorphic connection that allows one to kill the starting terms from $\mathcal{F}^{n-|k|}$ in eq. (4.15). For example, we have $\partial_{z_k}\Omega(\underline{z}) \in \mathcal{F}^{n-1} = \mathcal{H}^{n,0} \oplus \mathcal{H}^{n-1,1}$, but one checks from eqs. (4.2) and (4.17) that the application of $D_k = \partial_{z_k} + (\partial_{z_k}K)$ yields $D_k\Omega(\underline{z}) \in \mathcal{H}^{n-1,1}$. Writing down higher iterations of this non-holomorphic connection with this property is more involved, but possible, and is known as *special Kähler geometry* for $n = 3$, and generalizes to higher dimensions, see, e.g., ref. [49].

Since eq. (4.15) is a cohomological inclusion into the finite-dimensional space $\mathcal{H}$, there must be, up to exact terms, linear relations between the derivatives. The coefficients of these linear relations turn out to be rational functions in the complex moduli $\underline{z}$. The relations form a finitely-generated differential ideal called the *Picard-Fuchs differential ideal*. One can find its generators $\mathcal{L}_i$, $i = 1, \ldots, r$ concretely, for example, by the *Griffiths reduction method* pioneered in ref. [116] or for Calabi-Yau spaces embedded in toric varieties by the *Gel′fand-Kapranov-Zelevinskǐ (GKZ) systems* [117], see also refs. [48, 118]. A complete Picard-Fuchs differential ideal is equivalent to the flat Gauss-Manin connection. In fact, it often allows one to construct more easily the global flat sections (and other important structures, like the n-points couplings [115], see section 4.2.2). Since exact terms vanish when integrated over

any closed cycle, the period functions are annihilated by the $\mathcal{L}_i$:

$$\mathcal{L}_i \Pi_*(\underline{z}) = 0 \qquad \text{for } i = 1, \ldots, r \,. \tag{4.16}$$

Here the index $*$ refers to period integrals in any basis. The differential ideal is complete if it has b_n independent solutions near any $\underline{z}_0 \in \mathcal{M}_{\text{cs}}$.

4.2.2 Quadratic relations from Griffiths transversality

In this section we explore an important consequence of Calabi-Yau geometries for the maximal cuts of Feynman integrals. More precisely, we will show that the Calabi-Yau geometry leads to quadratic relations among the maximal cuts (in integer dimensions). We limit the exposition here to the mathematical background, and we will describe the resulting relations explicitly in the context of the equal-mass banana integrals in $D = 2$ dimensions in section 5.2.

Our starting point is the Griffiths transversality in eq. (4.15). Combing eq. (4.15) with the first polarization condition in eq. (4.5) and considerations of type, one gets as a generalization of the observations of Bryant and Griffiths [115] for Calabi-Yau manifolds in any dimension n:

$$\underline{\Pi}(\underline{z})^T \, \mathbf{\Sigma} \, \partial_{\underline{z}}^{\underline{k}} \underline{\Pi}(\underline{z}) = \int_{M_n} \Omega \wedge \partial_{\underline{z}}^{\underline{k}} \Omega = \begin{cases} 0 & \text{for } 0 \leq r < n \\ C_{\underline{k}}(\underline{z}) & \text{for } |k| = n \end{cases} \,, \tag{4.17}$$

where the $C_{\underline{k}}(\underline{z})$ are rational functions in the complex structure parameters $\underline{z}$. For the first equality in eq. (4.17), we used eq. (4.7) and the properties of the integer basis described earlier. The second equality follows very generally from eqs. (4.15) and (4.5). We point out that even in an arbitrary local basis $\underline{\tilde{\Pi}}(\underline{z})$ corresponding to an (implicit) choice of a basis of cycles $\tilde{\Gamma}^i \in H_n(M_n, \mathbb{C})$ (obtained, for example, as independent local solutions of the Picard-Fuchs differential ideal), one can find a $\tilde{\mathbf{\Sigma}}$ and write down the corresponding relations $\underline{\tilde{\Pi}}(\underline{z})^T \, \tilde{\mathbf{\Sigma}} \, \partial_{\underline{z}}^{\underline{k}} \underline{\tilde{\Pi}}(\underline{z})$ among the solutions very explicitly.

The quadratic relations in eq. (4.17) have important implications for Feynman integrals. Since the vector of periods $\underline{\Pi}(\underline{z})$ describes the maximal cuts, the relations in eq. (4.17) can equally be interpreted as a *set of quadratic relations among the maximal cuts*! Note that these relations are not obvious from a pure physics point of view, e.g., the momentum-space representation of the Feynman integrals. We will describe these relations among maximal cuts explicitly for the equal-mass banana integrals in section 5.2. Here we only mention that for the equal-mass banana graphs one finds $l(l+1)/2$ quadratic relations for $l - 1 = n$ even and $l(l-1)/2$ for n odd. The reason for this difference is that in the latter case the intersection form $\mathbf{\Sigma}$ is antisymmetric, so symmetric quadratic relations are trivially fulfilled.

The n-point (Yukawa) couplings and self-adjoint operators

In order to understand the quadratic relations in eq. (4.17) and to write them down explicitly, we need to know the functions $C_{\underline{k}}(\underline{z})$, sometimes referred to as the *Yukawa n-point couplings*. They can be obtained from the rational coefficients in front of the derivatives in the Picard-Fuchs differential operators, if and only if the latter generate the Picard-Fuchs ideal completely, see ref. [49] for details.

If the Picard-Fuchs differential ideal is generated by a single differential operator (see [45] for a proof) with normalization such that

$$\mathcal{L}^{(n+1)} = \partial_z^{n+1} + \sum_{i=0}^{n} a_i(z)\, \partial_z^i \,, \tag{4.18}$$

then the Yukawa coupling fulfills the differential equation

$$\frac{\partial_z C_n(z)}{C_n(z)} = \frac{2}{n+1} a_n(z) \,. \tag{4.19}$$

One can define the *adjoint differential operator* [119]

$$\mathcal{L}^{*(n+1)} = \sum_{i=0}^{n+1} (-\partial_z)^i \, a_i(z) \,. \tag{4.20}$$

An operator is called *essentially self-adjoint* if

$$\mathcal{L}^{*(n+1)} A(z) = (-1)^{n+1} A(z) \mathcal{L}^{(n+1)} \,, \tag{4.21}$$

where $A(z)$ satisfies the differential relation $\frac{\partial_z A(z)}{A(z)} = \frac{2}{n+1} a_n(z)$. Note that $A(z)$ is up to a multiplicative constant given by the Yukawa coupling $C_n(z)$. It was noticed in the search for Calabi-Yau operators [120] that the self-adjointness of an abstractly constructed differential operator with regular singularities implies that the solutions admit an even or odd intersection form for n even or odd, respectively, if $A(z)$ is an algebraic function. This gives an easy criterium to decide whether one-parameter specializations of Picard-Fuchs operators can come from a Calabi-Yau motive[8]: This can only be the case if eqs. (4.21) and (4.17) are fulfilled and in addition the global monodromy is in $O(\mathbf{\Sigma}, \mathbb{Z})$. In other words, imagine that the maximal cut of a Feynman integral depends on a single dimensionless variable (if there are more kinematic variables, we may consider a one-parameter slice in the rescaled kinematic space), and that its maximal cut is annihilated by some Picard-Fuchs operator

[8] By a motive we mean in this thesis a subspace of the cohomology group $H^r(X)$ for $0 \leq r \leq 2n$ of a n-dimensional variety X that is compatible with the Hodge decomposition and the action of the Galois group. For a more precise definition we refer to [47] or to the mathematical literature [121, 122].

$\mathcal{L}^{(n+1)}$. The previous discussion gives an easy criterion to determine from the Picard-Fuchs operator if the Feynman integral is associated with a Calabi-Yau motive. One can check that this criterion is satisfied for all the Picard-Fuchs operators for the maximal cuts of the banana integrals in $D = 2$ dimensions. On the other hand in dimensional regularization, i.e. $D = 2 - 2\epsilon$, these Picard-Fuchs operators cease to be self-adjoint as can be seen in [47].

4.2.3 Monodromy and limiting mixed Hodge structure on the boundary of $\mathcal{M}_{cs}$

Now we turn in this section to the structures related to the boundaries of the moduli space that are related to the special monodromies of the periods when we analytically continue them around the critical divisors which form the boundaries of $\mathcal{M}_{cs}$. This will give additional structures to the periods which also characterizes the upcoming period functions a lot. Additionally, this will constrain the form of the l-loop banana Feynman integral considerably such that at the end together with mirror symmetry it is possible to determine these completely in $D = 2$ dimensions.

A normal crossing model for the boundaries of $\mathcal{M}_{cs}$.

By going in a loop γ_{Δ_k} from a base-point $\underline{z}_0$ around a divisor given by $\Delta_k(\underline{z}) = 0$, induces a monodromy on the period integrals,[9] and hence on the maximal cut Feynman integral identified with the latter. These monodromies are very characteristic for the type of singularity that the fibre $M_{\{\Delta_k=0\}}$ over $\{\Delta_k(\underline{z}) = 0\}$ acquires. The branching behavior of the periods at all crictical loci is crucial to understand the analytic structure of the Feynman integral in all regions of its physical parameters. Mirror symmetry suggests that Calabi-Yau n-folds have a maximal degenerate singular point (see subsection 3.3.1) in their complex moduli space, called point of *maximal unipotent monodromy*. This point was identified with the large momentum regime of the banana integrals in ref. [45] and used with the monodromy at other singularities to clarify the analytic structure of these integrals in $D = 2$ dimensions completely to all loop orders.

The boundary of the moduli space $\mathcal{M}_{cs}$ refers to the critical divisors at which the Calabi-Yau fibre becomes singular. As we mentioned in section 4.1, we assume to be able to compactify and to resolve the moduli space to achieve a situation where all divisors are normal crossing in the compactified moduli space $\overline{\mathcal{M}}_{cs}$. We refer to $\mathcal{M}_{cs}$ as $\mathcal{M}_{cs} = \overline{\mathcal{M}}_{cs} \setminus D$, where D is a divisor with normal crossings, $D = \bigcup_k D_k$.

Let us begin with explainining how we can find the boundary components $\Delta_k(\underline{z}) = 0$. The first method to find them is to identify the sub-loci of $\mathcal{M}_{cs}$ over which the fibre of the family becomes singular. For example, for a Calabi-Yau manifold defined by $P_1 = \ldots = P_s = 0$, we have to find values in $\overline{\mathcal{M}}_{cs}$ such that $P_1 = \ldots = P_s = 0$ and $\mathrm{d}P_1 \wedge \ldots \wedge \mathrm{d}P_s = 0$ admits a solution. We can also determine the critical loci from the Picard-Fuchs differential ideal J that is generated by differential operators of order ord_k, $\mathcal{L}_k^{\mathrm{ord}_k}(\underline{z}, \partial_{\underline{z}}) \in \mathbb{C}\left[z_1, \ldots, z_m, \partial_{z_1}, \ldots, \partial_{z_m}\right]$,

[9] See section 4.2.1 for a detailed introduction to period integrals on Calabi-Yau varieties.

$k = 1, \ldots, |J|$. We can replace the derivatives $\partial_{z_i} \mapsto \xi_i$, $i = 1, \ldots, m = \dim(M_{\text{cs}})$ by formal variables $\underline{\xi}$ to get $|J|$ elements in the polynomial ring in $\underline{z}$ and $\underline{\xi}$. Then we consider the smallest differential ideal that characterizes the periods and restrict to the leading pieces, i.e., to the elements $S_k(\underline{z}, \underline{\xi}) := \mathcal{L}_k^{\text{ord}_k}(\underline{z}, \underline{\xi})\Big|_{\deg(\xi)=\text{ord}_k}$, which are homogeneous of order ord_k in the variables $\underline{\xi}$. One refers to the S_k as the *symbol* of the differential operator $\mathcal{L}_k^{\text{ord}_k}$. The critical loci $\tilde{\Delta}_j(\underline{z}) = 0$ are now given by the resultant of the $S_k(\underline{z}, \underline{\xi}) = 0$ in the $\underline{z}$ parameters, i.e., resultant$(\{S_k(\underline{z}, \underline{\xi}) = 0,\ \forall k\}, \underline{z})$. The resultant characterizes all divisors $\tilde{\Delta}_j(\underline{z}) = 0$ for which the system $\{S_k(\underline{z}, \underline{\xi}) = 0,\ \forall k\}$ has non-trivial solutions and it contains, in particular, the critical divisors of the family. For the Picard-Fuchs ideal generated by a single ordinary differential operator in one variable this amounts to find all zeroes of the coefficient of the highest derivative for $z \in \mathbb{P}^1$. This second method to find the boundary components is in general superior as it detects also the apparent singularities, which are not present in our examples of the banana family as can be checked since both methods lead to the same result.

Let us note that for moduli spaces $\overline{\mathcal{M}}_{\text{cs}}$ of dimension greater than one, non-generic intersections, e.g., tangencies of order m between the $\{\tilde{\Delta}_k(z) = 0\}$ or singularities of the $\{\tilde{\Delta}_k(z) = 0\}$, generally occur. In a procedure that can involve several steps of blow ups, they can be resolved to achieve a geometry of $\overline{\mathcal{M}}_{\text{cs}}$ with only normal crossing divisors. Adding all the exceptional divisors of the blow ups, the critical locus $D \subset \overline{\mathcal{M}}_{\text{cs}}$ is described as the set of irreducible normal crossing divisors $\{D_k\}$, $k = 1, \ldots, \#D$. Normal crossing means that locally we can describe the intersections of components in D as $w_1 = 0, \cdots, w_p = 0$, $p \leq r$ in local coordinates w_i, $i = 1, \ldots, r = \dim(\mathcal{M}_{\text{cs}})$. In this case we say that the family $\pi : \mathcal{M}_n \to \mathcal{M}_{\text{cs}}$ can be extended to a family $\overline{\pi} : \overline{\mathcal{M}}_n \to \overline{\mathcal{M}}_{\text{cs}}$. Concrete examples for the blow up procedure in Calabi-Yau moduli spaces can be found in refs. [96, 97].

Local and global monodromies.

We now analyze the monodromies that the vectors of periods undergo, when we take $\underline{z}$ around a loop γ_{Δ_i} around the critical divisor D given by $\Delta_i(z) = 0$. We illustrate this first on the example of a one-parameter differential operator $\mathcal{L}$ of order l. In that case, the compactification of $\mathcal{M}_{\text{cs}}$ is $\mathbb{P}^1$, and the divisors are just isolated points, $\Delta_i(z) = z - z_i$, $i = 1, \ldots, \#p_{\text{crit}}$. We can find a basis for the solution space at z_0 using the Frobenius method we explained in subsection 3.3.1.

Let us discuss in some detail the case of the Legendre family $\mathcal{E}_{\text{Leg}}$ of elliptic curves. This family is defined by the cubic constraint

$$y^2 = x(x-1)(x-z) \tag{4.22}$$

in $\mathbb{P}^2$ in the patch where we have set the third coordinate $w = 1$. The corresponding Picard-Fuchs equation is given by the operator

$$\mathcal{L}_{\text{Leg}} = z^2(1-z)\partial_z^2 + z(1-2z)\partial_z - z/4 = \theta^2 - z(\theta - 1/2)^2\,. \tag{4.23}$$

and the periods are solutions to $\mathcal{L}_{\text{Leg}} = 0$. We can apply the Frobenius method and solve the indicial equation for each singular point $z_0 \in \{0, 1, \infty\}$. The local exponents at all critical points are summarized in the Riemann $\mathcal{P}$-symbol:

$$\mathcal{P}_{\text{Leg}} \left\{ \begin{array}{ccc} 0 & 1 & \infty \\ \hline 0 & 0 & \frac{1}{2} \\ 0 & 0 & \frac{1}{2} \end{array} \right\} . \tag{4.24}$$

Since the local exponents at each singular point are equal to α, say, at each singular point there is a power series solution $\omega(\Delta) = \Delta^\alpha + \mathcal{O}(\Delta^{\alpha+1})$ (with $\Delta = z - z_0$) and a logarithmic solution $\hat{\omega}(\Delta) = \frac{m}{2\pi i}\omega(\Delta)\log(\Delta) + \mathcal{O}(\Delta^\alpha)$. In particular, if $\alpha \in \mathbb{Z}$, then the period vector transforms for a positively oriented loop γ_{Δ_i} around $\Delta_i(z) = 0$ with a $\mathbf{T}_{\gamma_{\Delta_i}}$ monodromy matrix

$$\begin{pmatrix} \hat{\omega} \\ \omega \end{pmatrix} \mapsto \begin{pmatrix} 1 & m \\ 0 & 1 \end{pmatrix} \begin{pmatrix} \hat{\omega} \\ \omega \end{pmatrix} =: \mathbf{T}_{\gamma_{\Delta_i}} \begin{pmatrix} \hat{\omega} \\ \omega \end{pmatrix} . \tag{4.25}$$

In particular, let the period be $\omega(\Delta) = \int_{S^1_\nu} \mathrm{d}x/y(z)$ and the dual period defined over the dual cycle be $\hat{\omega}(\Delta) = \int_{S^1_{\hat{\nu}}} \mathrm{d}x/y(z)$. Without loss of generality we can assume that $S^1_\nu = S^1_a$ and $S^1_{\hat{\nu}} = mS^1_b$ in an integral symplectic basis (a, b) of $H_1(E, \mathbb{Z})$. Then m has to be an integer. Generally, a monodromy matrix $\mathbf{T}$ in an integral basis has to be integral and has to respect the intersection form, $\mathbf{T}^T \boldsymbol{\Sigma} \mathbf{T} = \boldsymbol{\Sigma}$. We denote the group of all integer matrices that respect the intersection form $\boldsymbol{\Sigma}$ on the middle cohomology of rank $b_n(M) = r$ (or the rank of the Calabi-Yau motive r) by

$$\mathrm{O}(\boldsymbol{\Sigma}, \mathbb{Z}) = \left\{ \mathbf{T} \in \mathrm{GL}(r, \mathbb{Z}) \;\middle|\; \mathbf{T}^T \boldsymbol{\Sigma} \mathbf{T} = \boldsymbol{\Sigma} \right\} . \tag{4.26}$$

The subgroup of $\mathrm{O}(\boldsymbol{\Sigma}, \mathbb{Z})$ that is generated by the actual monodromies of the family is denoted by $\Gamma_{\mathcal{M}_n}$. For example, in odd dimensions n, the intersection pairing $\boldsymbol{\Sigma}$ is the standard symplectic pairing, and so $\Gamma_{\mathcal{M}_n}$ has to be a subgroup of the group of integral symplectic matrices $\mathrm{Sp}(b_n, \mathbb{Z})$. In particular, for elliptic curves ($n = 1$), it is a subgroup of $\mathrm{SL}(2, \mathbb{Z})$. Note that the Kähler potential in eq. (4.2) is single-valued under all monodromies.

A famous theorem of Landman [123] states that all possible monodromy matrices on an algebraic n-dimensional manifold have to obey

$$(\mathbf{T}^k - \mathbb{1})^{n+1} = 0 . \tag{4.27}$$

Here $k \in \mathbb{N}_0$ implies that the indicial α has to be a rational number. A monodromy matrix $\mathbf{T}$ can be unipotent of lower order $m < n$, i.e., $(\mathbf{T}^k - \mathbb{1})^{m+1} = 0$. It is clear that m is the size of the biggest Jordan block in $\mathbf{T}$. The maximal n that can appear is $n = \dim(M)$. It is not

too hard to see that the unipotency of order $m \leq n$ implies that a period on a n-dimensional manifold cannot degenerate worse than with a logarithmic singularity of type $\log(\Delta)^n$. This has an important consequence for Feynman integrals. Assume that we have a maximal cut of a Feynman integral in integer dimensions that degenerates in a dimensionless physical parameter Δ (or, more generally, some polynomial combination thereof) as $\log(\Delta)^m$. Then it follows from Landman's theorem that the geometry associated to this integral cannot be an algebraic manifold of dimension less than m, or a Calabi-Yau motive of weight less than m!

In the example of the Legendre family $\mathcal{E}_{\text{Leg}}$ one sees that for $z_0 \in \{0, 1, \infty\}$ the curve is singular, i.e., $P = 0$ and $\mathrm{d}P = 0$ have at least one common solution. This happens at a point on the curve, say $(x, y) = (x_0, y_0)$ (we assume that the singularity is not at $w = 0$ and use again the corresponding local patch $w = 1$). Using local coordinates $(x, y) = (x_0 + \tilde{\epsilon}_x, y_0 + \tilde{\epsilon}_y)$ the expansion around this point is given after a linear change in the deformation parameters up to quadratic order by $P = \epsilon_x^2 + \epsilon_y^2 = 0$. Allowing in addition small perturbations around the critical point $z = z_0 + \mu$ in $\mathcal{M}_{\text{cs}}$, the local singularity becomes

$$\epsilon_x^2 + \epsilon_y^2 = \mu^2 \,. \tag{4.28}$$

This describes a node, where a S^1-cycle ν shrinks with $\mu \to 0$. The vanishing S^1-cycle ν can be literally seen by taking the real slice of the equation (4.28), which describes the S^1 with radius $r^2 = \mathrm{Re}(\mu)^2$. This can be generalized to higher dimensions and the period integral over the S^n can be performed perturbatively, see eq. (3.3) in ref. [124]. The corresponding critical locus in $\mathcal{M}_{\text{cs}}$ is hence a conifold, while the singularity in the fibre is a node. The corresponding monodromy follows purely topologically from the Picard-Lefshetz formula

$$W(\Gamma) = \Gamma + (-1)^{(n+1)(n+2)/2}(\Gamma \cap \nu)\nu \,, \tag{4.29}$$

in any dimension n, see ref. [125] for a clarification regarding the signs in higher dimensions. The formula says that the conifold monodromy action W on any cycle $\Gamma \in H_n(M, \mathbb{Z})$, which can be identified (up to finite multi-covering issues in the choice of parametrization $\underline{z}$ of $\mathcal{M}_{\text{cs}}$) with the monodromy on the periods, depends only on its intersection with the vanishing cycle. Together with the self intersection of n spheres in projective n-folds [125],

$$S^n \cap S^n = \begin{cases} 0 & \text{for } n \text{ odd}\,, \\ 2(-1)^{\frac{n}{2}} & \text{for } n \text{ even}\,, \end{cases} \tag{4.30}$$

eqs. (4.29) and (4.30) give eq. (4.25) with $S^1_{\hat{\nu}} \cap S^1_{\nu} = -m$. They also imply something completely general for the degenerations of Feynman integrals. If the maximal cut integral corresponds to a period of a n-dimensional algebraic variety, then the most generic singularity will be a square root cut if n is even, and a logarithmic cut if n is odd (cf. the fact that $(l = n + 1)$-loop banana integrals have square roots cuts when l is odd and only logarithmic

singularities when l is even). This follows simply because eqs. (4.29) and (4.30) imply in odd dimensions an infinite-order operation, a so-called *symplectic reflection*, and in even dimensions a standard *Euclidean $\mathbb{Z}_2$-reflection*.

A simple application of this structure is that the logarithmic/square root cut behavior of the solutions to the Picard-Fuchs differential ideal at the conifold detects uniquely the period over the geometric vanishing cycle. As an actual cycle the latter might contain information about to the Feynman integral. Let us illustrate this for the banana integrals. In section 2.8 we have argued that as a consequence of the optical theorem, the imaginary part of the banana integral is proportional to a specific maximal cut. The corresponding cycle must be such that this maximal cut vanishes at the threshold $z = 1/(l+1)^2$, which is a conifold divisor. There is a unique period that vanishes at this conifold divisor, and so this period corresponds to the maximal cut that describes the imaginary part of the banana integral above threshold [45]. Note that the cycle that describes the imaginary part is different from the cycles T^l or Γ_T which give rise to the maximal cut in eq. (2.44), and we will comment further on this at the end of the this section.

The analysis of the solutions from the Picard-Fuchs differential ideal or eq. (4.29) yields the local monodromies. To determine the global monodromy group $\Gamma_{\mathcal{M}_n}$ in an integral symplectic basis requires global knowledge of the periods. For the elliptic curve case this can be obtained by analyzing the behavior of the explicit elliptic integrals near the critical points. Let the period vector of the Legendre curve be $(\Pi_b, \Pi_a) = (\int_b \Omega, \int_a \Omega)$, and let Π_b be the logarithmic period as in eq. (4.25). Then, up to $\mathrm{SL}(2,\mathbb{Z})$ conjugation, the monodromy group $\Gamma_{\mathcal{E}_{\text{Leg}}}$ of the Legendre family is generated by the following two matrices (we use here the notation $\mathbf{T}_{\gamma_{z-a}} =: \mathbf{T}_a$ with $a \in \{0, 1, \infty\}$):

$$\mathbf{T}_0 = \begin{pmatrix} 1 & 2 \\ 0 & 1 \end{pmatrix} \qquad \text{and} \qquad \mathbf{T}_1 = \begin{pmatrix} 1 & 0 \\ -2 & 1 \end{pmatrix} . \tag{4.31}$$

One can check that these matrices generate the congruence subgroup $\Gamma(2)$ of index 6 in $\mathrm{SL}(2,\mathbb{Z})$, and so the monodromy group of the Legendre family is $\Gamma_{\mathcal{E}_{\text{Leg}}} = \Gamma(2)$. One can also check that the matrices in eq. (4.31) satisfy Landman's theorem in eq. (4.27) with $n = k = 1$. Due to the obvious relation by successively going around all the loops γ_{Δ_i} for $i = 1, 2, 3$ in $\mathbb{P}^1$ one has $\mathbf{T}_0\mathbf{T}_1\mathbf{T}_\infty = \mathbb{1}$, and therefore $\mathbf{T}_\infty = \begin{pmatrix} 1 & -2 \\ 2 & -3 \end{pmatrix}$. We can conjugate the basis by $\Pi_b \to \Pi_b, \Pi_a \to \Pi_a + \Pi_b$ to get $\mathbf{T}^c_\infty = \begin{pmatrix} -1 & 2 \\ 0 & -1 \end{pmatrix}$. Comparing with eq. (4.27), we see that $\mathbf{T}^c_\infty$ (and thus also $\mathbf{T}_\infty$) satisfies Landman's theorem with $k = 2$ and $n = 1$. For the differential equation associated to the banana graph one finds the corresponding monodromy group to be $\Gamma_{\mathcal{E}_{\text{ban}_2}} = \Gamma_1(6)$, cf. refs. [20, 24, 78]. Finding the integral basis and the monodromy group $\Gamma_{\mathcal{M}_n}$ for families of higher-dimensional Calabi-Yau manifolds with higher-dimensional moduli spaces can become a formidable task. We comment on some strategies to do this at the very end of this section.

It follows generally from eq. (4.27) that $\mathbf{T}$ can always be factored as $\mathbf{T} = \mathbf{T}^{(s)}\mathbf{T}^{(u)}$, where $\mathbf{T}^{(s)}$ is semi-simple and of finite order and $\mathbf{T}^{(u)}$ is unipotent, i.e., $(\mathbf{T}^{(u)} - \mathbb{1})^{n+1} = 0$. For example, all singularities of the fibres in the Legendre family $\mathcal{E}_{\text{Leg}}$ are nodes and a homologically different cycle S^1_Γ with Γ primitive in $H_1(E, \mathbb{Z})$ vanishes at each conifold point. The square root cut at $z = \infty$ ($k = 2$), as well as the shifts by two at the other points, are due to the global choice of the parameter z. Locally, one can get rid of the semi-simple piece by choosing different local variables, e.g., for the Legendre family at $z = \infty$, one can choose $v = \sqrt{w}$ instead of $w = 1/z$. Only for elliptic curves the conifold points are also MUM-points.

The limiting mixed Hodge structure.

The general situation of more involved singularities in families with higher-dimensional fibers is described by the limiting mixed Hodge structure. The first statement of Deligne [126] is that the bundle $\mathcal{F}^0$ on $\mathcal{M}_{\text{cs}}$ has a canonical extension $\overline{\mathcal{F}^0}$ over $\overline{\mathcal{M}}_{\text{cs}}$. As we have learned from the theorem of Landman applied to the monodromy matrices, the forms the singularities of $\overline{\mathcal{F}^0}$ are only logarithmic. This is referred also as regular singularities (see section 3.3), and allows one to define an extension of the Gauss-Manin connection to

$$\overline{\nabla} : \overline{\mathcal{F}^0} \to \overline{\mathcal{F}^0} \otimes \Omega^1_{\overline{\mathcal{M}}_{\text{cs}}}(\log(D)) \,. \tag{4.32}$$

Here $\Omega^1_{\overline{\mathcal{M}}_{\text{cs}}}(\log(D))$ are meromorphic one-forms on $\overline{\mathcal{M}}_{\text{cs}}$ which can have the indicated logarithmic coefficients. In local coordinates where the divisor D is defined by $z_1 = \cdots = z_p = 0$, $\Omega^1_{\overline{\mathcal{M}}_{\text{cs}}}(\log(D))$ is generated by $\mathrm{d}z_1/z_1, \ldots, \mathrm{d}z_p/z_p, z_{p+1}, \ldots, z_r$. This means that in the first-order form of the Picard-Fuchs equation, the entries in the matrix $\tilde{\mathbf{A}}(z)$ in eq. (3.3) for families of any dimension of fibre and base can have only first-order poles at the singular loci! Locally, we can model $\mathcal{M}_{\text{cs}}$ as products of punctured discs $(\mathfrak{D}^*)^r$ and $\overline{\mathcal{M}}_{\text{cs}}$ as products of full discs $(\mathfrak{D})^r$. We assume to have changed coordinates such that we got rid of the semi-simple piece, and that going clockwise around a loop in the k^{th} disc we generate the unipotent piece $\mathbf{T}^{(u)}_k$ of the monodromy. We define

$$\mathbf{N}_k = -\log(\mathbf{T}^{(u)}_k) = -\log(1 + [\mathbf{T}^{(u)}_k - 1]) = \sum_{l=1}^{\max\left|J_{\mathbf{T}^{(u)}_k}\right|} (-1)^l [\mathbf{T}^{(u)}_k - 1]^l / l \,. \tag{4.33}$$

It is obvious that the sum is bounded by the maximal size of a Jordan block in $\mathbf{T}^{(u)}_k$. Now a section s of $\mathcal{F}^0$ defined on $(\mathfrak{D}^*)^r$ transforms like $s \mapsto \mathbf{T}^{(u)}_k s$, but one can construct a monondromy invariant section $\bar{s}$, i.e., one that is single-valued on $(\mathfrak{D}^*)^r$, by

$$\bar{s} = \exp\left(-\frac{1}{2\pi i}\sum_{k=1}^{r} N_k \log(z_k)\right) s =: \mathcal{O}(\underline{N})s \,, \tag{4.34}$$

and extend it canonically over $\mathfrak{D}^r$. This defines a natural extension of $\overline{\mathcal{F}^0}$ over $\mathfrak{D}^r$. The so-called nilpotent orbit theorem of W. Schmid [127] guarantees further that the $\mathcal{F}^p$ extend in a canonical way to sub-bundles $\overline{\mathcal{F}^p}$ of $\overline{\mathcal{F}^0}$ that extend the fibration in eq. (4.9) to $\mathfrak{D}^r$. In particular, at the origin $z = 0 \in \mathfrak{D}^r$, the $\overline{\mathcal{F}^p}$ define the *limiting Hodge filtration* $F^p_{\lim}$. The N_k fulfill a transversality $N_k(F^p_{\lim}) \subset F^{p-1}_{\lim}$ like the Griffiths transversality in eq. (4.14). One can show that the action of the extension of the Gauss-Manin connection $\overline{\nabla}_{\theta_k}$ (with $\theta_k = z_k \partial_{z_k}$) to $\mathfrak{D}^r$ becomes proportional to the action of N_k on $F^p_{\lim}$ as well as on $\mathrm{Gr}^p_{\lim} = F^p_{\lim}/F^{p+1}_{\lim}$:

$$\overline{\nabla}_{\theta_k} = -\frac{1}{2\pi i} N_k \,. \tag{4.35}$$

Also a section $s_{\mathbb{Z}} \in \mathcal{H}_{\mathbb{Z}}$ of the integer local system $\mathcal{H}_{\mathbb{Z}}$ on $\mathfrak{D}^r$ can be extended as $\bar{s}_{\mathbb{Z}} = \mathcal{O}(\underline{N}) s_{\mathbb{Z}}$ to $\mathfrak{D}^r$ and defines an integral structure $\bar{s}_{\mathbb{Z}}(0)$ over $z = 0$. However, there is a freedom in the choice of coordinates on the discs $\mathfrak{D}^r$. More precisely, the change of coordinates $\underline{z} \to \underline{\tilde{z}}(\underline{z})$ induces a choice $\exp\left(2\pi i \alpha_k (d\tilde{z}/dz)_k(0) N_k\right)$, referred to as nilpotent orbit, in the choice of the integral structure $\bar{s}_{\mathbb{Z}}(0)$.

The second filtration of the *limiting mixed Hodge structure* at the boundary is the ascending *monodromy weight filtration*:

$$W_\bullet : W_0 \subset W_1 \subset \cdots \subset W_{2n-1} \subset W_{2n} = H^n(M_{\underline{z}}, \mathbb{C}) \,, \tag{4.36}$$

with $\mathrm{Gr}^W_k = W_p / W_{p-1}$. The spaces $W_\bullet$ are defined by the action of the operator

$$\begin{aligned} &\text{(i.)} && N(W_k) \subset N(W_{k-2}) \,, \\ &\text{(ii.)} && N^k : \mathrm{Gr}^W_{n+k} \xrightarrow{\sim} \mathrm{Gr}^W_{n-k} \,. \end{aligned} \tag{4.37}$$

The first few and the last $W_\bullet$ are explicitly given by

$$\begin{aligned} W_0 &= \mathrm{Im}(N^n) \,, \\ W_1 &= \mathrm{Im}(N^{n-1}) \cap \mathrm{Ker}(N) \,, \\ W_2 &= \mathrm{Im}(N^{n-2}) \cap \mathrm{Ker}(N) + \mathrm{Im}(N^{n-1}) \cap \mathrm{Ker}(N^2) \,, \\ &\vdots \\ W_{2n-1} &= \mathrm{Ker}(N^n) \,. \end{aligned} \tag{4.38}$$

A key point is that $F^\bullet_{\lim}$ induces a Hodge structure of pure weight k on Gr^W_k [127], and the triple $(s_{\mathbb{Z}}(0), F^\bullet_{\lim}, W_\bullet)$ fits together to define a polarized limiting mixed Hodge structure. Its

limiting Hodge diamond is given according to Lemma 1.2.8 of ref. [104] by (see also ref. [128])

$$H_{\lim}^{p,q} = F_{\lim}^{p} \cap W_{p+q} \cap (\bar{F}_{\lim}^{p} \cap W_{p+q} + \sum_{j\geq 1} \bar{F}_{\lim}^{q-j} \cap W_{p+q-j-1}) \,, \tag{4.39}$$

with the property that $W_l = \oplus_{p+q\leq l} H_{\lim}^{p,q}$, $F_{\lim}^{p} = \oplus_{r\geq p} H_{\lim}^{r,s}$, $H_{\lim}^{p,q}$ projects isomorphically to $H^{p,q}(\mathrm{Gr}_{p+q}^{W})$ and $H_{\lim}^{p,q} = \overline{H^{p,q}}_{\lim}$ (mod W_{p+q-2}). From the Feynman integral point of view, one would like to have an application of this structure like for the conifold, i.e., one that relates the branching behavior of the periods to the singularity type in the fibre and predicts something concrete about the integral. Consider a filtration of a complex $K^\bullet$, with the standard definition $\mathrm{d}\cdot\mathrm{d} = 0$ and the cohomology $H^\bullet(K^\bullet) = \oplus_{p\geq 0} H^p(K^\bullet)$, where $H^p(K^\bullet) = \frac{Z^p}{\mathrm{d}K^{p-1}}$ and $Z^p = \ker\{\mathrm{d} : K^p \to K^{p+1}\}$ are cycles while $\mathrm{d}K^{p-1} = B^p \in Z^p$ are boundaries. One gets a spectral sequence $E_r = \oplus_{p,q\geq 0} E_r^{p,q}$ with $\mathrm{d}_r : E_r^{p,q} \to E_r^{p+1,q-r+1}$, $\mathrm{d}_r\cdot\mathrm{d}_r = 0$ and $H^\bullet(E_r) = E_{r+1}$, and this spectral sequence typically converges, i.e., there is an r_0 so that $E_r = E_{r+1} = \ldots =: E_\infty^{p,q}$ for all $r \geq r_0$. One says that E_r *degenerates* at r_0 and *abuts* to $H^\bullet(K^\bullet)$. The spectral sequence that comes from the filtration of K is given by

$$\begin{aligned} E_0 &= F^p K^{p+q}/F^{p+1}K^{p+q}, \\ E_1^{p,q} &= H^{p+q}(\mathrm{Gr}^p K^\bullet), \\ E_r^{p,q} &= \frac{\{c \in F^p K^{p+q} | \mathrm{d}c \in F^{p+r}K^{p+q+1}\}}{\mathrm{d}F^{p-r+1}K^{p+q+1} + F^{p+1}K^{p+q}}, \\ &\vdots \\ E_\infty^{p,q} &= \mathrm{Gr}^p(H^{p,q}(K^\bullet)) \,. \end{aligned} \tag{4.40}$$

A statement that relates logarithmic degenerations generally to the structure of the singularity of the fibre $M_0 = \pi^{-1}(0)$ in $\pi : M \mapsto \mathfrak{D}$, or rather to its resolutions, is as follows: If by a chain of blow ups the singularity of M_0 can be made to a reduced divisor E with normal crossing components E_i for $i = 0, \ldots, k$, then the Hodge spectral sequence based on $F_{\lim}^\bullet$ degenerates at ${}_{F_{\lim}}E_1^{pq}$, while the *monodromy weight spectral sequence* degenerates at ${}_W E_2$, and one has [106, 120]

$${}_W E_1^{p,q} = \bigoplus_{k=0}^{2p} H^{q+2(p-k)}(E[2p-k], \mathbb{Q}) \,, \tag{4.41}$$

where we define $E[k]$ by the disjoint union as $E[k] = \coprod_I E_{i_0} \cap E_{i_1} \cap \cdots \cap E_{i_k}$, $I = \{i_0 < i_1 < \cdots < i_k\}$. In particular, $E_1^{p,0}$ is identified with the complex $0 \to H^0(D[0]) \to H^0(D[1]) \to \cdots \to H^0(D[2n]) \to 0$ and $\mathrm{Gr}_0^W H_{\lim}^k(M_0) = H^k(\Gamma_I)$, where Γ_I is the dual intersection complex of M_0. What we said about the limiting mixed Hodge structures and monodromies in this section does not require the Calabi-Yau property $c_1(M) = 0$. Calabi-Yau manifolds, however, have generically a MUM-point.

A point of *maximal unipotent monodromy* short MUM-point fulfills the following conditions:

(i.) The point is defined by $P = \bigcap_{i=1}^{r} D_i$ in an r-dimensional moduli space $\mathcal{M}_{\text{cs}}$ and all monodromies $T_{\gamma_{D_i}}$ corresponding to the loops around all normal crossing divisors D_i are unipotent.

(ii.) One has $\dim(W_0) = \dim(W_1) = 1$ and $\dim(W_2) = 1 + r$.

(iii.) For a basis $g^0, g^1, \ldots, g^r$ of W_2, with g^0 a basis of W_0 and N_k defined by eq. (4.33), the $r \times r$ matrix m_k^j, $j, k = 1, \ldots, r$ defined by $N_k g^j = m_k^j g^0$ is invertible.

These criteria given in ref. [129] might be sufficient, but there are easier necessary conditions in many cases. For example, for one-parameter Calabi-Yau three-folds with fourth-order differential operators, it is sufficient that all four local exponents α are equal [120] at z_0 to make z_0 a MUM-point. More generally, one can characterize the MUM-point by demanding that at z_0 the solutions of the leading order symbols of the complete set of generators of the differential ideal should be completely degenerate with local exponent α, say, and that there is one normalized holomorphic solution $\varpi_0(\underline{z}) = z^\alpha + \mathcal{O}(\underline{z}^{1+\alpha})$ with this local exponent and r independent single logarithmic solutions of the form $\varpi_k = \frac{1}{2\pi i}\varpi_0(\underline{z}) \log(z_k) + \Sigma_k(\underline{z})$ [118], where we have chosen $\Sigma_k(\underline{z}) = z_k^{\alpha+1} + \mathcal{O}(\underline{z}^{\alpha+2})$. That replaces a.)-c.).

More generally, let I_p an index set of order $|I_p| = p$ and define the *Frobenius basis*:

$$S_{(p),k}(\underline{z}) = \frac{1}{(2\pi i)^p p!} \sum_{I_p} \kappa_{(p),k}^{i_1,\ldots,i_p} \varpi_0(\underline{z}) \log(z_{i_1}) \cdots \log(z_{i_p}) + \mathcal{O}(\underline{z}^{1+\alpha}) \,, \tag{4.42}$$

where $\mathcal{O}(\underline{z}^{1+\alpha})$ can also include logarithmic terms of total power up to $p-1$. The isomorphism in eq. (4.37) (ii.) implies that there is a non-degenerate pairing over $\mathbb{Q}$ between the solutions $S_{(n-p),k}$ and $S_{(p),k}$ for $k = 1, \ldots, |S_{(p)}(\underline{z})| = |S_{(n-p)}(\underline{z})|$ and $p = 0, \ldots, n$. Here $|S_{(p)}(\underline{z})|$ denotes the total number of solutions which are of leading order p in $\log(z_i)$. The statement is, roughly, that solutions of degree $n-p$ ($n = l-1$) in the logarithms $\log(z_k)$ are dual to solutions of degree p in the logarithms. In particular, the unique holomorphic solution with $p = 0$, $S_{(0),1} = \varpi_0(\underline{z})$, is dual to the unique solution which is of maximal degree n in the logarithms. The paring of the other solutions in this Frobenius basis depends on the details of the intersection numbers $\kappa_{(p),k}^{i_1,\ldots,i_p}$. To define this pairing over $\mathbb{Z}$ and to get a basis of solutions that correspond to period integrals over an integral basis of cycles in $H_n(M_n, \mathbb{Z})$, one has to analyze the pairing in eq. (8.6) and the map $\mathfrak{M}^{-1}$ defined by the $\widehat{\Gamma}$-class, as we will explain in section 8.2. The basis change which transforms the Frobenius basis in eq. (4.42) to this integer basis is *triangular* with respect to the grading by the logarithmic degree, i.e., it adds to solutions of degree p in the logarithms only solutions of lower degree in the logarithms, with coefficients that depend on the global topology of M_n and zeta values.

Note that the leading symbols of the differential ideal allow one to calculate the $\kappa_{(0),0}^{i_1,\ldots,i_n}$ up to a constant. In the case of mirror symmetry, these are the classical intersections $\kappa_{(0),0}^{i_1,\ldots,i_n} = D_{i_1} \cap \cdots \cap D_{i_n}$ of the basis of divisors in the mirror W_n to M_n, and the pairing over $\mathbb{Q}$ can be identified with the intersection pairing in its Chow ring. Much of the structure

of the logarithmic solutions will survive if $n = \dim(M_n)$ is replaced with the size of the Jordan block for a non-complete degeneration. For example, in ref. [120] it is argued that the limiting mixed Hodge structure of one-parameter Calabi-Yau three-folds can be one of the following types:

- The generic point F is characterized by generic local exponents.
- The conifold point C has local exponents (a, b, b, c) and a single 2×2 Jordan block.
- The K point has local exponents (a, a, b, b) and two 2×2 Jordan blocks.
- Finally, the MUM-point M has local exponents (a, a, a, a) and a 4×4 Jordan block.

Here different characters stand for different rational numbers and the *limiting mixed Hodge diamond* $H_{\lim}^{p,q}$ in eq. (4.39) for the different degenerations at $F-, C-, K-, M-$ points are depicted below:

$$
F: \begin{array}{ccccccc} & & & 0 & & & \\ & & 0 & & 0 & & \\ & 0 & & 0 & & 0 & \\ 1 & & 1 & & 1 & & 1 \\ & 0 & & 0 & & 0 & \\ & & 0 & & 0 & & \\ & & & 0 & & & \end{array}
\qquad
C: \begin{array}{ccccccc} & & & 0 & & & \\ & & 0 & & 0 & & \\ & 0 & & 1 & & 0 & \\ 1 & & 0 & & 0 & & 1 \\ & 0 & & 1 & & 0 & \\ & & 0 & & 0 & & \\ & & & 0 & & & \end{array}
$$

$$
K: \begin{array}{ccccccc} & & & 0 & & & \\ & & 0 & & 0 & & \\ & 1 & & 0 & & 1 & \\ 0 & & 0 & & 0 & & 0 \\ & 1 & & 0 & & 1 & \\ & & 0 & & 0 & & \\ & & & 0 & & & \end{array}
\qquad
M: \begin{array}{ccccccc} & & & 1 & & & \\ & & 0 & & 0 & & \\ & 0 & & 1 & & 0 & \\ 0 & & 0 & & 0 & & 0 \\ & 0 & & 1 & & 0 & \\ & & 0 & & 0 & & \\ & & & 1 & & & \end{array}
\,. \tag{4.43}
$$

For example, the previous considerations allow us to completely classify the singular points of the Calabi-Yau three-fold associated to the four-loop banana integral. The complex moduli space is $\mathcal{M}_{\text{4-loop}} = \mathbb{P}^1 \setminus \{z = 0, 1/25, 1/9, 1, \infty\}$. The local exponents of the singular points are summarized in the Riemann $\mathcal{P}$-symbol in eq. (5.4). In particular, using eq. (4.43), we immediately see that $z = 0$ is a M-point (MUM-point), $z = 1/25, 1/9, 1$ are C-points (conifolds), and $z = \infty$ is a K-point.

The $SL(2, \mathbb{C})$ *orbit theorem* [127] extends the standard $\mathrm{SL}(2, \mathbb{C})$ Lefshetz decomposition on polarized Kähler structures [130] to the limiting Hodge structure. Using this one can see for example that a 3×3 Jordan block in the above decomposition is not possible. The generic form of the limiting Hodge structures for multi-parameter families has been studied in refs. [131, 132]. These works characterize the types of *limiting mixed Hodge structures* that can occur in these cases, and one finds as a consequence which types of critical divisors can intersect. A generic feature is that at the MUM-point the horizontal middle cohomology with the degeneracies $1 = h_{n,0}, h^{\text{hor}}_{n-1,1}, \ldots, h^{\text{hor}}_{1,n-1}, h_{0,n} = 1$ is mapped to the vertical entries

of the limiting mixed Hodge structure $1 = h^{0,0}_{\lim}, h^{1,1}_{\lim}, \ldots, h^{n-1,n-1}_{\lim}, h^{n,n}_{\lim} = 1$ as explained in refs. [133, 134]. This has clearly bearings on the degenerations that can occur in maximal cut Feynman integrals as illustrated at the end of section 8.2. Since the Kähler potential is given in terms of the periods in eq. (4.2), the mixed Hodge structure in eq. (4.39), together with eq. (4.42), determines its leading logarithmic degeneration. One can therefore determine the leading behavior of the Weil-Peterssen metric and distinguish for example whether the critical divisors are at finite or infinite distance from the bulk of the moduli space. This leading behavior is enough to make statements about the swampland distance conjectures for Calabi-Yau three-folds, see refs. [135–137] and [138] for a review. The exact metric has been fixed using the Barnes integral representation and derivatives of the gamma function at the MUM-point before [48, 118, 124, 139]. In ref. [137] the Weil-Peterssen metric was determined exactly at the possible degenerations (4.43) of hypergeometric one-parameter Calabi-Yau three-folds.

The Frobenius basis and the integer basis.

So far, even if all classical constants in the symmetric tensors $\kappa_{(p),k}$ have been determined, the basis in eq. (4.42) for the periods is only what is called a *Frobenius basis* by mathematicians. In fact, eq. (4.17) extends to the singular locus z_0 and gives non-trivial relations between the intersection numbers. A Frobenius basis does not correspond to a basis of cycles Γ for $H_n(M_n, \mathbb{Q})$, which is sometimes called a *Betti basis*, and, of course, not to a basis in $H_n(M_n, \mathbb{Z})$, which we call an *integral basis*. Whereas, a maximal cut integral does correspond to an integral over an element in $H_n(M_n, \mathbb{Z})$ and so the latter has to be found if one is interested in the maximal cuts computed with an integral basis of cycles. A basis transformation from a generic Frobenius basis to a rational or integral basis will involve interesting *transcendental numbers*.

A pedestrian way to construct an integral basis proceeds by the following method: Resolve the critical loci in the moduli space to divisors with normal crossings. After that step, we construct near sufficiently many points $\underline{z}_i$ and, in particular, around the intersections of the critical divisors, local Frobenius bases of solutions $\underline{\tilde{\Pi}}_{\underline{z}_i}$ of the Picard-Fuchs operators. Here 'sufficient' means that the finite regions of convergence of the $\underline{\tilde{\Pi}}_{\underline{z}_i}$ define sufficiently many overlapping patches U_i to cover $\mathcal{M}_{\text{cs}}$. Once one has picked such a system of local solutions $\underline{\tilde{\Pi}}_{\underline{z}_i}$, $i = 1, \ldots, s$, one finds a global basis by analytic continuation of the solutions into all patches. Between neighboring patches U_i and U_j with $U_j \cap U_j \neq \emptyset$, one can construct numerically connection matrices $\mathbf{C}_{ij}$ such that $\underline{\tilde{\Pi}}_{\underline{z}_i} = \mathbf{C}_{ij}\, \underline{\tilde{\Pi}}_{\underline{z}_j}$ between patches, eventually in intermediate steps to achieve the necessary numerical precision. In this globally defined basis one can construct the simultaneous action of all independent generators of the monodromy group $\Gamma_{\mathcal{M}_n}$. The latter generate (not freely, but with the so-called Van Kampen relations) the monodromies around all critical divisors. A basis change, involving transcendental entries, makes all these generators simultaneously elements of $O(\mathbf{\Sigma}, \mathbb{Z})$ and leads up to conjugation in $O(\mathbf{\Sigma}, \mathbb{Z})$ to the desired integer basis of solutions $\underline{\Pi}$.

This complicated procedure can be much simplified if one knows certain integral geometric

cycles a priori. For example, at the conifolds the vanishing S^n-spheres can be identified, and the corresponding integrals over Ω can be perturbatively performed to low order in the moduli to get the exact normalization. Most information concerning the integral basis can be extracted at the MUM-point. As can be seen from eq. (6.17), the holomorphic solution at the MUM-point is an integral over a n-torus $\mathbf{T} = T^n = T^{l-1}$, which can be performed by taking residues, cf. eq. (7.7). Consider now the unique cycle $\mathbf{S}$, whose period degenerates at the MUM-point with the highest power of the logarithms, i.e., with order $\log^n$. The latter is dual to $\mathbf{T}$, whose period has no logarithm, according to eq. (4.37) (ii), as explained after eq. (4.42). Since both cycles are unique, they are dual with respect to the intersection form $\mathbf{\Sigma}$. The cycle $\mathbf{S} = S^n$ corresponds to the S^n-sphere that vanishes at the conifold locus that is nearest to the MUM-point under consideration. This property of the dual periods is known to hold quite generally and plays an important role in homological mirror symmetry, where the shift monodromy by the maximal degenerating cycle of the MUM-point at the nearest conifold is known as Seidel-Thomas twist [140].

It is a very remarkable fact found in ref. [45] that for the banana integral the maximal cut integral that corresponds to the period over this cycle $\mathbf{S}$ yields the imaginary part of the integral above threshold. We have thus been able to identify two distinguished cycles in the Calabi-Yau: The sphere $\mathbf{S}$ provides the imaginary part above threshold. It corresponds in loop momentum space to the maximal cut contour Γ_{Im}, and so it has a direct physical interpretation and relevance. The torus $\mathbf{T}$ considered in ref. [43], which corresponds in loop momentum space to the maximal cut contour Γ_T from eqs. (2.44) and (6.17), does not seem to have any known physical interpretation. Its importance, however, lies in the fact that it furnishes the unique holomorphic period at the MUM-point. This integral allows one to reconstruct the generators of the Picard-Fuchs differential ideal and plays an important role in understanding this ideal (cf. ref. [45], as well as chapters 6 and 7). Amazingly, these two distinguished cycles are exactly the dual cycles that play a crucial role in homological mirror symmetry, as discussed above.

Finally, let us mention the important observation by Deligne that the mixed Hodge structure becomes a mixed Hodge-Tate structure at the MUM-point [141]. In this situation one expects that the $\widehat{\Gamma}$-class governs the integral structure and the *transcendental weight* of the periods. As it turns out, this $\widehat{\Gamma}$-class (and the closely related Mellin-Barnes representation of the banana integrals) are the most effective analytic tools to find the integral basis and to perform some of its analytic continuations, respectively. We explain in section 8.2 that the $\widehat{\Gamma}$-class can also be extended to include the inhomogeneous solutions, i.e., the full Feynman integral. In section 9.1 we show that the Mellin-Barnes representation of the banana integral allows one to prove this $\widehat{\Gamma}$-conjecture if one considers the right contours.

CHAPTER 5

The Equal-Mass Banana Graphs

In this chapter we want to collect all information about the equal-mass banana graphs such that we can compute them to arbitrary loop order in $D = 2$ dimensions. For this we use the techniques and insights of the last chapters. We focus here on the results we made in [45, 47].

5.1 Frobenius method for equal-mass banana graphs

We want to compute the equal-mass banana graphs in $D = 2$ dimensions using differential equations. It is known that the maximal cuts $J_{l,0}(z;0)$ (cf. eq (2.19)) of the banana family are annihilated by a differential operator $\mathcal{L}_l$ of order l. For low loop order, the explicit form of $\mathcal{L}_l$ (and of its solutions) can be found in refs. [20, 33, 86, 87, 108, 109, 112, 113, 142]. One can construct the operator $\mathcal{L}_l$ by a procedure developed in [8, 45]. Furthermore, the operator $\mathcal{L}_l$ is the Picard-Fuchs operator associated to a family of Calabi-Yau $(l-1)$-folds M_{l-1} (chapter 4) parametrized by $z = m^2/p^2 \in \mathbb{R}$.[1]

Let us collect some properties of the operators $\mathcal{L}_l$. The singularities of $\mathcal{L}_l$ are located at the points

$$z \in \{0, \infty\} \cup \bigcup_{j=0}^{\lceil \frac{l-1}{2} \rceil} \left\{ \frac{1}{(l+1-2j)^2} \right\} , \tag{5.1}$$

and they form the discriminant of the operator by

$$\text{Disc}(\mathcal{L}_l) = (-z)^l \prod_{k \in \Delta^{(l)}} (1 - kz) , \tag{5.2}$$

[1] We could also consider complex values z, but for physics applications it is sufficient to consider z real.

with the short hand notation

$$\Delta^{(l)} := \bigcup_{j=0}^{\lceil \frac{l-1}{2} \rceil} \left\{ (l+1-2j)^2 \right\} . \tag{5.3}$$

The discriminant multiplies the highest θ-derivatives times a factor z^l. We can collect the singularity structure of the operators $\mathcal{L}_l$ in the Riemann $\mathcal{P}$-symbol, see subsection 3.3.1. At the point $z = 0$ we have for each loop order l a MUM-point with indicials $\alpha_i = 1$ for $i = 1, \ldots, l$. At the closest singularity, i.e. $p^2/m^2 = (l+1)^2$, one has for even l a single logarithmic solution and for l odd a square root solution, i.e. $\alpha_i \in \mathbb{N}/2$ for a single $i \in \{1, \ldots, l\}$. In total the Riemann $\mathcal{P}$-symbol is given for even l by

$$\mathcal{P}_{\text{even}} \left\{ \begin{array}{cccccc} 0 & \frac{1}{(l+1)^2} & \frac{1}{(l-1)^2} & \cdots & 1 & \infty \\ \hline 1 & 0 & 0 & \cdots & 0 & 0 \\ 1 & 1 & 1 & \cdots & 1 & 0 \\ 1 & 2 & 2 & \cdots & 2 & 1 \\ & & & & & 1 \\ \vdots & \vdots & \vdots & \vdots & \vdots & \vdots \\ 1 & l-2 & l-2 & \cdots & l-2 & \frac{l}{2}-1 \\ 1 & \frac{l}{2}-1 & \frac{l}{2}-1 & \cdots & \frac{l}{2}-1 & \frac{l}{2}-1 \end{array} \right\} \tag{5.4}$$

and for odd l by

$$\mathcal{P}_{\text{odd}} \left\{ \begin{array}{cccccc} 0 & \frac{1}{(l+1)^2} & \frac{1}{(l-1)^2} & \cdots & \frac{1}{4} & \infty \\ \hline 1 & 0 & 0 & \cdots & 0 & 0 \\ 1 & 1 & 1 & \cdots & 1 & 0 \\ 1 & 2 & 2 & \cdots & 2 & 1 \\ & & & & & 1 \\ \vdots & \vdots & \vdots & \vdots & \vdots & \vdots \\ & & & & & \frac{l-3}{2} \\ 1 & l-2 & l-2 & \cdots & l-2 & \frac{l-3}{2} \\ 1 & \frac{l}{2}-1 & \frac{l}{2}-1 & \cdots & \frac{l}{2}-1 & \frac{l-3}{4} \end{array} \right\} . \tag{5.5}$$

Around the MUM-point we can construct with the Frobenius method (subsection 3.3.1) a basis of solutions $\underline{\Pi}_l(z) := \left(\varpi_{l,0}(z), \ldots, \varpi_{l,l-1}(z)\right)^T$ given by

$$\varpi_{l,k}(z) = \sum_{j=0}^{k} \frac{1}{(k-j)!} \log^{k-j}(z)\, \Sigma_{l,j}(z) , \tag{5.6}$$

where the $\Sigma_{l,k}(z)$ are holomorphic in a neighbourhood around the MUM-point $z = 0$, normalized such that $\Sigma_{l,k}(z) = \delta_{k0}\, z + \mathcal{O}(z^2)$. For $k = 0$ we have explicitly

$$\varpi_{l,0}(z) = \Sigma_{l,0}(z) = \sum_{k_1,\ldots,k_{l+1}\geq 0} \binom{|k|}{k_1,\ldots,k_{l+1}}^2 z^{|k|+1}\,, \tag{5.7}$$

with $|k| = k_1 + \ldots + k_{l+1}$ and the multinomial coefficient $\binom{k}{k_1,\ldots,k_{l+1}} = \frac{k!}{k_1!\cdots k_{l+1}!}$. To extend this basis to the whole parameter space one has to perform a careful analytic continuation which was explained and demonstrated through a `PariGP` program in [45].

Using the basis of solutions $\underline{\Pi}_l(z)$ we can get the maximal cuts of $J_{l,1}(z;0)$ (cf. eq (2.19)) by

$$J^{\Gamma}_{l,1}(z) = \underline{\alpha}^{\Gamma} \cdot \underline{\Pi}_l(z) = \sum_{j=1}^{l} \alpha^{\Gamma}_j\, \varpi_{l,j-1}(z) \qquad \text{for } \underline{\alpha}^{\Gamma} \in \mathbb{C}^l\,. \tag{5.8}$$

These maximal cuts form a basis of the Calabi-Yau periods of M_{l-1}. Notice that the maximal cut contours are defined in integral homology, they are 'genuine geometric objects', whereas the Frobenius basis elements $\varpi_{l,j}(z)$ are not, they are not obtained by integrating over a cycle in integer homology.

5.2 Bilinear relations for equal-mass banana graphs

To find the bilinear relations between the periods $\varpi_{l,j}(z)$ as described in subsection 4.2.2 we write the Picard-Fuchs operator in the terms of usual derivatives

$$\mathcal{L}_l = \sum_{k=0}^{l} B_{l,k}(z)\partial_z^k\,, \tag{5.9}$$

where the $B_{l,k}(z)$ are polynomials. We can choose for the Wronskian

$$\mathbf{W}_l(z) := \begin{pmatrix} \varpi_{l,0}(z) & \varpi_{l,1}(z) & \ldots & \varpi_{l,l-1}(z) \\ \partial_z\varpi_{l,0}(z) & \partial_z\varpi_{l,1}(z) & \ldots & \partial_z\varpi_{l,l-1}(z) \\ \vdots & \vdots & & \vdots \\ \partial_z^{l-1}\varpi_{l,0}(z) & \partial_z^{l-1}\varpi_{l,1}(z) & \ldots & \partial_z^{l-1}\varpi_{l,l-1}(z) \end{pmatrix}, \tag{5.10}$$

which is related to the master integrals by $\underline{J}^{\Gamma}_l(z) = \mathbf{W}_l(z)\underline{\alpha}^{\Gamma}$. A small calculation shows [47] that the determinant of the Wronskian $\mathbf{W}_l(z)$ yields

$$\det \mathbf{W}_l(z) = \Big((-1)^l z^{-3}\,\mathrm{Disc}(\mathcal{L}_l)\Big)^{-l/2} = \left(z^{l-3}\prod_{k\in\Delta^{(l)}}(1-kz)\right)^{-l/2}, \tag{5.11}$$

where $\mathrm{Disc}(\mathcal{L}_l)$ is given in eq. (5.2). In section 3.2 we have seen the important role of the Wronskian $\mathbf{W}_l(z)$ for solving the Gauss-Manin system. For this one has to compute its inverse. Now we will see that the structure of the inverse Wronskian will be reduced due to the bilinear relations as a result from Griffiths transversality.

Recall from subsection 4.2.1 that there is a bilinear pairing – the intersection pairing $\mathbf{\Sigma}$ – on the entries of $\mathbf{W}_l(z)$. If we work with the Frobenius basis $\underline{\Pi}_l(z)$, Griffiths transversality in eq. (4.17) takes the form

$$\underline{\Pi}_l(z)^T\,\mathbf{\Sigma}_l\,\partial_z^k\underline{\Pi}_l(z) = \begin{cases} 0 & , k < l-1\,, \\ C_{l-1}(z) & , k = l-1\,, \end{cases} \tag{5.12}$$

where the intersection matrix $\mathbf{\Sigma}_l$ is given by

$$\mathbf{\Sigma}_l = \begin{pmatrix} & & & 1 \\ & & -1 & \\ & 1 & & \\ \iddots & & & \end{pmatrix}. \tag{5.13}$$

Equation (5.12) can be interpreted as a collection of bilinear relations between the maximal cuts of $J_{l,1}(z;0)$ and $J_{l,k}(z;0)$ for $k > 1$. One can derive (c.f. 4.2.2 and [47] for a more thorough derivation) a differential equation for $C_{l-1}(z)$ from the Picard-Fuchs operator $\mathcal{L}_l$

$$\partial_z C_l(z) + \frac{2}{l}\frac{B_{l,l-1}(z)}{B_{l,l}(z)}C_l(z) = 0\,. \tag{5.14}$$

With our normalization of Frobenius basis $\underline{\Pi}_l(z)$ (c.f. equation (5.6)) we find

$$C_l(z) = \frac{1}{z^{l-3}\prod_{k\in\Delta^{(l)}}(1-kz)}\,. \tag{5.15}$$

With further differentiation of eq. (5.12) we can obtain more relations. One can even find a hole matrix of bilinear relations of the

$$\mathbf{Z}_l(z) = \begin{pmatrix} \underline{\Pi}_l(z)^T\,\mathbf{\Sigma}_l\,\underline{\Pi}_l(z) & \cdots & \underline{\Pi}_l(z)^T\,\mathbf{\Sigma}_l\,\partial_z^{l-1}\underline{\Pi}_l(z) \\ \vdots & \ddots & \vdots \\ \partial_z^{l-1}\underline{\Pi}_l(z)^T\,\mathbf{\Sigma}_l\,\underline{\Pi}_l(z) & \cdots & \partial_z^{l-1}\underline{\Pi}_l(z)^T\,\mathbf{\Sigma}_l\,\partial_z^{l-1}\underline{\Pi}_l(z) \end{pmatrix}. \tag{5.16}$$

One can show that all entries of this matrix are rational functions and that $\mathbf{Z}_l(z)^T = (-1)^{l+1}\,\mathbf{Z}_l(z)$.

Let us make some comments and examples for these relations. For low loop orders these relations are well-known. At $l = 1$ the period is an algebraic function and for $l = 2$ the relations are the familiar Legendre relations. More interesting is that at three loops the operator is a symmetric square. For $l = 4$ we want to give the relations explicitly. It turns out that the inverse $\mathbf{Z}_l^{-1}(z)$ has a more compact form. We find

$$\mathbf{Z}_4^{-1}(z) = \begin{pmatrix} 0 & -\frac{1}{z} + 28 - 285z + 450z^2 & -1 + 70z - 777z^2 + 900z^3 & -z + 35z^2 - 259z^3 + 225z^4 \\ \frac{1}{z} - 28 + 285z - 450z^2 & 0 & z - 35z^2 + 259z^3 - 225z^4 & 0 \\ 1 - 70z + 777z^2 - 900z^3 & -z + 35z^2 - 259z^3 + 225z^4 & 0 & 0 \\ z - 35z^2 + 259z^3 - 225z^4 & 0 & 0 & 0 \end{pmatrix}.$$

As a final remark let us state that we could not find additional relations between the periods which are not captured by Griffiths transversality, for more details we refer to [47].

With the relations or better the matrix of relations $\mathbf{Z}_l(z)$ we can express the inverse of the Wronskian matrix $\mathbf{W}_l(z)$ through

$$\mathbf{W}_l(z)^{-1} = \mathbf{\Sigma}_l \mathbf{W}_l(z)^T \mathbf{Z}_l(z)^{-1}. \tag{5.17}$$

Note that this implies polynomial relations of higher degree between the entries of $\mathbf{W}_l(z)$, because the entries of the inverse are proportional to $(l-1) \times (l-1)$ minors. Moreover, we see that Griffiths transversality also determines $\det \mathbf{W}_l(z)$. Using eq. (5.17) one finds

$$\det \mathbf{W}_l(z) = C_l(z)^{l/2}, \tag{5.18}$$

which is also a cross check for eq. (5.11).

Let us conclude this section with some comments: First, we mention that this is not the first time that bilinear relations between maximal cuts of banana integrals were considered. In particular, refs. [143–146] considered quadratic relations between moments of Bessel functions, which are closely related to banana integrals and their cuts. Quadratic relations for maximal cuts for $l = 2$ and $l = 3$ were also studied in ref. [147], and such relations also arise from the twisted Riemann bilinear relations [148, 149]. Finally, in this section we have only discussed the equal-mass case. Griffiths transversality holds more generally also for the periods, i.e., the maximal cuts, in the case of distinct propagator masses.

5.3 Explicit set of master integrals for banana graphs

Having analyzed the Frobenius basis of solutions and the relations between them let us know use this to obtain the banana integrals for arbitrary loop orders in $D = 2$ dimensions as (iterated) integrals of Calabi-Yau periods as explained in section 3.2.

We start with eq. (3.7) for $D = 2$:

$$\partial_z \underline{J}_l(z;0) = \mathbf{B}_{l,0}(z)\, \underline{J}_l(z;0) + (-1)^{l+1}(l+1)!\, \frac{z}{z^l \prod_{k\in\Delta^{(l)}}(1-kz)}\, \underline{\hat{e}}_l\,, \tag{5.19}$$

with $\underline{\hat{e}}_l = (0,\ldots,0,1)^T$. Changing variables like in eq. (3.9), we obtain

$$\partial_z \underline{L}_l^{(0)}(z) = (-1)^{l+1}(l+1)!\, \frac{z}{z^l \prod_{k\in\Delta^{(l)}}(1-kz)}\, \mathbf{W}_l(z)^{-1}\underline{\hat{e}}_l = (l+1)!\, \frac{\boldsymbol{\Sigma}_l\, \underline{\Pi}_l(z)}{z^2}\,, \tag{5.20}$$

where in the last step we have used the identity $\mathbf{W}_l(z)^{-1}\, \underline{\hat{e}}_l = (-1)^{l+1}\frac{\boldsymbol{\Sigma}_l \underline{\Pi}_l(z)}{C_l(z)}$, which follows from (5.17). This equation can easily be solved by quadrature

$$\underline{L}_l^{(0)}(z) \;= \underline{L}_l^{(0)}(0) + (l+1)!\, \boldsymbol{\Sigma}_l \int_{\vec{1}_0}^{z} \mathrm{d}w\, \frac{\underline{\Pi}_l(w)}{w^2}\,, \tag{5.21}$$

or equivalently

$$\underline{J}_l^{(0)}(z) \;= \mathbf{W}_l(z)\underline{L}_l^{(0)}(0) + (l+1)!\, \mathbf{W}_l(z)\, \boldsymbol{\Sigma}_l \int_{\vec{1}_0}^{z} \mathrm{d}w\, \frac{\underline{\Pi}_l(w)}{w^2}\,. \tag{5.22}$$

For the individual master integrals, i.e., the individual components of $\underline{J}_l^{(0)}$, we find:

$$J_{l,k}^{(0)}(z) \;= \partial_z^{k-1}\underline{\Pi}_l(z)^T\, \boldsymbol{\Sigma}_l\, \underline{L}_l^{(0)}(0) + (l+1)!\, \partial_z^{k-1}\underline{\Pi}_l(z)^T\, \boldsymbol{\Sigma}_l \int_{\vec{1}_0}^{z} \mathrm{d}w\, \frac{\underline{\Pi}_l(w)}{w^2}\,. \tag{5.23}$$

Here $\vec{1}_0$ denotes the unit tangent vector at 0. In the limit $z \to 0$, we have

$$\underline{\Pi}_l(z) = z\, \left(1, \log z, \frac{1}{2}\log^2 z, \ldots, \frac{1}{(l-1)!}\log^{l-1} z\right)^T + \mathcal{O}(z^2)\,, \tag{5.24}$$

so that the integral in eq. (5.22) diverges if the lower integration limit is zero. The divergency is regulated by introducing the tangential base point $\vec{1}_0$. For a comprehensive review of how this regularization can be practically implemented into the framework of iterated integrals on curves see, e.g., ref. [150]. In the present case, the tangential base point regularization

(often called shuffle regularization) reduces to the prescription:

$$\int_{\vec{1}_0}^{z} \mathrm{d}w \, \frac{\omega_{l,k}(w)}{w^2} := \frac{1}{(k+1)!} \log^{k+1} z + \int_0^z \frac{\mathrm{d}w}{w} \left(\frac{\omega_{l,k}(w)}{w} - \frac{1}{k!} \log^k w \right) . \tag{5.25}$$

It is easy to check that the remaining integral in eq. (5.25) is absolutely convergent (as long as the range $[0, z]$ does not contain any singular point of $\mathcal{L}_l$).

Finally, we have to determine the initial condition $\underline{L}_l^{(0)}(0)$. We start from eq. (5.23) for $k = 1$. Since the integral in the second term in eq. (5.25) is convergent, this integral vanishes like a power in the limit $z \to 0$, and so this term behaves like $\mathcal{O}(z^2)$. Using eq. (5.24), we find:

$$J_{l,1}(z;0) \; = -(-1)^l (l+1)\, z \log^l z + z \sum_{j=0}^{l-1} L^{(0)}_{l,l-j}(0) \frac{(-\log z)^j}{j!} + \mathcal{O}(z^2) \, . \tag{5.26}$$

We see that the vector $\underline{L}_l^{(0)}(0)$ is uniquely determined once we know the leading asymptotics of $J_{l,1}(z;0)$ in the limit $z \to 0$. This limit can be related for arbitrary loop order to a novel $\widehat{\Gamma}$-class which we explain in chapter 8. In particular, one will show that the coefficients $L^{(0)}_{l,k}(0)$ are given as $\mathbb{Q}[i\pi]$-linear combinations of zeta values of uniform transcendental weight k, c.f. eqs. (8.19) - (8.21).

Equation (5.22) was one of the main results of my publication [47] because it expresses all master integrals for the equal-mass banana integral in $D = 2$ dimensions for arbitrary loop order l as an integral of Calabi-Yau periods. Furthermore, the initial condition can be given in a closed form, namely in terms of a generating functional determined from the $\widehat{\Gamma}$-class, so purely from geometry. We find it remarkable that such a compact formula of geometric origin exists for all loop orders. Notice that the relations among maximal cuts from Griffiths transversality play an important role in deriving eq. (5.22).

CHAPTER 6

Hypersurface Motive of the Banana Graphs

In the previous chapters we have learned the basics of Feynman integrals, especially differential equational techniques to compute them, and the mathematics of Calabi-Yau manifolds. Now we want to combine both to compute the banana integrals for generic masses. In this chapter we associate a first geometry to the l-loop banana integral which enabled us to solve them in the generic-mass case for $l \leq 4$. This is the so-called hypersuface motive, since the Calabi-Yau manifold is realized as a hypersurface in a toric ambient space. This was originally done in my first paper [44] for $l \leq 3$ and was later extended with the $l = 4$ case in my second publication [45].

The geometry will directly originate from the graph polynomial representation of the Feynman integral, see section 2.4. It is very special for the banana family that in $D = 2$ dimensions the exponent of the first Symanzik polynomial vanishes and the exponent of the second Symanzik polynomial is equal to one. This simplifies a lot the form of these integrals and offers us our first geometric description. We use the second Symanzik polynomial as a Newton polynomial which then defines our Calabi-Yau variety. Using the Gel′fand-Kapranov-Zelevinskĭ system of differential equations for this geometry we can construct a basis of periods of the Calabi-Yau variety which first describe the maximal cut integrals of the banana graph. This will be done around the MUM-point corresponding in physical terms to the large momentum region. Furthermore, we explain then how one can extend these homogeneous differential equations to a set of inhomogeneous differential equations such that its solution space yields a full set of functions parametrizing the full banana integral.

6.1 Hypersurface geometry associated to the l-loop banana graph

As already mentioned we start with the second Symanzik polynomial which is also the denominator of the banana integral in $D = 2$ dimensions

$$\int_{\sigma_l} \frac{\mu_l}{\mathcal{F}_l(p^2, \underline{m}^2; \underline{x})}\,, \tag{6.1}$$

see also section 2.4 and in particular eqs. (2.29) - (2.31). The zero locus of this integrand defines a singular[1] family of $(l-1)$-dimensional Calabi-Yau hypersurfaces M^s_{l-1} by

$$M_s = \{\mathcal{F}_l(p^2, \underline{m}^2; \underline{x}) = 0 \,|\, (x_1 : \ldots : x_{l+1}) \in \mathbb{P}^l\}\,. \tag{6.2}$$

From standard arguments, see e.g. [151], M^s_{l-1} is a complex Kähler manifold with trivial canonical class, hence a Calabi-Yau space, see section 4.1. The first fact follows by the definition of M^s_{l-1} as a hypersurface in projective space $\mathbb{P}^l$, which is Kähler, and the second since for a homogeneous polynomial P with degree $\deg(P)$ in $\mathbb{P}^l$ the canonical class is given in terms of the hyperplane class H of $\mathbb{P}^l$ as [151]

$$-K = c_1(TM^s_{l-1}) = ((l+1) - \deg(P))\, H\,. \tag{6.3}$$

So for the banana graph polynomial we have $\deg(P_l) = l+1$ and therefore the canonical class is trivial. Notice that it is important that the integrand in (6.1) is well defined under the $\mathbb{C}^*$ scaling of the homogeneous coordinates of $\mathbb{P}^l$. This is guaranteed by the degree of the second Symanzik polynomial and the measure μ_l. As we have said the hypersurface constraint (6.2) defines a singular Calabi-Yau variety. Fortunately, there is a canonical resolution known. This method is known as the Batyrev construction [49, 152–154] and yields a smooth family of Calabi-Yau varieties M_{l-1} with typically more parameters than the singular one.

6.1.1 Calabi-Yau hypersurfaces in toric ambient spaces

Now we want to describe the Batyrev construction which will furnishes for us a smooth Calabi-Yau manifold and its mirror in a toric ambient space. Moreover, we can compute some characteristics of the Calabi-Yau spaces and their moduli spaces in this formalism and find also a suitable set of coordinates, the so-called Batyrev coordinates.

We first define a Newton polynomial P_{Δ_l} as

$$\mathcal{F}_l(p^2, \underline{m}^2; \underline{x}) =: P_{\Delta_l} \prod_i^{l+1} x_i\,. \tag{6.4}$$

The exponents of each monomial of P_{Δ_l} w.r.t. to the coordinates x_i for $i = 1, \ldots, l+1$ define a point in a lattice $\mathbb{Z}^{l+1}$. The convex hull of all these points in the natural embedding of $\mathbb{Z}^{l+1} \subset \mathbb{R}^{l+1}$ defines a l-dimensional lattice polyhedron. The dimension is reduced due to the homogeneity of P_{Δ_l}. We denote the polyhedron that lies in the induced lattice $\mathbb{Z}^l \subset \mathbb{R}^l$ by Δ_l. One calls P_{Δ_l} the Newton polynomial of Δ_l and Δ_l the Newton polyhedron of P_{Δ_l}.

[1] For $l = 1, 2$ actually the family is generically non-singular.

More concretely, picking the canonical basis e_i for $\Lambda = \mathbb{Z}^l \subset \mathbb{R}^l = \Lambda_{\mathbb{R}}$ the $l(l+1)$ vertices defined by (6.4) span the polytope Δ_l [2], i.e.

$$\Delta_l = \text{Conv}\left(\{\pm e_i\}_{i=1}^{l} \cup \{\pm(e_i - e_j)\}_{1\leq i<j\leq l}\right) . \tag{6.5}$$

Note that Δ_l contains beside these vertices no further integral point other then the origen $\nu_0 = (0,\ldots,0)$. Moreover, Δ_l is integral and reflexive, which implies that the dual polytope $\hat{\Delta}_l \subset \hat{\Lambda}_{\mathbb{R}}$

$$\hat{\Delta}_l = \{y \in \hat{\Lambda}_{\mathbb{R}} | \langle y, x\rangle \geq -1, \forall\, x \ \in \Delta_l\} \tag{6.6}$$

is also an integral lattice polyhedron. Note that the dual of the dual polyhedron is the polyhedron itself, i.e. $\hat{\hat{\Delta}}_l = \Delta_l$. The dual polyhedron $\hat{\Delta}_l$ is concretely given by

$$\hat{\Delta}_l = \text{Conv}\left(\bigcup_{k=1}^{l}\bigcup_{r=1}^{\binom{l}{k}}\sum_{i=1}^{l} I_i^{(k),r}\hat{e}_i \cup \bigcup_{k=1}^{l}\bigcup_{r=1}^{\binom{l}{k}}\sum_{i=1}^{l}(-I_i^{(k),r}\hat{e}_i)\right) , \tag{6.7}$$

where $\hat{e}_i$ is a basis of the lattice $\hat{\Lambda}_{\mathbb{R}}$ and the $I^{(k),r}$ for $r = 1,\ldots,\binom{l}{k}$ are the sets of all distinct permutations of k ones and $l-k$ zeros. Indeed the $2(2^l-1)$ points listed in (6.7) are all integral points of $\hat{\Delta}_l$ beside the origin. For the polytope Δ_l itself it means that it has $2(2^l-1)$ faces. From the structure of the vertices of Δ_l it can be proven that there is no integral point in the facets of the dual polytope. The combinatorics of all facets of $\hat{\Delta}$ are equal, in particular, they all have 2^{l-1} vertices.

A central theorem in the toric mirror construction of Batyrev [152] says that a smooth resolution M_{l-1} of M_{l-1}^s with trivial canonical class is given by the constraint

$$P_{\Delta_l} = \sum_{\nu^{(i)}\in\Delta_l} a_i \prod_{\hat{\nu}^{(k)}\in\hat{\Delta}_l} x_k^{\langle \nu^{(i)},\hat{\nu}^{(k)}\rangle} = 0 \tag{6.8}$$

in the coordinate ring X_i of $\mathbb{P}_{\hat{\Delta}_l}$, where $\nu^{(i)}$, $i = 0,\ldots,n_p$ and $\hat{\nu}^{(k)}$, $i = 1,\ldots,n_{\hat{p}}$ run over all integer points in Δ_l and $\hat{\Delta}_l$, respectively[3]. Here $I(\Delta_l)$ is the number of lattice points in Δ_l and $n_p = I(\Delta_l) - 1$. Analogous definitions apply for $\hat{\Delta}_l$. Note that (6.8) defines an embedding of the physical parameters p^2 and $\underline{m}^2$, into convenient but redundant complex structure variables $a_i \in \mathbb{C}$ for $i = 0,\ldots,n_p$. Both the physical as well as the $\underline{a}$ parameters are only defined up to scale. Note that we are a little cavaliar with the notations: The coordinate rings x_i, $i = 1,\ldots,l+1$ in the definition (6.4) and the one x_i, $i = 0,\ldots,n_{\hat{p}}$ in (6.8) are, of course,

[2] For $l = 3$ this polytope is depicted in Figure 6.1.

[3] P_{Δ_l} is a Laurent polynomial in which the minimal degree of the x_i is -1, while $\mathcal{F}_l(p^2, \underline{m}^2; \underline{x}) = 0$ is a polynomial constraint.

different. However, we can get the former by blowing down the latter. This is achieved by setting a suitable subset of $n_{\hat{p}} - (l+1)$ of the latter x_i variables to one. Likewise, given P_{Δ_l} in x_i, $i = 1, \ldots, l+1$ as in (6.4) and all $\mathbb{C}^*$ actions (6.10) we can uniquely extend it to $n_{\hat{p}}$ variables X_i by requiring that the extended polynomial (or strictly speaking the proper transform of (6.4)) is homogeneous w.r.t. to all $\mathbb{C}^*$ rescalings in (6.10).

The space $\mathbb{P}_{\Delta_l}$ is a l-dimensional projective toric variety that can be associated to any reflexive lattice polyhedra Δ_l given a star triangulation [4] $\mathcal{T}$ of Δ_l as

$$\mathbb{P}_{\Delta_l} = \frac{\mathbb{C}^{n_p}[x_0, \ldots, x_{n_p}] \setminus Z_{\mathcal{T}}}{(\mathbb{C}^*)^{n_p - l}} \,. \tag{6.9}$$

Here the $\mathbb{C}^*$ actions that are divided out are generated by

$$x_i \longmapsto x_i (\mu^{(k)})^{\ell_i^{(k)}} \quad \text{for } i = 0, \ldots, n_p \,, \tag{6.10}$$

where $\mu^{(k)} \in \mathbb{C}^*$ and the $\ell^{(k)}$ vectors span the $(n_p - l)$-dimensional space of all linear relations

$$L = \{(\ell_0^*, \ell_1^*, ..., \ell_{n_p}^*) \in \mathbb{Z}^{n_p+1} \,|\, l_0^* \bar{\nu}_0 + \ell_1^* \bar{\nu}_1 + ... + \ell_{n_p}^* \bar{\nu}_{n_p} = 0\} \tag{6.11}$$

among the points

$$\mathcal{A} = \{\bar{\nu}_0, \bar{\nu}_1, ..., \bar{\nu}_{n_p} | \bar{\nu}_i = (1, \nu_i), \nu_i \in \Delta_l \cap \mathbb{Z}^l\} \,. \tag{6.12}$$

From a triangulation [5] $\mathcal{T}$ of the polytope Δ_l one can determine the set of generators $\ell^{(k)}$ of L and the Stanley-Reisner ideal $Z_{\mathcal{T}}$. The latter describes loci in $\mathbb{C}^p[x_0, \ldots, x_p]$, which have to be excluded so that the orbits of the $\mathbb{C}^*$ action (6.10) have a well defined dimension. Positive linear combinations of $\ell^{(k)}$ for $k = 1, \ldots, n$ span the Mori cone, which is not necessary simplicial if $n > n_p - l$. It is dual to the Kähler cone of $\mathbb{P}_{\Delta_l}$ and all cones corresponding to all triangulations $\mathcal{T}$ of Σ_{Δ_l} form the secondary fan, see [156] for a review how to calculate the $\ell^{(k)}$ vectors and the Stanley-Reisner ideal combinatorial from a triangulation $\mathcal{T}$. This combinatorics is implemented in the computer package `SageMath` [157], which calculates the possible triangulations $\mathcal{T}$ and from them the generators $\ell^{(k)}$ and the Stanley Reisner ideal $Z_{\mathcal{T}}$. For the project [44] we could write a code in `SageMath` which could generate a star triangulation for the polytopes of the banana family. Here we used the special form of them such that we could simply triangulate the codimensional one facets and connected these triangulations with the inner point. These gave at least a few triangulations of the

[4] In a star triangulation all l-dimensional simplices of the triangulation covering the reflexive polyhedron share the inner point as one of their vertices.

[5] Δ_l defines canonically a fan Σ_{Δ_l} and the definition of a smooth $\mathbb{P}_{\Delta_l}$ may require to add integer points outside Δ_l and to triangulate the fan Σ_{Δ_l}. Such cases are discussed in [153, 155].

polyhedrons Δ_l for $l \geq 4$ since the combinatorics grows too fast to list all triangulations. For $l \leq 3$ all triangulations could be found.

The family of $(l-1)$-dimensional Calabi-Yau varieties defined as section of the canonical bundle $P_{\hat{\Delta}_l} = 0$ of $\mathbb{P}_{\Delta_l}$ is by Batryrev [152] conjectured to be the mirror manifold $W_{l-1} = X_{\hat{\Delta}_l}$ of the manifold M_{l-1}, i.e. (M_{l-1}, W_{l-1}) form a mirror pair with dual properties, see for more details chapter 8. A main implication of this proposal is that the complex structure deformation space of M_{l-1} denoted by $\mathcal{M}_{\text{cs}}(M_{l-1})$ is identified with the complexified Kähler or stringy Kähler moduli space $\mathcal{M}_{\text{cKs}}(W_{l-1})$

$$\mathcal{M}_{\text{cKs}}(W_{l-1}) = \mathcal{M}_{\text{cs}}(M_{l-1}) \tag{6.13}$$

and vice versa. Note that the real Kähler moduli space is parametrized by the Kähler parameters $t_k^{\mathbb{R}} = \int_{\mathcal{C}_k} \omega$, where $\omega \in H^{1,1}(M_{l-1})$ and $\mathcal{C}_k$ span a basis of holomorphic curves in $H_{1,1}(M_{l-1}, \mathbb{Z})$. In string theory the complexification is due to the Neveu-Schwarz two-form field b also in $H^{1,1}(M_{l-1})$. The complex variables $t_k = \int_{\mathcal{C}_k} \omega + ib$, $k = 1, \ldots, h_{1,1}(M_{l-1})$ parametrize locally the complexified moduli space $\mathcal{M}_{\text{cKs}}(W_{l-1})$ of W_{l-1}. We will elaborate on the concept of mirror symmetry and its implications in chapter 8.

We will next discuss the space $\mathcal{M}_{\text{cs}}(M_{l-1})$ of complex structure deformations of M_{l-1}. This space is redundantly parametrized by the complex coefficients a_i for $i = 0, \ldots, n_p$ in (6.8). The $\underline{a}$ are identified by $l+1$ scaling relations on the coordinates of $\mathbb{P}_{\hat{\Delta}_l}$ and the automorphism of $\mathbb{P}_{\hat{\Delta}_l}$ that leaves M_{l-1} invariant but acts on the parametrization of the polynomial constraint P_{Δ_l}. The latter one-parameter families of identifications of the deformation parameters are in an one-to-one correspondence to the points inside codimension one faces of Δ_l. Let us denote by Θ_k^j all faces of codimension k in Δ_l labeled by j. $I(\Theta_k^j)$ denotes the number of lattice points contained in Θ_k^j, while $I'(\Theta_k^j)$ denotes the number of lattice points that lie in the interior of $\Theta_k^{(j)}$. With this notation M_{l-1} has $I(\Delta_l) - (l+1) - \sum_j I'(\Theta_1^j)$ independent complex structure deformations. They correspond to elements in $H^1(M_{l-1}, TM_{l-1})$ and are unobstructed on a Calabi-Yau manifold M_{l-1}. The cohomology group $H^1(M_{l-1}, TM_{l-1})$ is related to the cohomology group $H^{l-2,1}(M_{l-1})$ via the contraction with the unique holomorphic $(l-1,0)$-form, see also section 4.1.

Equation (6.13) implies that, in particular, the complex dimensions of these spaces have to match, i.e. $h_{1,1}(X_{\hat{\Delta}_l}) = h_{l-2,1}(X_{\Delta_l})$ and $h_{1,1}(X_{\Delta_l}) = h_{l-2,1}(X_{\hat{\Delta}_l})$. From theses facts it follows that the dimensions of these important cohomology groups are given by counting integral

points in the polytops[6]

$$\begin{aligned} h_{1,1}(X_{\Delta_l}) &= I(\hat{\Delta}_l) - (l+1) - \sum_j I'(\hat{\Theta}_1^j) + \sum_j I'(\hat{\Theta}_2^i) I'(\Theta_{l-2}^i)) = 2^{l+1} - l - 2 \\ h_{l-2,1}(X_{\Delta_l}) &= I(\Delta_l) - (l+1) - \sum_i I'(\Theta_1^i) + \sum_i I'(\Theta_2^i) I'(\hat{\Theta}_{l-2}^i)) = l^2 \,. \end{aligned} \tag{6.14}$$

For $l = 3$ the Calabi-Yau manifold M_2 will be a nine-parameter family of polarized K3 surfaces. In this case the transversal cycles in h_{11} are counted $h_{11}^T = I(\Delta_l) - (l+1) = 9$, i.e. in total one has eleven transcendental and eleven algebraic two-cycles, which are counted by $h_{11}^A = I(\hat{\Delta}_l) - (l+1) = 11$. For $l = 4$ the 16-parameter family of Calabi-Yau three-folds M_3 has $h_{11} = 26$ and $h_{21} = 16$ and hence Euler number $\chi = 20$. For $l = 5$ the Calabi-Yau four-fold M_4 has $h_{31} = 25$, $h_{11} = 57$, $h_{21} = 0$ and $\chi = 540$. Using an index theorem [133] one gets $h_{22} = 422$. These numbers are important topological data of the $(l-1)$-dimensional Calabi-Yau varieties and they can be used to distinguish them. We notice this at this point because later we will define another Calabi-Yau geometry associated to the banana graph which is topological different to the hypersurface geometry defined here simply because the Euler numbers computed here differ. We will discuss this point later in more detail.

Since our polytope (6.5) has only $\sum_i I(\Theta_l^i) = l(l+1)$ corners and one inner point the manifold M_{l-1} has l^2 complex structure deformations, which at the end have to be mapped to our physical parameters p^2 and $\underline{m}^2$. Due to the scaling behavior (2.4) we can scale one parameter away such that we have only $l+1$ independent physical parameters. Therefore, the map to the physical parameter space has a huge kernel for high loop l and special effort has to be made to specify the relevant physical subspace of $\mathcal{M}_{\text{phys}}(M) \subset \mathcal{M}_{\text{cs}}(M)$ as described concretely in the example section 6.3. This is also why later we prefer the other geometry associated to the l-loop banana graph since there the dimension of the complex structure deformation space equals the relevant physical parameter space.

Actual properties of the smooth canonical resolution of M_{l-1}^s, in particular its Kähler cone, depend on the choice of the star triangulation $\hat{\mathcal{T}}$ of $\hat{\Delta}_l$. However, these detailed properties of the Kähler moduli space $\mathcal{M}_{\text{cKs}}(M_{l-1})$ of M_{l-1} do not affect the complex moduli space $\mathcal{M}_{\text{cs}}(M_{l-1})$ and also not the maximal cuts of the banana integral. The maximal cut integrals depend only on the complex structure parameters. The blow up coordinate ring allows, however, a useful description of the boundary contribution to the full Feynman integral, see [113]. Moreover, the identification (6.13) turns out to be very useful to introduce suitable coordinates on $\mathcal{M}_{\text{cs}}(M_{l-1})$ to obtain solutions for the integral (6.1). Different star triangulations $\mathcal{T}$ of the polyhedra Δ_l correspond to different Kähler cones of the ambient space $\mathbb{P}_{\Delta_l}$ of W_{l-1} and correspond eventually[7] to different Kähler cones of W_{l-1}. Each choice

[6] The last terms after the first equal sign in the formulas in each line of (6.14) correspond to Kähler— or complex structure deformations, which are frozen by the toric realization of the manifolds, respectively. Likewise the third terms are absent in our case. The last equality holds only for the polyhedra given in (6.5) and (6.7).

[7] If all curves that bound the Kähler cone of $\mathbb{P}_{\Delta_l}$ descend to the hypersurface W_{l-1}.

of the Kähler cone of W_{l-1} defines by mirror symmetry and the identification (6.13) canonical so called Batyrev coordinates z_i^{B} for $i = 1, \ldots, h_{l-2,1}(M_{l-1}) = h_{1,1}(W_{l-1}) =: h$ on $\mathcal{M}_{\mathrm{cs}}(M_{l-1})$. These are very useful and good coordinates since they reflect best the symmetries of the complex structure moduli space $\mathcal{M}_{\mathrm{cs}}(M_{l-1})$. Moreover, at their origin $z_i^{\mathrm{B}} = 0$ for all i there is a MUM-point of $\mathcal{M}_{\mathrm{cs}}(M)$. The coordinates $\underline{z}^{\mathrm{B}}$ are ratios of the coefficients $\underline{a}$ of P_{Δ_l} given for each triangulation by

$$z_i^{\mathrm{B}} = (-a_0)^{\ell_0^{(i)}} \prod_k a_k^{\ell_k^{(i)}}, \quad i = 1, \ldots, n_p - l = h \,. \tag{6.15}$$

The definition of the $\underline{z}^{\mathrm{B}}$ eliminates the scaling relation. Since in our case we have no codimension one points, i.e., no automorphism of $\mathbb{P}_{\hat{\Delta}}$ leaving the hypersurface invariant and further identifying the $\underline{a}$ deformations, the $\underline{z}^{\mathrm{B}}$ are actual coordinates on $\mathcal{M}_{\mathrm{cs}}(M_{l-1})$. In other simple cases one can restrict in the definition of L (6.11) to linear relations of points, which are not in codimensions one, the general case is discussed in [153, 155]. In the moduli space of $\mathcal{M}_{\mathrm{cs}}(M_{l-1})$ as parametrized only by the independent a_i, the $\underline{z}^{\mathrm{B}}$ are blow up coordinates resolving singular loci in discriminant components of the hypersurface $P_{\Delta_l} = 0$ in $\mathcal{M}_{\mathrm{cs}}(M_{l-1})$, so that these become in the resolved model of the complex moduli space $\widehat{\mathcal{M}_{\mathrm{cs}}}(M_{l-1})$ intersection points of normal crossing divisors $D_i = \{z_i = 0\}$, $i = 1, \ldots, h_{l-2,1}(M_{l-1})$.

Of particular significance in the geometric toric construction of the differentials on M_{l-1} is the coefficient a_0 of the monomial $\prod_{i=1}^{l+1} x_i$ in $\mathcal{F}_l(p^2, \underline{m}^2; \underline{x})$ corresponding to the inner point in Δ_l, which is given in the physical parameters by[8]

$$a_0 = -p^2 + \sum_{i=1}^{l+1} m_i^2 \,. \tag{6.16}$$

6.1.2 Period integrals of the hypersurface model M_{l-1}

The Baytrev coordinates $\underline{z}^{\mathrm{B}}$ defined by the Mori cone $\ell^{(k)}$ vectors of the mirror W_{l-1} are so constructed, as already said, that at their origin $z_i^{\mathrm{B}} = 0$ for all $i = 1, \ldots h$ one has a point of MUM-point. Now we can use all the beautiful structures of a MUM-point as explained in chapter 4. For instance, we can simply compute the period ϖ_0 which is given at the MUM-point by an integral over the cycle $\mathbf{T} = T^{l-1}$ in the Calabi-Yau M_{l-1}. This period ϖ_0 is the holomorphic period at the MUM-point and is given as the unique power series in the Frobenius basis, see section 3.3. In the toric ambient space this integral can be written as a

[8] Notice here an additional minus sign compared to the works [44, 45] since there the second Symanzik polynomial is normalized with this additional -1 factor. This difference will continue through this thesis to guarantee consistent conventions.

residue integral over a T^l of the holomorphic $(l-1,0)$-form $\Omega_{l-1}(\underline{z}^{\mathrm{B}})$. With the $\ell^{(k)}$ vectors we can compute

$$\begin{aligned}\varpi_0(\underline{z}^{\mathrm{B}}) &= \frac{1}{(2\pi i)^l}\int_{T^l}\frac{a_0\mu_l}{\mathcal{F}_l(\underline{a};\underline{x})} = \frac{1}{(2\pi i)^{l-1}}\int_{T^{l-1}}\Omega_{l-1}(\underline{z}^{\mathrm{B}}) \\ &= \sum_{\{\underline{k}\}}\frac{\Gamma\left(-\sum_{\alpha=1}^{h}\ell_0^{(\alpha)}k_\alpha+1\right)}{\prod_{l=1}^{n_p}\Gamma\left(\sum_{\alpha=1}^{h}\ell_l^{(\alpha)}k_\alpha+1\right)}\prod_{\alpha=1}^{h}z_\alpha^{\mathrm{B}\,k_\alpha}\,.\end{aligned} \tag{6.17}$$

First, notice the factor of a_0 in the numerator such that the integral is invariant under rescalings of the paramters $\underline{a}$. This factor has to be divided out later to get the actual Feynman integral. In eq. (6.17) we use the coordinate ring $\underline{x}$ as in (6.4) and set $x_{l+1}=1$. In the tuple $\{\underline{k}\}=\{k_1,\ldots,k_h\}$ each k_i runs over non negative integers $k_i\in\mathbb{N}_0$. Note that by definition the sum of the integer entries in each $\ell^{(k)}$ is zero. Therefore, they have also negative entries. For hypersurfaces and complete intersections the $\ell_0^{(k)}$ entry is non-positive $\ell_0^{(k)}\leq 0$ for all k. However, for $i>0$ the $\ell_i^{(k)}$ can have either sign. Poles of the gamma function at negative integers in the denominator make the summand vanishing. This effectively restricts the range of the $\{k_1,\ldots,k_h\}$ to a positive cone

$$\sum_{\alpha=1}^{h}\ell_j^{(\alpha)}k_\alpha\geq 0\,. \tag{6.18}$$

Restricting to the physical slice means to parametrize the a_i, $i=0,\ldots,n_p$ by the physical variables $p^2,\underline{m}^2$ and, therefore, we have $\underline{z}^{\mathrm{B}}=\underline{z}^{\mathrm{B}}(p^2,\underline{m}^2)$. Due to the definition of (6.15) one can find a splitting of the set of indices $\{\alpha_1,\ldots,\alpha_h\}$ into $\{\alpha_1,\ldots,\alpha_{l+1}\}$ and $\{\alpha_{l+2},\ldots,\alpha_h\}$ so that the variables $\{z^{\mathrm{B}}_{\alpha_{l+2}},\ldots,z^{\mathrm{B}}_{\alpha_h}\}$ are either set to constant values[9] or identified with the variables $z^{\mathrm{B}}_{\alpha_j}(p^2,\underline{m}^2)$ for $i=1,\ldots,l+1$. A key observation in the examples of the banana family is that the range (6.18) is such that the contribution from the summation over the k_{α_j}, $j=l+2,\ldots,h$ to each monomial $\prod_{i=1}^{l+1}z_{\alpha_i}^{\mathrm{B}\,k_i}$ is finite. This implies that we can also give (6.17) non-redundantly in the $l+1$ physical parameters $z^{\mathrm{B}}_{\alpha_i}(p^2,\underline{m}^2)$ for $i=1,\ldots,l+1$ exactly to arbitrary order. The range (6.18) and (6.17) can also be calculated directly as follows: Expanding in the integrand $a_0/\mathcal{F}_l(\underline{a};\underline{x})=[1/\prod_i x_i]\,[1/(1-1/a_0(\ldots))]$ the second factor as a geometric series and noticing that only the constant terms of it contribute to the integral yields the result. Applying this to the torus integral ϖ_0 we find for the maximal cut after

[9] In principle, this can also mean zero or infinity where both limits have to be treated carefully since they can result in divergencies of the period integrals on this subslice. Problems of divergencies if one goes onto the subslice will be discussed later in the text in more detail.

dividing through the inner point a_0 given in (6.16)

$$M_l^{T^{l-1}}(p^2, \underline{m}^2) = \frac{\varpi_0\left(\underline{z}^{\mathrm{B}}(p^2, \underline{m}^2)\right)}{-p^2 + \sum_{i=1}^{l+1} m_i^2} \tag{6.19}$$

This is an exact series expansion with finite radius of convergence for regions in the physical parameters in which $\underline{z}^{\mathrm{B}}(p^2, \underline{m}^2)$ are all small.

The other periods around the MUM-point can be computed with the Frobenius method, see section 3.3. For this we introduce h auxiliary deformation parameters ρ_α in

$$\varpi(\underline{z}^{\mathrm{B}}, \underline{\rho}) = \sum_{n_1,\dots,n_h \geq 0} c(\underline{n}, \underline{\rho}) \underline{z}^{\mathrm{B}\underline{n}+\underline{\rho}}, \tag{6.20}$$

where $\underline{z}^{\mathrm{B}\underline{n}+\underline{\rho}} := \prod_{\alpha=1}^{h} z_\alpha^{\mathrm{B}n_\alpha+\rho_\alpha}$ and

$$c(\underline{k}, \underline{\rho}) = \frac{\Gamma\left(-\sum_{\alpha=1}^{h} \ell_0^{(\alpha)}(n_\alpha + \rho_\alpha) + 1\right)}{\prod_{l=1}^{n_p} \Gamma\left(\sum_{\alpha=1}^{h} \ell_l^{(\alpha)}(n_\alpha + \rho_\alpha) + 1\right)}\,. \tag{6.21}$$

With this definition $\varpi_0(\underline{z}^{\mathrm{B}}) = \varpi(\underline{z}^{\mathrm{B}}, \underline{\rho})|_{\underline{\rho}=0}$ and the $h^{n-1,1}$ linear logarithmic solutions are given by

$$\varpi_1^{(\alpha)}(\underline{z}^{\mathrm{B}}) = [(1/(2\pi i)\partial_{\rho_\alpha}\varpi(\underline{z}^{\mathrm{B}}, \underline{\rho})]|_{\underline{\rho}=0} = 1/(2\pi i)\varpi_0(\underline{z}^{\mathrm{B}})\log(z_\alpha^{\mathrm{B}}) + \mathcal{O}(z) \tag{6.22}$$

for $\alpha = 1, \cdots, h$. All other solutions of degree $2 \leq k \leq l-1$ in the logarithms are of the form

$$\varpi_k^{(i)}(\underline{z}^{\mathrm{B}}) = [c_i^{\alpha_1\dots\alpha_k}\partial_{\rho_{\alpha_1}}\dots\partial_{\rho_{\alpha_k}}\varpi(\underline{z}^{\mathrm{B}}, \underline{\rho})]|_{\underline{\rho}=0} \tag{6.23}$$

for $i = 1, \dots, n_{\text{k-log. sol.}}$. The tensors $c_i^{\alpha_1\dots\alpha_k}$ can be chosen such that the functions ϖ_k are period integrals of actual cycles in integral homology when they contain the correct transcendental numbers which are dictated by the $\widehat{\Gamma}$-class conjecture and classical intersection theory on W. We will demonstrate this in chapter 8 at least for some particular cycles but also for the other geometric realization we introduce in chapter 7. There we also comment why this is much more difficult for the hypersurfaces.

6.1.3 GKZ method for the banana integrals

Gel′fand, Kapranov and Zelevinskǐ [158] investigated integrals of the from

$$I_\sigma^{GKZ} = \int_\sigma \prod_{i=1}^{r} P(x_1,\dots,x_k)^{\alpha_i} x_1^{\beta_1}\cdots x_k^{\beta_k} \mathrm{d}x_1\cdots\mathrm{d}x_k\,, \tag{6.24}$$

where they consider σ to be a cycle without a precise definition in [158]. The full banana integral in $D=2$ dimensions (6.1) is a special case of the general integral (6.24) where the integration domain σ_l is given by a chain. In comparison the integral in (6.17) is over a closed cycle T^l but still a specialization of (6.24). For the GKZ method this means that for the former we obtain a set of inhomogeneous differential equations because the chain σ_l is an open cycle on the Calabi-Yau variety whereas the maximal cut integrals, as in particular the torus integral in (6.17), are governed by homogeneous equations.

In general the GKZ integrals I_σ^{GKZ} can be viewed as a systematic multivariable generalization of the Euler integral

$${}_2F_1(a,b,c;z) = \sum_{n=0}^{\infty} \frac{(a)_n (b)_n}{n!(c)_n} = \frac{\Gamma(c)}{\Gamma(b)\Gamma(b-c)} \int_0^1 t^{(b-1)}(1-t)^{(b-c-1)}(1-zt)^{-a}\,\mathrm{d}t\,, \tag{6.25}$$

which solves the Gauss hypergeometric system. In this sense ϖ_0 is a generalized multivariable hypergeometric series.

The power of the GKZ method goes back to a detailed analysis of the scaling properties of integrals as given in (6.24). Using these scaling properties one can write down a set of differential equations the integral (6.24) satisfies. These differential equations will be computed in a combinatorial fashion which is much easier and faster than the full Griffiths reduction method. But this set of differential equations is typically not large enough to uniquely determine the integral (6.24), in particular, since the GKZ method does not give boundary conditions for these differential equations. It does not even give the smallest set of functions which describe the integral (6.24). But later we show how one can deal with these issues at least in the context of the banana integrals.

The scaling relations of the l-loop banana integral follow from the linear relations between the points of the associated Newton polytope Δ_l. These were generated by the $\ell^{(k)}$ vectors. Now each $\ell^{(k)}$ give rise to a differential operator $\mathcal{D}_{\ell^{(k)}}$ in the redundant moduli $\underline{a}$. Moreover, the infinitesimal invariance under the $(\mathbb{C}^*)^{l+1}$ scaling relations yields further differential

operators $\mathcal{Z}_j$, $j = 1, \ldots, l+1$. Together they constitute a resonant GKZ system [117, 159]:

$$\begin{aligned} \hat{\mathcal{D}}_{\ell^{(k)}} M_l^\Gamma &= \left(\prod_{\ell_i^{(k)}>0} \left(\frac{\partial}{\partial a_i}\right)^{\ell_i^{(k)}} - \prod_{\ell_i^{(k)}<0} \left(\frac{\partial}{\partial a_i}\right)^{-\ell_i^{(k)}} \right) M_l^\Gamma = 0 \quad \text{and} \\ \mathcal{Z}_j M_l^\Gamma &= \left(\sum_{i=0}^{p} \bar{\nu}_{i,j} \theta_{a_i} - \beta_j \right) M_l^\Gamma = 0 \end{aligned} \tag{6.26}$$

with $\beta = (-1, 0, ..., 0) \in \mathbb{R}^{l+1}$ for the hypersurface case and $\theta_a = a\,\partial_a$ and Γ a cycle defining a maximal cut. This form applies to the period integrals of Calabi-Yau hypersurfaces in toric varieties [152, 153]. Notice that these operators are given in terms of the redundant variables $\underline{a}$. To turn them into operators of our favorite Batyrev coordinates $\underline{z}^{\mathrm{B}}$ we have to include an additional factor of a_0 such that they annihilate $a_0 M_l^\Gamma$ which at the end has to be divided out again since we are only interested in M_l^Γ. We can use the relations $\mathcal{Z}_j M_l^\Gamma = 0$ to eliminate the $\underline{a}$ in favour of the scale invariant $\underline{z}^{\mathrm{B}}$ defined in (6.15) using $a_i \partial_{a_i} = \sum_{k=1}^{l^2} \ell_i^{(k)} z_k^{\mathrm{B}} \partial_{z_k^{\mathrm{B}}}$ and by the commutation relation $[\theta_a, a^r] = r a^r$ applied previously to a_0 we obtain operators $\mathcal{D}_{\ell^{(k)}}(\underline{z}^{\mathrm{B}})$ that annihilate $a_0 M_l^\Gamma$. As it turns out these operators do not only determine the $a_0 M_l^\Gamma$ since they admit further solutions [153]. To obtain the actual Picard-Fuchs differential ideal one can factorize the $\mathcal{D}_{\ell^{(k)}}(\underline{z}^{\mathrm{B}})$ and disregard trivial factors that allow for additional solutions which have the wrong asymptotic to be periods [48, 153]. In practice, the most efficient way to get the Picard-Fuchs differential ideal is often to make an ansatz for additional minimal order differential operators that annihilate (6.17) and check that the total system of differential operators allows no additional solutions then the ones specified in (6.22) and (6.23). Or, as we do in section 9.2 cf. eq. (9.11), one can analyze the structure of the quotient of gamma functions in (6.17) to write down additional differential operators simply from the combinatorics of these gamma functions.

One of our main results of [44] is that we give the general strategy to derive the Picard-Fuchs differential ideal in the physical parameters $\underline{z}^{\mathrm{B}}(p, \underline{m}^2)$ for $i = 1, \ldots, l+1$. We recall this in this thesis for the three-loop case which corresponds to a two-dimensional Calabi-Yau also known as K3 surface. These operators determine the maximal cut integrals everywhere in the parameter space. By applying these operators to the geometrical chain integral

$$\int_{\sigma_l} \frac{a_0\, \mu_l}{\mathcal{F}_l(\underline{a}; \underline{x})} \tag{6.27}$$

and integrating explicitly over the boundary of the chain σ_l we can find the inhomogeneous differential equations and the corresponding special solutions describing the full l-loop banana graph explicitly. With this method we could reach loop orders $l = 1, 2, 3$ in [44] and $l = 4$ in [45] where for $l = 3, 4$ the generic mass case was not known before. For even higher loop orders this method gets too time consuming and we would recommend to use

the methods explained in chapter 7 which give also results for much higher loop orders.

6.1.4 Mori cone generators and subslice problem

There are two main difficulties in the case of the banana family if one wants to use the GKZ method of a hypersurface Calabi-Yau. The first problem concerns the number of ℓ-vectors which can be too large although an appropriate triangulation of the polytope Δ_l is used. The second problem is that the smooth hypersurface Calabi-Yau has to many parameters compared to the actual number of physical parameters. Therefore, one has to deal with a subslice problem. Both difficulties could be solved in [44] where also a longer discussion about them is given.

The minimal number of ℓ-vectors should be equal to l^2 which is also the number of complex structure deformations of the Calabi-Yau M_{l-1} as given in (6.14). But it can happen that an appropriate triangulation $\mathcal{T}$ give rise to more ℓ-vectors. In this case one has to select only l^2 ℓ-vectors such that the following conditions we made and claimed in [44] are fulfilled. Firstly, the selected ℓ-vectors should be linear independent over the reals. Secondly, we want that at least for each entry of a ℓ-vector corresponding to a vertex of the polytope different to the origin there is a ℓ-vector which has a positive entry at this position. With these conditions we were able to choose a correct set of ℓ-vectors for the banana integrals.

To restrict onto the physical subslice one has to analyze the holomorphic solution (6.17) carefully. Using the inequalities (6.18) it is possible to resum the summations in (6.17) of the unphysical Batyrev coordinates, i.e., the ones which have no counterpart in the physical parameters p^2 and $\underline{m}^2$ since they have to be set to unity or another value. This means that the infinite sums in (6.17) of the unphysical Batyrev coordinates are actually finite and these can be simply set to unity or another value without causing divergencies. Then one can use ϖ_0 expressed only in the physical important Batyrev coordinates to generate the other solutions. For this one makes an ansatz of operators spanning a differential operator ideal which describes this holomorphic solution together with other logarithmic solutions such that all solutions describe a Calabi-Yau motive with $l+1$ logarithmic solutions. One should start first with second order operators and extends then with higher-order operators if necessary. For more details see section 2.2.4 of [44].

6.2 The complete banana diagram and inhomogeneous differential equations

So far we have only described the solutions corresponding to the maximal cuts of the banana graphs. These correspond to the period integrals of a Calabi-Yau hypersurface M_{l-1} and can be described by a differential operator ideal which can be found with the prescription given in the last subsection. But now we have to extend this to yield the actual full Feynman integral (6.1) in $D = 2$ dimensions.

For this we want to extend the differential operator ideal of the maximal cuts to a set

of inhomogeneous differential operators. Here we simply apply these operators on the full Feynman integral (6.1) for some fixed value of the Batyrev coordinates and perform the resulting integral numerically. This integration can be done with standard numerical integration routines implemented, for example in `mathematica`. Then the crucial step is to guess the analytic form of the result. For this one has to do the numerical integration for different values of the Batyrev coordinates and analyze the form of the result. Fortunately, there is a good guess how the inhomogeneities have to look like. From integration by parts section 2.3.2 and the construction of the Gauss-Manin connection section 3.2 we know that the inhomogeneities are given by the subtopologies having less propagators. For the banana graphs there is only one type of subtopology which is a tadpole, cf. eq. (2.19). In $D = 2$ a tadpole has roughly the form of $\log(z_i^B)$. Therefore, we can make an ansatz out of $\log(z_i^B)$ for the inhomogeneities of the differential operators. For more details we refer again to [44] section 2.3.

6.3 Example: The generic mass three-loop banana integral

In this section we want to demonstrate our method for the three-loop banana integral. This was before our paper [44] the first unknown generic mass case in the infinite series of l-loop banana graphs. In [44] we have given more details and also more examples are shown for the interesting reader.

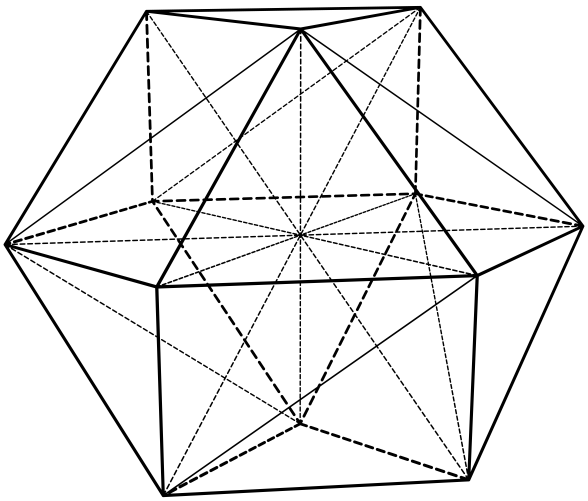

Figure 6.1: Polytope Δ_3 together with a triangulation for the three-loop banana graph.

The geometry underlying the three-loop banana integral is a K3 surface. In the hypersurface description this K3 surface can be constructed from the polytope shown in figure 6.1.

This polytope is constructed from the vertices

$$\begin{aligned}&\{(-1,1,0),(1,0,0),(0,-1,1),(0,0,1),(1,-1,0),(1,0,-1),(0,0,-1),(-1,0,1),\\&\quad(0,-1,0),(-1,0,0),(0,1,0),(0,1,-1),(0,0,0)\}\,,\end{aligned} \tag{6.28}$$

which are the exponents of the monomials in the second Symanzik Polynomial $\mathcal{F}_3(p^2,\underline{m}^2;\underline{x})$ given in (2.30). In figure 6.1 we have also drawn a triangulation which give the following nine ℓ-vectors

$$\begin{aligned}\ell_1&=(0,0,-1,0,1,0,0,1,0,0,0,0,-1)\,, & \ell_2&=(0,-1,0,0,1,0,0,0,0,0,1,0,-1)\\ \ell_3&=(0,-1,0,1,0,1,0,0,0,0,0,0,-1)\,, & \ell_4&=(0,0,-1,1,0,0,0,0,1,0,0,0,-1)\\ \ell_5&=(-1,0,0,-1,0,0,0,1,0,0,1,0,0)\,, & \ell_6&=(0,0,0,0,-1,1,-1,0,1,0,0,0,0)\\ \ell_7&=(0,0,1,0,0,0,0,-1,-1,1,0,0,0)\,, & \ell_8&=(0,1,0,0,0,-1,0,0,0,0,-1,1,0)\\ \ell_9&=(1,0,0,0,0,0,1,0,0,-1,0,-1,0)\,.\end{aligned} \tag{6.29}$$

This set of ℓ-vectors yields directly a minimal set and the Batyrev coordinates. On the physical subslice, i.e., expressed only through the physical parameters p^2 and $\underline{m}^2$, they are given by

$$\begin{aligned}z_1^{\mathrm{B}}&=\frac{m_1^2}{p^2-m_1^2+m_2^2+m_3^2+m_4^2}\,,\\ z_2^{\mathrm{B}}&=\frac{m_2^2}{p^2-m_1^2+m_2^2+m_3^2+m_4^2}\,,\\ z_3^{\mathrm{B}}&=\frac{m_3^2}{p^2-m_1^2+m_2^2+m_3^2+m_4^2}\,,\\ z_4^{\mathrm{B}}&=\frac{m_4^2}{p^2-m_1^2+m_2^2+m_3^2+m_4^2}\end{aligned} \tag{6.30}$$

and $z_5^{\mathrm{B}}=\cdots=z_9^{\mathrm{B}}=1$. From the ℓ-vectors we can find the holomorphic solution which is given on the physical subslice by

$$\begin{aligned}\omega_0(z_1^{\mathrm{B}},z_2^{\mathrm{B}},z_3^{\mathrm{B}},z_4^{\mathrm{B}})&=\sum_{\mathcal{J}}\frac{\Gamma(1+m_1+m_2+m_3+m_4)}{\Gamma(1+m_3+m_4-m_5)\Gamma(1+m_1+m_2-m_6)\Gamma(1+m_1+m_5-m_7)\Gamma(1+m_4+m_6-m_7)}\\&\quad\cdot\frac{{z_2^{\mathrm{B}}}^{m_1}{z_3^{\mathrm{B}}}^{m_2}{z_4^{\mathrm{B}}}^{m_3}{z_5^{\mathrm{B}}}^{m_4}}{\Gamma(1-m_1-m_4+m_7)\Gamma(1+m_2+m_5-m_8)\Gamma(1+m_3+m_6-m_8)\Gamma(1-m_2-m_3+m_8)}\\&\quad\cdot\frac{1}{\Gamma(1+m_7-m_9)\Gamma(1+m_8-m_9)\Gamma(1-m_5+m_9)\Gamma(1-m_6+m_9)}\\&=1+2\left(z_1^{\mathrm{B}}z_2^{\mathrm{B}}+z_1^{\mathrm{B}}z_3^{\mathrm{B}}+z_1^{\mathrm{B}}z_4^{\mathrm{B}}+z_2^{\mathrm{B}}z_3^{\mathrm{B}}+z_2^{\mathrm{B}}z_4^{\mathrm{B}}+z_3^{\mathrm{B}}z_4^{\mathrm{B}}\right)\\&\quad+12\left(z_1^{\mathrm{B}}z_2^{\mathrm{B}}z_3^{\mathrm{B}}+z_1^{\mathrm{B}}z_2^{\mathrm{B}}z_4^{\mathrm{B}}+z_1^{\mathrm{B}}z_3^{\mathrm{B}}z_4^{\mathrm{B}}+z_2^{\mathrm{B}}z_3^{\mathrm{B}}z_4^{\mathrm{B}}\right)+\cdots\,,\end{aligned} \tag{6.31}$$

where the summation range is

$$\begin{aligned}\mathcal{J} = \{&0 \leq m_1 \leq \infty,\ 0 \leq m_2 \leq \infty,\ 0 \leq m_3 \leq \infty,\ 0 \leq m_4 \leq \infty,\ 0 \leq m_5 \leq m_3 + m_4,\\ &m_2 + m_3 \leq m_8 \leq m_2 + m_5,\ 0 \leq m_6 \leq m_1 + m_2,\ m_1 + m_4 \leq m_7 \leq m_1 + m_5,\\ &m_6 \leq m_9 \leq m_7\}\end{aligned} \tag{6.32}$$

after having used the inequalities (6.18) appropriate. Then one can find the differential operators $\mathcal{D}_1, \ldots, \mathcal{D}_4$ generating a differential operator ideal for the K3 periods. These are listed in appendix A. The single-logarithmic solutions of these operators are

$$\begin{aligned}\varpi_1^{(1)}(\underline{z}^{\mathrm{B}}) &= \varpi_0 \log(z_1^{\mathrm{B}}) + \Sigma_1^1\\ \varpi_1^{(2)}(\underline{z}^{\mathrm{B}}) &= \varpi_0 \log(z_2^{\mathrm{B}}) + \Sigma_1^2\\ \varpi_1^{(3)}(\underline{z}^{\mathrm{B}}) &= \varpi_0 \log(z_3^{\mathrm{B}}) + \Sigma_1^3\\ \varpi_1^{(4)}(\underline{z}^{\mathrm{B}}) &= \varpi_0 \log(z_4^{\mathrm{B}}) + \Sigma_1^4\end{aligned} \tag{6.33}$$

with

$$\begin{aligned}\Sigma_1^1 = &-z_1^{\mathrm{B}} + z_2^{\mathrm{B}} + z_3^{\mathrm{B}} + z_4^{\mathrm{B}} + \tfrac{z_1^{\mathrm{B}2}}{2} - \tfrac{z_2^{\mathrm{B}2}}{2} - \tfrac{z_3^{\mathrm{B}2}}{2} - \tfrac{z_4^{\mathrm{B}2}}{2}\\ &+ z_1^{\mathrm{B}} z_2^{\mathrm{B}} + z_1^{\mathrm{B}} z_3^{\mathrm{B}} + z_1^{\mathrm{B}} z_4^{\mathrm{B}} + z_2^{\mathrm{B}} z_3^{\mathrm{B}} + 5 z_2^{\mathrm{B}} z_3^{\mathrm{B}} + 5 z_2^{\mathrm{B}} z_4^{\mathrm{B}} + 5 z_3^{\mathrm{B}} z_4^{\mathrm{B}} + \cdots .\end{aligned} \tag{6.34}$$

The other Σ_1^i for $i = 2, 3, 4$ are given as permutations, namely $\Sigma_1^2 = \Sigma_1^1(z_1^{\mathrm{B}} \leftrightarrow z_2^{\mathrm{B}})$, $\Sigma_1^3 = \Sigma_1^1(z_1^{\mathrm{B}} \leftrightarrow z_3^{\mathrm{B}})$ and $\Sigma_1^4 = \Sigma_1^1(z_1^{\mathrm{B}} \leftrightarrow z_4^{\mathrm{B}})$. The double-logarithmic solution is given by

$$\begin{aligned}\varpi_2(\underline{z}^{\mathrm{B}}) = \varpi_0 z^{\mathrm{B}} \Big[&\log(z_1^{\mathrm{B}}) \log(z_2^{\mathrm{B}}) + \log(z_1^{\mathrm{B}}) \log(z_3^{\mathrm{B}}) + \log(z_1^{\mathrm{B}}) \log(z_4^{\mathrm{B}}) + \log(z_2^{\mathrm{B}}) \log(z_3^{\mathrm{B}})\\ &+ \log(z_2^{\mathrm{B}}) \log(z_4^{\mathrm{B}}) + \log(z_3^{\mathrm{B}}) \log(z_4^{\mathrm{B}})\Big] + \left(\Sigma_1^2 + \Sigma_1^3 + \Sigma_1^4\right) \log(z_1^{\mathrm{B}})\\ &+ \left(\Sigma_1^1 + \Sigma_1^3 + \Sigma_1^4\right) \log(z_2^{\mathrm{B}}) + \left(\Sigma_1^1 + \Sigma_1^2 + \Sigma_1^4\right) \log(z_3^{\mathrm{B}})\\ &+ \left(\Sigma_1^1 + \Sigma_1^2 + \Sigma_1^3\right) \log(z_4^{\mathrm{B}}) + \Sigma_2\end{aligned} \tag{6.35}$$

with

$$\Sigma_2 = 4 \left(z_1^{\mathrm{B}} z_2^{\mathrm{B}} + z_3^{\mathrm{B}} z_2^{\mathrm{B}} + z_4^{\mathrm{B}} z_2^{\mathrm{B}} + z_1^{\mathrm{B}} z_3^{\mathrm{B}} + z_1^{\mathrm{B}} z_4^{\mathrm{B}} + z_3^{\mathrm{B}} z_4^{\mathrm{B}}\right) + \cdots . \tag{6.36}$$

The differential operators $\mathcal{D}_1, \ldots, \mathcal{D}_4$ do not allow for further solutions as expected.

From numerics we can find for the inhomogeneities

$$\begin{aligned}
\mathcal{D}_1 &\to 0 \\
\mathcal{D}_2 &\to 5\log(z_1^{\mathrm{B}}) - 5\log(z_2^{\mathrm{B}}) \\
\mathcal{D}_3 &\to \log(z_1^{\mathrm{B}}) + \log(z_2^{\mathrm{B}}) + \log(z_3^{\mathrm{B}}) - 3\log(z_4^{\mathrm{B}}) \\
\mathcal{D}_4 &\to -5\log(z_3^{\mathrm{B}}) + 5\log(z_4^{\mathrm{B}})\,.
\end{aligned} \tag{6.37}$$

These inhomogeneous differential equations have an additional cubic-logarithmic solution

$$\begin{aligned}
\varpi_S = &-\varpi\Big[\log\left(z_1^{\mathrm{B}}\right)\log\left(z_2^{\mathrm{B}}\right)\log\left(z_3^{\mathrm{B}}\right) + \log\left(z_1^{\mathrm{B}}\right)\log\left(z_3^{\mathrm{B}}\right)\log\left(z_4^{\mathrm{B}}\right) \\
&+\log\left(z_1^{\mathrm{B}}\right)\log\left(z_3^{\mathrm{B}}\right)\log\left(z_4^{\mathrm{B}}\right) + \log\left(z_2^{\mathrm{B}}\right)\log\left(z_3^{\mathrm{B}}\right)\log\left(z_4^{\mathrm{B}}\right)\Big] \\
&-2\Big[(z_1^{\mathrm{B}}+z_2^{\mathrm{B}})\left(\log(z_1^{\mathrm{B}})+\log(z_2^{\mathrm{B}})\right) + (z_1^{\mathrm{B}}+z_3^{\mathrm{B}})\left(\log(z_1^{\mathrm{B}})+\log(z_3^{\mathrm{B}})\right) \\
&+(z_1^{\mathrm{B}}+z_4^{\mathrm{B}})\left(\log(z_1^{\mathrm{B}})+\log(z_4^{\mathrm{B}})\right) + (z_2^{\mathrm{B}}+z_3^{\mathrm{B}})\left(\log(z_2^{\mathrm{B}})+\log(z_3^{\mathrm{B}})\right) \\
&+(z_2^{\mathrm{B}}+z_4^{\mathrm{B}})\left(\log(z_2^{\mathrm{B}})+\log(z_4^{\mathrm{B}})\right) + (z_3^{\mathrm{B}}+z_4^{\mathrm{B}})\left(\log(z_2^{\mathrm{B}})+\log(z_4^{\mathrm{B}})\right)\Big] \\
&+2\Big[(-3z_1^{\mathrm{B}}+z_2^{\mathrm{B}}+z_3^{\mathrm{B}}+z_4^{\mathrm{B}})\log(z_1^{\mathrm{B}}) + (z_1^{\mathrm{B}}-3z_2^{\mathrm{B}}+z_3^{\mathrm{B}}+z_4^{\mathrm{B}})\log(z_2^{\mathrm{B}}) \\
&+(z_1^{\mathrm{B}}+z_2^{\mathrm{B}}-3z_3^{\mathrm{B}}+z_4^{\mathrm{B}})\log(z_3^{\mathrm{B}}) + (z_1^{\mathrm{B}}+z_2^{\mathrm{B}}+z_3^{\mathrm{B}}-3z_4^{\mathrm{B}})\log(z_4^{\mathrm{B}})\Big] \\
&+12(z_1^{\mathrm{B}}+z_2^{\mathrm{B}}+z_3^{\mathrm{B}}+z_4^{\mathrm{B}}) + \cdots\,.
\end{aligned} \tag{6.38}$$

One can then construct the full Feynman integral as a linear combination of the solutions 6.31, (7.13), (6.35) and (6.38). Additionally, one has to divide through the inner point a_0. Later in chapter 8 we will explain how one can determine the coefficients of this linear combination from mirror symmetry and the $\widehat{\Gamma}$-class.

CHAPTER 7

Complete Intersection Motive of the Banana Graphs

In the last chapter we have introduced a Calabi-Yau geometry defined by a hypersurface in a toric ambient such that the periods of this Calabi-Yau correspond to the maximal cuts of the banana graphs. Now we want to associate another and topological different Calabi-Yau geometry to the banana graphs such that again their periods describe the maximal cuts. This will be a complete intersection Calabi-Yau and we will argue that this motive is superior to the hypersurface motive. At the end we will compute the periods for the four-loop banana integral and demonstrate the power of this technique.

The complete intersection description was from us used in [45, 47] for the banana graphs.

7.1 A complete intersection Calabi-Yau for the l-loop banana graph

In the hypersurface geometry it was quite obvious that their period integrals correspond to the banana integral because they were literally the same integral expressions. Only the integration range was different. The cycle T^l give rise to the holomorphic period at the MUM-point and could be related to a maximal cut integral. The simplex integral over σ_l was a relative period of the hypersurface Calabi-Yau. So this was a direct identification between the banana integrals and the Calabi-Yau periods. For the complete intersection Calabi-Yau this identification is a little bit more indirect and one has really to compare the periods and not the integral expressions.

So let us start with a direct computation of the holomorphic period at the MUM-point[1]

$$\begin{aligned}\varpi_0(p^2,\underline{m}_i^2) &= -\frac{p^2}{(2\pi i)^l}\int_{T^l}\frac{1}{\left(\sum_{i=1}^{l+1}m_i^2x_i\right)\left(\sum_{i=1}^{l+1}\frac{1}{x_i}\right)-p^2}\frac{\mu_l}{\prod_{i=1}^{l+1}x_i}\\ &= \frac{1}{(2\pi i)^l}\int_{T^l}\sum_{n=0}^{\infty}\left(\frac{1}{p^2}\right)^n\left(\sum_{|k|=n}\binom{n}{k_1,\ldots,k_l+1}\prod_{i=1}^{l+1}(m_i^2x_i)^{k_i}\right)\\ &\qquad\times\left(\sum_{|\tilde{k}|=n}\binom{n}{\tilde{k}_1,\ldots,\tilde{k}_{l+1}}\prod_{i=1}^{l+1}x_i^{-\tilde{k}_i}\right)\frac{\mu_l}{\prod_{i=1}^{l+1}x_i}\\ &= \sum_{n=0}^{\infty}\sum_{|k|=n}\binom{n}{k_1,\ldots,k_l+1}^2\prod_{i=1}^{l+1}\left(\frac{m_i^2}{p^2}\right)^{k_i}\end{aligned} \tag{7.1}$$

with $|k|=\sum_{i=1}^{l+1}k_i$. For the second equality we have used the geometrical series and in the last line we evaluated all residues. We see that ϖ_0 is actually only a function of the ratios $z_i=m_i^2/p^2$ for $i=1,\ldots,l+1$ as expected from section 2.3. These parameters $\underline{z}$ are now the good parameters for the complete intersection geometry compared to the Batyrev coordinates $\underline{z}^{\mathrm{B}}$ for the hypersurface model. Before we move on let us emphasize that this is exactly the same as the holomorphic period we found from the hypersurface Calabi-Yau (6.17). The only difference is that in (6.17) we have used the Batyrev coordinates $\underline{z}^{\mathrm{B}}$ and one has to divide by the inner point contribution a_0. If one does this both expressions are the same.

The idea is that we want to build a Calabi-Yau geometry such that its holomorphic period is exactly (7.1). Moreover, we want that this geometry has naturally only the $l+1$ coordinates $\underline{z}$ and no further auxiallary parameters such that we do not have to worry about subslice problems as in the hypersurface case. To be honest this is not a simple task and in [45] we were lucky that we could find an appropriate candidate in the data base [160] after a hint from Matt Kerr.

This geometry is defined as a complete intersection of two polynomials in an ambient space. Therefore, we call it the complete intersection model. More precisely, these two polynomials are of degree $(1,\ldots,1)$ in

$$\mathbb{P}_{l+1}:=\bigotimes_{i=1}^{l+1}\mathbb{P}^1_{(i)}, \tag{7.2}$$

i.e.,

$$M_{l-1}=\left\{P_1(w_1^{(i)},w_2^{(i)})=P_2(w_1^{(i)},w_2^{(i)})=0|(w_1^{(i)}:w_2^{(i)})\in\mathbb{P}^1_{(i)},\forall i=1,\ldots,l+1\right\}\subset\mathbb{P}_{l+1} \tag{7.3}$$

[1] We have rescaled the integral by a factor of p^2 to compensate the scaling behavior from (2.4).

with the two degree $(1,\ldots,1)$ polynomial constraints

$$\begin{aligned} P_1 &= w_2^{(1)}\cdots w_2^{(l+1)}\left(\kappa - m_1^2\frac{w_1^{(1)}}{w_2^{(1)}} - \ldots - m_{l+1}^2\frac{w_1^{(l+1)}}{w_2^{(l+1)}}\right) \\ P_2 &= w_1^{(1)}\cdots w_1^{(l+1)}\left(-p^2 + \kappa\frac{w_2^{(1)}}{w_1^{(1)}} + \ldots + \kappa\frac{w_1^{(l+1)}}{w_1^{(l+1)}}\right) . \end{aligned} \tag{7.4}$$

Here we used as parameters the momentum p^2, the masses $\underline{m}^2$ and an additional parameter we call κ. The parameter κ can be scaled out and is only introduced for relating the complete intersection description to the hypersurface one. We can denote our complete intersection in a product of manifolds as

$$M_{l-1} = \left(\begin{array}{c|c} \mathbb{P}_1^1 & 1 \quad 1 \\ \vdots & \vdots \quad \vdots \\ \mathbb{P}_{l+1}^1 & 1 \quad 1 \end{array} \middle\} \, l+1\right) \subset \left(\begin{array}{c|c} \mathbb{P}_1^1 & 1 \\ \vdots & \vdots \\ \mathbb{P}_{l+1}^1 & 1 \end{array} \middle\} \, l+1\right) = F_l \subset \mathbb{P}_{l+1} \, . \tag{7.5}$$

The ambient manifold F_l is a Fano variety and we will see that it also plays an important role for the full banana integral.

We can construct a birational map from the smooth geometry in eq. (7.3) to the singular hypersurface geometry in eq. (6.2). First we go to a patch in $\mathbb{P}_{l+1}$ in which we can set all $w_2^{(i)}$ to unity. Then solving $P_1 = 0$ for the parameter κ one obtains $\kappa = \sum_{i=1}^{l+1} m_i^2 w_1^{(i)}$. Plugging this into the second constraint we immediately see that it is given by the second graph polynomial

$$P_2 = w_1^{(1)}\cdots w_1^{(l+1)}\left(-p^2 + \left(\sum_{i=1}^{l+1} m_i^2 w_1^{(i)}\right)\left(\sum_{i=1}^{l+1}\frac{1}{w_1^{(i)}}\right)\right) , \tag{7.6}$$

which defines the hypersurface geometry by (6.2). So we see that booth geometries are related through a birational map and so we expect that they should also both describe the maximal cuts of the banana graphs. But to make this even more explicit we can compute the holomorphic period of the complete intersection model directly from (7.3) and (7.4). Setting

$\kappa = 1$ and going to the patch with $w_2^{(i)} = 1$ for all $i = 1, \ldots, l+1$, we find for the torus period

$$\begin{aligned}
&\frac{-p^2}{(2\pi i)^{l+1}} \oint_{w_1^{(1)}=0} \cdots \oint_{w_1^{(l+1)}=0} \frac{1}{P_1 P_2} \mathrm{d}w_1^{(1)} \wedge \ldots \wedge \mathrm{d}w_1^{(l+1)} \\
&= \frac{1}{(2\pi i)^{l+1}} \oint_{w_1^{(1)}=0} \cdots \oint_{w_1^{(l+1)}=0} \frac{1}{1 - \sum_{i=1}^{l+1} m_i^2 w_1^{(i)}} \frac{1}{1 - \sum_{i=1}^{l+1} \frac{1}{p^2} \frac{1}{w_1^{(i)}}} \frac{\mathrm{d}w_1^{(1)}}{w_1^{(1)}} \wedge \ldots \wedge \frac{\mathrm{d}w_1^{(l+1)}}{w_1^{(l+1)}} \\
&= \frac{1}{(2\pi i)^{l+1}} \oint_{w_1^{(1)}=0} \cdots \oint_{w_1^{(l+1)}=0} \sum_{\substack{|m|=m \\ |n|=n}} \binom{m}{m_1 \ldots m_{l+1}} \binom{n}{n_1 \ldots n_{l+1}} \prod_{i=1}^{l+1} (m_i^2 w_1^{(i)})^{m_i} \left(\frac{1}{p^2 w_1^{(i)}} \right)^{n_i} \\
&\qquad \cdot \frac{\mathrm{d}w_1^{(1)}}{w_1^{(1)}} \wedge \ldots \wedge \frac{\mathrm{d}w_1^{(l+1)}}{w_1^{(l+1)}} \\
&= \sum_{n=0}^{\infty} \sum_{|k|=n} \binom{n}{k_1, \ldots, k_{l+1}}^2 \prod_{i=1}^{l+1} z_i^{k_i} = \varpi_0(\underline{z}) \,.
\end{aligned} \tag{7.7}$$

The last identity is obtained by performing all the residues and using the coordinates $z_i = \frac{m_i^2}{p^2}$. From this small computation we really see that the complete intersection Calabi-Yau provides the correct holomorphic period with the correct number of parameters for us.

7.1.1 Frobenius method for complete intersection geometry

So far we have only computed the holomorphic period for the complete intersection geometry. Similar as in the hypersurface model (6.20) - (6.23) one can construct all periods using the Frobenius method for complete intersections [48]. The crucial point is the knowledge of the ℓ-vectors which have for a complete intersection the form $\ell^{(k)} = (\ell_{01}^{(k)}, \ldots, \ell_{0h}^{(k)}\,;\, \ell_1^{(k)}, \ldots, \ell_c^{(k)})$ for $k = 1, \ldots, h^{l-2,1}(M_{l-1})$. Here h is the number of complete intersection constraints, c is the number of homogeneous coordinates of the ambient space and the $\ell_i^{(k)}$ for $i = 1, \ldots, c$ are the degrees of the constraints. For simple ambient spaces being products of (weighted) projective spaces one can directly write down the ℓ-vectors using the rules in [48]. For general toric ambient spaces one has to do a similar procedure as we did in the hypersurface case, namely one has to analyze the associated polyhedron and a triangulation of it is necessary. Also here we refer for more details to [48]. Fortunately, in the case of the banana graphs the ambient space is a product of $l+1$ copies of $\mathbb{P}^1$ and by (7.5) we have $h = 2$, $c = 2(l+1)$ and the $\ell^{(k)}$

read

$$\begin{aligned}
\ell^{(1)} &= (-1,-1;1,1,0,0,\cdots,0,0,0,0)\\
\ell^{(2)} &= (-1,-1;0,0,1,1,\cdots,0,0,0,0)\\
&\vdots\\
\ell^{(l)} &= (-1,-1;0,0,0,0,\cdots,1,1,0,0)\\
\ell^{(l+1)} &= (-1,-1;0,0,0,0,\cdots,0,0,1,1)\ .
\end{aligned} \tag{7.8}$$

From the ℓ-vectors we get first the natural variables of the geometry which are also called the Batyrev coordinates but now for a complete intersection. A general formula is given in [48] which is quite similar to the one in the hypersurface case (6.15). For the banana graph geometry one finds

$$z_i = \frac{m_i^2}{p^2} \quad \text{for } i = 1,\ldots,l+1\,, \tag{7.9}$$

which are exactly the right dimensionless parameters one would expect from eq. (7.1).

Secondly, one can construct from the ℓ-vectors a generalized Gelfand-Kapranov-Zelevinskĭ differential ideal with holomorphic solution

$$\omega(\underline{z};\underline{\rho}) = \sum_{n_1,\ldots,n_{l+1}\geq 0} c(\underline{n}+\underline{\rho})\,\underline{z}^{\underline{n}+\underline{\rho}}\,, \tag{7.10}$$

where the series coefficients $c(\underline{n})$ are determined by the $l+1$ ℓ-vectors via

$$c(\underline{n},\underline{\rho}) = \frac{\prod_{j=1}^{2}\Gamma\left(-\sum_{\alpha=1}^{l+1}\ell_{0j}^{(\alpha)}\,(n_\alpha+\rho_\alpha)+1\right)}{\prod_{i=1}^{2l+2}\Gamma\left(\sum_{\alpha=1}^{l+1}\ell_i^{(\alpha)}\,(n_\alpha+\rho_\alpha)+1\right)}\,. \tag{7.11}$$

In particular, the unique holomorphic solution at the point of maximal unipotent monodromy, i.e., $z_i = \frac{m_i^2}{p^2} = 0$ for $i = 1,\ldots,l+1$, is given by

$$\varpi_0(\underline{z}) = \omega(\underline{z};\underline{\rho})|_{\underline{\epsilon}=\underline{0}} = \sum_{n_1,\ldots,n_{l+1}\geq 0}\binom{|n|}{n_1,\ldots,n_{l+1}}^2\prod_{k=1}^{l+1}z_k^{n_k}\,. \tag{7.12}$$

The other periods are given as certain combinations of derivatives w.r.t. the deformation parameters

$$\varpi_k^{(i)}(\underline{z}) = [c_i^{\alpha_1\ldots\alpha_k}\partial_{\rho_{\alpha_1}}\ldots\partial_{\rho_{\alpha_k}}\varpi(\underline{z},\underline{\rho})]|_{\underline{\rho}=0}\,, \tag{7.13}$$

where the index i labels the different k-logarithmic solutions. For certain tensors $c_i^{\alpha_1\ldots\alpha_k}$

these solutions correspond to actual period integrals of integral homology of M_{l-1}. We will determine them with the $\widehat{\Gamma}$-class in chapter 8.

From the ℓ-vectors we can actually determine not only the periods but also a set of differential operators annihilating them. For every ℓ-vector $\ell^{(i)}$ one can compute using the rules of [48] a differential operator $\mathcal{D}_i$. For the ℓ-vectors of the banana graphs (7.8) we get the following ones

$$\begin{aligned}\mathcal{D}_i &= \theta_i^2 - \left(\sum_{j=1}^{l+1}\theta_j\right)^2 z_i \\ &= \theta_i^2 - z_i\left(1+\sum_{j=1}^{l+1}\theta_j\right)^2 \quad \text{for } i = 1,\dots,l+1.\end{aligned} \tag{7.14}$$

These $l+1$ operators are not enough to determine the periods of M_{l-1} uniquely, i.e., the solution space of all $\mathcal{D}_i$ contain more solutions than periods exist. Therefore, one has to find more differential operators such that the non-geometric solutions disappear. There are several techniques known to find such operators. The naiv one is to make an ansatz. Here one makes an ansatz of an additional operator such that it annihilates the known holomorphic solution. Then one assumes that such an operator should also annihilate the higher-logarithmic solutions. By this procedure one can construct the desired additional operators. Another more difficult method is to try to factor the operators $\mathcal{D}_i$ and require that the resulting operator after factorization also annihilates the geometric periods. In practice this is a hard task, in particular in the multi-parameter case, because often only certain linear combinations of the operators $\mathcal{D}_i$ are factorizable and not the single one. As a last method one can also use the combinatorics of (7.11) to simply guess additional differential operators. In contrast to the naive ansatz method there are muss less parameters to fix. In section 9.2 we will explain this in more detail and in section 7.3 we demonstrate the hole GKZ method on the four-loop generic-mass banana graph.

7.2 Comparison of the hypersurface motive and the complete intersection motive

There are at least four reasons why the smooth complete intersection representation in eq. (7.3) is superior to the hypersurface representation in eq. (6.2). First, after using the $\mathrm{SL}_i(2,\mathbb{C})$ symmetries, it contains exactly the right number of deformations which are very easily identifiable with the physical parameters $p^2, \underline{m}^2$ or their ratios $\underline{z}$. Second, and even more importantly, eq. (7.3) defines a natural closed sub-motive (see below) $H^{\text{hor}}_{l-1}(M^{\text{CI}}_{l-1})$ and $H^{l-1}_{\text{hor}}(M^{\text{CI}}_{l-1},\mathbb{Z})$ of the total homology and cohomology of M^{CI}_{l-1}.[2] In particular, $H^{l-1}_{\text{hor}}(M^{\text{CI}}_{l-1})$ is generated by derivatives w.r.t. the deformation parameters in (7.5) of the holomorphic

[2] Which similar to the cohomology and homology of M^{HS}_{l-1} is much bigger then the desired physical sub-motive.

$(l-1,0)$-form as can be seen from (4.15) and the discussion around. We find for the respective cohomology groups

$$h_{\text{hor}}^{l-1-k,k}(M_{l-1}^{\text{CI}}) = \begin{cases} \binom{l+1}{k} & \text{if } k \leq \left\lceil \frac{l}{2} \right\rceil - 1 \\ \binom{l+1}{l-1-k} & \text{otherwise} \end{cases}, \tag{7.15}$$

which is much smaller than the full cohomology group for high loop orders. Among this cohomology group we can identify the integrands of the master integrals in $D = 2$ dimensions, while among the dual homology group $H_{l-1}^{\text{hor}}(M_{l-1}^{\text{CI}})$ we find a basis of different maximal cut contours. Third, it allows one to extract the Picard-Fuchs differential ideal with general masses straightforwardly as a simpler GKZ system only in the physical masses, as pioneered for these cases in ref. [48]. The last point is that, according to ref. [48], mirror symmetry maps the horizontal middle cohomology $H_{\text{hor}}^{l-1}(M_{l-1}^{\text{CI}})$ to the vertical cohomology $H_{\text{vert}}^{k,k}(W_{l-1}^{\text{CI}})$, i.e., the one that is inherited from the ambient space, and the corresponding middle homology $H_{\text{hor}}^{l-1}(M_{l-1}^{\text{CI}})$ to the even homology $H_{\text{even}}^{\text{vert}}(W_{l-1}^{\text{CY}})$, that is obtained by restricting the Chow group of the ambient space, on the same manifold. If we restrict ourselves to these vertical– and horizontal subspaces of homology and cohomology parametrized by the physical subspace of the moduli spaces and denote the restriction by the superscript res then the restricted complete intersection geometries for the banana graphs are self mirrors

$$M_{l-1}^{\text{CI, res}} = W_{l-1}^{\text{CI, res}}\,. \tag{7.16}$$

The latter fact allowed some of us in ref. [45] to find the full banana integral in $D = 2$ dimensions using the $\widehat{\Gamma}$-classes of the mirror geometry $W_{l-1}^{\text{CI, res}}$ in the large volume regions for the full physical parameter space and to specify the exact branching behavior of the Feynman integral at the conifold divisors. We will demonstrate this in chapter 8.

The important lesson to draw from the two geometrical representations for the banana graphs is that there is no such thing as a unique Calabi-Yau geometry (or its extension) associated to a Feynman graph. To underline the point, we note that M_{l-1}^{HS} and M_{l-1}^{CY} have different topologies, e.g., the Euler numbers for M_{l-1}^{HS} were already computed after eq. (6.14) and are listed here again

$$\chi(M_3^{\text{HS}}) = 20\,, \qquad \chi(M_4^{\text{HS}}) = 540\,, \qquad \ldots\,. \tag{7.17}$$

For the complete intersection one can find M_{l-1}^{CI}

$$\chi(M_3^{\text{CI}}) = -80\,, \qquad \chi(M_4^{\text{CI}}) = 720\,, \qquad \ldots\,. \tag{7.18}$$

Therefore, one cannot find a smooth map relating these geometries. Rather, one must

focus on finding the uniquely defined *family of Calabi-Yau motives*, preferably in the easiest geometrical setting.

7.3 The four-loop generic-mass banana integral

Before we end this chapter on the complete intersection Calabi-Yau motive associated to the banana family we want to demonstrate on the four-loop generic-mass case the strength of this description. This is a five-parameter model, i.e. $z_1 = m_1^2/p^2, \ldots, z_5 = m_5^2/p^2$. The ℓ-vectors were already defined in (7.8) and the holomorphic solution is given in (7.12) which reads for the four-loop case

$$\begin{aligned}\varpi_0(\underline{z}) &= \sum_{n_1,\ldots,n_5\geq 0} \binom{|n|}{n_1,\ldots,n_5}^2 \prod_{k=1}^{5} z_k^{n_k} \\ &= 1 + z_1 + z_2 + z_3 + z_4 + z_5 + z_1^2 + z_2^2 + z_3^2 + z_4^2 + z_5^2 \\ &\quad + 4(z_1z_2 + z_1z_3 + z_2z_3 + z_1z_4 + z_2z_4 + z_3z_4 + z_1z_5 + z_2z_5 + z_3z_5 + z_4z_5) + \cdots .\end{aligned} \tag{7.19}$$

For the logarithmic solutions we promote the faculties to gamma functions as in (7.11) and compute the derivatives. Here every derivative w.r.t each ρ_α, $\alpha = 1, \ldots, 5$ is actually a solution. We find

$$\begin{aligned}\varpi_1^{(1)}(\underline{z}) &= [\partial_{\rho_1}\varpi(\underline{z},\underline{\rho})]|_{\underline{\rho}=0} \\ &= \varpi_0 \log(z_1) + 2(z_2 + z_3 + z_4 + z_5) + \mathcal{O}(z_iz_j)\,.\end{aligned} \tag{7.20}$$

The other four single-logarithmic solutions are obtained by replacing $z_1 \leftrightarrow z_i$ for $i = 2, \ldots, 5$.

For the higher k-logarithmic solutions not all derivatives w.r.t. any k-tuple of $\underline{\rho}$-derivatives are actually solutions to the desired differential ideal. To find the correct linear combinations of ρ-derivatives we first have to find a generating set of operators such that their solutions span the whole cohomology group $H^{l-1}_{\text{hor}}(M_{l-1})$. More precisely, we want at the MUM-point a single holomorphic and single triple-logarithmic solution as well as five single-logarithmic and five double-logarithmic solutions as predicted from the Calabi-Yau geometry such that in total we have twelve solutions generating $H^{l-1}_{\text{hor}}(M_{l-1})$.

These operators are best determined by analyzing the gamma functions in (7.11) by the techniques explained in section 9.2 for $\epsilon = 0$. A `mathematica` code for generating them is supplemented to my publication [47]. As a possible generating set of operators one can take first the five operators from the ℓ-vectors given in eq. (7.14) and additional five more

complicated operators which start in leading order in $\underline{z}$ as

$$\begin{aligned}
\mathcal{D}_6 &= (\theta_1 - \theta_4)(\theta_3 - \theta_5) + \mathcal{O}(z_i) \\
\mathcal{D}_7 &= (\theta_1 - \theta_3)(\theta_4 - \theta_5) + \mathcal{O}(z_i) \\
\mathcal{D}_8 &= (\theta_2 - \theta_4)(\theta_3 - \theta_5) + \mathcal{O}(z_i) \\
\mathcal{D}_9 &= (\theta_2 - \theta_3)(\theta_4 - \theta_5) + \mathcal{O}(z_i) \\
\mathcal{D}_{10} &= \theta_1(\theta_2 - \theta_5) + (-\theta_2 + \theta_4)\theta_5 + \theta_3(-\theta_4 + \theta_5) + \mathcal{O}(z_i)\,.
\end{aligned} \tag{7.21}$$

The full form can be found in appendix B.

With the operators $\{\mathcal{D}_1, \ldots, D_{10}\}$ the five double-logarithmic solutions are

$$\begin{aligned}
\varpi_2^{(1)}(\underline{z}) &= [(\partial_{\rho_1}\partial_{\rho_2} + \partial_{\rho_1}\partial_{\rho_3} + \partial_{\rho_1}\partial_{\rho_4} + \partial_{\rho_1}\partial_{\rho_5})\varpi(\underline{z}, \underline{\rho})]|_{\underline{\rho}=0} \\
&= \varpi_0 \log(z_1)(\log(z_2) + \log(z_3) + \log(z_4) + \log(z_5)) + 8z_1\log(z_1) \\
&\quad + 2(z_2 + z_3 + z_4 + z_5)(3\log(z_1) + \log(z_2) + \log(z_3) + \log(z_4) + \log(z_5)) \\
&\quad + \mathcal{O}(z_i z_j)
\end{aligned} \tag{7.22}$$

and again the other four are found by replacing $z_1 \leftrightarrow z_i$ for $i = 2, \ldots, 5$.

The tripple-logarithmic solution is given by

$$\begin{aligned}
\varpi_3(\underline{z}) &= \left[\left(\sum_{1\le\alpha_1<\alpha_2<\alpha_3\le 5} \partial_{\rho_{\alpha_1}}\partial_{\rho_{\alpha_2}}\partial_{\rho_{\alpha_3}}\right)\varpi(\underline{z}, \underline{\rho})\right]\Bigg|_{\underline{\rho}=0} \\
&= \varpi_0 \left(\sum_{1\le\alpha_1<\alpha_2<\alpha_3\le 5} \log(z_{\alpha_1})\log(z_{\alpha_2})\log(z_{\alpha_3})\right) + \mathcal{O}(z_i)\,.
\end{aligned} \tag{7.23}$$

The twelve solutions in eqs. (7.20), (7.20), (7.22) and (7.23) span the cohomology $H^{l-1}_{\text{hor}}(M_{l-1})$. In chapter 8 we explain how one can construct out of these solutions geometrical period integrals of $H^{l-1}_{\text{hor}}(M_{l-1}, \mathbb{Z})$ using the $\widehat{\Gamma}$-class formalism.

At the end we want to mention that as in the hypersurface case one can extend the homogeneous differential operators $\{\mathcal{D}_1, \ldots, D_{10}\}$ to a set of inhomogeneous differential equations such that their solution space describes the whole banana four-loop integral and not only its maximal cuts. The corresponding inhomogeneities are obtained as explained in

section 6.2. They are given for the choice of the operators $\{\mathcal{D}_1, \ldots, D_{10}\}$ by

$$\begin{aligned}
\mathcal{D}_6 &\to (\log(z_1) - \log(z_4))(\log(z_3) - \log(z_5)) \\
\mathcal{D}_7 &\to (\log(z_1) - \log(z_3))(\log(z_4) - \log(z_5)) \\
\mathcal{D}_8 &\to (\log(z_2) - \log(z_4))(\log(z_3) - \log(z_5)) \\
\mathcal{D}_9 &\to (\log(z_2) - \log(z_3))(\log(z_4) - \log(z_5)) \\
\mathcal{D}_{10} &\to \log(z_1)(\log(z_2) - \log(z_5)) + (-\log(z_2) + \log(z_4))\log(z_5) \\
&\qquad + \log(z_3)(-\log(z_4) + \log(z_5)) \,,
\end{aligned} \tag{7.24}$$

whereas the operators $D_1, \ldots, D_5$ have vanishing inhomogeneities, i.e., they stay homogeneous also for the whole Feynman integral.

The additional special solution to (7.24) can be chosen to be

$$\varpi_4(\underline{z}) = \varpi_0 \left(\sum_{1 \leq \alpha_1 < \alpha_2 < \alpha_3 < \alpha_4 \leq 5} \log(z_{\alpha_1}) \log(z_{\alpha_2}) \log(z_{\alpha_3}) \log(z_{\alpha_4}) \right) + \mathcal{O}(z_i) \,. \tag{7.25}$$

Also here we discuss the correct linear combination of solutions of (7.20), (7.20), (7.22), (7.23) and (7.25) to yield the banana four-loop Feynman integral in chapter 8.

CHAPTER 8

Mirror Symmetry and the $\widehat{\Gamma}$-Class

In this chapter we want to introduce techniques from mirror symmetry to determine from the non-geometric Frobenius basis of periods the geometrical, integral basis of periods. For the Calabi-Yau geometry this means that we want to find a geometrical basis of maximal cut integrals. For the full Feynman integral we want to find the correct linear combination of Calabi-Yau periods and the additional special solution of the extended set of inhomogeneous differential equations. These problems can be solved with the $\widehat{\Gamma}$-class formalism which is a technique from mirror symmetry.

We began this chapter with an introduction of mirror symmetry and a recapitulation of its most important consequences and concepts. In particular, we explain the $\widehat{\Gamma}$-class and its extension to the fano variety F_1. Then we use the $\widehat{\Gamma}$-class technique to determine in the equal-mass case the linear combination of Frobenius basis elements to describe the full banana integral.

8.1 Mirror symmetry

There is a quite *remarkable fact*, namely that Calabi-Yau manifolds come quite generically in *mirror pairs* (M_n, W_n). This can be understood as the exchange of two deformation– or moduli spaces. It has precise implications on how the l-loop banana integral can degenerate, e.g., in the large momentum regime.

So far we have only described the complex structure moduli space $\mathcal{M}_{\text{cs}}$ of the manifold M_n. One can depicture the infinitessimal directions of this moduli space as infinitessimal deformations $\delta g_{i\bar{j}}$ of the Calabi-Yau Kähler metric $g_{i\bar{j}}$ that preserve the Calabi-Yau property namely its Ricci-flatness, $R_{i\bar{j}}(g_{i\bar{\imath}} + \delta g_{\bar{\imath}\bar{j}}) = 0$. While the Kähler metric in a given complex structure has mixed index structure $i\bar{j}$, the deformation $\delta g_{\bar{\imath}\bar{j}}$ can have any index structure. It is clear that the pure deformations correspond to the *complex* complex structure deformations, which change the meaning of the unbarred and barred indices. Morevover, using the Weitzenböck formula [130], one shows that the latter are related to harmonic forms spanning $H^1(M_n, TM_n)$, i.e., to complex structure deformations [99]. Deformations with mixed index

structure are identified with *real* Kähler structure deformations. They correspond to a choice of the Kähler form ω as a real linear combination of $h^{1,1}(M_n)$ harmonic $(1,1)$-forms. The classical Kähler moduli space is hence of real dimension $h^{1,1}(M_n)$. It has been suggested by type II string theory on M_n (see ref. [49]) that one should complete the choice of the real Kähler form ω with the choice of a real Neveu-Schwartz B-field $b = b_{i\bar{j}}\, dx^i d\bar{x}^{\bar{j}}$ whose equations of motion imply that it is also a harmonic $(1,1)$-form to describe a *complexified* Kähler moduli space. Let us fix topological curve classes C_i for $i = 1, \ldots, h^{1,1}$ in $H_2(M_n)$ dual to a reference basis of $H^{1,1}(M_n)$ at t_0 on M_n. The independent Kähler parameters of the large volume Calabi-Yau n-fold M_n are identified with the complexified areas

$$t^i = \int_{C_i} (\omega + ib) \qquad \text{for } i = 1, \ldots, h^{1,1}(M_n)\,. \tag{8.1}$$

These curves[1] parametrize the *complexified Kähler moduli space* $\mathcal{M}_{\text{cKs}}(M_n)$.

The mirror symmetry conjecture states that for a Calabi-Yau n-fold M_n there is a Calabi-Yau n-fold W_n so that the structures

$$H^{p,q}(M_n) \cong H^{n-p,q}(W_n) \tag{8.2}$$

are identified. On the one hand, as reviewed in section 4.1, the infinitesimal complex structure deformations are described by the cohomology groups $H^1(M_n, TM_n) \cong H^{n-1,1}(M_n)$. They are unobstructed and the dimension of $\mathcal{M}_{\text{cs}}^{h^{n-1,1}}(M_n)$ is $h^{n-1,1}$, as indicated. On the other hand, we know from eq. (8.1) that the complexified Kähler moduli space $\mathcal{M}_{\text{cKs}}^{h^{1,1}}(M_n)$ has dimension $h^{n-1,1}(M_n)$. So, schematically, mirror symmetry states that the structures associated to the following moduli spaces are identified:[2]

$$\mathcal{M}_{\text{cs}}^{h^{n-1,1}(M_n)}(M_n) \Longleftrightarrow \mathcal{M}_{\text{cKs}}^{h^{1,1}(W_n)}(W_n) \quad \text{and} \quad \mathcal{M}_{\text{cKs}}^{h^{1,1}(M_n)}(M_n) \Longleftrightarrow \mathcal{M}_{\text{cs}}^{h^{n-1,1}(W_n)}(W_n)\,. \tag{8.3}$$

Note that eq. (8.2) corresponds to a 90 degree rotation of the Hodge diamond of M_n relative to the one of W_n, in which the unique $(n,0)$– and $(0,n)$-forms on M_n and the unique $(0,0)$-cohomology element and the unique (n,n)-volume form on W_n, respectively, are identified. In other words, mirror symmetry exchanges the vertical– and horizontal cohomologies and their associated structures. In particular, it exchanges $H^n_{\text{hor}}(M_n)$ with $H_{\text{vert}} = \oplus_{k=0}^n H^{k,k}_{\text{vert}}$. This is also what we see when comparing the middle cohomology of M_n with the limiting mixed

[1] Recall that the area of a curve (C_i) is given by $\text{area}(C_i) = \int_{C_i} \omega$.

[2] The statement also applies to K3 surfaces where $H^{1,1}(M_{\text{K3}}) \sim H^{1,1}(W_{\text{K3}})$, and there is anyways only a universal K3, albeit in a more subtle sense. The exchange means in this case that the polarization is changed, so that the role of the transcendental– and the holomorphic cycles are exchanged. More generally, in the symmetric cohomology groups, like $H^{\frac{n}{2},\frac{n}{2}}(X)$ for n even, one can define vertical– and horizontal pieces, that get exchanged.

Hodge structure at the MUM-points according to eq. (4.39), for example when comparing the F-point with the M-point in eq. (4.43). Using monodromy considerations and the notation from eq. (4.42), the following *mirror map* can be identified at the MUM-points:

$$t^k(z) = \frac{S_{(1),k}(\underline{z})}{S_{(0),0}(\underline{z})} = \frac{1}{2\pi i}\left(\log(z_k) + \frac{\Sigma_k(\underline{z})}{\omega_0(\underline{z})}\right) \qquad \text{for } k = 1, \ldots, h^{11}(W_n) = h^{n-1,1}(M_n)\ . \tag{8.4}$$

The last ingredient is the *homological mirror symmetry conjecture* which states the equivalence of the derived categories on M_n and W_n:

$$\begin{array}{l} D^\pi(\text{Fukaya}(M_n)) \\ \text{the bounded derived Fukaya} \\ \text{category of } M_n \end{array} \quad \Longleftrightarrow \quad \begin{array}{l} D^b(\text{Coh}(W_n)) \\ \text{the bounded derived category} \\ \text{of coherent sheaves on } W_n\ , \end{array} \tag{8.5}$$

According to the conjecture, mirror symmetry is really supposed to be an order two isomorphism $\mathfrak{M} : D^b(\text{Coh}(W_n)) \to D^\pi(\text{Fukaya}(M_n))$ between these categories respecting all structures. The objects in $D^\pi(\text{Fukaya}(M_n))$ are *Lagrangian cycles* supporting local systems. The definition of the Lagrangian cycles L uses the symplectic structure $L|_\omega = 0$, as it is familiar from classical mechanics. They have real dimension n and can be characterized by their homology classes Γ in $H_n(M_n, \mathbb{Z})$ that carry a *mass* $M_\Gamma(\underline{z})$ given by $M_\Gamma(\underline{z}) = e^{K(\underline{z})/2}|Z_\Gamma(\underline{z})|$ related to the period or charge $\Pi_\Gamma(\underline{z})$. The objects in $D^b(\text{Coh}(W_n))$ are *coherent holomorphic sheaves*. They are supported on holomorphic sub-manifolds and carry additional bundle structures and can be characterized by their class $\mathcal{G}$ in the algebraic K-theory group K^0_{alg}. A key point is that, on the one hand, their *charge* $\Pi_\mathcal{G}(\underline{t})$ can be calculated using the $\widehat{\Gamma}$-class of $\mathcal{G}$ in the large volume regime in terms of classical intersections of divisors and characteriztic classes on W_n, and on the other hand, they can be identified at the MUM-points with the periods of the mirror using the mirror map in eq. (8.4) as $\Pi_\mathcal{G}(\underline{t}) = \Pi_{\mathfrak{M}(\mathcal{G})}(\underline{t})$. Here we introduced the convention that $\Pi_\Gamma(\underline{t})$ is evaluated in the Kähler gauge $X^0 = S_{(0),0} = 1$. Note that $M_\Gamma(\underline{z})$ is invariant under Kähler gauge transformations.

8.2 The $\widehat{\Gamma}$-class

The motivation for defining the $\widehat{\Gamma}$-class orginated in the idea of identifying the pairing in both categories more naturally. Both categories have such a pairing between the charge classes of objects and auto-equivalences that leave the pairing invariant. In the Fukaya category the pairing is induced by the intersection pairing coming from $\mathbf{\Sigma}$ (we abbreviate it as $\Gamma \circ \Gamma'$), and the auto equivalences can be identifyied with the monodromy group action on Γ. The natural pairing for objects in $D^b(\text{Coh}(W_n))$, after mapping K^0_{alg} to H_{vert} using the

Chern map, is the Euler pairing

$$\mathcal{G} \circ \mathcal{G}' = \int_{W_n} \mathrm{ch}(\mathcal{G}^*)\,\mathrm{ch}(\mathcal{G}')\,\mathrm{Td}(TW_n)\,. \tag{8.6}$$

The *Strominger-Yau-Zaslow conjecture* implies that the sky-scrapper sheaf $\mathcal{O}_{\mathrm{pt}}$ and the structure sheaf $\mathcal{O}_{W_n}$ are mapped to $\mathfrak{M}(\mathcal{O}_{\mathrm{pt}}) = \mathbf{T}$ and $\mathfrak{M}(\mathcal{O}_{W_n}) = \mathbf{S}$, where the classes of the two special Lagrangian n-cycles **T,S** have been specified at the end of section 4.2.3. In simple cases, $\Pi_{\mathbf{S}}$ could be analytically continued to the MUM-point and some data of $Z_{\mathcal{O}_{W_n}}(t) = \Pi_{\mathbf{S}}$ for $\mathcal{O}_{W_n} = \mathfrak{M}(\mathbf{S})$ were known for three-folds, like the famous $\zeta(3)\chi(W_n)$ term [124] and the $\frac{(2\pi i)^2}{24} c_2 \cdot D$ terms [48]. The Todd class Td is a multiplicative class generated by [161]

$$\frac{x}{1-e^{-x}}\,. \tag{8.7}$$

The $\widehat{\Gamma}$-class proposal [162–165] is to take a 'square root' of the Todd class using the following identity

$$\Gamma\left(1+\frac{x}{2\pi i}\right)\Gamma\left(1-\frac{x}{2\pi i}\right) = e^{-x/2}\frac{x}{1-e^{-x}}\,, \tag{8.8}$$

and define the $\widehat{\Gamma}$-class by

$$\widehat{\Gamma}(TW_n) = \prod_i \Gamma\left(1+\frac{\delta_i}{2\pi i}\right) = \exp\left(-\gamma c_1(TW_n) + \sum_{k\geq 2}(-1)^k(k-1)!\,\zeta(k)\,\mathrm{ch}_k(\mathcal{G})\right) \tag{8.9}$$

with the Euler-Mascheroni constant γ. Here δ_i are the Chern roots of TW_n. The transition from the Chern characters to the Chern classes c_k is decribed by Newton's formula

$$\mathrm{ch}_k = (-1)^{(k+1)} k \left[\log\left(1+\sum_{i=1}^{\infty} c_i\, x^i\right)\right]_k\,, \tag{8.10}$$

where $[*]_k$ means to take the k^{th} coefficient (in x) of the expansion of the expression $*$. The Chern classes in turn can be computed from the adjunction formula

$$c_k(W_{l-1}) = \left[\frac{\prod_{i=1}^{l+1}(1+H_i)^2}{(1+\sum_{i=1}^{l+1} H_i)^2}\right]_k\,, \tag{8.11}$$

where one has to take the term of multi-degree k in the hyperplane classes H_i. More precisely, since the hyperplane classes in each $\mathbb{P}^1$ fulfill $H_i^2 = 0$ we can express c_k in terms of elementary

symmetric polynomials $s_k(\underline{H}) = \sum_{i_1<\ldots<i_k} H_{i_1}\cdots H_{i_k}$ as

$$c_k(W_{l-1}) = (-1)^k k! \sum_{j=0}^{k} \frac{(-2)^j(k+1-j)}{j!} s_k(\underline{H}) =: \mathcal{N}_k^{W_{l-1}} s_k(\underline{H})\,. \tag{8.12}$$

Similarly, considering the power one of the normal bundle in the denominator of (8.11) (instead of two) we can write for the Chern classes of the ambient space

$$c_k(F_l) = (-1)^k k! \sum_{j=0}^{k} \frac{(-2)^j}{j!} s_k(\underline{H}) =: \mathcal{N}_k^{F_l} s_k(\underline{H})\,. \tag{8.13}$$

Moreover, we notice that the integral of a top degree product of Chern classes c_{k_n} over $X = W_{l-1}$ or $X = F_l$ is given by

$$\int_X \prod_n c_{k_n} = (l+1)! \prod_n \frac{\mathcal{N}_{k_n}^X}{k_n!}\,. \tag{8.14}$$

On Calabi-Yau spaces one defines $\mathcal{G}\circ\mathcal{G}' = \int_{W_n} \overline{\psi(\mathcal{G})}\psi(\mathcal{G}')$ with $\Psi(\mathcal{G}) = \mathrm{ch}(\mathcal{G})\cdot\widehat{\Gamma}(TW_n)$. The operation $\overline{\psi(\mathcal{G})}$ gives a sign $(-1)^k$ on elements in H^{2k}, and one gets as desired $\mathcal{G}\circ\mathcal{G}' = \Gamma\circ\Gamma'$ with $\Gamma = \mathfrak{M}(\mathcal{G})$ and $\Gamma' = \mathfrak{M}(\mathcal{G}')$. Moreover, the charges of $\mathcal{G}$ in the large volume limit of W_n, which corresponds to a MUM-point of M_n, can be calculated as [134, 162–166]

$$\Pi_{\mathcal{G}}(\underline{t}) = \int_{W_n} e^{\underline{\omega}\cdot\underline{t}}\,\widehat{\Gamma}(TW_n)\mathrm{ch}(\mathcal{G}) + \mathcal{O}(e^{-\underline{t}})\,. \tag{8.15}$$

If we know the image of the class of the cycle of a maximal cut, we can use eq. (8.15) to compute its precise asymptotic at the MUM-point. For the banana integral the maximal cut contour related to the imaginary part of the integral was identified with **S** in ref. [45], and it has the dual $\mathcal{G} = \mathcal{O}_{W_n}$ with $\mathrm{ch}(\mathcal{O}_{W_n}) = 1$. Therefore, it was possible to extract the asymptotic expansion of the Feynman integral involving all the transcendental numbers by identifying

$$\Pi_{\mathbf{S}}(\underline{t}(\underline{z})) = \int_{W_n} e^{\underline{\omega}\cdot\underline{t}}\,\widehat{\Gamma}(TW_n) + \mathcal{O}(e^{-\underline{t}}) = Z_{\mathcal{O}_{W_n}}(\underline{t})\,, \tag{8.16}$$

and comparing the powers of t^k on both sides using the mirror map in eq. (8.4), see also below. This uniquely defines the transformation from the Frobenius basis in eq. (4.42) to the integer cycle basis and relates the large momentum behavior of the banana integrals to the topological data of the Calabi-Yau space W_n given in eq. (7.5), where the dimension of the Calabi-Yau space $n = \dim(M_n) = \dim(W_n) = l-1$ is determined by the loop order l. We also note that the cycle $\mathbf{T}\sim T^n$ can be identified with the skyscraper sheaf $\mathcal{O}_{\mathrm{pt}}$ and

$\Pi_{\mathcal{O}_{\text{pt}}} = 1$ [163]. Hence, in this case we get no logarithm and the corresponding solution is the holomorphic one and $\mathcal{O}_W \circ \mathcal{O}_{pt} = \mathbf{S} \cap \mathbf{T} = 1$. It is possible to get the full set of integral K-theory classes and specify a complete integral basis of periods using eq. (8.15). This is reviewed for three-folds and four-folds in ref. [134], but should be possible for all W_{l-1}.

The last point to make here goes beyond the case of maximal cuts and should fit into the framework of the third generalization of Deligne to define mixed Hodge structures on singular manifolds for open cycles. It was found in ref. [45] and proven by Hiroshi Iritani in ref. [50] that the full banana integral, which is defined over the open cycle σ_l in the l-dimensional Fano variety F_l with $W_{l-1} \subset F_l$ such that the $l-1$-dimensional W_{l-1} embeds as canonical hypersurface, is determined by an extended $\widehat{\Gamma}$-class

$$\widehat{\Gamma}_{F_l}(TF_l) = \frac{\widehat{A}(TF_l)}{\widehat{\Gamma}^2(TF_l)} = \frac{\Gamma(1-c_1)}{\Gamma(1+c_1)} \cos(\pi c_1) \,, \tag{8.17}$$

where $\widehat{A}$ is the Hirzebruch A-roof genus [161] and $c_1 = c_1(F_l) \neq 0$. Using this we can get the asymptotic behavior of the full Feynman integral by the identification

$$J_{l,\underline{0}}(\underline{z}, 0) = \int_{F_l} e^{\frac{\omega \cdot \underline{t}}{}} \widehat{\Gamma}_{F_l}(TF_l) + \mathcal{O}(e^{-\underline{t}}) \,. \tag{8.18}$$

The integer symplectic basis element that corresponds to $J_{l,\underline{0}}(\underline{z}, 0)$ can now be determined by expanding eq. (8.18) in the parameters $\underline{t}(\underline{z})$. To do this one has to calculate the classical topological intersection data that occur in this expansion. Let $I^{(k)}$ a set of k indices, with $1 \leq I_p^{(k)} \leq h_{11}(F_l)$ for all $p = 1, \ldots, k$. Then typical terms that appear are the intersections of l divisors D_i for $i = 1, \ldots, h_{11}(F_l)$ in F_l, i.e., $\int_F \bigwedge_{p=1}^{l} \omega_{I_p^{(l)}} = \bigcap_{p=1}^{l} D_{I_p^{(l)}}$ or the intersection of the k^{th} Chern class c_k with $l-k$ such divisors in F, i.e., $\int_F c_k \bigwedge_{p=1}^{l-k} \omega_{I_p^{l-k}} = [c_k] \cap \bigcap_{p=1}^{l-k} D_{I_p^{(l-k)}}$ etc.. The evaluation is feasible by simple and fundamental techniques in algebraic geometry and fixes the numerical coefficients of a degree l polynomial in $\underline{t}$ that represents $J_{l,\underline{0}}(\underline{z}, 0)$ up to $\mathcal{O}(e^{-\underline{t}})$ corrections. For the Fano variety F_l in eq. (7.5), the calculation was performed in ref. [45] in detail. Inserting the mirror map in eq. (8.4), we can hence get the precise coefficients of the leading logarithmic terms and since $J_{l,\underline{0}}(\underline{z}, 0)$ is a solution to a linear differential equation we can uniquely combine the Frobenius solutions in eq. (4.42) to get the exact linear combination that specifies an integer basis element of periods.

These coefficients can also nicely be expressed through a generating functional as we found in [45] before the proof with the $\widehat{\Gamma}$-class was performed. If one expands the l-loop banana Feynman integral in terms of the Frobenius basis (5.6) as

$$J_{l,\underline{0}}(\underline{z}, 0) = \sum_{k=0}^{l} \lambda_k^{(l)} \varpi_k \tag{8.19}$$

then the coefficients $\lambda_k^{(l)}$ can be computed through[3]

$$\sum_{l=0}^{\infty} \lambda_0^{(l)} \frac{x^l}{(l+1)!} = -\frac{\Gamma(1-x)}{\Gamma(1+x)} \mathrm{e}^{-2\gamma x - i\pi x}, \tag{8.20}$$

and the other coefficients are related by

$$\lambda_k^{(l)} = (-1)^k k! \binom{l+1}{k} \lambda_0^{(l-k)}. \tag{8.21}$$

For the generic mass case the coefficients $\lambda_k^{(l)}$ split symmetrically for multiple higher-logarithmic solutions if these are constructed also symmetrically. This is actually the case for our bases of generic-mass solutions in the hypersurfaces as well as in the complete intersection geometry. For the hypersurface motive, cf. (6.2), this splitting[4] can be found in table 4 of [45] and equation (5.17). For the four-loop banana integral with solutions (7.20), (7.20), (7.22), (7.23) and (7.25) the correct linear combination to obtain the full banana integral is given by

$$\begin{aligned}
\lambda_0^{(4)} &= -450\zeta(4) + 80\pi\zeta(3)i \\
\lambda_{1,1}^{(4)} &= \ldots = \lambda_{1,5}^{(4)} = 16\zeta(3) + 24\pi\zeta(2)i \\
\lambda_{2,1}^{(4)} &= \ldots = \lambda_{2,5}^{(4)} = 6\zeta(2) \\
\lambda_{3,1}^{(4)} &= 2\pi i \\
\lambda_{5,1}^{(4)} &= 1\,.
\end{aligned} \tag{8.22}$$

Before we end this chapter we also want to mention that there is also another possibility to determine the leading asymptotic of the banana integral which can also be seen as a check of the $\widehat{\Gamma}$-class results, namely the hypergeometric series representation of the banana integrals. We determined through a lengthy computation in [47] the leading asympotic of the banana integrals using the Mellin-Barnes representation also in dimensional regularization. In the following chapter we will recall shortly this computation and its implications. But in $D = 2$ this again confirms the results presented in this section.

[3] Notice that here the coefficients are slightly different than the ones in [45] due to a different normalization of the Frobenius basis, cf. (5.6).

[4] Notice that in [45] the different convention in the analytic continuation which gives the imaginary part of the banana integral a negative sign compared to the conventions used here. The convention in this thesis follow the standard physical ones.

CHAPTER 9

Banana Feynman Integrals in Dimensional Regularization

So far we have only considered the banana integrals in $D = 2$ dimensions. In this final chapter we now want to extend this to dimensional regularization and we want to elaborate a formalism to systematically compute the expansion in the dimensional regulator ϵ. As a first step we compute an explicit *hypergeometric series representation* for the generic-mass banana integral in the large momentum limit, $p^2 \gg m_i^2 > 0$. This hypergeometric representation serves a twofold purpose: First, it allows us to obtain the leading asymptotic behavior of all banana integrals in the large momentum limit, which provides the boundary condition for solving the differential equations, reproducing in leading order in ϵ the coefficients given in eqs. (8.20) and (8.21) found by numerics and the $\widehat{\Gamma}$-class. Second, we use this representation to derive a complete set of differential equations satisfied by the banana integrals.

This chapter is mostly based on my last publication [47] abound the banana integrals in dimensional regularization. We collect here only the most important aspects to explain the computation of the banana integrals in $D = 2 - 2\epsilon$ dimensions as an extension of the previous chapters. For the complete derivation of the hypergeometric series expansion of the banana integrals and the intermediate *Mellin-Barnes representation* we refer to the original work [47].

9.1 A hypergeometric series representation of the banana integral

In this section we want shortly to recapitulate the most important steps to compute the hypergeometric series expansion of the l-loop banana integral eqrefsymbanana. For this one first starts to find a Mellin-Barnes integral representation which for the banana integrals can be evaluated in the large momentum regime $p^2 \gg m_i^2 > 0$ yielding the hypergeometric series expansion. This determines the leading asymptotic of the banana integrals to all orders in the dimensional regulator ϵ.

Our derivation of the hypergeometric series expansion is valid for generic masses m_i^2 and

exponents ν_i of the propagators. Nevertheless, we present here only the results for the case $\nu_i = 1$ for all $i = 1, \ldots, l+1$. If all propagator masses are zero, the integral is trivial and can be evaluated in terms of gamma functions. Therefore, we assume from now on that at least one propagator is massive.

To derive the MB representation for $\tilde{I} := I^{\text{Ban}}_{\underline{\nu}}(p^2, \underline{m}^2; D)$, we start from the Feynman parameter representation in eq. (2.31) and adapt the approach of ref. [33, app. A] to the l-loop case (the two-loop case was treated in ref. [167]; see also ref. [168]). There are two important identities. The first one is the identity

$$\frac{1}{(A+B)^\lambda} = \int_{c-i\infty}^{c+i\infty} \frac{\mathrm{d}\xi}{2\pi i}\, A^\xi B^{-\xi-\lambda} \frac{\Gamma(-\xi)\Gamma(\xi+\lambda)}{\Gamma(\lambda)}\,, \tag{9.1}$$

where for appropriate c the contour runs parallel to the imaginary axis and separates the left poles (due to $\Gamma(\xi+\lambda)$) from the right poles of the integrand (due to $\Gamma(-\xi)$). Secondly, we use a formula of a Euler beta type integral

$$\int_0^\infty \mathrm{d}x\, x^\alpha\, (A+Bx)^\beta = A^{1+\alpha+\beta} B^{-1-\alpha} \frac{\Gamma(1+\alpha)\Gamma(-1-\alpha-\beta)}{\Gamma(-\beta)}\,. \tag{9.2}$$

With these two identities we can compute a Mellin-Barnes representation of the banana integral. For a careful derivation we refer to [47]. Afterwards this Mellin-Barnes integral can be computed in the large momentum region, i.e. for $p^2 \gg m_i^2$. This is a very technical procedure and again the details can be looked up in [47]. We only cite here the final hypergeometric series representation of the banana integral for the generic-mass case and with unit propagator powers

$$\begin{aligned} I^{\text{Ban}}_{1,\ldots,1}(p^2, \underline{m}^2; 2-2\epsilon) = {} & \frac{1}{\Gamma(1+l\epsilon)} \left(\frac{1}{-p^2-i0}\right)^{1+l\epsilon} \sum_{\underline{j}\in\{0,1\}^{l+1}} \frac{\Gamma(-\epsilon)^j\, \Gamma(\epsilon)^{l+1-j}\, \Gamma(1+(j-1)\epsilon)}{\Gamma(-j\epsilon)} \\ & \times \left[\prod_{i=1}^{l+1} \left(\frac{m_i^2}{-p^2-i0}\right)^{(j_i-1)\epsilon} \sum_{\underline{n}\in\mathbb{N}_0^{l+1}} \frac{(1+j\epsilon)_n\, (1+(j-1)\epsilon)_n}{\prod_{i=1}^{l+1}(1+(-1)^{j_i+1}\epsilon)_{n_i}} \prod_{i=1}^{l+1} \frac{1}{n_i!} \left(\frac{m_i^2}{p^2}\right)^{n_i}\right]. \end{aligned} \tag{9.3}$$

We can see here that, similar to the case $D = 2$, the generic-mass banana integral is symmetric in variables m_i^2/p^2 for $i = 1, \ldots, l+1$. Or the other way round, the equal-mass case is somehow the diagonal of the generic-mass case. This reflects the fact that the banana graphs have a symmetry which interchanges the propagators.

At the end we want to give the leading asymptotic behavior of the banana integral (9.3) at large momentum. So let $\underline{n} = (0, \ldots, 0)$ in eq. (9.3), we can immediately extract the leading

behavior of the banana integrals at large momentum. For the generic-mass case one obtains:

$$I^{\text{Ban}}_{1,\dots,1}(p^2,\underline{m}^2;2-2\epsilon) = -\frac{1}{\Gamma(1+l\epsilon)}e^{i\pi l\epsilon}\left(\frac{1}{p^2}\right)^{1+l\epsilon} \times \sum_{\underline{j}\in\{0,1\}^{l+1}} e^{i\pi(j-1)\epsilon}\frac{\Gamma(-\epsilon)^j\,\Gamma(\epsilon)^{l+1-j}\,\Gamma(1+(j-1)\epsilon)}{\Gamma(-j\epsilon)}\prod_{i=1}^{l+1} z_i^{(j_i-1)\epsilon} + \mathcal{O}\left(z_i^2\right) . \tag{9.4}$$

Equation (9.4) gives the leading asymptotics of $I^{\text{Ban}}_{1,\dots,1}(p^2,\underline{m}^2;2-2\epsilon)$ and can be used as a boundary condition to solve the differential equations for the banana graphs. In the equal-mass case, eq. (9.4) can be further simplified to

$$J_{l,1}(z;\epsilon) = -\sum_{k=1}^{l+1}\binom{l+1}{k}\frac{\Gamma(-\epsilon)^k\,\Gamma(\epsilon)^{l+1-k}}{\Gamma(-k\epsilon)}\frac{\Gamma(1+(k-1)\epsilon)}{\Gamma(1+l\epsilon)}e^{(k-1)i\pi\epsilon}\,z^{1+(k-1)\epsilon} + \mathcal{O}\left(z^2\right) . \tag{9.5}$$

Expanding eq. (9.5) around $\epsilon = 0$, one obtains

$$J_{l,1}(z;\epsilon) = \sum_{n=0}^{\infty} J^{(n)}_{l,1}(z)\,\epsilon^n , \tag{9.6}$$

and inspecting the leading order in ϵ, $J^{(0)}_{l,1}$ *precisely* reproduces the logarithmic structure of the l-loop banana Feynman integral in $D = 2$ spacetime dimensions described in chapter 4. Moreover, eq. (9.5) confirms the combinatorial pattern of Riemann zeta values in the constants $\lambda^{(l)}_k$ in eqs. (8.20) and (8.21), and extends it to higher orders in ϵ. It was also observed that the transcendental weight of $\lambda^{(l)}_k$, which is $l-k$, and the highest occurring power of logarithms in $\varpi_{l,k}(z)$, which is k, always add up to the loop order l.

We can now partially generalize these observations to higher orders in the ϵ-expansion. For simplicity we discuss the equal-mass case, while the generic-mass case can be treated similarly. At order ϵ^n we find powers of $\log(z)$ up to $L = l+n$ and coefficients with transcendental weight up to $T = l+n$. Indeed, at any order ϵ^n, the constant of highest occurring transcendental weight $T = l+n$ always multiplies the holomorphic period $\varpi_{l,0}(z)$ of the Calabi-Yau $(l-1)$-fold. More generally, at order ϵ^n, consider all terms that multiply constants of a certain transcendental weight T and a certain power L of logarithms, i.e., $\log^L(z)$. We find that there are only non-zero terms for $L+T \leq l+n$. For the maximum value $L+T = l+n$, these terms are again proportional to the holomorphic Calabi-Yau period $\varpi_{l,0}(z)$ (with a rational number as proportionality constant), independently of the splitting between L and T and the value of n.

9.2 Differential equations for banana Feynman integrals

The goal of this section is to present a method to derive differential equations for banana integrals at arbitrary loop order and in dimensional regularization. In principle, the differential equations can be derived using IBP relations (see section 2.3.2). However, for high numbers of loops l and for many distinct values of the masses m_i^2, publicly available computer codes can be rather inefficient, and it can be hard to obtain the explicit form of the differential equations. Here we present an alternative method to derive a set of operators that define inhomogeneous differential equations for $I^{\text{Ban}}_{1,\ldots,1}(\underline{z}; 2-2\epsilon)$, cf. eq. (3.15). As explained in section 9.2, these differential operators form an ideal, and there may be substantial freedom in choosing a generating set for this ideal. As a consequence, our set of operators may look substantially different from the one obtained from first-order differential equations and IBP relations.

For the generic-mass case we use a purely combinatorial method to find the desired differential operators by analyzing the structure of the gamma functions appearing in the second line of eq. (9.3). We work with gamma functions instead of rising factorials, because this will simplify the formulas. This can be achieved simply be rescaling the coefficient in the first line of eq. (9.3). We define the ϵ-Frobenius basis with an explicit ϵ-dependent indicial by:

$$\mathcal{I}_{(j_1,\ldots,j_{l+1})}(\underline{z},\epsilon) := \sum_{\underline{n}\in\mathbb{N}_0^{l+1}} \frac{\Gamma(1+n+j\epsilon)\,\Gamma(1+n+(j-1)\epsilon)}{\prod_{i=1}^{l+1}\Gamma(1+n_i)\,\Gamma(1+n_i+(-1)^{j_i+1}\epsilon)} \prod_{i=1}^{l+1} z_i^{n_i+j_i\epsilon}\,. \tag{9.7}$$

Indeed, it is easy to see that eq. (9.3) can be written as a linear combination of the $\mathcal{I}_{(j_1,\ldots,j_{l+1})}$. The power series in eq. (9.7), however, have a finite radius of convergence. Our goal is to derive a set of $1 < j \leq l+1$ differential operators that annihilate the elements of the ϵ-Frobenius basis, where we again use the notation $j = \sum_{i=1}^{l+1} j_i$. and similarly for n. The set of differential operators is then extended to a set of inhomogeneous differential equations by including the case $j = 1$ (for now, we exclude the case $j = 0$, but we briefly comment on it at the very end). These differential equations then serve as a starting point to analytically continue the ϵ-Frobenius basis to all values of the z_i.

Let us start by analyzing the maximal cuts. We want to find a set of differential operators $\{\mathcal{L}_k\}$ whose solution space is spanned by the ϵ-Frobenius basis in eq. (9.7) (and only those):

$$\text{Sol}(\{\mathcal{L}_k\}) = \left\langle \mathcal{I}_{(j_1,\ldots,j_{l+1})}(\underline{z},\epsilon) \right\rangle_{1<j\leq l+1}\,. \tag{9.8}$$

Clearly, this solution space will then also contain the maximal cuts of the banana integral for a given loop order l.

The most general linear differential operator with polynomial coefficients acting on the

ϵ-Frobenius basis can be written in the form

$$\mathcal{L}_{\underline{\alpha},\underline{\beta}} = \sum_{\underline{\alpha},\underline{\beta}} a_{\underline{\alpha},\underline{\beta}}\, \underline{z}^{\underline{\alpha}} \underline{\theta}^{\underline{\beta}}\,, \tag{9.9}$$

where $a_{\underline{\alpha},\underline{\beta}}$ are constants and $\underline{\alpha}, \underline{\beta}$ are multi-indices, and $\underline{z}^{\underline{\alpha}} := \prod_{k=1}^{l+1} z_k^{\alpha_k}$ and $\underline{\theta}^{\underline{\beta}} := \prod_{k=1}^{l+1} \theta_k^{\alpha_k}$. It is therefore sufficient to understand the action of the $\underline{z}^{\underline{\alpha}} \underline{\theta}^{\underline{\beta}}$ on the elements of the ϵ-Frobenius basis.

Let us start by analyzing the maximally symmetric index $\underline{j} = (1, \ldots, 1)$. With the rising and falling factorial[1]

$$\begin{aligned} (x)_n &= x(x+1)\cdots(x+n-1)\,, \\ [x]_n &= x(x-1)\cdots(x-n+1) \end{aligned} \tag{9.10}$$

we find

$$\begin{aligned} \underline{z}^{\underline{\alpha}} \underline{\theta}^{\underline{\beta}}\, \mathcal{I}_{(1,\ldots,1)} = \sum_{\underline{n} \in \mathbb{N}_0^{l+1}} & \frac{\prod_{i=1}^{l+1} [n_i]_{\alpha_i} [n_i + \epsilon]_{\alpha_i}}{[n + l\epsilon]_{\alpha} [n + (l+1)\epsilon]_{\alpha}} \prod_{k=1}^{l+1} (n_k - \alpha_k + \epsilon)^{\beta_k} \\ & \times \frac{\Gamma(1 + n + (l+1)\epsilon)\, \Gamma(1 + n + l\epsilon)}{\prod_{i=1}^{l+1} \Gamma(1 + n_i)\, \Gamma(1 + n_i + \epsilon)} \prod_{i=1}^{l+1} z_i^{n_i + \epsilon}\,, \end{aligned} \tag{9.11}$$

where in the left-hand side we again use the simplified notation $\alpha = \sum_i \alpha_i$. Using a computer algebra system we can now solve for the coefficients $a_{\underline{\alpha},\underline{\beta}}$ in eq. (9.9) such that the operator $\mathcal{L}_{\underline{\alpha},\underline{\beta}}$ annihilates the ϵ-Frobenius basis element with $\underline{j} = (1, \ldots, 1)$,

$$\mathcal{L}_{\underline{\alpha},\underline{\beta}}\, \mathcal{I}_{(1,\ldots,1)} = 0\,. \tag{9.12}$$

For fixed α and β, any linear combination that annihilates $\mathcal{I}_{(1,\ldots,1)}$ can be computed in this way[2].

As an example, let us consider the two-loop case. Here we can construct the operators

$$\begin{aligned} \mathcal{L}_1 &= (1 - z_1)(\theta_2 - \epsilon)(\theta_3 - \epsilon) - (z_2(\theta_3 - \epsilon) + z_3(\theta_2 - \epsilon))(2\theta_1 + \theta_2 + \theta_3 + 1 - \epsilon)\,, \\ \mathcal{L}_4 &= \theta_1(\theta_1 - \epsilon) - z_1(\theta_1 + \theta_2 + \theta_3 + 1)(\theta_1 + \theta_2 + \theta_3 + 1 - \epsilon)\,, \end{aligned} \tag{9.13}$$

and $\mathcal{L}_2 = \mathcal{L}_1(1 \leftrightarrow 2)$, $\mathcal{L}_3 = \mathcal{L}_1(1 \leftrightarrow 3)$, $\mathcal{L}_5 = \mathcal{L}_4(1 \leftrightarrow 2)$ and $\mathcal{L}_6 = \mathcal{L}_4(1 \leftrightarrow 3)$. For these

[1] The rising factorial is also known as the Pochhammer function. Note that there are different notations for rising and falling factorials used in the literature.

[2] A `Mathematica`-code which generates these operators can be downloaded from `http://www.th.physik.uni-bonn.de/Groups/Klemm/data.php` as supplementary data to [47].

operators we have chosen $\alpha \leq 1$ and $\beta \leq 2$. The set of operators

$$\mathcal{L}^{(2)} := \{\mathcal{L}_1, \ldots, \mathcal{L}_6\} \tag{9.14}$$

is enough to uniquely determine the ϵ-Frobenius basis elements with $j = 2, 3$, and no other solutions.

More generally, for α and β chosen large enough, the operators $\mathcal{L}_{\underline{\alpha},\underline{\beta}}$ will generate the solution space in eq. (9.15), i.e., $\text{Sol}(\{\mathcal{L}_{\underline{\alpha},\underline{\beta}}\}) = \langle \mathcal{I}_{(j_1,\ldots,j_{l+1})}(\underline{z}, \epsilon) \rangle_{1<j\leq l+1}$. From our computations we actually found that the operators with $\alpha \leq 1$ and $\beta \leq l$ are enough to generate the desired solution space:

$$\text{Sol}(\{\mathcal{L}_{\underline{\alpha},\underline{\beta}}\}_{\alpha\leq 1,\beta\leq l}) = \left\langle \mathcal{I}_{(j_1,\ldots,j_{l+1})}(\underline{z}, \epsilon) \right\rangle_{1<j\leq l+1} . \tag{9.15}$$

The set $\{\mathcal{L}_{\underline{\alpha},\underline{\beta}}\}_{\alpha\leq 1,\beta\leq l}$ is still overcomplete: A properly chosen subset of $\{\mathcal{L}_{\underline{\alpha},\underline{\beta}}\}_{\alpha\leq 1,\beta\leq l}$ can be sufficient to generate the whole solution space. For example, the operators from the set $\mathcal{L}^{(2)}$ are sufficient to generate the desired ϵ-Frobenius basis elements in the sunset case, although there exist 9 linearly independent operators for $\alpha \leq 1$ and $\beta \leq 2$.

As mentioned in subsection 3.3.2, it is in general not clear what is the best way of representing an ideal such that it yields the desired solution space. For instance, naively, the maximal cuts of the two-loop banana integral were found to satisfy a fourth order homogeneous differential equation, cf., e.g., ref. [169]. Later, it was shown that a second-order differential operator suffices (in two space-time dimensions), cf. refs. [7, 109, 170]. Using our method, we would obtain the set $\mathcal{L}^{(2)}$ of six operators, which has still the same solution space. Our set $\mathcal{L}^{(2)}$ consists of more operators, but of simpler type. For example, the polynomials appearing in the operators in eq. (9.13) are of small degree. The question of which representation is more appropriate depends on the concrete application that one has in mind.

So far we have only discussed how to find a set of operators $\{\mathcal{L}_{\underline{\alpha},\underline{\beta}}\}$ that annihilate the functions $\mathcal{I}_{(j_1,\ldots,j_{l+1})}(\underline{z}, \epsilon)$ with $1 < j \leq l + 1$. Equivalently, the solution space $\text{Sol}(\{\mathcal{L}_{\underline{\alpha},\underline{\beta}}\})$ will be generated by all the maximal cuts of the l-loop banana graph. In order to describe the full uncut Feynman integral, we need to include the corresponding functions with $j = 1$. There are $\binom{l+1}{1} = l + 1$ different functions of this type (and there is the same number of l-loop tadpole graphs for generic masses). These functions, however, are not elements of $\text{Sol}(\{\mathcal{L}_{\underline{\alpha},\underline{\beta}}\})$ (i.e., they are not simultaneously annihilated by all the $\mathcal{L}_{\underline{\alpha},\underline{\beta}}$). Instead, they are special solutions to certain inhomogeneous differential equations obtained from the $\mathcal{L}_{\underline{\alpha},\underline{\beta}}$. In analogy with eq. (3.25), we define the solution space of a set of inhomogeneous differential equations:

$$\text{SolInhom}(\{(\mathcal{L}_k, g_k)\}) = \{f(\underline{z}) | \mathcal{L}_i f(\underline{z}) = g_i(\underline{z}) \text{ for all } (\mathcal{L}_i, g_i) \in \{(\mathcal{L}_k, g_k)\}\} . \tag{9.16}$$

In this language, an element of the ϵ-Frobenius basis with $j = 1$ lies in the solution space $\text{SolInhom}(\{(\mathcal{L}_{\underline{\alpha},\underline{\beta}}, g_{\underline{\alpha},\underline{\beta}})\})$, for a specific set of inhomogeneities $\{g_{\underline{\alpha},\underline{\beta}}\}$ depending on the particular chosen j-vector. In order to determine these inhomogeneities, we simply apply every generator $\mathcal{L}_{\underline{\alpha},\underline{\beta}}$ to every element of the Frobenius basis with $j = 1$. By this procedure one finds for each basis element with $j = 1$ inhomogeneities of the form z_i^ϵ.

Let us illustrate this again on the example of the two-loop banana integral. Acting with the the operators from $\mathcal{L}^{(2)}$ yields the following inhomogeneities:

$$\begin{aligned}
\mathcal{L}_1 \mathcal{I}_{(1,0,0)}(\underline{z}, \epsilon) &= \frac{1}{\Gamma(-\epsilon)^2}\, z_1^\epsilon\,, \\
\mathcal{L}_2 \mathcal{I}_{(0,1,0)}(\underline{z}, \epsilon) &= \frac{1}{\Gamma(-\epsilon)^2}\, z_2^\epsilon\,, \\
\mathcal{L}_3 \mathcal{I}_{(0,0,1)}(\underline{z}, \epsilon) &= \frac{1}{\Gamma(-\epsilon)^2}\, z_3^\epsilon\,.
\end{aligned} \tag{9.17}$$

All other operators give zero when applied to the three ϵ-Frobenius solutions with $j = 1$. We stress that there is still a freedom in how we choose the set $\{(\mathcal{L}_{\underline{\alpha},\underline{\beta}}, g_{\underline{\alpha},\underline{\beta}})\}$ and construct the corresponding solution spaces. For example, we could write the vector space $\text{SolInhom}(\{(\mathcal{L}_{\underline{\alpha},\underline{\beta}}, g_{\underline{\alpha},\underline{\beta}})\})$ as a sum of three solution spaces

$$\text{SolInhom}(\{\mathcal{L}_{\underline{\alpha},\underline{\beta}}, g_{\underline{\alpha},\underline{\beta}}\}) = \sum_{p=1}^{3} \text{SolInhom}(\mathcal{L}^{(2,p)}) = \left\langle \mathcal{I}_{(j_1,j_2,j_3)}(\underline{z}, \epsilon) \right\rangle_{1 \le j \le 3}, \tag{9.18}$$

with

$$\mathcal{L}^{(2,p)} = \{(\mathcal{L}_i, g_i) : g_i(\underline{z}) = \delta_{ip}\, z_p^\epsilon\, \Gamma(-\epsilon)^{-2}, 1 \le i \le 6\}\,. \tag{9.19}$$

Since $I_{1,1,1}(\underline{z}, \epsilon)$ is symmetric under a permutation of the z_i, the inhomogeneous term must also have this property. It is therefore sufficient to consider $\{(\mathcal{L}_{\underline{\alpha},\underline{\beta}}, g_{\underline{\alpha},\underline{\beta}})\}$ such that the solution space contains the sum $\mathcal{I}_{(1,0,0)} + \mathcal{I}_{(0,1,0)} + \mathcal{I}_{(0,0,1)}$, but it does not contain each summand separately. This is achieved by the choice

$$\text{SolInhom}(\{(\mathcal{L}_{\underline{\alpha},\underline{\beta}}, g_{\underline{\alpha},\underline{\beta}})\}) = \text{SolInhom}(\mathcal{L}^{(2)}_{\text{inhom}})\,, \tag{9.20}$$

with

$$\mathcal{L}^{(2)}_{\text{inhom}} = \{(\mathcal{L}_1, \Gamma(-\epsilon)^{-2}\, z_1^\epsilon), (\mathcal{L}_2, \Gamma(-\epsilon)^{-2}\, z_2^\epsilon), (\mathcal{L}_3, \Gamma(-\epsilon)^{-2}\, z_3^\epsilon), (\mathcal{L}_4, 0), (\mathcal{L}_5, 0), (\mathcal{L}_6, 0)\}\,. \tag{9.21}$$

Note that SolInhom($\mathcal{L}^{(2)}_{\text{inhom}}$) is contained in the sum of vector spaces in eq. (9.18), but the converse is not true. Finally, we can also describe the solution space of a set of homogeneous equations, by multiplying $\mathcal{L}_1$, $\mathcal{L}_2$ and $\mathcal{L}_3$ from left by an operator that annihilates the inhomogeneity. We have

$$\text{Sol}(\tilde{\mathcal{L}}^{(2)}) = \left\langle \mathcal{I}_{(j_1,j_2,j_3)}(\underline{z},\epsilon) \right\rangle_{1\leq j\leq 3}, \tag{9.22}$$

with

$$\tilde{\mathcal{L}}^{(2)} := \{(\theta_1-\epsilon)\mathcal{L}_1, (\theta_2-\epsilon)\mathcal{L}_2, (\theta_3-\epsilon)\mathcal{L}_3, \mathcal{L}_4, \mathcal{L}_5, \mathcal{L}_6\}\,. \tag{9.23}$$

The previous discussion makes it clear that it is a matter of taste whether we consider a set of inhomogeneous differential operators or a set of higher-order differential operators; the resulting solution spaces contain all functions necessary to solve the problem at hand. Our strategy of first constructing combinatorially an ideal which can then be extended to a set of inhomogeneous differential equations guarantees that we generate the correct solution space.

The method we have just described can easily be implemented into a computer algebra system. We can in this way derive a set of inhomogeneous differential equations satisfied by $J_{l,\underline{0}}(\underline{z},\epsilon)$. The coefficients of the linear combination in the Frobenius basis in eq. (9.7) can be read off by comparing to the hypergeometric series representation in eq. (9.3) (or by using eq. (9.4) as a boundary condition in the large momentum limit). At this point we have to make an important comment. Our strategy to obtain the differential equations consisted in starting from the MB representation, which leads to the hypergeometric series representation in eq. (9.3). It may thus appear that we did not gain anything, because we have derived the differential equations *after* we knew the solution, cf. eq. (9.3). The series representation in eq. (9.3), however, does not converge for all values of $\underline{z}$. The differential equations allow us to analytically continue the series in eq. (9.3), e.g., by transforming the differential equation to another point and to obtain local power series representations close to that point (see the discussion in chapter 3).

Let us make some comments about our differential equations. First, we emphazise that our procedure allows us to derive differential equations for arbitrary values of $\underline{z}$, including zero masses. This follows immediately from the fact that eq. (9.3) is valid also in the case of massless propagators. Second, we point out that from our higher-order inhomogeneous differential equation for $J_{l,\underline{0}}(\underline{z},\epsilon)$, we can easily obtain the first-order Gauss-Manin system for the master integrals in eq. (2.18). When extracting the entries of the matrix $\tilde{\mathbf{A}}(\underline{z};\epsilon)$ in eq. (3.3), we need to divide by the discriminant of the system. This introduces typically a very long and complicated polynomial, especially in the multi-parameter case. Therefore, the matrix $\tilde{\mathbf{A}}(\underline{z};\epsilon)$ is usually very complicated, and we prefer to work with the larger, but simpler, set of differential operators $\{\mathcal{L}_{\alpha,\beta}\}$ constructed in this section.

Finally, we want to emphasize that our combinatorial method of constructing a set of

differential operators such that its solution space contains a specific set of functions starting from an analysis of a power series as in eq. (9.7) can be applied not only with the dimensional regulator ϵ but also for $\epsilon = 0$ and we think also to other functions given as a power series with coefficients being fractions of gamma functions. In particular, in the $\epsilon = 0$ case one can construct easily a complete set of operators generating the function space of the l-loop banana integral in $D = 2$ dimensions. In chapter 7 we used the GKZ method for complete intersection Calabi-Yau manifolds to compute the banana integrals. The GKZ method does not directly yield a complete set of operators such that one has to find additional operators. In section 7.3 we explicitly solved the four-loop case where we used the methods explained in this section to generate the additional operators listed in eq. (7.21) and in appendix B.

9.2.1 Comments on the number of solutions

We conclude with some comments about the number of elements in the ϵ-Frobenius basis in eq. (9.7) for a given loop order l. We count the number of solutions with the same value of j, which itself counts how many ϵ parameters appear in the indicials to the differential operators. Thereby, we find for fixed j exactly $\binom{l+1}{j}$ different solutions. In total we obtain the following sequence:

$$\underbrace{\binom{l+1}{1} = l+1}_{j=1} \;\Big|\; \underbrace{\binom{l+1}{2}}_{j=2} \; \underbrace{\binom{l+1}{3}}_{j=3} \; \cdots \; \underbrace{\binom{l+1}{l+1} = 1}_{j=l+1} . \tag{9.24}$$

Here the vertical line separates the special solutions of the inhomogeneous equations from the homogeneous ones. For example, for the two-loop case this reduces to

$$3 \quad | \quad 3 \quad 1 , \tag{9.25}$$

in agreement with the discussion above. If we compare the number of solutions in the generic-mass case for $\epsilon = 0$ and $\epsilon \neq 0$, we observe that for $\epsilon \neq 0$ we have more solutions. For example, at two-loop order the number of solutions for $\epsilon = 0$ is

$$1 \quad | \quad 1 \quad 1 . \tag{9.26}$$

The fact that the number of master integrals is smaller in exactly $D = 2$ dimensions was already observed in refs. [7, 109, 170] for the two-loop banana graph. Comparing to the number of solutions for $\epsilon = 0$ for the maximal cut in $D = 2$ dimensions in ref. [45], we see that generically the dimension of the solution space, and therefore the number of master integrals, increases by introducing a non-vanishing dimensional regularization parameter ϵ.

Let us make another comment about the number of solutions for different values of j.

We can extend the sequence in eq. (9.24) by including the function in eq. (9.7) for $j = 0$. There is exactly one such function. Note that this solution can also be included into eq. (9.3), because it would enter the linear combination with a vanishing prefactor. We then obtain the sequence:

$$\underbrace{1 = \binom{l+1}{0}}_{j=0} \;\Big\|\; \underbrace{\binom{l+1}{1} = l+1}_{j=1} \;\Big|\; \underbrace{\binom{l+1}{2}}_{j=2} \; \underbrace{\binom{l+1}{3}}_{j=3} \; \cdots \; \underbrace{\binom{l+1}{l+1} = 1}_{j=l+1} . \tag{9.27}$$

The solution space of the functions in eq. (9.7) with $0 \leq j \leq l+1$ can be described in terms of differential equations in different ways. One possibility is that one allows only certain linear combinations of operators determining the solution space corresponding to the sequence in eq. (9.24). One may apply appropriate θ-derivatives to the same operators, similar to the procedure of extending the solution space by the ϵ-Frobenius solutions with $j = 1$. To be precise, let us look again at the two-loop case. Here the ϵ-Frobenius element with $j = 0$ can be included into the solution space if one considers the following ideal $\{\theta_1(\theta_1 - \epsilon)\mathcal{D}_1, \theta_2(\theta_2 - \epsilon)\mathcal{D}_2, \theta_3(\theta_3 - \epsilon)\mathcal{D}_3, \mathcal{D}_4, \mathcal{D}_5, \mathcal{D}_6\}$. This ideal allows exactly the 8 desired solutions which can be grouped into

$$1 \;||\; \quad 3 \quad | \quad 3 \quad 1 . \tag{9.28}$$

More generally, the pattern of the number of solutions in eq. (9.27) corresponds to the pattern of the dimensions of the (co)homology groups of the ambient space $\mathbb{P}_{l+1}$, which is first the ambient space of the Fano variety F_l in which in turn the Calabi-Yau variety M_{l-1} for the critical spacetime dimensions $\epsilon = 0$ is embedded, as it is explained in eq. (7.5). It is tantalising to speculate that in dimensional regularization the solutions can be interpreted as some kind of twisted quantum deformation of the cohomology of $\mathbb{P}_{l+1}$.

9.3 Some comments on the equal-mass case

The techniques introduced in the last two sections can also be applied on the equal-mass banana integrals to compute them in dimensional regularization. In this case the equal-mass case is considered as a one-parameter subslice in the generic-mass parameter space. As we have already seen in subsection 6.1.4 restricting a high-parameter moduli space to a smaller here even a one-parameter slice is typically a hard technical problem. One cannot simply restrict the partial differential equations obtained in the previous section to the equal-mass case. Furthermore, the dimension of the ϵ-Frobenius basis is much smaller in the equal-mass case where it is the same in $D = 2$ and $D = 2 - 2\epsilon$ dimensions, namely $l + 1$.

In this thesis we do not want to recapitulate in detail the additional methods which were

elaborated in [47] but only want to give some comments about them.

In the equal-mass case it turns out that one can compute directly a Picard-Fuchs differential equation starting from a Bessel function representation [8, 167] of the banana integral given by

$$J_{l,1}(z=1/t;\epsilon) = \frac{2^{l(1-\epsilon)}}{\Gamma(1+l\epsilon)} t^{\frac{\epsilon}{2}} \int_0^\infty x^{1+l\epsilon}\, I_{-\epsilon}(\sqrt{t}x) K_\epsilon(x)^{l+1}\, \mathrm{d}x\,, \tag{9.29}$$

valid for $t := 1/z < (l+1)^2$, where $I_\alpha(x)$ and $K_\alpha(x)$ are the modified Bessel functions. From a detailed analysis of this representation and, in particular, of the Bessel functions we could derive in [47] an inhomogeneous differential equation for the l-loop equal-mass banana integral. A list of these equations can be found in table 2 of [47].

These differential equations could be solved with the Frobenius method where now the indicials get an ϵ-dependence and therefore the basis of solutions as well, similarly as the ϵ-Frobenius basis is (9.7). Also the Riemann $\mathcal{P}$-symbol gets a ϵ-dependence since also at the other singular points the indicials get shifted by ϵ-terms. Only the location of the singular points is unchanged. For details see section 6.2 of [47].

With eq. (9.5) we could find also the correct linear combination of the ϵ-Frobenius basis to obtain the full l-loop equal-mass banana integral in $D = 2 - 2\epsilon$ dimensions. Again at zeroth order in the regulator ϵ this reproduced the results found from numerics and the $\widehat{\Gamma}$-class. This also extended the results in the literature of the equal-mass banana integrals to arbitrary loop order.

9.4 Special solutions and cut integrals

In this section we provide an interpretation of the additional special solutions to the inhomogeneous Picard-Fuchs differential ideal in terms of non-maximal cut integrals. This interpretation complements and extends the interpretation of the maximal cut integrals as solutions to the associated homogeneous system and its relationship to the Frobenius basis for the solution space of the Picard-Fuchs differential ideals for the maximal cuts. We start by defining non-maximal cuts in general (not restricted to banana integrals), and then comment on the relationship to the solution space of the Picard-Fuchs differential ideal at the end of this section. This section is also an extension of section 2.7.

Let us consider the setup and the notation of chapter 2, in particular section 2.7. A *non-maximal cut contour* Γ for the integral $I^G_{\underline{\nu}}(\underline{x}; D)$ is a contour that encircles some of the propagators of $I^G_{\underline{\nu}}(\underline{x}; D)$. We assume that Γ encircles at least one propagator. At this point we have to make an important comment about dimensional regularization. In *integer* dimension the integration contour Γ has an immediate geometrical interpretation. The extension of this contour to dimensional regularization will be necessary for the following discussion. One can still define the contour geometrically, but it needs to be interpreted as a *twisted cycle* [171], see also refs. [66, 172–175]. The distinction will not be crucial for the discussion that follows, and it is sufficient to apply intuition from ordinary cycles in integer dimensions.

It is important, however, to point out that beyond one loop non-maximal cut integrals may diverge even if the original Feynman integral is finite, cf., e.g., refs. [80, 176]. The divergences are of infrared origin and arise from massless particles that are put on-shell when taking the residues. Therefore, it is important to work with an appropriate infrared regulator when discussing non-maximal cut integrals. Dimensional regularization provides such a regulator.

Following sections 2.7 and 2.8, if Γ is a cut contour and $J_i(\underline{z};\epsilon)$ denotes a master integral, then we denote the corresponding cut integral by $J_i^\Gamma(\underline{z};\epsilon)$. The vector $\underline{J}^\Gamma(\underline{z};\epsilon)$ then satisfies the same system of differential equations as the vector of master intergals $J_i(\underline{z};\epsilon)$ in eq. (3.3), i.e., we have

$$\mathrm{d}\underline{J}^\Gamma(\underline{z};\epsilon) = \widetilde{A}(\underline{z};\epsilon)\underline{J}^\Gamma(\underline{z};\epsilon) \quad \text{for every cut contour } \Gamma\,. \tag{9.30}$$

Let us discuss how we can construct a basis of cut integrals. We say that a sector is *reducible* if every integral from this sector can be written as a linear combination of integrals from lower sectors. Let $\Theta_1,\ldots,\Theta_s$ denote the set of irreducible sectors. There is a natural partial order on the Θ_r (coming from the partial order on sectors, see subsection 2.3.2). In particular, we choose $\Theta_1 = (1,\ldots,1)$. We denote by $\underline{J}_r(\underline{z};\epsilon) = (J_{r,1}(\underline{z};\epsilon),\ldots,J_{r,M_r}(\underline{z};\epsilon))^T$ the master integrals in the sector Θ_r (by which we mean that those master integrals cannot be expressed as linear combinations of integrals from lower sectors; cf. eq. (3.6)). In each sector Θ_r we can now choose a basis of M_r maximal cut contours, i.e., a set of M_r independent cut contours that encircle precisely the propagators that define the sector Θ_r. Let us denote the basis of maximal cut contours in the sector Θ_r by $\Gamma_{r,1},\ldots,\Gamma_{r,M_r}$. Note that for $r=1$ and integer D, we recover the maximal cut contours defined in section 2.7. Each contour $\Gamma_{r,i}$ defines a valid non-maximal cut contour for integrals from sectors with more propagators.

Consider the $M\times M$ matrix (where $M=\sum_{r=1}^s M_r$ is the total number of master integrals):

$$\mathbf{J}(\underline{z};\epsilon) =: \left(\underline{J}^{\Gamma_{1,1}}(\underline{z};\epsilon),\ldots,\underline{J}^{\Gamma_{1,M_1}}(\underline{z};\epsilon),\underline{J}^{\Gamma_{2,1}}(\underline{z};\epsilon),\ldots,\underline{J}^{\Gamma_{s,M_s}}(\underline{z};\epsilon)\right). \tag{9.31}$$

It is easy to check that the columns of $\mathbf{J}(\underline{z};\epsilon)$ are linearly independent (for generic $\underline{z}$), and so $\mathbf{J}(\underline{z};\epsilon)$ is a fundamental solution matrix for the system in eq. (9.30). As a corollary, we conclude that every master integral can be written as a linear combination of its cut integrals in the basis of cut contours $\Gamma_{r,i}$:

$$J_k(\underline{z};\epsilon) = \sum_{r=1}^{s}\sum_{i=1}^{M_r} a_{r,i}(\epsilon)\, J_k^{\Gamma_{r,i}}(\underline{z};\epsilon)\,, \tag{9.32}$$

where the coefficients $a_{r,i}(\epsilon)$ may depend on ϵ, but they are independent of $\underline{z}$. Note that this relation is very reminiscient of the celebrated *Feynman Tree Theorem* [177, 178]. It would be interesting to work out the relationship between the basis decomposition in eq. (9.32) and the Feynman Tree Theorem in the future.

Assume now that $\mathcal{D}^{(k)}$ generates the Picard-Fuchs differential ideal that annihilates $J_k(\underline{z};\epsilon)$, i.e., it is a complete set of differential operators that annihilate $J_k(\underline{z};\epsilon)$. Since the solution space of the Picard-Fuchs differential ideal must agree with the general solution obtained from the system in eq. (9.30), eq. (9.32) implies that

$$\mathrm{Sol}(\mathcal{D}^{(k)}) = \left\langle J_k^{\Gamma_{r,i}}(\underline{z};\epsilon) \right\rangle_{1\leq r\leq s; 1\leq i\leq M_r} = \sum_{r=1}^{s} \left\langle J_k^{\Gamma_{r,i}}(\underline{z};\epsilon) \right\rangle_{1\leq i\leq M_r}, \tag{9.33}$$

where in the second inequality we have made explicit the fact that the solution space can be decomposed into contributions from cut contours from different sectors. The previous considerations show that we can, at least in principle, obtain a basis of the solution space of the system of differential equations satisfied by the master integrals that consists entirely of cut integrals. Just like in the case of maximal cuts, however, constructing such a basis of cycles explicitly can be a monumental task, and it is in general not possible to follow this route.

In the following, we argue that the special solutions from section 9.2 that extend the solution space for the Picard-Fuchs differential ideal for the maximal cuts can be identified with non-maximal cuts. However, similar to the discussion of the relationship between the Frobenius basis and the maximal cuts defined via cycles from integral homology, the special solutions constructed in the previous section will not be obtained from non-maximal cut contours defined over the integers.

Let us illustrate this on the example of the two-loop case. In particular, let us discuss the two-loop master integral $J_{1,\underline{0}}(\underline{z};\epsilon)$. The Picard-Fuchs differential ideal is generated by the set $\tilde{\mathcal{L}}^{(2)}$ in eq. (9.23). Its solution space admits the decomposition

$$\mathrm{Sol}(\tilde{\mathcal{L}}^{(2)}) = \mathrm{Sol}(\mathcal{L}^{(2)}) + \left\langle \mathcal{I}_{(1,0,0)}(\underline{z},\epsilon) \right\rangle + \left\langle \mathcal{I}_{(0,1,0)}(\underline{z},\epsilon) \right\rangle + \left\langle \mathcal{I}_{(0,0,1)}(\underline{z},\epsilon) \right\rangle, \tag{9.34}$$

where $\mathcal{L}^{(2)}$ was defined in eq. (9.14). Let us interpret eq. (9.34) in the light of eq. (9.33). We know from section 9.2 that there are four irreducible sectors for the two-loop banana integral, namely

$$\Theta_1 = (1,1,1)\,, \quad \Theta_2 = (1,1,0)\,, \quad \Theta_3 = (1,0,1)\,, \quad \Theta_4 = (0,1,1)\,, \tag{9.35}$$

and $M_1 = 4$ and $M_2 = M_3 = M_4 = 1$. Let us start by discussing the first term in eq. (9.34). Its interpretation is similar to the discussion in section 4.2.3 (which was restricted to $D = 2$ dimensions): The cut contours $\Gamma_{1,i}$, $1 \leq i \leq 4$, define a basis for the maximal cut contours of $J_{1,\underline{0}}(\underline{z};\epsilon)$.[3] The maximal cut integrals $J_{1,\underline{0}}^{\Gamma_{1,i}}(\underline{z};\epsilon)$ are annihilated by the differential operators

[3] Note that these contours define the maximal cuts in $D = 2 - 2\epsilon$ dimensions. Consequently, there are four maximal cut contours, and not only two, just like there are more master integrals in $D = 2 - 2\epsilon$ than in $D = 2$ dimensions, cf. (9.24).

from $\mathcal{L}^{(2)}$, and they form an integral basis for the solution space:

$$\text{Sol}(\mathcal{L}^{(2)}) = \left\langle J^{\Gamma_{1,i}}_{1,\underline{0}}(\underline{z};\epsilon) \right\rangle_{1\leq i\leq 4}. \tag{9.36}$$

This integral basis may be hard to construct, as it requires a detailed knowledge of the cycles. We know, however, that the solution space $\text{Sol}(\mathcal{L}^{(2)})$ is equally generated by the ϵ-Frobenius basis in eq. (9.15). The ϵ-Frobenius basis is not an integral basis, but its advantage is that we can construct it explicitly.

Next, let us discuss the remaining three terms in eq. (9.34). The non-maximal cut integrals $J^{\Gamma_{r,1}}_{1,\underline{0}}(\underline{z};\epsilon)$ for $2 \leq r \leq 4$ are not annihilated by the elements of $\mathcal{L}^{(2)}$ (because for each sector there is a tadpole integral whose maximal cut is non-zero). As a consequence, $J^{\Gamma_{r,1}}_{1,\underline{0}}(\underline{z};\epsilon)$ for $2 \leq r \leq 4$ satisfies an inhomogeneous equation, i.e., it is annihilated by the elements of $\tilde{\mathcal{L}}^{(2)}$! Thus, we see that the last three terms in eq. (9.34) represent the contributions from the non-maximal cuts in eq. (9.33), which we quote here for the two-loop case:

$$\text{Sol}(\tilde{\mathcal{L}}^{(2)}) = \left\langle J^{\Gamma_{1,i}}_{1,\underline{0}}(\underline{z};\epsilon) \right\rangle_{1\leq i\leq 4} + \sum_{r=2}^{4} \left\langle J^{\Gamma_{r,1}}_{1,\underline{0}}(\underline{z};\epsilon) \right\rangle = \text{Sol}(\mathcal{L}^{(2)}) + \sum_{r=2}^{4} \left\langle J^{\Gamma_{r,1}}_{1,\underline{0}}(\underline{z};\epsilon) \right\rangle. \tag{9.37}$$

Again, constructing explicitly the integer cycles $\Gamma_{r,1}$ with $r > 1$ can be extremely complicated, but we can work with the elements of the non-integer ϵ-Frobenius basis with $j = 1$. Note that it would be wrong to conclude that the elements of the ϵ-Frobenius basis with $j = 1$ are the non-maximal cut integrals $J^{\Gamma_{r,1}}_{1,\underline{0}}(\underline{z};\epsilon)$ for $r > 1$, defined by integrating over cycles from integral homology. Just like for the maximal cuts, the elements of the ϵ-Frobenius basis correspond to cut integrals over cycles that are not defined in integral homology, and a given non-maximal cut integral $J^{\Gamma_{r,1}}_{1,\underline{0}}(\underline{z};\epsilon)$ is in general for $r > 1$ a linear combination with transcendental coefficients of different terms in the ϵ -Frobenius basis, including those with $j > 1$.

CHAPTER 10

Conclusion

In this thesis we have seen that there is a strong connection between computations of multi-loop Feynman integrals and modern algebraic geometry. Only from a deep understanding of the geometry associated to the l-loop banana Feynman graph it was possible to compute the Feynman integral for generic masses and high loop orders. Characteristics of the Feynman integral as the branching behavior, singularity and monodromy structure, its differential equations and many more are reflected by the geometry. On the geometrical side these properties are often better understood and under control such that they determine the Feynman integral. But still this connection is not fully elaborated and in particular, the physicists and mathematicians have to learn a lot from each other in order to increase the power of computing multi-loop Feynman graphs.

During my PhD several important results could be achieved:

On a practical side the generic-mass banana integrals could be computed for arbitrary loop orders which was possible before only for loop orders $l \leq 2$ (chapters 6 and 7). These Feynman graphs have an important role for improving the accuracy of theoretical predictions for scattering processes of fundamental particles. Using two different Calabi-Yau geometries, which lead to the same motive, the maximal cuts of the banana integrals were computed. Additionally, differential equations governing them were found with the GKZ method. This leads to an analytic continuation over the whole parameter space. An extension of these differential equations to inhomogeneous ones determined the missing special solution to describe the full Feynman integral. We also gave an interpretation of these special solutions as non-maximal cut integrals. Finally, with the help of a novel $\widehat{\Gamma}$-class we were able to find the correct linear combination of solutions.

But also in the equal-mass case new results were obtained (chapter 5). In $D = 2$ dimensions we could find a compact and simple form of the l-loop integral in terms of iterated Calabi-Yau periods. This representation is a generalization of the results found for $l \leq 3$ [24, 25, 33, 112, 150, 179, 180]. Due to our contribution the banana family joins now the set of infinite families of Feynman integrals where an explicit analytic result is known [181–188]. But this

is the first of these families which can not be expressed in terms of multiple polylogarithms.

From a conceptional perspective we were also able to extend the connection between Calabi-Yau motives and multi-loop Feynman integrals. We reviewed basic concepts of Feynman graph computations (chapter 2), fundamental properties and solution techniques for differential equations (chapter 3) and the mathematics of Calabi-Yau manifolds (chapter 4) together with mirror symmetry (chapter 8). This has hopefully boosted the connection between geometry and Feynman integrals.

There are many continuations of our work possible. First of all, the most obvious one would be to extend our methods also to other classes of Feynman integrals beside the banana ones. In this direction it would be interesting to see how one can use the GKZ method and some intuition from geometry to find differential equations for Feynman integrals without usage of the traditional integration by parts approach. Secondly, the mathematics of iterated Calabi-Yau periods has to be enhanced similarly to the theory of iterated modular forms. The concept of iterated integrals in Feynman integral computations is so fundamental that also for Calabi-Yau periods these concepts have to be implemented. Probably, this will give better numerical control over these functions. But in general it would be very interesting and advisable to check what geometric objects or motives can show up in Feynman graph computations. In our examples Calabi-Yau motives were the most generic objects and also the most natural ones. But there are some observations [189–191] that also other geometries such as Riemann surfaces of higher genus[1] can show up, in particular, for non-planar Feynman diagrams. But there are also possibilities to include these geometries in Calabi-Yau motives such that one can still claim that Calabi-Yau motives are the most complicated geometric structures appearing in Feynman graph computations. A clarification of this relation would be very interesting.

[1] Only Riemann surfaces of genus one, i.e. elliptic curves, are Calabi-Yau manifolds. For higher genera they are not strictly speaking Calabi-Yau manifolds. But they can give rise to so-called local Calabi-Yau spaces.

APPENDIX A

Differential operators for the three-loop banana integral

Here we list the four differential operators $\mathcal{D}_1, \ldots, \mathcal{D}_4$ for the three-loop banana integral.

$$\begin{aligned}\mathcal{D}_1 = &\left(\theta_1 - \theta_2\right)\left(\theta_3 - \theta_4\right) \\ &+ z_1(\theta_3 - \theta_4)(\theta_1 - \theta_2 - \theta_3 - \theta_4) + z_2(\theta_3 - \theta_4)(\theta_1 - \theta_2 + \theta_3 + \theta_4) \\ &- 2(z_1 - z_2)\left(z_3(\theta_3 + 1) - z_4(\theta_4 + 1)\right)(\theta_1 + \theta_2 + \theta_3 + \theta_4 + 1)\end{aligned} \tag{A.1}$$

$$\begin{aligned}\mathcal{D}_2 = &\, 5(\theta_1 - \theta_2)\theta_4 - 6\theta_2^2 \\ &+ z_1\left(2\theta_1^2 - 8\theta_1\theta_2 + 6\theta_2^2 - 6\theta_3^2 - 11\theta_4^2 + 4\left(\theta_1 + \theta_2\right)\theta_3 + \left(9\theta_1 - \theta_2 - 13\theta_3\right)\theta_4\right) \\ &+ z_2\left(17\theta_4^2 + \left(13\theta_1 - 9\theta_2 + 25\theta_3 + 6\right)\theta_4 - 2\left(\theta_2 - \theta_3\right)\left(4\theta_2 + 6\theta_3 + 3\right) + \theta_1\left(8\theta_2 + 8\theta_3 + 6\right)\right) \\ &+ 2\Big[5z_3z_4(\theta_2 - \theta_1) + z_1^2(\theta_1 - \theta_2 - \theta_3 - \theta_4) + z_2^2(\theta_1 - \theta_2 + \theta_3 + \theta_4) \\ &+ z_1z_4(3\theta_1 + 3\theta_2 - 2\theta_3 - 8\theta_4 - 5) + z_1z_3(3\left(\theta_1 + \theta_2 - \theta_3\right) - 2\theta_4) \\ &+ 3z_1z_2(-\theta_1 + 3\theta_2 + \theta_3 + \theta_4 + 2) + z_2z_3(6\theta_3 + 5\theta_4 + 6) \\ &+ z_2z_4(5\theta_3 + 11\theta_4 + 11)\Big]\left(\theta_1 + \theta_2 + \theta_3 + \theta_4 + 1\right)\end{aligned} \tag{A.2}$$

$$\begin{aligned}\mathcal{D}_3 = &-3\theta_2^2 - 2\theta_2\theta_4 + \theta_1\left(3\theta_2 - 2\theta_4\right) + \theta_4\left(\theta_3 + \theta_4\right) \\ &- 3z_1\theta_2\left(-\theta_1 + \theta_2 + \theta_3\right) - z_1\theta_4(2\theta_1 + \theta_2 - 2\theta_3) - z_3\theta_4(\theta_1 + \theta_2 - \theta_3) + (2z_1 - z_3)\theta_4^2 \\ &- z_4\left(\theta_1 + \theta_2 + \theta_3 - \theta_4\right)\left(\theta_4 + 1\right) + z_2\left(\theta_1 - \theta_2 + \theta_3 + \theta_4\right)\left(3\theta_2 + 8\theta_4 + 3\right) \\ &+ 2\left[-2z_3z_4(\theta_4 + 1) + z_1z_4 - 3z_1z_3\theta_2 + z_1(z_3 + z_4)\theta_4 + z_2z_3(3\theta_2 + 4\theta_4 + 3)\right. \\ &\left.+ 4z_2z_4 + 4z_2(z_1 + z_4)\theta_4\right]\left(\theta_1 + \theta_2 + \theta_3 + \theta_4 + 1\right)\end{aligned} \tag{A.3}$$

$$
\begin{aligned}
\mathcal{D}_4 = & -\theta_2\left(\theta_2+5\theta_3-5\theta_4\right) \\
& +z_1(2\theta_1^2-\left(3\theta_2+\theta_3-4\theta_4\right)\theta_1+\theta_2^2-\theta_3^2-6\theta_4^2+4\theta_2\theta_3-\left(\theta_2+3\theta_3\right)\theta_4) \\
& +5z_4\left(\theta_1-\theta_2-\theta_3\right)\left(\theta_1+\theta_2+\theta_3-\theta_4\right)+5z_3\theta_4\left(\theta_1+\theta_2-\theta_3+\theta_4\right) \\
& +z_2\Big[-3\theta_2^2+\left(-14\theta_3+11\theta_4-1\right)\theta_2+17\theta_3^2-8\theta_4^2+\theta_3+\theta_1\left(3\theta_2+13\theta_3-12\theta_4+1\right) \\
& +5\theta_3\theta_4+\theta_4\Big] \\
& +\Big[2z_1^2(\theta_1-\theta_2-\theta_3-\theta_4)+z_1z_4(11\theta_1-9\theta_2+\theta_3-11\theta_4) \\
& +z_1z_2(-\theta_1+3\theta_2+11\theta_3-9\theta_4+2)+z_1z_3(\theta_1+11\theta_2-\theta_3+\theta_4) \\
& +2z_2z_3(-5\theta_2+11\theta_3-5\theta_4+6)+2z_2z_4(5\theta_3-4\theta_4-4)+10z_3z_4(\theta_4-\theta_3) \\
& +2z_2^2(\theta_1-\theta_2+\theta_3+\theta_4)\Big]\left(\theta_1+\theta_2+\theta_3+\theta_4+1\right)
\end{aligned}
\tag{A.4}
$$

APPENDIX B

Differential operators for the four-loop banana integral

Here we list the four differential operators $\mathcal{D}_6, \ldots, \mathcal{D}_{10}$ for the four-loop banana integral.

$$\begin{aligned}\mathcal{D}_6 = &(\theta_1 - \theta_4)\,(\theta_3 - \theta_5) - z_1\,(\theta_3 - \theta_5)\,(\theta_1 + 2\theta_2 + \theta_4 + 1)\\ &- z_2\,(\theta_1 - \theta_4)\,(\theta_3 - \theta_5) + z_3(2\theta_1^2 + \theta_1\,(2\theta_2 + \theta_3 + \theta_5 + 1) - \theta_4\,(2\theta_2 + \theta_3 + \theta_5 + 1))\\ &+ z_4(2\theta_3^2 + \theta_3\,(\theta_1 + 2\theta_2 + \theta_4 + 1) - \theta_5\,(\theta_1 + 2\theta_2 + \theta_4 + 1))\\ &+ z_5\,(\theta_1 - \theta_4)\,(2\theta_1 + 2\theta_2 + \theta_3 + 2\theta_4 + \theta_5 + 1)\end{aligned} \tag{B.1}$$

$$\begin{aligned}\mathcal{D}_7 = &(\theta_1 - \theta_3)\,(\theta_4 - \theta_5) - z_1(\theta_4 - \theta_5)(\theta_1 + 2\theta_2 + \theta_3 + 1)\\ &- z_2\,(\theta_1 - \theta_3)\,(\theta_4 - \theta_5) + z_3\,(\theta_4 - \theta_5)\,(\theta_1 + 2\theta_2 + \theta_3 + 1)\\ &- z_4\,(\theta_1 - \theta_3)\,(2\theta_1 + 2\theta_2 + 2\theta_3 + \theta_4 + \theta_5 + 1)\\ &+ z_5\,(\theta_1 - \theta_3)\,(2\theta_1 + 2\theta_2 + 2\theta_3 + \theta_4 + \theta_5 + 1)\end{aligned} \tag{B.2}$$

$$\begin{aligned}\mathcal{D}_8 = &(\theta_2 - \theta_4)\,(\theta_3 - \theta_5) - z_1\,(\theta_2 - \theta_4)\,(\theta_3 - \theta_5)\\ &- z_2\,(\theta_3 - \theta_5)\,(2\theta_1 + \theta_2 + \theta_4 + 1)\\ &- z_3(2\theta_2^2 + \theta_2\,(2\theta_1 + \theta_3 + \theta_5 + 1) - \theta_4\,(2\theta_1 + \theta_3 + \theta_5 + 1))\\ &+ z_4(2\theta_3^2 + \theta_3\,(2\theta_1 + \theta_2 + \theta_4 + 1) - \theta_5\,(2\theta_1 + \theta_2 + \theta_4 + 1))\\ &+ z_5\,(\theta_2 - \theta_4)\,(2\theta_1 + 2\theta_2 + \theta_3 + 2\theta_4 + \theta_5 + 1)\end{aligned} \tag{B.3}$$

$$\begin{aligned}\mathcal{D}_9 = &(\theta_2-\theta_3)(\theta_4-\theta_5) - z_1(\theta_2-\theta_3)(\theta_4-\theta_5)\\ &- z_2(\theta_4-\theta_5)(2\theta_1+\theta_2+\theta_3+1) + z_3(\theta_4-\theta_5)(2\theta_1+\theta_2+\theta_3+1)\\ &- z_4(\theta_2-\theta_3)(2\theta_1+2\theta_2+2\theta_3+\theta_4+\theta_5+1)\\ &+ z_5(\theta_2-\theta_3)(2\theta_1+2\theta_2+2\theta_3+\theta_4+\theta_5+1)\end{aligned} \tag{B.4}$$

$$\begin{aligned}\mathcal{D}_{10} = &\theta_1(\theta_2-\theta_5) + (-\theta_2+\theta_4)\theta_5 + \theta_3(-\theta_4+\theta_5)\\ &- z_1(\theta_2(\theta_1+2\theta_3+2\theta_4-\theta_5+1) - \theta_5(\theta_1+\theta_4+1) - \theta_3(\theta_4+\theta_5))\\ &- z_2(2\theta_1^2+\theta_1(\theta_2+2\theta_3+2\theta_4-\theta_5+1) - \theta_5(\theta_2+\theta_4+1) + \theta_3(\theta_4+\theta_5))\\ &- z_3(\theta_4(2\theta_2+\theta_3-\theta_5+1) - \theta_5(\theta_2+\theta_3+1) - \theta_1(\theta_2-2\theta_4+\theta_5))\\ &+ z_4(2\theta_3^2+\theta_3(2\theta_2+\theta_4-\theta_5+1) - \theta_5(\theta_2+\theta_4+1) - \theta_1(\theta_2-2\theta_3+\theta_5))\\ &+ z_5(2\theta_1^2+2\theta_2^2-2\theta_3^2-\theta_4(2\theta_4+1) - \theta_3(3\theta_4+1) - \theta_5(\theta_3+\theta_4) + \theta_2(\theta_5+1)\\ &\quad + \theta_1(1+3\theta_2+\theta_5))\end{aligned} \tag{B.5}$$

Bibliography

[1] M. Kontsevich and D. Zagier, "Periods," *Mathematics unlimited—2001 and beyond*, Springer, Berlin, 2001 771 (cit. on p. 1).

[2] A. V. Kotikov, *Differential equations method: The Calculation of vertex type Feynman diagrams*, Phys. Lett. **B259** (1991) 314 (cit. on pp. 2, 30).

[3] A. V. Kotikov, *Differential equation method: The Calculation of N point Feynman diagrams*, Phys. Lett. **B267** (1991) 123 (cit. on pp. 2, 30).

[4] A. Kotikov, *Differential equations method. New technique for massive Feynman diagram calculation*, Physics Letters B **254** (1991) 158, ISSN: 03702693, URL: http://linkinghub.elsevier.com/retrieve/pii/037026939190413K (cit. on p. 2).

[5] T. Gehrmann and E. Remiddi, *Differential equations for two-loop four-point functions*, Nuclear Physics B **580** (2000) 485, ISSN: 05503213, URL: http://linkinghub.elsevier.com/retrieve/pii/S0550321300002236 (cit. on p. 2).

[6] J. M. Henn, *Multiloop integrals in dimensional regularization made simple*, Phys. Rev. Lett. **110** (2013) 251601, arXiv: 1304.1806 [hep-th] (cit. on pp. 2, 30, 31).

[7] S. Müller-Stach, S. Weinzierl, and R. Zayadeh, *Picard-Fuchs equations for Feynman integrals*, Commun. Math. Phys. **326** (2014) 237, arXiv: 1212.4389 [hep-ph] (cit. on pp. 2, 43, 108, 111).

[8] P. Vanhove, *The physics and the mixed Hodge structure of Feynman integrals*, Proc. Symp. Pure Math. **88** (2014) 161, ed. by R. Donagi, M. R. Douglas, L. Kamenova, and M. Rocek, arXiv: 1401.6438 [hep-th] (cit. on pp. 2, 61, 113).

[9] S. Bauberger, M. Böhm, G. Weiglein, F. A. Berends, and M. Buza, *Calculation of two-loop self-energies in the electroweak Standard Model*, Nucl. Phys. B Proc. Suppl. **37B** (1994) 95, ed. by T. Riemann and J. Blümlein, arXiv: hep-ph/9406404 (cit. on p. 2).

[10] S. Abreu, M. Becchetti, C. Duhr, and R. Marzucca, *Three-loop contributions to the ρ parameter and iterated integrals of modular forms*, JHEP **02** (2020) 050, arXiv: 1912.02747 [hep-th] (cit. on pp. 2, 3).

[11] S. Laporta, *Analytical expressions of 3 and 4-loop sunrise Feynman integrals and 4-dimensional lattice integrals*, Int. J. Mod. Phys. A **23** (2008) 5007, arXiv: 0803.1007 [hep-ph] (cit. on p. 2).

[12] E. E. Kummer, *Über die Transcendenten, welche aus wiederholten Integrationen rationaler Formeln entstehen*, J. reine ang. Mathematik **21** (1840) 74, 193, 328 (cit. on p. 3).

[13] J. A. Lappo-Danilevsky, *Théorie algorithmique des corps de Riemann*, Rec. Math. Moscou **34** (1927) 113 (cit. on p. 3).

[14] A. B. Goncharov, *Multiple polylogarithms and mixed Tate motives*, (), arXiv: math/0103059 (cit. on p. 3).

[15] A. B. Goncharov, *Multiple polylogarithms, cyclotomy and modular complexes*, Math.Res.Lett. **5** (1998) 497, arXiv: 1105.2076 [math.AG] (cit. on p. 3).

[16] F. Brown, "On the decomposition of motivic multiple zeta values," *Galois-Teichmüller theory and arithmetic geometry*, vol. 68, Adv. Studies in Pure Math. Math. Soc. Japan, 2012 31, arXiv: 1102.1310 [math.NT] (cit. on p. 3).

[17] E. Remiddi and J. A. M. Vermaseren, *Harmonic polylogarithms*, Int. J. Mod. Phys. **A15** (2000) 725, arXiv: hep-ph/9905237 [hep-ph] (cit. on p. 3).

[18] T. Gehrmann and E. Remiddi, *Two loop master integrals for $\gamma^* \to 3$ jets: The Planar topologies*, Nucl.Phys. **B601** (2001) 248, arXiv: hep-ph/0008287 [hep-ph] (cit. on p. 3).

[19] J. Ablinger, J. Blumlein, and C. Schneider, *Harmonic Sums and Polylogarithms Generated by Cyclotomic Polynomials*, J. Math. Phys. **52** (2011) 102301, arXiv: 1105.6063 [math-ph] (cit. on p. 3).

[20] S. Bloch and P. Vanhove, *The elliptic dilogarithm for the sunset graph*, J. Number Theor. **148** (2015) 328, arXiv: 1309.5865 [hep-th] (cit. on pp. 3, 52, 61).

[21] A. Beilinson and A. Levin, "The elliptic polylogarithm," *Motives (Seattle, WA, 1991)*, vol. 55, Proc. Sympos. Pure Math. Amer. Math. Soc., Providence, RI, 1994 123, URL: https://doi.org/10.1007/s00208-018-1645-4 (cit. on p. 3).

[22] A. Levin and G. Racinet, *Towards multiple elliptic polylogarithms*, (2007), eprint: math/0703237 (math) (cit. on p. 3).

[23] F. Brown and A. Levin, *Multiple Elliptic Polylogarithms*, (2011), arXiv: 1110.6917 [math.NT] (cit. on p. 3).

[24] L. Adams and S. Weinzierl, *Feynman integrals and iterated integrals of modular forms*, Commun. Num. Theor. Phys. **12** (2018) 193, arXiv: 1704.08895 [hep-ph] (cit. on pp. 3, 26, 52, 117).

[25] J. Broedel, C. Duhr, F. Dulat, B. Penante, and L. Tancredi,
Elliptic symbol calculus: from elliptic polylogarithms to iterated integrals of Eisenstein series,
JHEP **08** (2018) 014, arXiv: 1803.10256 [hep-th] (cit. on pp. 3, 117).

[26] J. Broedel, C. Duhr, F. Dulat, and L. Tancredi,
Elliptic polylogarithms and iterated integrals on elliptic curves. Part I: general formalism,
JHEP **05** (2018) 093, arXiv: 1712.07089 [hep-th] (cit. on p. 3).

[27] J. Broedel, C. Duhr, F. Dulat, and L. Tancredi, *Elliptic polylogarithms and iterated integrals on elliptic curves II: an application to the sunrise integral*,
Phys. Rev. D **97** (2018) 116009, arXiv: 1712.07095 [hep-ph] (cit. on p. 3).

[28] J. Broedel, C. Duhr, F. Dulat, B. Penante, and L. Tancredi,
Elliptic Feynman integrals and pure functions, JHEP **01** (2019) 023,
arXiv: 1809.10698 [hep-th] (cit. on p. 3).

[29] L. Adams and S. Weinzierl,
The ε-form of the differential equations for Feynman integrals in the elliptic case,
Phys. Lett. **B781** (2018) 270, arXiv: 1802.05020 [hep-ph] (cit. on pp. 3, 31).

[30] L. Adams, E. Chaubey, and S. Weinzierl,
Planar Double Box Integral for Top Pair Production with a Closed Top Loop to all orders in the Dimensional Regularization Parameter, Phys. Rev. Lett. **121** (2018) 142001,
arXiv: 1804.11144 [hep-ph] (cit. on pp. 3, 31).

[31] L. Adams, E. Chaubey, and S. Weinzierl, *Analytic results for the planar double box integral relevant to top-pair production with a closed top loop*, JHEP **10** (2018) 206,
arXiv: 1806.04981 [hep-ph] (cit. on pp. 3, 31).

[32] J. Broedel, C. Duhr, F. Dulat, B. Penante, and L. Tancredi,
Elliptic polylogarithms and Feynman parameter integrals, JHEP **05** (2019) 120,
arXiv: 1902.09971 [hep-ph] (cit. on p. 3).

[33] J. Broedel et al., *An analytic solution for the equal-mass banana graph*, JHEP **09** (2019) 112,
arXiv: 1907.03787 [hep-th] (cit. on pp. 3, 61, 104, 117).

[34] C. Duhr and L. Tancredi, *Algorithms and tools for iterated Eisenstein integrals*,
JHEP **02** (2020) 105, arXiv: 1912.00077 [hep-th] (cit. on p. 3).

[35] C. Bogner, S. Müller-Stach, and S. Weinzierl,
The unequal mass sunrise integral expressed through iterated integrals on $\overline{\mathcal{M}}_{1,3}$,
Nucl. Phys. B **954** (2020) 114991, arXiv: 1907.01251 [hep-th] (cit. on pp. 3, 31).

[36] J. Campert, F. Moriello, and A. Kotikov, *Sunrise integral with two internal masses and pseudo-threshold kinematics in terms of elliptic polylogarithms*, (2020),
arXiv: 2011.01904 [hep-ph] (cit. on p. 3).

[37] M. Walden and S. Weinzierl,
Numerical evaluation of iterated integrals related to elliptic Feynman integrals,
Comput. Phys. Commun. **265** (2021) 108020, arXiv: 2010.05271 [hep-ph]
(cit. on p. 3).

[38] M. A. Bezuglov, A. I. Onishchenko, and O. L. Veretin,
Massive kite diagrams with elliptics, Nucl. Phys. B **963** (2021) 115302,
arXiv: 2011.13337 [hep-ph] (cit. on p. 3).

[39] S. Weinzierl, *Modular transformations of elliptic Feynman integrals*,
Nucl. Phys. B **964** (2021) 115309, arXiv: 2011.07311 [hep-th] (cit. on p. 3).

[40] A. Kristensson, M. Wilhelm, and C. Zhang,
The elliptic double box and symbology beyond polylogarithms, (2021),
arXiv: 2106.14902 [hep-th] (cit. on p. 3).

[41] J. Ablinger et al., *Iterated Elliptic and Hypergeometric Integrals for Feynman Diagrams*,
J. Math. Phys. **59** (2018) 062305, arXiv: 1706.01299 [hep-th] (cit. on p. 3).

[42] C. Bogner, A. Schweitzer, and S. Weinzierl, *Analytic continuation and numerical evaluation of the kite integral and the equal mass sunrise integral*,
Nucl. Phys. **B922** (2017) 528, arXiv: 1705.08952 [hep-ph] (cit. on p. 3).

[43] P. Vanhove, "Feynman integrals, toric geometry and mirror symmetry,"
KMPB Conference: Elliptic Integrals, Elliptic Functions and Modular Forms in Quantum Field Theory, 2019 415, arXiv: 1807.11466 [hep-th] (cit. on pp. 3, 59).

[44] A. Klemm, C. Nega, and R. Safari,
The l-loop Banana Amplitude from GKZ Systems and relative Calabi-Yau Periods,
JHEP **04** (2020) 088, arXiv: 1912.06201 [hep-th]
(cit. on pp. 3, 16, 34, 43, 69, 72, 75, 79–81).

[45] K. Bönisch, F. Fischbach, A. Klemm, C. Nega, and R. Safari,
Analytic structure of all loop banana integrals, JHEP **05** (2021) 066,
arXiv: 2008.10574 [hep-th]
(cit. on pp. 3, 16, 34, 39, 43, 47, 48, 52, 59, 61, 63, 69, 75, 79, 85, 86, 91, 99–101, 111).

[46] J. L. Bourjaily, Y.-H. He, A. J. Mcleod, M. Von Hippel, and M. Wilhelm, *Traintracks through Calabi-Yau Manifolds: Scattering Amplitudes beyond Elliptic Polylogarithms*,
Phys. Rev. Lett. **121** (2018) 071603, arXiv: 1805.09326 [hep-th] (cit. on pp. 3, 43).

[47] K. Bönisch, C. Duhr, F. Fischbach, A. Klemm, and C. Nega,
Feynman Integrals in Dimensional Regularization and Extensions of Calabi-Yau Motives,
(2021), arXiv: 2108.05310 [hep-th]
(cit. on pp. 3, 16, 29, 37, 39, 41, 43, 47, 48, 61, 63–65, 67, 85, 92, 101, 103, 104, 107, 113).

[48] S. Hosono, A. Klemm, S. Theisen, and S.-T. Yau,
Mirror symmetry, mirror map and applications to complete intersection Calabi-Yau spaces,
Nucl. Phys. **B433** (1995) 501, [AMS/IP Stud. Adv. Math.1,545(1996)],
arXiv: hep-th/9406055 [hep-th] (cit. on pp. 3, 45, 58, 79, 88–91, 98).

[49] A. Klemm,
"The B-model approach to topological string theory on Calabi-Yau n-folds,"
B-model Gromov-Witten theory, Trends Math. Birkhäuser/Springer, Cham, 2018 79
(cit. on pp. 3, 45, 47, 70, 96).

[50] H. Iritani,
Asymptotics of the banana Feynman amplitudes at the large complex structure limit, (2020), arXiv: 2011.05901 [math.AG] (cit. on pp. 3, 100).

[51] J. M. Henn, *Lectures on differential equations for Feynman integrals*,
J. Phys. **A48** (2015) 153001, arXiv: 1412.2296 [hep-ph] (cit. on p. 5).

[52] G. Passarino and M. J. G. Veltman,
One Loop Corrections for e+ e- Annihilation Into mu+ mu- in the Weinberg Model,
Nucl. Phys. B **160** (1979) 151 (cit. on p. 6).

[53] G. 't Hooft and M. J. G. Veltman, *Scalar One Loop Integrals*,
Nucl. Phys. B **153** (1979) 365 (cit. on p. 6).

[54] T. Hahn and M. Perez-Victoria,
Automatized one loop calculations in four-dimensions and D-dimensions,
Comput. Phys. Commun. **118** (1999) 153, arXiv: hep-ph/9807565 (cit. on p. 6).

[55] C. Itzykson and J. B. Zuber, *Quantum Field Theory*,
International Series In Pure and Applied Physics, New York: McGraw-Hill, 1980,
ISBN: 9780486445687, 0486445682,
URL: http://dx.doi.org/10.1063/1.2916419 (cit. on pp. 6, 14).

[56] M. E. Peskin and D. V. Schroeder, *An Introduction to quantum field theory*,
Reading, USA: Addison-Wesley, 1995, ISBN: 978-0-201-50397-5 (cit. on pp. 6, 8).

[57] M. Srednicki, *Quantum Field Theory*, Cambridge University Press, 2007 (cit. on p. 6).

[58] V. A. Smirnov, *Analytic tools for Feynman integrals*, vol. 250, 2012 (cit. on p. 6).

[59] E. R. Speer and M. J. Westwater, *GENERIC FEYNMAN AMPLITUDES*, (1970)
(cit. on p. 9).

[60] E. Panzer, *Feynman integrals and hyperlogarithms*, PhD thesis: Humboldt U., 2015,
arXiv: 1506.07243 [math-ph] (cit. on pp. 9, 14).

[61] K. Chetyrkin and F. Tkachov,
Integration by Parts: The Algorithm to Calculate beta Functions in 4 Loops,
Nucl. Phys. B **192** (1981) 159 (cit. on p. 11).

[62] F. Tkachov,
A Theorem on Analytical Calculability of Four Loop Renormalization Group Functions,
Phys. Lett. B **100** (1981) 65 (cit. on p. 11).

[63] A. Grozin, *Integration by parts: An Introduction*, Int. J. Mod. Phys. A **26** (2011) 2807,
arXiv: 1104.3993 [hep-ph] (cit. on pp. 11, 20, 21).

[64] A. V. Smirnov and A. V. Petukhov, *The Number of Master Integrals is Finite*,
Lett. Math. Phys. **97** (2011) 37, arXiv: 1004.4199 [hep-th] (cit. on p. 12).

[65] T. Bitoun, C. Bogner, R. P. Klausen, and E. Panzer,
Feynman integral relations from parametric annihilators, Lett. Math. Phys. **109** (2019) 497,
arXiv: 1712.09215 [hep-th] (cit. on p. 12).

[66] P. Mastrolia and S. Mizera, *Feynman Integrals and Intersection Theory*, JHEP **02** (2019) 139, arXiv: 1810.03818 [hep-th] (cit. on pp. 12, 113).

[67] M. Y. Kalmykov and B. A. Kniehl, *Counting the number of master integrals for sunrise diagrams via the Mellin-Barnes representation*, JHEP **07** (2017) 031, arXiv: 1612.06637 [hep-th] (cit. on p. 13).

[68] C. Bogner and S. Weinzierl, *Feynman graph polynomials*, Int. J. Mod. Phys. A **25** (2010) 2585, arXiv: 1002.3458 [hep-ph] (cit. on pp. 14, 16).

[69] O. Tarasov, *Connection between Feynman integrals having different values of the space-time dimension*, Phys. Rev. D **54** (1996) 6479, arXiv: hep-th/9606018 (cit. on p. 19).

[70] H. Frellesvig and C. G. Papadopoulos, *Cuts of Feynman Integrals in Baikov representation*, JHEP **04** (2017) 083, arXiv: 1701.07356 [hep-ph] (cit. on pp. 20, 22).

[71] URL: http://staff.ustc.edu.cn/~yzhphy/teaching/PH16212/Integral_representations.pdf (cit. on pp. 20, 22).

[72] P. A. Baikov, *Explicit solutions of the three loop vacuum integral recurrence relations*, Phys. Lett. B **385** (1996) 404, arXiv: hep-ph/9603267 (cit. on pp. 20, 21).

[73] P. A. Baikov, *Explicit solutions of n loop vacuum integral recurrence relations*, (1996), arXiv: hep-ph/9604254 (cit. on pp. 20, 21).

[74] D. A. Kosower and K. J. Larsen, *Maximal Unitarity at Two Loops*, Phys. Rev. D **85** (2012) 045017, arXiv: 1108.1180 [hep-th] (cit. on p. 23).

[75] M. Søgaard and Y. Zhang, *Multivariate Residues and Maximal Unitarity*, JHEP **12** (2013) 008, arXiv: 1310.6006 [hep-th] (cit. on p. 23).

[76] J. L. Bourjaily, N. Kalyanapuram, C. Langer, and K. Patatoukos, *Prescriptive Unitarity with Elliptic Leading Singularities*, (2021), arXiv: 2102.02210 [hep-th] (cit. on p. 23).

[77] C. Dlapa, X. Li, and Y. Zhang, *Leading singularities in Baikov representation and Feynman integrals with uniform transcendental weight*, (2021), arXiv: 2103.04638 [hep-th] (cit. on p. 23).

[78] H. Frellesvig, C. Vergu, M. Volk, and M. von Hippel, *Cuts and Isogenies*, JHEP **05** (2021) 064, arXiv: 2102.02769 [hep-th] (cit. on pp. 26, 52).

[79] G. 't Hooft and M. J. G. Veltman, *DIAGRAMMAR*, NATO Sci. Ser. B **4** (1974) 177 (cit. on p. 26).

[80] S. Abreu, R. Britto, C. Duhr, and E. Gardi, *From multiple unitarity cuts to the coproduct of Feynman integrals*, JHEP **10** (2014) 125, arXiv: 1401.3546 [hep-th] (cit. on pp. 26, 27, 114).

[81] A. V. Kotikov,
Differential equations method: New technique for massive Feynman diagrams calculation,
Phys. Lett. **B254** (1991) 158 (cit. on p. 30).

[82] T. Gehrmann and E. Remiddi, *Differential equations for two loop four point functions*,
Nucl.Phys. **B580** (2000) 485, arXiv: hep-ph/9912329 [hep-ph] (cit. on p. 30).

[83] R. N. Lee and A. I. Onishchenko, *ϵ-regular basis for non-polylogarithmic multiloop integrals and total cross section of the process $e^+e^- \to 2(Q\bar{Q})$*, JHEP **12** (2019) 084,
arXiv: 1909.07710 [hep-ph] (cit. on pp. 31, 33).

[84] K. G. Chetyrkin, M. Faisst, C. Sturm, and M. Tentyukov,
epsilon-finite basis of master integrals for the integration-by-parts method,
Nucl. Phys. B **742** (2006) 208, arXiv: hep-ph/0601165 (cit. on p. 31).

[85] J. Broedel, C. Duhr, F. Dulat, B. Penante, and L. Tancredi,
"From modular forms to differential equations for Feynman integrals,"
KMPB Conference: Elliptic Integrals, Elliptic Functions and Modular Forms in Quantum Field Theory, 2019 107, arXiv: 1807.00842 [hep-th] (cit. on p. 31).

[86] E. Remiddi and L. Tancredi, *Differential equations and dispersion relations for Feynman amplitudes. The two-loop massive sunrise and the kite integral*,
Nucl. Phys. **B907** (2016) 400, arXiv: 1602.01481 [hep-ph] (cit. on pp. 33, 61).

[87] A. Primo and L. Tancredi, *Maximal cuts and differential equations for Feynman integrals. An application to the three-loop massive banana graph*, Nucl. Phys. **B921** (2017) 316,
arXiv: 1704.05465 [hep-ph] (cit. on pp. 33, 61).

[88] A. von Manteuffel and L. Tancredi,
A non-planar two-loop three-point function beyond multiple polylogarithms,
JHEP **06** (2017) 127, arXiv: 1701.05905 [hep-ph] (cit. on p. 33).

[89] L.-B. Chen, Y. Liang, and C.-F. Qiao,
NNLO QCD corrections to $\gamma + \eta_c(\eta_b)$ exclusive production in electron-positron collision,
JHEP **01** (2018) 091, arXiv: 1710.07865 [hep-ph] (cit. on p. 33).

[90] B. A. Kniehl, A. V. Kotikov, A. I. Onishchenko, and O. L. Veretin,
Two-loop diagrams in non-relativistic QCD with elliptics, Nucl. Phys. B **948** (2019) 114780,
arXiv: 1907.04638 [hep-ph] (cit. on p. 33).

[91] R. N. Lee, A. A. Lyubyakin, and V. A. Stotsky,
Total cross sections of $e\gamma \to eX\bar{X}$ processes with $X = \mu, \gamma, e$ via multiloop methods,
JHEP **01** (2021) 144, arXiv: 2010.15430 [hep-ph] (cit. on p. 33).

[92] R. N. Lee and A. I. Onishchenko,
Master integrals for bipartite cuts of three-loop photon self energy, JHEP **04** (2021) 177,
arXiv: 2012.04230 [hep-ph] (cit. on p. 33).

[93] E. L. Ince, *Ordinary Differential Equations*, Dover Publications, New York, 1944
viii+558 (cit. on p. 34).

[94] C. M. Bender and S. A. Orszag,
Advanced Mathematical Methods for Scientists and Engineers I,
Springer-Verlag New York, 1999 (cit. on p. 34).

[95] M. Yoshida, *Fuchsian Differential Equations*, Vieweg+Teubner Verlag, 1987
(cit. on p. 34).

[96] P. Candelas, X. De La Ossa, A. Font, S. H. Katz, and D. R. Morrison,
Mirror symmetry for two parameter models. 1.,
Nucl. Phys. B **416** (1994) 481, ed. by B. Greene and S.-T. Yau,
arXiv: hep-th/9308083 (cit. on pp. 37, 49).

[97] P. Candelas, A. Font, S. H. Katz, and D. R. Morrison,
Mirror symmetry for two parameter models. 2., Nucl. Phys. B **429** (1994) 626,
arXiv: hep-th/9403187 (cit. on pp. 37, 49).

[98] S. T. Yau, *On the Ricci curvature of a compact Kähler manifold and the complex Monge-Ampère equation. I*, Comm. Pure Appl. Math. **31** (1978) 339, ISSN: 0010-3640,
URL: https://doi.org/10.1002/cpa.3160310304 (cit. on p. 40).

[99] K. Kodaira, *Complex manifolds and deformation of complex structures*, English,
Classics in Mathematics, Translated from the 1981 Japanese original by Kazuo Akao,
Springer-Verlag, Berlin, 2005 x+465, ISBN: 3-540-22614-1,
URL: https://doi.org/10.1007/b138372 (cit. on pp. 40, 95).

[100] G. Tian, "Smoothness of the universal deformation space of compact Calabi-Yau manifolds and its Petersson-Weil metric,"
Mathematical aspects of string theory (San Diego, Calif., 1986), vol. 1,
Adv. Ser. Math. Phys. World Sci. Publishing, Singapore, 1987 629 (cit. on p. 40).

[101] A. N. Todorov,
The Weil-Petersson geometry of the moduli space of $SU(n \geq 3)$ (Calabi-Yau) manifolds. I,
Comm. Math. Phys. **126** (1989) 325, ISSN: 0010-3616,
URL: http://projecteuclid.org/euclid.cmp/1104179854 (cit. on p. 40).

[102] H. Hironaka,
Resolution of singularities of an algebraic variety over a field of characteristic zero. I, II,
Ann. of Math. (2) 79 (1964), 109–203; ibid. (2) **79** (1964) 205, ISSN: 0003-486X,
URL: https://doi.org/10.2307/1970547 (cit. on p. 41).

[103] P. Deligne, "Théorie de Hodge. I,"
Actes du Congrès International des Mathématiciens (Nice, 1970), Tome 1, 1971 425
(cit. on p. 41).

[104] P. Deligne, *Théorie de Hodge. II*, Inst. Hautes Études Sci. Publ. Math. (1971) 5,
ISSN: 0073-8301,
URL: http://www.numdam.org/item?id=PMIHES_1971__40__5_0
(cit. on pp. 41, 55).

[105] P. Deligne, *Théorie de Hodge. III*, Inst. Hautes Études Sci. Publ. Math. (1974) 5, ISSN: 0073-8301, URL: http://www.numdam.org/item?id=PMIHES_1974__44__5_0 (cit. on p. 41).

[106] C. A. M. Peters and J. H. M. Steenbrink, *Mixed Hodge structures*, vol. 52, Ergebnisse der Mathematik und ihrer Grenzgebiete. 3. Folge. A Series of Modern Surveys in Mathematics [Results in Mathematics and Related Areas. 3rd Series. A Series of Modern Surveys in Mathematics], Springer-Verlag, Berlin, 2008 xiv+470, ISBN: 978-3-540-77015-2 (cit. on pp. 42, 44, 55).

[107] D. A. Cox and S. Katz, *Mirror symmetry and algebraic geometry*, vol. 68, Mathematical Surveys and Monographs, American Mathematical Society, Providence, RI, 1999 xxii+469, ISBN: 0-8218-1059-6, URL: https://doi.org/10.1090/surv/068 (cit. on pp. 42, 44).

[108] S. Laporta and E. Remiddi, *Analytic treatment of the two loop equal mass sunrise graph*, Nucl. Phys. B **704** (2005) 349, arXiv: hep-ph/0406160 (cit. on pp. 43, 61).

[109] S. Müller-Stach, S. Weinzierl, and R. Zayadeh, *A Second-Order Differential Equation for the Two-Loop Sunrise Graph with Arbitrary Masses*, Commun. Num. Theor. Phys. **6** (2012) 203, arXiv: 1112.4360 [hep-ph] (cit. on pp. 43, 61, 108, 111).

[110] J. L. Bourjaily, A. J. McLeod, M. Spradlin, M. von Hippel, and M. Wilhelm, *Elliptic Double-Box Integrals: Massless Scattering Amplitudes beyond Polylogarithms*, Phys. Rev. Lett. **120** (2018) 121603, arXiv: 1712.02785 [hep-th] (cit. on p. 43).

[111] D. Zagier, "Elliptic modular forms and their applications," *The 1-2-3 of modular forms*, Universitext, Springer, Berlin, 2008 1, URL: https://doi.org/10.1007/978-3-540-74119-0_1 (cit. on p. 43).

[112] S. Bloch, M. Kerr, and P. Vanhove, *A Feynman integral via higher normal functions*, Compos. Math. **151** (2015) 2329, arXiv: 1406.2664 [hep-th] (cit. on pp. 43, 61, 117).

[113] S. Bloch, M. Kerr, and P. Vanhove, *Local mirror symmetry and the sunset Feynman integral*, Adv. Theor. Math. Phys. **21** (2017) 1373, arXiv: 1601.08181 [hep-th] (cit. on pp. 43, 61, 74).

[114] C. Voisin, *Hodge theory and complex algebraic geometry. I*, English, vol. 76, Cambridge Studies in Advanced Mathematics, Translated from the French by Leila Schneps, Cambridge University Press, Cambridge, 2007 x+322, ISBN: 978-0-521-71801-1 (cit. on p. 45).

[115] R. L. Bryant and P. A. Griffiths, "Some observations on the infinitesimal period relations for regular threefolds with trivial canonical bundle," *Arithmetic and geometry, Vol. II*, vol. 36, Progr. Math. Birkhäuser Boston, Boston, MA, 1983 77 (cit. on pp. 45, 46).

[116] P. A. Griffiths, *On the periods of certain rational integrals. I, II*, Ann. of Math. (2) 90 (1969), 460-495; ibid. (2) **90** (1969) 496, ISSN: 0003-486X, URL: https://doi.org/10.2307/1970746 (cit. on p. 45).

[117] I. M. Gel'fand, A. V. Zelevinsky, and M. M. Kapranov, *Hypergeometric functions and toric varieties*, Funktsional. Anal. i Prilozhen. **23** (1989) 12, ISSN: 0374-1990, URL: https://doi.org/10.1007/BF01078777 (cit. on pp. 45, 79).

[118] S. Hosono, A. Klemm, S. Theisen, and S.-T. Yau, *Mirror symmetry, mirror map and applications to Calabi-Yau hypersurfaces*, Comm. Math. Phys. **167** (1995) 301, ISSN: 0010-3616, URL: http://projecteuclid.org/euclid.cmp/1104271994 (cit. on pp. 45, 56, 58).

[119] G. Frobenius, *Ueber adjungirte lineare Differentialausdrücke*, J. Reine Angew. Math. **85** (1878) 185, ISSN: 0075-4102, URL: https://doi.org/10.1515/crll.1878.85.185 (cit. on p. 47).

[120] D. van Straten, "Calabi-Yau operators," *Uniformization, Riemann-Hilbert correspondence, Calabi-Yau manifolds & Picard-Fuchs equations*, vol. 42, Adv. Lect. Math. (ALM), Int. Press, Somerville, MA, 2018 401 (cit. on pp. 47, 55–57).

[121] J. S. Milne, "Motives—Grothendieck's dream," *Open problems and surveys of contemporary mathematics*, vol. 6, Surv. Mod. Math. Int. Press, Somerville, MA, 2013 325 (cit. on p. 47).

[122] D. Zagier, "The arithmetic and topology of differential equations," *European Congress of Mathematics*, Eur. Math. Soc., Zürich, 2018 717 (cit. on p. 47).

[123] A. Landman, *On the Picard-Lefschetz transformation for algebraic manifolds acquiring general singularities*, Trans. Amer. Math. Soc. **181** (1973) 89, ISSN: 0002-9947, URL: https://doi.org/10.2307/1996622 (cit. on p. 50).

[124] P. Candelas, X. C. de la Ossa, P. S. Green, and L. Parkes, *A pair of Calabi-Yau manifolds as an exactly soluble superconformal theory*, Nuclear Phys. B **359** (1991) 21, ISSN: 0550-3213, URL: https://doi.org/10.1016/0550-3213(91)90292-6 (cit. on pp. 51, 58, 98).

[125] K. Lamotke, *The topology of complex projective varieties after S. Lefschetz*, Topology **20** (1981) 15, ISSN: 0040-9383, URL: https://doi.org/10.1016/0040-9383(81)90013-6 (cit. on p. 51).

[126] P. Deligne, *Equations Differentielles a Points Singuliers Reguliers by Pierre Deligne.* fre, 1st ed. 1970., Lecture Notes in Mathematics, 163, Berlin, Heidelberg: Springer Berlin Heidelberg, 1970, ISBN: 3-540-36373-4 (cit. on p. 53).

[127] W. Schmid, *Variation of Hodge structure: the singularities of the period mapping*, Invent. Math. **22** (1973) 211, ISSN: 0020-9910, URL: https://doi.org/10.1007/BF01389674 (cit. on pp. 54, 57).

[128] E. Cattani and A. Kaplan, *Polarized mixed Hodge structures and the local monodromy of a variation of Hodge structure*, Invent. Math. **67** (1982) 101, ISSN: 0020-9910, URL: https://doi.org/10.1007/BF01393374 (cit. on p. 55).

[129] D. R. Morrison, "Making enumerative predictions by means of mirror symmetry," *Mirror symmetry, II*, vol. 1, AMS/IP Stud. Adv. Math. Amer. Math. Soc., Providence, RI, 1997 457 (cit. on p. 56).

[130] P. Griffiths and J. Harris, *Principles of algebraic geometry*, Wiley Classics Library, Reprint of the 1978 original, John Wiley & Sons, Inc., New York, 1994 xiv+813, ISBN: 0-471-05059-8, URL: https://doi.org/10.1002/9781118032527 (cit. on pp. 57, 95).

[131] C. Robles, *Classification of horizontal* $SL(2)$*s*, Compos. Math. **152** (2016) 918, ISSN: 0010-437X, URL: https://doi.org/10.1112/S0010437X15007691 (cit. on p. 57).

[132] M. Kerr, G. J. Pearlstein, and C. Robles, *Polarized relations on horizontal* $\mathrm{SL}(2)$*'s*, Doc. Math. **24** (2019) 1295, ISSN: 1431-0635 (cit. on p. 57).

[133] A. Klemm, B. Lian, S. Roan, and S.-T. Yau, *Calabi-Yau fourfolds for M theory and F theory compactifications*, Nucl. Phys. B **518** (1998) 515, arXiv: hep-th/9701023 (cit. on pp. 58, 74).

[134] N. Cabo Bizet, A. Klemm, and D. Vieira Lopes, *Landscaping with fluxes and the E8 Yukawa Point in F-theory*, (2014), arXiv: 1404.7645 [hep-th] (cit. on pp. 58, 99, 100).

[135] R. Blumenhagen, D. Kläwer, L. Schlechter, and F. Wolf, *The Refined Swampland Distance Conjecture in Calabi-Yau Moduli Spaces*, JHEP **06** (2018) 052, arXiv: 1803.04989 [hep-th] (cit. on p. 58).

[136] T. W. Grimm, E. Palti, and I. Valenzuela, *Infinite Distances in Field Space and Massless Towers of States*, JHEP **08** (2018) 143, arXiv: 1802.08264 [hep-th] (cit. on p. 58).

[137] A. Joshi and A. Klemm, *Swampland Distance Conjecture for One-Parameter Calabi-Yau Threefolds*, JHEP **08** (2019) 086, arXiv: 1903.00596 [hep-th] (cit. on p. 58).

[138] E. Palti, *The Swampland: Introduction and Review*, Fortsch. Phys. **67** (2019) 1900037, arXiv: 1903.06239 [hep-th] (cit. on p. 58).

[139] A. Klemm and S. Theisen, *Considerations of one modulus Calabi-Yau compactifications: Picard-Fuchs equations, Kahler potentials and mirror maps*, Nucl. Phys. B **389** (1993) 153, arXiv: hep-th/9205041 (cit. on p. 58).

[140] P. Seidel and R. Thomas, *Braid group actions on derived categories of coherent sheaves*, Duke Math. J. **108** (2001) 37, ISSN: 0012-7094, URL: https://doi.org/10.1215/S0012-7094-01-10812-0 (cit. on p. 59).

[141] P. Deligne, "Local behavior of Hodge structures at infinity," *Mirror symmetry, II*, vol. 1, AMS/IP Stud. Adv. Math. Amer. Math. Soc., Providence, RI, 1997 683, URL: https://doi.org/10.24033/msmf.276 (cit. on p. 59).

[142] L. Adams, C. Bogner, and S. Weinzierl, *The two-loop sunrise graph in two space-time dimensions with arbitrary masses in terms of elliptic dilogarithms*, J. Math. Phys. **55** (2014) 102301, arXiv: 1405.5640 [hep-ph] (cit. on p. 61).

[143] D. Broadhurst and D. P. Roberts, *Quadratic relations between Feynman integrals*, PoS **LL2018** (2018) 053 (cit. on p. 65).

[144] Y. Zhou, $\mathbb{Q}$*-linear dependence of certain Bessel moments*, (2019), arXiv: 1911.04141 [math.NT] (cit. on p. 65).

[145] Y. Zhou, *Wrońskian algebra and Broadhurst-Roberts quadratic relations*, (2020), arXiv: 2012.03523 [math.NT] (cit. on p. 65).

[146] J. Fresán, C. Sabbah, and J.-D. Yu, *Quadratic relations between Bessel moments*, (2020), arXiv: 2006.02702 [math.AG] (cit. on p. 65).

[147] R. N. Lee, *Symmetric ϵ- and $(\epsilon + 1/2)$-forms and quadratic constraints in "elliptic" sectors*, JHEP **10** (2018) 176, arXiv: 1806.04846 [hep-ph] (cit. on p. 65).

[148] K. Cho and K. Matsumoto, *Intersection theory for twisted cohomologies and twisted Riemann's period relations I*, Nagoya Math. J. **139** (1995) 67 (cit. on p. 65).

[149] H. Frellesvig et al., *Decomposition of Feynman Integrals by Multivariate Intersection Numbers*, JHEP **03** (2021) 027, arXiv: 2008.04823 [hep-th] (cit. on p. 65).

[150] F. Brown, *Multiple modular values and the relative completion of the fundamental group of $\mathcal{M}_{1,1}$*, (2014), arXiv: 1407.5167v4 [math.NT] (cit. on pp. 66, 117).

[151] R. Bott and L. W. Tu, *Differential forms in algebraic topology*, vol. 82, Graduate Texts in Mathematics, Springer-Verlag, New York-Berlin, 1982 xiv+331, ISBN: 0-387-90613-4 (cit. on p. 70).

[152] V. V. Batyrev,
Dual polyhedra and mirror symmetry for Calabi-Yau hypersurfaces in toric varieties,
J. Algebraic Geom. **3** (1994) 493, ISSN: 1056-3911 (cit. on pp. 70, 71, 73, 79).

[153] S. Hosono, A. Klemm, S. Theisen, and S.-T. Yau,
Mirror symmetry, mirror map and applications to Calabi-Yau hypersurfaces,
Commun. Math. Phys. **167** (1995) 301, arXiv: hep-th/9308122
(cit. on pp. 70, 72, 75, 79).

[154] V. V. Batyrev and D. van Straten, *Generalized hypergeometric functions and rational curves on Calabi-Yau complete intersections in toric varieties*,
Comm. Math. Phys. **168** (1995) 493, ISSN: 0010-3616,
URL: http://projecteuclid.org/euclid.cmp/1104272487 (cit. on p. 70).

[155] S. Hosono, B. H. Lian, and S.-T. Yau,
GKZ generalized hypergeometric systems in mirror symmetry of Calabi-Yau hypersurfaces,
Commun. Math. Phys. **182** (1996) 535, arXiv: alg-geom/9511001 [alg-geom]
(cit. on pp. 72, 75).

[156] D. A. Cox, J. B. Little, and H. K. Schenck, *Toric varieties*, vol. 124,
Graduate Studies in Mathematics,
American Mathematical Society, Providence, RI, 2011 xxiv+841,
ISBN: 978-0-8218-4819-7, URL: https://doi.org/10.1090/gsm/124
(cit. on p. 72).

[157] URL: http://doc.sagemath.org/html/en/reference/schemes/sage/schemes/toric/variety.html (cit. on p. 72).

[158] Gel'fand, I. M. and Zelevinsky, A. V. and Kapranov, M. M.,
Newton polyhedra of principal A-determinants, Dokl. Akad. Nauk SSSR **308** (1989) 20,
ISSN: 0002-3264 (cit. on p. 78).

[159] Gel'fand, I. M. and Kapranov, M. M. and Zelevinsky, A. V.,
Generalized Euler integrals and A-hypergeometric functions, Adv. Math. **84** (1990) 255,
ISSN: 0001-8708, URL: https://doi.org/10.1016/0001-8708(90)90048-R
(cit. on p. 79).

[160] T. Coates, A. Corti, S. Galkin, V. Golyshev, and A. Kasprzyk,
"Fano Varieties and Extremal Laurent Polynomials: A collaborative research blog,"
since December 2012 (cit. on p. 86).

[161] F. Hirzebruch, *Topological methods in algebraic geometry*, Classics in Mathematics,
Translated from the German and Appendix One by R. L. E. Schwarzenberger, With a preface to the third English edition by the author and Schwarzenberger, Appendix Two by A. Borel, Reprint of the 1978 edition, Springer-Verlag, Berlin, 1995 xii+234,
ISBN: 3-540-58663-6 (cit. on pp. 98, 100).

[162] S. Hosono, "Central charges, symplectic forms, and hypergeometric series in local mirror symmetry," *Mirror symmetry. V*, vol. 38, AMS/IP Stud. Adv. Math. Amer. Math. Soc., Providence, RI, 2006 405 (cit. on pp. 98, 99).

[163] H. Iritani, "Ruan's conjecture and integral structures in quantum cohomology," *New developments in algebraic geometry, integrable systems and mirror symmetry (RIMS, Kyoto, 2008)*, vol. 59, Adv. Stud. Pure Math. Math. Soc. Japan, Tokyo, 2010 111, URL: https://doi.org/10.2969/aspm/05910111 (cit. on pp. 98–100).

[164] L. Katzarkov, M. Kontsevich, and T. Pantev, "Hodge theoretic aspects of mirror symmetry," *From Hodge theory to integrability and TQFT tt*-geometry*, vol. 78, Proc. Sympos. Pure Math. Amer. Math. Soc., Providence, RI, 2008 87, URL: https://doi.org/10.1090/pspum/078/2483750 (cit. on pp. 98, 99).

[165] S. Galkin, V. Golyshev, and H. Iritani, *Gamma classes and quantum cohomology of Fano manifolds: gamma conjectures*, Duke Math. J. **165** (2016) 2005, ISSN: 0012-7094, URL: https://doi.org/10.1215/00127094-3476593 (cit. on pp. 98, 99).

[166] A. Gerhardus and H. Jockers, *Quantum periods of Calabi–Yau fourfolds*, Nucl. Phys. B **913** (2016) 425, arXiv: 1604.05325 [hep-th] (cit. on p. 99).

[167] F. A. Berends, M. Buza, M. Bohm, and R. Scharf, *Closed expressions for specific massive multiloop selfenergy integrals*, Z. Phys. C **63** (1994) 227 (cit. on pp. 104, 113).

[168] L. Adams, C. Bogner, and S. Weinzierl, *The two-loop sunrise graph with arbitrary masses*, J. Math. Phys. **54** (2013) 052303, arXiv: 1302.7004 [hep-ph] (cit. on p. 104).

[169] M. Caffo, H. Czyz, S. Laporta, and E. Remiddi, *The Master differential equations for the two loop sunrise selfmass amplitudes*, Nuovo Cim. A **111** (1998) 365, arXiv: hep-th/9805118 (cit. on p. 108).

[170] E. Remiddi and L. Tancredi, *Schouten identities for Feynman graph amplitudes; The Master Integrals for the two-loop massive sunrise graph*, Nucl. Phys. B **880** (2014) 343, arXiv: 1311.3342 [hep-ph] (cit. on pp. 108, 111).

[171] K. Aomoto and M. Kita, *Theory of Hypergeometric Functions*, Springer Monographs in Mathematics, Springer Japan, 2011 (cit. on p. 113).

[172] S. Mizera, *Scattering Amplitudes from Intersection Theory*, Phys. Rev. Lett. **120** (2018) 141602, arXiv: 1711.00469 [hep-th] (cit. on p. 113).

[173] S. Mizera, *Aspects of Scattering Amplitudes and Moduli Space Localization*, PhD thesis: Perimeter Inst. Theor. Phys., 2019, arXiv: 1906.02099 [hep-th] (cit. on p. 113).

[174] H. Frellesvig et al., *Decomposition of Feynman Integrals on the Maximal Cut by Intersection Numbers*, JHEP **05** (2019) 153, arXiv: 1901.11510 [hep-ph] (cit. on p. 113).

[175] H. Frellesvig et al.,
Vector Space of Feynman Integrals and Multivariate Intersection Numbers,
Phys. Rev. Lett. **123** (2019) 201602, arXiv: 1907.02000 [hep-th] (cit. on p. 113).

[176] B. Ananthanarayan, A. B. Das, and D. Wyler,
The Hopf Algebra Structure of the Two Loop Three Mass Non-Planar Feynman Diagram,
(2021), arXiv: 2104.00967 [hep-th] (cit. on p. 114).

[177] R. P. Feynman, *Quantum theory of gravitation*,
Acta Phys. Polon. **24** (1963) 697, ed. by J.-P. Hsu and D. Fine (cit. on p. 114).

[178] R. P. Feynman, "Closed Loop and Tree Diagrams," *Magic without MAgic*,
ed. by L. M. Brown, 1972 (cit. on p. 114).

[179] Y. I. Manin,
"Iterated integrals of modular forms and noncommutative modular symbols,"
Algebraic geometry and number theory, vol. 253, Progr. Math.
Boston: Birkhäuser Boston, 2006 565, arXiv: math/0502576 (cit. on p. 117).

[180] S. Bloch, M. Kerr, and P. Vanhove,
Local mirror symmetry and the sunset Feynman integral,
Adv. Theor. Math. Phys. **21** (2017) 1373, ISSN: 1095-0761,
URL: https://doi.org/10.4310/ATMP.2017.v21.n6.a1 (cit. on p. 117).

[181] N. I. Usyukina and A. I. Davydychev,
Exact results for three and four point ladder diagrams with an arbitrary number of rungs,
Phys. Lett. B **305** (1993) 136 (cit. on p. 117).

[182] N. I. Usyukina and A. I. Davydychev,
An Approach to the evaluation of three and four point ladder diagrams,
Phys. Lett. B **298** (1993) 363 (cit. on p. 117).

[183] D. J. Broadhurst and D. Kreimer,
*Knots and numbers in Phi**4 theory to 7 loops and beyond*,
Int. J. Mod. Phys. C **6** (1995) 519, ed. by B. H. Denby and D. Perret-Gallix,
arXiv: hep-ph/9504352 (cit. on p. 117).

[184] F. Brown and O. Schnetz,
Single-valued multiple polylogarithms and a proof of the zig–zag conjecture,
J. Number Theor. **148** (2015) 478, arXiv: 1208.1890 [math.NT] (cit. on p. 117).

[185] O. Schnetz, *Evaluation of the period of a family of triangle and box ladder graphs*, (2012),
arXiv: 1210.5376 [math.NT] (cit. on p. 117).

[186] J. M. Drummond, *Generalised ladders and single-valued polylogarithms*,
JHEP **02** (2013) 092, arXiv: 1207.3824 [hep-th] (cit. on p. 117).

[187] S. Caron-Huot, L. J. Dixon, M. von Hippel, A. J. McLeod, and G. Papathanasiou,
The Double Pentaladder Integral to All Orders, JHEP **07** (2018) 170,
arXiv: 1806.01361 [hep-th] (cit. on p. 117).

[188] B. Basso and L. J. Dixon, *Gluing Ladder Feynman Diagrams into Fishnets*, Phys. Rev. Lett. **119** (2017) 071601, arXiv: 1705.03545 [hep-th] (cit. on p. 117).

[189] R. Huang and Y. Zhang, *On Genera of Curves from High-loop Generalized Unitarity Cuts*, JHEP **04** (2013) 080, arXiv: 1302.1023 [hep-ph] (cit. on p. 118).

[190] A. Georgoudis and Y. Zhang, *Two-loop Integral Reduction from Elliptic and Hyperelliptic Curves*, JHEP **12** (2015) 086, arXiv: 1507.06310 [hep-th] (cit. on p. 118).

[191] J. D. Hauenstein, R. Huang, D. Mehta, and Y. Zhang, *Global Structure of Curves from Generalized Unitarity Cut of Three-loop Diagrams*, JHEP **02** (2015) 136, arXiv: 1408.3355 [hep-th] (cit. on p. 118).